



Modeling Hand Motor Outcome Following Stroke using Multimodal MRI

Firdaus Fabrice Hannanu

► To cite this version:

Firdaus Fabrice Hannanu. Modeling Hand Motor Outcome Following Stroke using Multimodal MRI. Neuroscience. Université Grenoble Alpes [2020-..], 2022. English. NNT : 2022GRALS037 . tel-04095206

HAL Id: tel-04095206

<https://theses.hal.science/tel-04095206>

Submitted on 11 May 2023

HAL is a multi-disciplinary open access archive for the deposit and dissemination of scientific research documents, whether they are published or not. The documents may come from teaching and research institutions in France or abroad, or from public or private research centers.

L'archive ouverte pluridisciplinaire **HAL**, est destinée au dépôt et à la diffusion de documents scientifiques de niveau recherche, publiés ou non, émanant des établissements d'enseignement et de recherche français ou étrangers, des laboratoires publics ou privés.

THÈSE

Pour obtenir le grade de

DOCTEUR DE L'UNIVERSITÉ GRENOBLE ALPES

École doctorale : ISCE - Ingénierie pour la Santé la Cognition et l'Environnement

Spécialité : MBS - Modèles, méthodes et algorithmes en biologie, santé et environnement

Unité de recherche : AUTONOMIE, GÉRONTOLOGIE, E-SANTÉ, IMAGERIE & SOCIÉTÉ

Modélisation de la récupération motrice de la main en IRM multimodale après un infarctus cérébral

Modeling Hand Motor Outcome Following Stroke using Multimodal MRI

Présentée par :

Firdaus Fabrice HANNANU

Direction de thèse :

Assia JAILLARD

PRATICIEN HOSPITALIER, Université Grenoble Alpes

Directrice de thèse

Marc HOMMEL

PROFESSEUR DES UNIVERSITES - PRATICIEN HOSPITALIER,
Université Grenoble Alpes

Co-directeur de thèse

Rapporteurs :

ISABELLE BONAN

Professeur des Univ. - Praticien hosp., UNIVERSITE RENNES 1

GILLES ALLALI

Praticien-Hospitalier HDR, Université de Lausanne

Thèse soutenue publiquement le 16 novembre 2022, devant le jury composé de :

ASSIA JAILLARD

Praticien-Hospitalier HDR, UNIVERSITE GRENOBLE ALPES

Directrice de thèse

LEEANNE CAREY

Professeur associé, La Trobe University

Examinatrice

THIERRY MOULIN

Professeur des Univ. - Praticien hosp., UNIVERSITE DE FRANCHE-COMTE

Examineur

DOMINIC PERENNOU

Professeur des Univ. - Praticien hosp., UNIVERSITE GRENOBLE ALPES

Président

ISABELLE BONAN

Professeur des Univ. - Praticien hosp., UNIVERSITE RENNES 1

Rapporteuse

GILLES ALLALI

Praticien-Hospitalier HDR, Université de Lausanne

Rapporteur

Declaration

I hereby declare that except where specific reference is made to the work of others, the contents of this dissertation are original and have not been submitted in whole or in part for consideration for any other degree or qualification in this, or any other university. This dissertation is my own work and contains nothing which is the outcome of work done in collaboration with others, except as specified in the text and Acknowledgements. This dissertation contains fewer than 65,000 words including appendices, bibliography, footnotes, tables and equations and has fewer than 150 figures.

Firdaus Fabrice Hannanu
September 2022

Acknowledgements

This thesis is only made possible through work and dedication of many supporting people and institutions over several years.

First of all, this thesis is deeply indebted to all the patients and volunteers who have contributed to the studies, for their courage and valuable time, and for believing in research as our way of knowing and understanding the brain.

I would like to express my deepest gratitude to my supervisors, Assia Jaillard and Marc Hommel, who have showed sincere support, patience, and guidance since the first time they welcomed me to the lab for my master research project. They have given me invaluable insights over the years that helped me develop skills necessary to attain both my academic and personal goals. Thank you for the constant challenge, to get the best of me. I want to thank Nicolas Vuillerme, for his valuable advice and views during my doctoral study. I am forever grateful for the opportunity to learn and grow from them as my supervisors and role models.

I would like to thank my thesis committee members, Isabelle Bonan, Gilles Allali, Leeanne Carey, Thierry Moulin, and Dominic Perenneu for accepting to be part of the jury, and taking time to attentively read the manuscript. Also for Arnaud Attie and Chantal Delon-Martin as member of the yearly Comité de Suivi Individuel (CSI), who have given me insights and constructive critical advices during years of my Ph.D.

My profound thanks to all members of the ISIS-HERMES, IRMAS, and RESSTORE research group and co-authors, Alexandre Krainik, Bernadette Naegele, Olivier Detante, Charlotte Rosso, Flore Baronnet-Chauvet, Aliénor Jaillard, and Nicolas Hommel, who have contributed in data collection and analysis and reviewed the manuscripts for publications.

My sincere thanks are also for the people who have worked with me side-by-side, Bérengère Aubert-Broche, Issa Goundous, and Benjamin Darçot. In a relatively short time, they have helped me as partners for discussing ideas, asking stupid questions, exploring new tools, double-checking codes and data analysis, and even taught me some of my first french sentences.

This doctoral study is financially funded by Lembaga Pengelola Dana Pendidikan (LPDP), Ministry of Finance, government of Indonesia. I am highly grateful for this privilege, and while many opportunities will be open for me in the future, one thing will remain: *Aku pasti mengabdikan*.

My endless gratitude would go without saying for my parents, who got me started, and for my loving wife Rien and my son Fabien, who accompanied me along the way. Thank you, for never stop encouraging my fascination for science.

Abstract

Hand motor impairment is one of the most disabling neurological deficits following stroke, as hand play a crucial role in daily life activities. Moreover, the variability of hand motor recovery among patients and the incomplete understanding of contributing factors of recovery remains the key challenges in stroke research. Some biomarkers have been currently identified, such as initial motor severity, age, or lesion volume, but the predictive values are still considered insufficient. Non-routine neuroimaging MRI, providing non-invasive and quantitative measures of brain structural and functional changes after stroke, may help to explain the residual variance.

Using populations from three longitudinal studies (ISIS-HERMES, IRMAS, and RESTORE) with clinical, behavioral, and multimodal MRI assessments, the current thesis sought to investigate predictive models and neural correlates of hand motor recovery using 5 different MRI modalities, including task-fMRI, diffusion-weighted imaging (DWI), resting-state fMRI (rs-fMRI), surface-based morphometry, and voxel-based lesion-symptom mapping (VLSM), when used either independently or in combination.

The results of our first study, using functional MRI, showed that spatiotemporal patterns of task-related sensorimotor brain activity, specifically those involved in the dorsolateral and dorsomedial network, predict hand motor recovery. Second, using DWI, we showed that in addition to the integrity of the corticospinal tract (CST), other white matter tracts, such as the superior longitudinal fasciculus (SLF), corpus callosum (CC) and anterior corona radiata (ACR), contribute in ipsilateral hand impairment. Third, we showed that both visuomotor and motor functional connectivity can predict six-month hand motor outcome. In the fourth study, we found that cortical thickness may provide prediction accuracy that is comparable to that of initial clinical severity. Moreover, lesions in the CST, at the level of the posterior limb of internal capsule (PLIC) and corona radiata, were associated with a bad hand motor outcome at six-months follow-up. Lastly, we found that hand motor outcome was best predicted by task-fMRI with improved prediction if used together with DWI and that DWI would be the best predictor for more global measures.

Our findings suggest that MRI modalities may improve hand motor recovery models currently used in clinical settings, and that each modality provide predictive values depending on the specific type of outcome that is measured. This thesis also highlights the neural correlates involved in hand motor impairment and recovery. Moreover, MRI biomarkers may be useful to assess the effects of novel therapies in stroke.

Résumé

L'atteinte motrice de la main après un accident vasculaire cérébral (AVC) est une cause majeure de handicap, les gestes manuels étant indispensables aux activités de la vie quotidienne. En outre, la récupération motrice de la main est très hétérogène chez les patients AVC, et les facteurs intervenant dans la récupération restent mal connus. Certains de ces facteurs ont été identifiés, tels que l'âge, la sévérité initiale, ou le volume lésionnel, mais leur utilisation en tant que biomarqueurs est limitée, car ils n'expliquent que partiellement la récupération motrice de la main. La neuro-imagerie IRM, en apportant des mesures non invasives et quantifiées des modifications structurales et fonctionnelles observées après l'AVC, pourraient permettre d'expliquer une partie de la variance résiduelle de la récupération.

Le présent travail s'appuie sur les données cliniques, expérimentales et IRM acquises de façon longitudinale dans 3 études différentes (ISIS-HERMES, IRMAS, et RESSTORE), pour tester des modèles prédictifs et les corrélats neuronaux de la récupération motrice de la main en utilisant les 5 modalités IRM suivantes, de façon unimodale ou multimodale: IRM fonctionnelle (IRMf) d'activation basée sur une tâche motrice, IRMf de repos, IRM morphométrique, analyse de lésion par 'voxel-based lesion-symptom mapping (VLSM)', et IRM de diffusion.

Les résultats de notre première étude montrent que l'activation spatio-temporelle en IRMf des réseaux sensorimoteurs dorsolatéral et dorsomédial prédit la récupération motrice. Dans une deuxième étude basée sur l'IRM de diffusion, le degré d'intégrité du faisceau corticospinal (CST) et d'autres tracts de la substance blanche tels que le faisceau longitudinal supérieur, le corps calleux, et la corona radiata antérieure permettaient d'expliquer l'atteinte de la main ipsilatérale. Dans la troisième étude basée sur l'IRMf de repos, la connectivité fonctionnelle motrice et visuomotrice prédit la force de la main six mois après un AVC. Dans la quatrième étude, l'épaisseur corticale prédit la récupération motrice aussi bien voire mieux que le déficit moteur initial. En outre, l'étude des lésions en VLSM montre que les localisations du CST au niveau du bras postérieur de la capsule interne et de la corona radiata étaient associées à l'absence de récupération motrice de la main lors du suivi à 6 mois. Dans la dernière étude, basée sur une approche IRM multimodale, l'IRMf, associé ou non à la

diffusion, est le meilleur prédicteur de la récupération motrice de la main, alors que l'IRM de diffusion est un meilleur prédicteur pour les mesures de récupération globale.

L'ensemble de ces résultats suggère que l'utilisation de biomarqueurs IRM peut améliorer la prédiction de la récupération motrice dans un contexte clinique, et que la modalité à utiliser dépend de la fonction à prédire. Ce travail met également en évidence les corrélats neuronaux impliqués dans la récupération motrice de la main. Enfin, ces biomarqueurs IRM pourraient servir à évaluer l'effet de nouvelles thérapies dans l'AVC.

Table of contents

Abstract	vii
Résumé	ix
List of publications	xv
List of figures	xvii
List of tables	xix
Glossary	xxi
Introduction	1
1 Literature Review	5
1.1 Stroke	6
1.1.1 Definition and global burden	6
1.1.2 Post-stroke hand motor deficits and recovery	7
1.1.3 Ipsilateral hand - Impairment and mechanisms	10
1.2 Motor system	12
1.2.1 Anatomical organization of the motor system	12
1.2.2 Functional organization of the motor system	19
1.2.3 Lateral grasping network in macaque and its putative human homolog	20
1.2.4 Two visual streams theory - a brief history and its development . . .	21
1.3 MRI Neuroimaging modalities and prognostic models in stroke	22
1.3.1 Structural MRI	23
1.3.2 Functional MRI (fMRI)	36
1.3.3 Predictive models of hand motor outcome using multimodal MRI .	43
2 Materials and Methods	45
2.1 Materials	46
2.1.1 Participants	47
2.1.2 Clinical and behavioral scores	49
2.1.3 MRI acquisition	50
2.2 Methods	53

2.2.1	MRI Data Processing	53
2.2.2	Statistical analysis	56
3	Thesis Work	59
3.1	Study I. Task-fMRI	61
3.1.1	Overview	61
3.1.2	Article	62
3.1.3	Methodological considerations	82
3.2	Study II. DTI	83
3.2.1	Overview	83
3.2.2	Article	83
3.3	Study III. Resting-state fMRI	95
3.3.1	Overview	95
3.3.2	Article	96
3.4	Study IV (Surface-based morphometry)	126
3.4.1	Introduction	126
3.4.2	Methods	127
3.4.3	Results	128
3.4.4	Discussion	130
3.5	Study V (VLSM)	135
3.5.1	Introduction	135
3.5.2	Methods	137
3.5.3	Results	137
3.5.4	Discussion	141
3.6	Study VI (Multimodal MRI)	145
3.6.1	Introduction	145
3.6.2	Methods	146
3.6.3	Results	147
3.6.4	Discussion	147
4	Discussion and Conclusion	153
4.1	Summary of the main findings	154
4.2	Hand motor impairment after stroke	156
4.3	Predictive models and neural correlates of hand motor recovery	157
4.3.1	Clinical assessments	157
4.3.2	Lesion characteristics	158

4.3.3	Structural Imaging	159
4.3.4	Functional MRI	160
4.4	Methodological Considerations	162
4.4.1	Generalizability of the results	162
4.4.2	Sample size	162
4.4.3	Heterogeneity in study designs and confounding factors	163
4.4.4	Brain asymmetry: to flip or not to flip?	165
4.5	Clinical Implications	165
4.6	Perspectives	167
4.7	Conclusion	168
References		169
Appendix A Supplementary materials and methods		197
A.1	Inclusion and exclusion criteria of cohorts	197
A.1.1	ISIS-HERMES study	197
A.1.2	RESSTORE study	198
A.1.3	IRMAS study	199
A.2	Clinical score measurement	199
A.2.1	National Institutes of Health Stroke Scale	199
A.2.2	modified Rankin Scale	208
Appendix B Supplementary Results		211
B.1	Study IV. Surface-based Morphometry	211
B.2	Study VI. Multimodal MRI	214

List of Publications

Published articles

1. **Hannanu, F. F.**, Goundous, I., Detante, O., Naegele, B., & Jaillard, A. (2020). Spatiotemporal pattern of sensorimotor fMRI activity influence hand motor recovery in subacute stroke: A longitudinal task-related fMRI study. *Cortex; a journal devoted to the study of the nervous system and behavior*, 129, 80–98. <https://doi.org/10.1016/j.cortex.2020.03.024>
2. **Hannanu, F. F.**, Naegele, B., Hommel, M., Krainik, A., Detante, O., & Jaillard, A. (2022). White matter tract disruption is associated with ipsilateral hand impairment in subacute stroke: a diffusion MRI study. *Neuroradiology*, 10.1007/s00234-022-02927-8. Advance online publication. <https://doi.org/10.1007/s00234-022-02927-8>
3. Razak, R. A., **Hannanu, F. F.**, Naegele, B., Hommel, M., Detante, O., & Jaillard, A. (2022). Ipsilateral hand impairment predicts long-term outcome in patients with subacute stroke. *European journal of neurology*, 10.1111/ene.15323. Advance online publication. <https://doi.org/10.1111/ene.15323>

Submitted articles

1. **Hannanu, F. F.**, Baronnet-Chauvet, F., Naegele, B., Jaillard, A.V., Krainik, A., Detante, O., Rosso, C., & Jaillard, A. Visuomotor resting-state functional MRI connectivity predicts hand motor outcome following stroke. *Neurology*.

List of figures

1.1	Stroke incidence rates among countries	6
1.2	Arterial territory of the human brain	7
1.3	Time course of stroke	9
1.4	Primary motor cortex	13
1.5	Somatosensory and motor cortex	14
1.6	Premotor cortex	15
1.7	The corticospinal tract	18
1.8	Connections of the motor system	19
1.9	Lateral grasping network	21
1.10	Cortical thickness	24
1.11	Cortical thickness estimation using CAT12	24
1.12	Steps in VLSM analysis	28
1.13	Diffusion-weighted imaging signal intensity	32
1.14	White matter segmentation	35
1.15	The hemodynamic response function (HRF)	38
1.16	Task-fMRI design	38
1.17	Passive task-fMRI brain activity	40
1.18	Functional connectivity	42
2.1	Datasets used for each study	47
2.2	HCP Atlas	54
2.3	Preprocessing steps	57
3.1	Study III flowchart	128
3.2	Study III Lesion overlay	139
3.3	Study III VLSM Statistical map	140
3.4	MRI Biomarkers	149

List of figures

B.1	Heatplot of the whole dataset	214
-----	---	-----

List of tables

1.1	Studies reporting cortical thickness in stroke	27
1.2	Studies reporting the association between lesion location and hand and upper limb motor deficit in stroke	30
3.1	Characteristics of participants	128
3.2	Behavioral and clinical scores of stroke group	129
3.3	Between-group comparison (t-values) of CT, FD, and GI	129
3.4	CT comparison between patients and controls at ROI-level	131
3.5	Performance of the model represented by the area under the curve (AUC) of hand grip models using different algorithms	132
3.6	Patient characteristics with clinical and behavioral scores	138
3.7	Number of significant voxels included in each ROI for each scores	142
3.8	Characteristics, clinical and behavioral scores in patients and controls	150
3.9	Predictive value of each modality using different algorithms	151
3.10	Predictive value of MRI modalities when used in combination of two	152
B.1	Mean and SD of the SBM metrics for controls, patients at M0 and patients at M6	211
B.2	FD comparison between patients and controls at ROI-level	212
B.3	GI comparison between patients and controls at ROI-level	213
B.4	Predictive value of metrics in each modality using different methods	215

Glossary

Acronyms / Abbreviations

ADMSCs allogeneic adipose tissue-derived mesenchymal stem cells

BOLD Blood-Oxygen-Level Dependent

DTI Diffusion Tensor Imaging

FA Fractional Anisotropy

fMRI Functional Magnetic Resonance Imaging

FOD Fiber Orientation Distribution

GLM General Linear Model

HRF Hemodynamic Response Function

ICA Independent Component Analysis

LMM Linear Mixed Model

mNIHSS Motor subscale of National Institute of Health Stroke Scale

MRI Magnetic Resonance Imaging

mRS modified Rankin Scale

NIHSS National Institute of Health Stroke Scale

PPT Purdue Pegboard Test

ROI Region of Interest

rs-fMRI Resting-state functional Magnetic Resonance Imaging

Glossary

RSFC Resting-State Functional Connectivity

SBM Surface-Based Morphometry

VLSM Voxel based lesion-symptom mapping

Introduction

Stroke remains the second leading cause of death and disability-adjusted life years (DALYs) in adults, just second to ischemic heart disease (World Health Organization, 2019). One of the most common yet disabling effects following an ischemic stroke is the impairment of the voluntary movement of the hand. Motor deficits impairing the movements of the hand, such as reach and grasp actions, are crucial because they are used to manipulate tools and objects to perform functional tasks dexterously. Indeed, hand impairment due to stroke hampers the ability to perform daily life activities and patients' independence (Horn et al., 2016; Raghavan, 2007). Interestingly, while some patients eventually regained some degree of hand motor function, hand deficit persisted until six months following a stroke in more than two-thirds of stroke survivors, even with standard treatment procedures and active participation in rehabilitation programs. (Feigin et al., 2003) Therefore, hand recovery is a challenge in current stroke research with a question that remains to be addressed: why do some patients recover their hand motor function better than others?

The interest in answering this question is twofold. From a pathophysiological perspective, an understanding of the underlying mechanisms of recovery is necessary to promote the development of new therapies and rehabilitation strategies since the exact neural correlates of hand motor recovery after stroke are still far from being completely understood. Second, robust biomarkers and predictive models of outcome would serve several clinical purposes: to inform patients and caregivers about the prognostic course of the disease, to determine groups of patients that could benefit from interventions to promote recovery, and to plan better therapeutical strategies that best suit the functional requirements at the individual level.

In the quest for predictive biomarkers, motor initial severity assessed within a week after stroke has been consistently reported to be highly correlated with the outcome (Sato et al., 2008; Wouters et al., 2018) but explained less than 50% of outcome variance (Rost et al., 2016). Indeed, clinical scores are considered insufficient to discriminate between patients with good or bad motor outcomes reliably (Buch et al., 2016). A potential candidate to improve prediction may come from non-routine neuroimaging analysis, providing a non-invasive and quantitative measure of brain structural and functional properties (Heiss

Introduction

and Kidwell, 2014; Pinto et al., 2018). Ever since the development of advanced MRI neuroimaging tools, several studies have explored the cortical and subcortical correlates of hand motor impairment and recovery and biomarkers of motor recovery after stroke. Structurally, greater disruption of descending white matter pathways is associated with worse motor performance and outcome. Lesion load and fractional anisotropy (FA) of the corticospinal tract (CST) at the level of the posterior limb of the internal capsule or pons have been reported to best predict motor outcomes. (Feng et al., 2015; Koch et al., 2016; Kumar et al., 2016; Puig et al., 2010) In addition, there is evidence from functional neuroimaging that both task-related cortical activity and resting-state functional connectivity are associated with motor performance and outcomes. (Brihmat et al., 2020; Favre et al., 2014)

The research on neuroimaging biomarkers of outcome, however, mainly focused on the upper-limb motor outcome, assessed using motor clinical scores such as the Fugl-Meyer Score, (Buch et al., 2016; Zhang et al., 2015) or NIHSS (Puig et al., 2010; Radlinska et al., 2010) that primarily measure proximal or distal movements, but not the hand ability *per se*. Other studies used modified Rankin Score (mRS) and Barthel Index (Radlinska et al., 2010) to assess global functional outcomes. Among many hand motor task measurements, a hand dynamometer is frequently used to assess handgrip strength (Raghavan, 2007), and the Purdue pegboard test (PPT) is used to quantitatively assess manual dexterity that requires reach and grasp motor actions. (Schaechter et al., 2009) More specific hand abilities, such as detailed velocity, acceleration, or accuracy, would need customized kinematic tools to measure. (Kortier et al., 2014) As opposed to the upper limb, the hand is a phylogenetically and functionally specialized part of the human body, and therefore should deserve specific investigations. Only few studies, those that will be further discussed in the subsequent chapter, used neuroimaging tools to assess hand outcome after stroke.

The main objective of this thesis is to explore the modeling of hand motor recovery after stroke using longitudinal and multimodal MRI, with two goals: (1) to explore the mechanisms underlying hand impairment and recovery following stroke, and (2) to determine hand recovery predictors based on neuroimaging. In this context, several other questions may arise: When used independently, which MRI modality predicts hand motor outcome the best? Does a combination of two or more modalities (for example, diffusion MRI and RS-fMRI) provide better prediction than one, or do they bring redundant information to the model? Either way, which MRI modality combination provides the best prediction? Is it worth performing all MRI sequences to have a better prognostic model?

To answer these questions, several MRI modalities will be explored, including:

- Morphological structural MRI to assess surface-based morphometry (SBM), providing measures of surface such as cortical thickness, fractal dimension, and gyrification index, and voxel-based lesion-symptom mapping (VLSM), used to identify specific brain anatomical regions whose damage is associated with hand motor outcome
- Diffusion-weighted imaging (DWI), measuring the white matter microstructural information at the level of fiber bundles by using the fractional anisotropy (FA)
- Functional MRI (fMRI), that measures hemodynamical properties of neural activity, when performing motor task (Task-fMRI), and functional connectivity between cortical and subcortical regions at rest (Resting-state fMRI)

This work mainly used the existing data provided by a randomized controlled stem cell trial (ISIS-HERMES [Intravenous Stem cells after Ischemic Stroke and HEuristic value of multimodal MRI to assess MEsenchymal stem cell therapy in Stroke]), involving healthy participants and patients with subacute ischemic stroke, and a two-year follow-up. A major advantage of this dataset is its longitudinal design with multiple time points of clinical and MRI assessments that enables us to investigate stroke recovery more extensively, which is rarely found in the literature. In addition, data from other cohorts (IRMAS [Récupération après un Accident Ischémique Cérébrale: Mécanismes et Prédiction en IRM], and RESSTORE [REgenerative Stem cell therapy for STroke in Europe]) were used in this work, according to the issue that was explored (external validation and machine learning approaches).

This work includes the following chapters:

- Chapter 1 provides thesis background and reviews state-of-the-art of the topic, including stroke, motor systems, and predictive models using MRI neuroimaging.
- Chapter 2 presents the general material and methods, including the design of the three studies, the population used in each study, the clinical and behavioral measurements, the MRI acquisition parameters, and the statistical approach used in the thesis studies.
- Chapter 3 presents the main thesis work, including the published and submitted article, preliminary results, and methodological questions and problems that were encountered and addressed during the studies.
- Chapter 4 summarizes the main findings of each study, discusses the general findings, methodological considerations, clinical implications, and perspectives for future studies, and provides the concluding remarks.

Chapter 1

Literature Review

Chapter contents

1.1	Stroke	6
1.1.1	Definition and global burden	6
1.1.2	Post-stroke hand motor deficits and recovery	7
1.1.3	Ipsilateral hand - Impairment and mechanisms	10
1.2	Motor system	12
1.2.1	Anatomical organization of the motor system	12
1.2.2	Functional organization of the motor system	19
1.2.3	Lateral grasping network in macaque and its putative human homolog	20
1.2.4	Two visual streams theory - a brief history and its development . . .	21
1.3	MRI Neuroimaging modalities and prognostic models in stroke	22
1.3.1	Structural MRI	23
1.3.2	Functional MRI (fMRI)	36
1.3.3	Predictive models of hand motor outcome using multimodal MRI .	43

1.1 Stroke

1.1.1 Definition and global burden

Stroke is defined as a sudden focal neurologic syndrome, specifically the type caused by cerebrovascular disease. (Ropper et al., 2014) The term cerebrovascular disease designates any abnormality of the brain resulting from a pathologic process of the blood vessels, including occlusion of the lumen by embolus or thrombus, rupture of a vessel, altered permeability of the vessel wall, or increased viscosity or other change in the quality of the blood flowing through the cerebral vessels. Based on these pathologies, stroke is classified into two major types: ischemic, blood obstruction to the brain; and hemorrhagic, rupture of weakened blood vessels. Among all stroke cases, more than 85% are ischemic (Benjamin et al., 2018) and therefore will be the focus of the present work. The main stroke risk factors are hypertension, diabetes, tobacco, hyperlipidemia, and arterial fibrillation. Many others risk factors have been identified, such as arteritis, aneurysmal dilatation, hematologic disorders, PFO, arterial dissection, oral contraception, developmental malformation, and many more.

According to the Global Burden of Disease Study 2019 (Feigin et al., 2021), stroke remains the third-leading cause of death and disability combined. Despite the substantial reductions in age-standardized rates, particularly among people older than 70 years, the prevalence, incidence, deaths from stroke, and disability-adjusted life years (DALYs) of ischaemic stroke had increased (by 88%, 95%, 61%, and 57%, respectively) from 1990 to 2019. There are substantial between-country variations, with higher incidence rates in low than in high-income countries, as shown in figure 1.1.

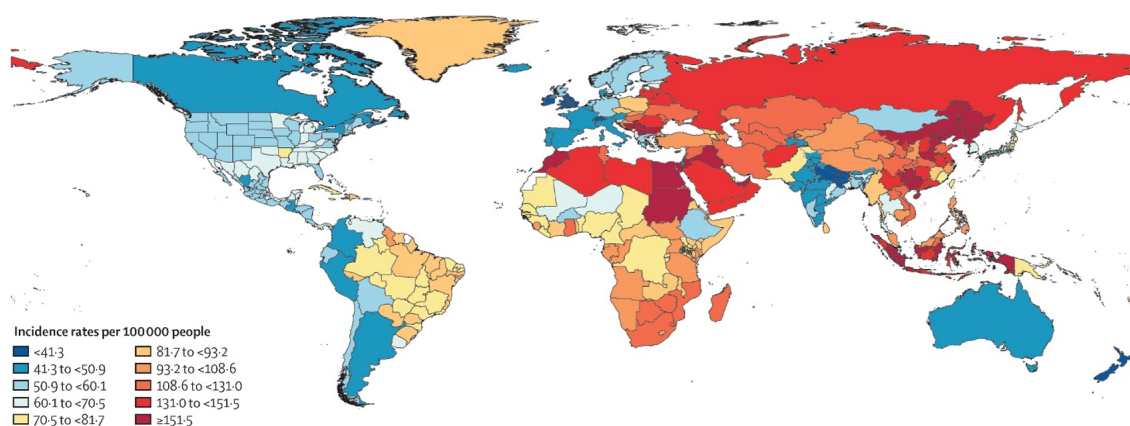


Fig. 1.1 Between-country variations in age-standardized stroke incidence rates per 100000 people, 2019. Adapted from Global Burden of Disease Study 2019 (Feigin et al., 2021)

1.1.2 Post-stroke hand motor deficits and recovery

The neurological deficits caused by stroke are related of the location and extent of the lesion. In ischemic stroke, the symptoms depend on the territory of the occluded artery. In stroke cases affecting middle cerebral artery (MCA) territory (see arterial territory, figure 1.2), accounting for half of all ischemic stroke incidence, the most frequent symptom is unilateral weakness or loss of voluntary movement in the upper limb contralateral to the lesion (Ng et al., 2007; Rathore et al., 2002). In addition, other manifestations may occur in combinations, such as facial paresis, lower-limb weakness, aphasia, agnosia, visual field defects, and so forth (Ropper et al., 2014).

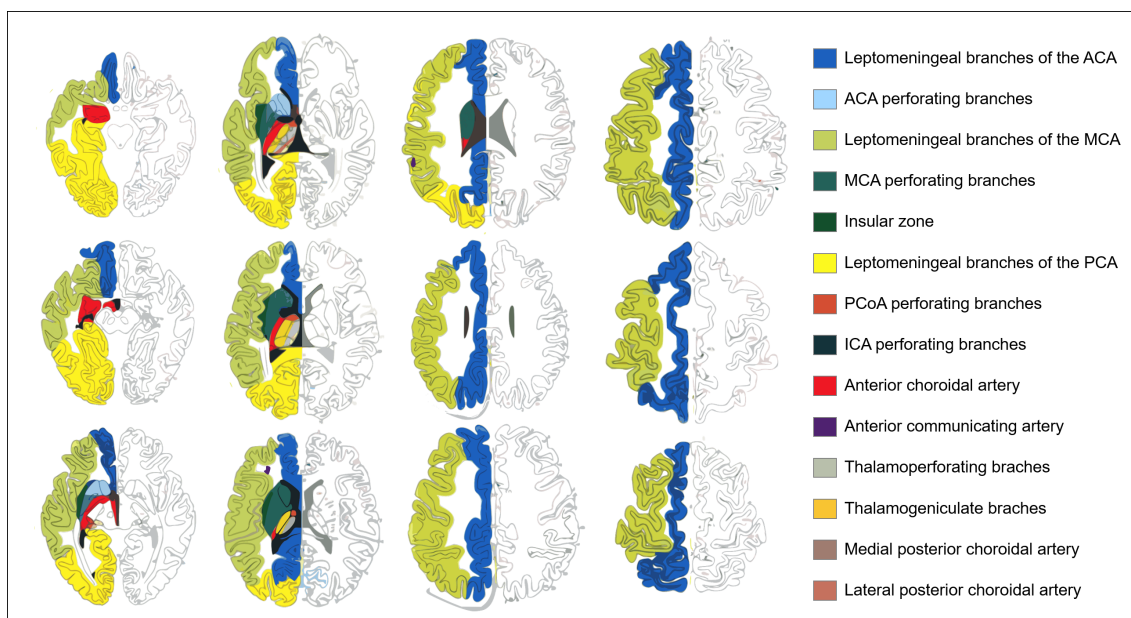


Fig. 1.2 Arterial territory of the human brain (Tatu et al., 1998)

Among the motor clinical manifestations following stroke, one of the most important symptoms is the deficit of the hand. As hand motor function plays an important role in daily life activities to manipulate objects and use tools, such as brushing teeth, writing, cooking, or touching a screen, any type of motor deficit or lack of recovery would be highly disabling. Indeed, it is well reported that the severity of hand impairment is associated with a decrease in quality of life (Franceschini et al., 2010), restricted social participation (Wolfe, 2000), and subjective well-being (Nichols-Larsen et al., 2005). Motor hand deficit is known as a result of damage to the motor cortex located around the hand knob and/or the corticospinal tract (CST) (Kuypers, 2011; Morecraft et al., 2002), frequently featured as impairment of distal movements, such as a decrease of finger strength, loss of dexterity, and abnormal hand flexion synergy (Mawase et al., 2020). In addition, there is a body of evidence from anatomical and

Literature Review

neuroimaging works in both nonhuman primates (Dum and Strick, 2002; Kuypers, 2011) and humans (Carey et al., 2005; Favre et al., 2014; Howells et al., 2018; Manto et al., 2012; Rosso et al., 2013) showing the participation of other brain regions for hand movements, such as the premotor and parietal cortices, thalamus, basal ganglia, cerebellum, and white motor tracts other than the CST such as the superior longitudinal fasciculus (SLF).

An essential feature of stroke is its temporal profile on recovery, with the arrest and then the regression of the neurological deficit in most strokes. In most ischemic strokes, improvement occurs in the first days and then gradually over weeks and months with considerable variations in residual disability (Ropper et al., 2014). The Stroke Roundtable Consortium (Bernhardt et al., 2017) proposed to define four periods of stroke recovery: the first 24 hours as the hyperacute phase, the days 1 to 7 or 8 as the acute phase, the first 3 months as the early sub-acute phase, the months 4 to 6 as the late sub-acute phase, and after six month as the chronic phase. The rationale behind this classification is that recovery-related processes following stroke, such as necrosis, inflammation, neural plasticity, and apoptosis, are time-dependent (Figure 1.3). The generally accepted view is that natural recovery (without any intervention) occurs within first months after stroke, and therefore the chance of recovery is higher in acute than in chronic strokes.

Motor recovery also follows distinct patterns depending on the topography of the deficit. While walking abilities or other motor actions supported by proximal musculature usually recover during the subacute period, hand paresis may persist until the chronic phase of stroke. Moreover, it is generally reported that patients with subcortical strokes tend to have a clinically worse prognosis than cortical strokes (Shelton and Reding, 2001). However, in the context of hand motor recovery, subcortical strokes involving part of the corona radiata and the internal capsule is worse than stroke in the motor cortex. This fact is somewhat explainable, assuming that a lesion in the primary motor cortex could be partially taken over by other cortical areas (either the perilesional cortices, other cortical areas within the sensorimotor network, or mirror areas on the other hemisphere), while a subcortical lesion would damage the output of these cortices, and therefore leaving less room for compensatory process. On the other hand, the effect of lesion volume is still disputed. Weak correlations were reported between stroke lesion volume and global outcome or upper limb motor outcome (Lövgren et al., 1997). Another study, including a larger sample size (n=139), found no relationship between lesion volume and upper limb impairment and motor function (Page et al., 2013).

Measuring motor performance in real-life relevance is a challenging task. A suggestion for standardizing outcome measurements is to apply a unified motor outcome assessment for

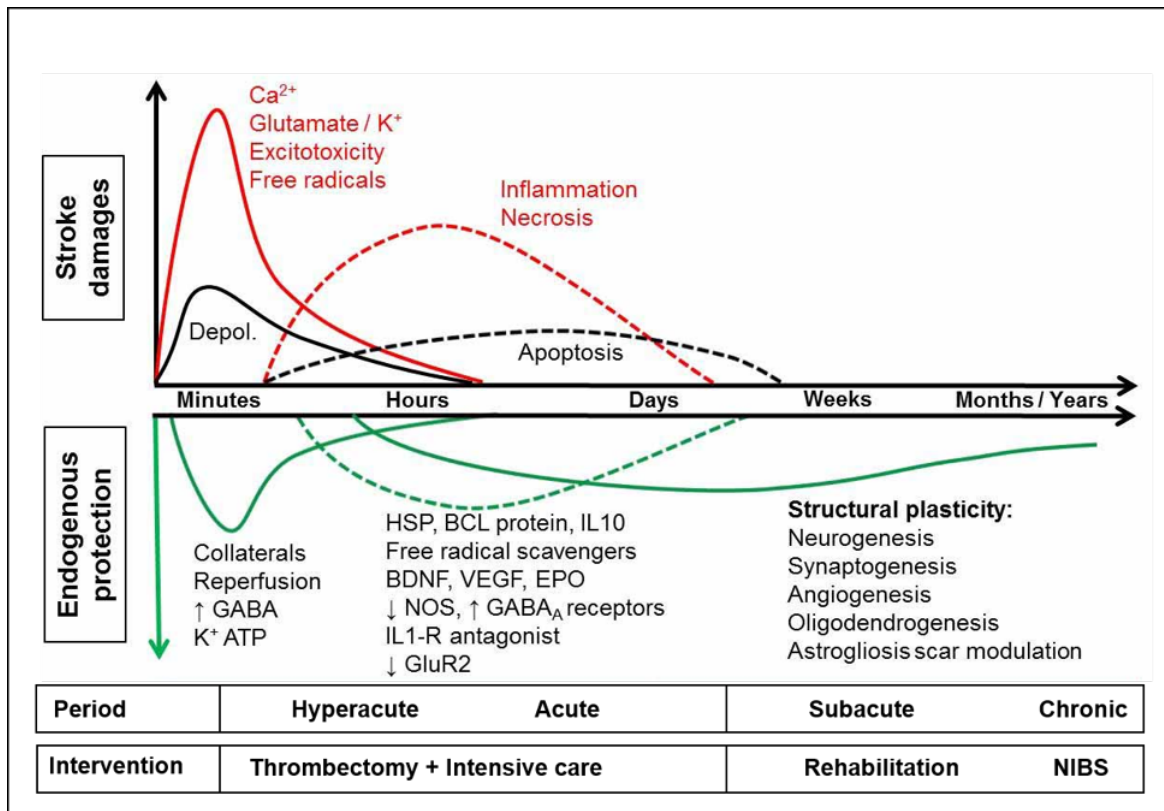


Fig. 1.3 Time course of stroke. BCL: B-cell lymphoma protein; BDNF: brain-derived neurotrophic factor; BP: blood pressure; Depol.: peri-infarct depolarization; EP: endothelial progenitors (CD34+); EPO: erythropoietin; GCSF: granulocyte-colony stimulating factor; GF: growth factors; GluR2: glutamate receptor (subunit 2); HSC: hematopoietic stem cells (CD34+); HSP: heat-shock protein; IL: interleukin; IP3: inositol tri-phosphate; IV: intravenous; MNC: mononuclear cells; MSC: mesenchymal stromal/stem cells; NOS: NO synthase; SRI: serotonin reuptake inhibitors; VEGF: vascular endothelial growth factor. NIBS indicates non-invasive brain stimulation. (Detante et al., 2014)

all patients with stroke. However, the choice of the outcome parameter is highly dependent on the group of patients being investigated: patients with low outcomes are not able to perform high demanding tests, while those with high motor outcome show ceiling effects in less demanding tests (Horn et al., 2016). The Fugl-Meyer Motor Assessment Scale is still predominantly used after stroke to assess motor impairment and recovery, but its items do not provide details on the level of hand motor impairment. Similarly, the motor subscore of Action Research Arm Test (ARAT), Motricity Index (M1), and Wolf Motor Function Test (WMFT) more closely describe overall upper-limb function rather than hand, as their motor subtests require only proximal arm movements. As the neural correlates of the proximal and distal parts of the upper limb are different (Kuypers, 2011), conclusions from studies using upper-limb measurements should not be generalized to hand function.

Different hand abilities can be assessed, such as measuring strength, aiming, pinch grip, and tapping tasks. Among many hand motor task measurements, hand dynamometer is frequently used to assess handgrip strength (Raghavan, 2007) -a pure grasp motor task, and is consistently reported to be impaired to 6 months after stroke (Prados-Román et al., 2021). Recovery of grip strength is an indication of the restored corticospinal tract but does not show a direct association with manual dexterity (Thickbroom et al., 2002). Instead, several quantitative tests are widely used to assess manual dexterity, such as the Purdue pegboard test (PPT), box and block test (BBT), nine-hole peg test (9HPT), and Jebson Taylor hand function test (JHFT). Similar to handgrip strength, manual dexterity was impaired in both acute (Lang et al., 2005) and chronic (Collins et al., 2018) stroke.

Nevertheless, even after accounting for initial clinical scores and stroke characteristics, a large part of explained variance of hand motor outcome remains to be determined. Several biomarkers have been identified which enable a considerable prediction of hand-motor outcome after cerebral damage in the subacute stage after stroke. A robust biomarker would serve several main clinical purposes, from informing patients and caregivers about the course of the disease to determining groups of patients that would benefit from interventions. From a physiological perspective, the understanding of the underlying mechanism of hand motor recovery and functional recruitment of motor resources would help to promote the development and evaluation of new therapies and rehabilitation strategies. The aim of this work is to assess the value of MRI biomarkers in the evaluation of motor recovery of the hand.

1.1.3 Ipsilateral hand - Impairment and mechanisms

Until recently, most stroke studies focused more on the impairment of the affected hand, the one on the side contralateral to the lesion, and to a lesser degree on the ipsilateral hand. This is understandable, given the fact that the performance of the ipsilateral hand is usually assumed as "normal" or "healthy" when compared to that of the affected hand. Indeed, in some assessments, motor impairment is often measured as a relative comparison of the affected side to the ipsilateral side, using the latter as a reference. Moreover, the degree of the sensorimotor deficit in the affected upper limb is a very useful clinical measure as it is consistently reported to be an independent predictor of motor recovery and long-term disability (Katrak et al., 1998; Nijland et al., 2010; Stinear, 2010). However, one limitation of the prognostic use of contralateral limb assessment is the floor effect when dealing with patients with hemiplegia or severe hemiparesis, as they cannot actively move their hand or

fingers and therefore scoring very low on hand motor assessment, and yet some of them manage to show significant sensorimotor recovery.

Meanwhile, a more subtle and variable level of motor impairment is observed in the limb ipsilateral to the lesion. Motor weakness in the ipsilateral hand has been consistently reported (Brodal, 1973; Colebatch and Gandevia, 1989; Jones et al., 1989; Kitsos et al., 2013; Varghese and Winstein, 2019). Ipsilateral hand impairment has been observed at both the acute and chronic phase of stroke for a large variety of sensorimotor tasks (Jones et al., 1989), including dexterity (Cunha et al., 2017; Desrosiers et al., 1996; Noskin et al., 2008; Nowak et al., 2007; Son et al., 2018; Yelnik et al., 1996), reach and grasp movements (Hermsdörfer et al., 1999; Ketcham et al., 2007; Kim et al., 2003; Yarosh et al., 2004), limb segment coordination (Debaere et al., 2001), motor speed (Bustrén et al., 2017; de Groot-Driessen et al., 2006; Prigatano and Wong, 1997), and, in some but not all studies, handgrip force (Colebatch and Gandevia, 1989; Jones et al., 1989; McCrea et al., 2003; Noskin et al., 2008; Prigatano and Wong, 1997; Sunderland et al., 1999).

Interestingly, this ipsilateral hand deficit was reported to be more prominent in severe stroke (Bustrén et al., 2017) and therefore opens up a possibility to provide more continuous and precise measures of stroke deficit and a surrogate clinical biomarker of motor deficit and recovery, particularly when the contralesional hand deficit cannot be assessed. A subacute stroke study suggested that ipsilateral finger-tapping speed predicted functional disability at 12 weeks of follow-up (de Groot-Driessen et al., 2006). However, a large part of the patients had bilateral, non-documented, or no stroke lesions, questioning the validity of the measures. A more recent study found no correlations between ipsilateral hand impairment assessed with dexterity and kinematics measures three weeks following stroke and the Barthel Index measured at three months (Metrot et al., 2013).

From patophysiological perspective, several underlying mechanisms have been postulated to account for ipsilateral hand deficits after unilateral stroke, but no consensus was reached. Since ipsilateral hand deficit is defined by the impairment of tests assessing sensorimotor functions, a first theory implicated the involvement of the sensorimotor system, whether directly by ipsilesional uncrossed corticospinal pathways (Ziemann et al., 1999) or through interhemispheric transcallosal fibers (Jung et al., 2002; Kitsos et al., 2013). Another mechanism relies on posterior parietal cortex damage responsible for altered bilateral motor control (Jones et al., 1989). Also, neuropsychological deficits such as apraxia and neglect were demonstrated to alter ipsilateral hand performance, particularly in complex tasks requiring cognitive functions. (Chestnut and Haaland, 2008; Sunderland et al., 1999; Varghese and Winstein, 2019; Wetter et al., 2005)

In this thesis, alongside the assessment of the affected hand, some works will be dedicated to assessing the ipsilateral hand, both from clinical and neuroimaging perspectives. More specifically, its frequency, its impact on stroke global outcome, and the possible explanatory mechanisms.

1.2 Motor system

The process of motor recovery from stroke can be seen as a motor relearning of skills with a damaged brain. With this notion, the brain areas mainly involved in motor recovery, which will then be the basis of the choice of the regions of interest (ROIs) and white matter tracts included in the following neuroimaging analysis, would be those that in a normal brain is involved in performing motor actions, and in learning the motor skills. The following part briefly describes the anatomical and functional organization of the motor system, together with the networks related to hand motor performance, including the lateral grasping network, and the two visual streams.

1.2.1 Anatomical organization of the motor system

Primary sensorimotor cortex (SM1)

Primary motor cortex (M1)

The primary motor cortex, or M1, or Brodmann area 4 (BA4), is located on the precentral gyrus and is in general cytoarchitecture characterized by few granule cells in layer IV and a high density of very large pyramidal cells (Betz cells) in layer V. M1 is organized topographically, in the way that hand and face area represents a very large area of BA4 compared to the rest of the body.

In both human (Geyer et al., 1996) and nonhuman primates (He et al., 1993), the M1 area can be divided into two subregions. In the human brain, M1-4a and M1-4p differ in terms of cyto-, myelo- and chemoarchitecture: M1-4a is lying in the rostral part of M1 located caudally to the dorsal pre-motor cortex, and M1-4p is the caudal part lying in the depth of the central sulcus next to SI-3a (Geyer et al., 1996). Rathelot et al. (Rathelot and Strick, 2009) showed a differential distribution of the cortico-motoneuronal cells for M1-4a and M1-4p in the macaque brain, resulting in a new view of M1 organization, with monosynaptic connections from M1-4a to interneurons in the intermediate zone of the spinal cord, and monosynaptic connections from M1-4p directly to motoneurons in the ventral horn of the spinal cord. Monosynaptic input from the cerebral cortex to motoneurons is a

relatively new phylogenetic feature (Kuypers et al., 2013), providing the ability to produce independent movements of the fingers and thus skilled movements such as precise grasp and tool manipulation. As a result, M1-4p is considered the new M1, as compared to the phylogenetically older M1-4a, which is associated with less complex motor patterns (Rathelot and Strick, 2009).

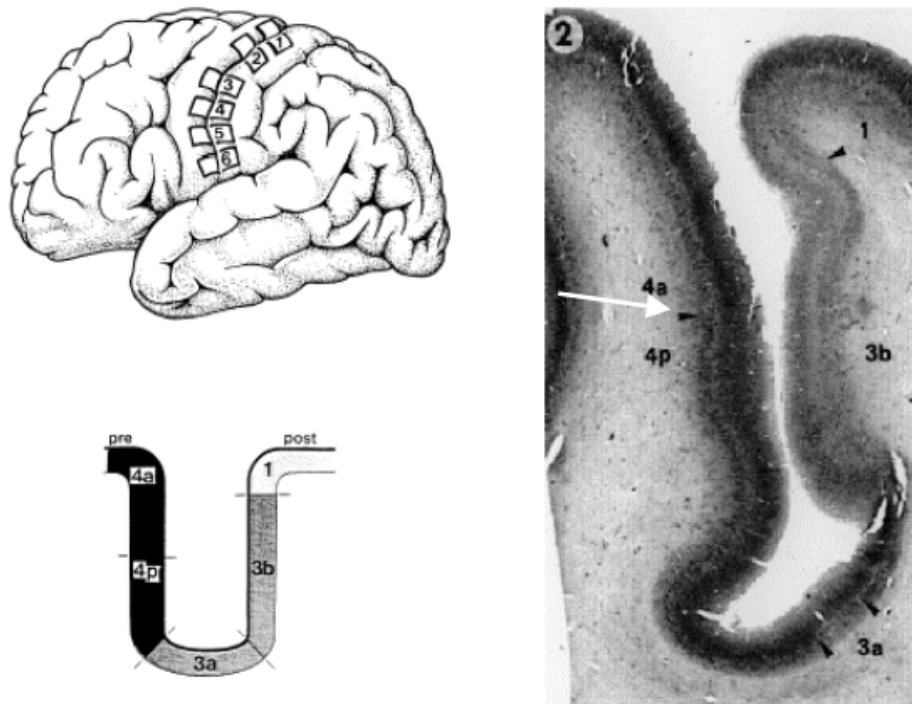


Fig. 1.4 A section through the central sulcus showing subregions of the primary motor cortex, 4a, and 4p (right). The primary somatosensory cortex (areas 1, 3a, 3b) is located in the posterior bank, while the primary motor cortex (areas 4a and 4p) is located in the anterior bank. The boundary between the two subregions is indicated by the white arrow. The lateral brain view (top left) shows levels at which sections were taken (section marked 2), and a diagram (bottom left) represents each subregion in a schematic view. Figures were taken from Hilbig et al. (2001)

In humans, the functional role of M1-4a and M1-4p in human studies remains debated. On one hand, an fMRI study in healthy participants has observed a functional dissociation between M1-4a and M1-4p, with higher fMRI activity related to a flexion-extension task of the fingers in M1-4a than in M1-4p, while the reverse was observed for a sequential finger tapping requiring to move the fingers independently (Jaillard et al., 2005). Similar dissociations were also found in other stroke studies. The anatomofunctional subdivision of the M1 hand area has been related to subregions subserving different roles in motor control with M1-4p recruited by tasks engaging cognitive (Sharma et al., 2008), attentional

Literature Review

(Binkofski et al., 2002), or distal components (Viganò et al., 2019). In contrast, a meta-analysis showed that M1-4a activity was related to precision (versus force) handgrip and M1-4p was related to dynamic (versus static) handgrip (King et al., 2014).

The hypotheses of the works in this thesis with regard to this topic were based on the assumption that M1-4p may be the output of precise grip tasks requiring independent finger movements, while M1-4a would drive simple motor tasks without independent finger movements.

Primary somatosensory cortex (S1)

The primary somatosensory cortex, S1 (areas 3a, 3b, 1, and 2), is located in the postcentral gyrus. It contributes to purposive hand movements in conjunction with M1 (Gemba and Sasaki, 1984; Sasaki and Gemba, 1984). In order to perform hand motor action, especially if it includes manipulating an object, real-time somatosensory information about the position and movement of the hand and perception about the form of an object (independently from visual and auditory input) from a tactile sensation are required (Okuda et al., 1995). Detailed spatial location of sensory and motor areas is provided in figure 1.5.

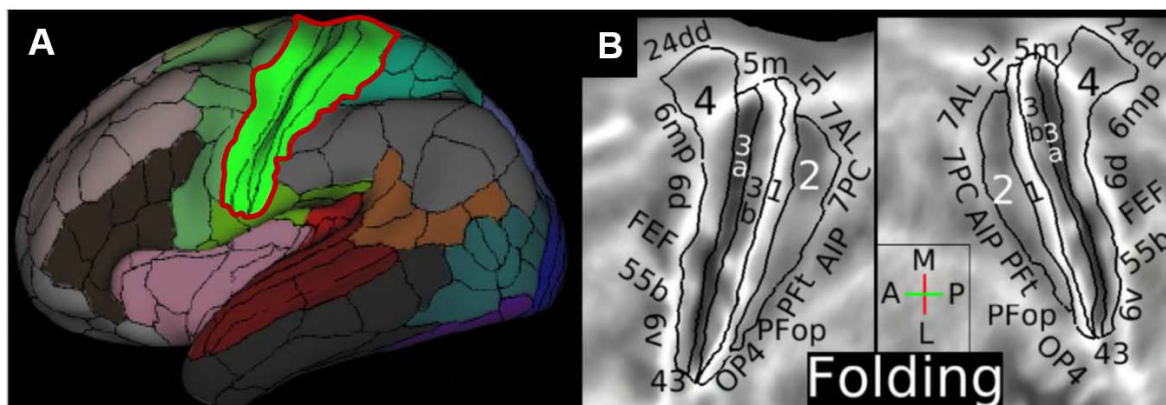


Fig. 1.5 Somatosensory and motor cortex. A. HCP Atlas, somatosensory and motor cortex regions are outlined in red. B. Detailed spatial location of early sensory (areas 1, 2, 3a, and 3b) and motor (area 4) areas with the neighboring areas on a folding map. Figures were taken from Glasser et al. (2016).

Premotor Cortex (PMC, BA6)

The premotor cortex is located anterior to the M1 and is responsible for several aspects of motor control. It is generally divided into two main regions: The medial and lateral parts, both of which send projections to M1 and have outputs through the pyramidal tract (Dum

and Strick, 1991; He et al., 1993; Muakkassa and Strick, 1979). Detailed spatial location of premotor region is provided in figure 1.6.

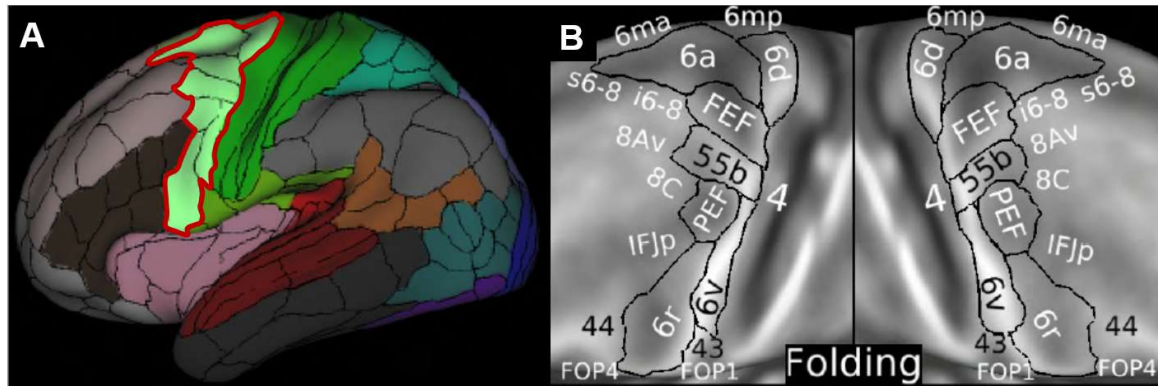


Fig. 1.6 Premotor cortex (PMC). A. HCP Atlas, Premotor areas are outlined in red. B. Detailed spatial location of 6 premotor areas plus area 55b, with neighboring areas (including primary motor cortex, area 4), on a folding map. PMC includes the medial PMC (6ma and 6mp), and lateral PMC (6v and 6d). Figures were taken from Glasser et al. (2016).

Medial PMC

The medial PMC is located on the midline of the hemisphere (medial side of the PMC) just anterior to the M1 and further subdivided into the supplementary motor area (SMA)-proper (6mp), pre-SMA (6ma), cingulate motor area (CMA). SMA and pre-SMA are located on the medial aspect of the brain, in the dorsomedial frontal cortex, just anterior to the leg representation of M1 (Picard and Strick, 1996). The term "pre-SMA" was introduced in 1992 to distinguish this more anterior region from the SMA proper because it has lower electrical excitability (Matsuzaka et al., 1992). In fact, anatomical studies have shown that the SMA comprises around 10% of all corticospinal cells, suggesting that SMA has direct connections to motor neurons, while pre-SMA has only sparse projection to the corticospinal system (Dum and Strick, 1991). As a main part of the medial premotor cortex, SMA is involved in higher-level processing, *i.e.*, planning and programming of voluntary movement, more specifically, self-initiated movements (relative to externally triggered movements) (Goldberg, 1985; Picard and Strick, 1996). It is also involved in complex sequences of movements, coordinating bilateral movements, and motor learning (Tanji and Shima, 1994).

Lateral PMC

The lateral part of the premotor cortex (often notated as PMC) is further divided into the ventrolateral part (vPMC, 6v) and dorsolateral part (dPMC, 6d). The vPMC is often associated with hand motor movements, in particular grasping and manipulation of objects

Literature Review

(Davare et al., 2006), while dPMC is associated with reaching and action selection (Lee and van Donkelaar, 2006) Some studies claim that vPMC is the human homolog for area F5 in macaque (Ferri et al., 2015) and therefore is part of the putative human mirror neuron system. Similarly, there is evidence for the role of the dPMC in imitation (de C Hamilton, 2015), or more specifically, goal-directed action imitation (Koski et al., 2002).

Subcortical motor regions

The two most important subcortical motor regions that are closely related to the motor cortex are the basal ganglia and the cerebellum. These structures are often called the extrapyramidal system to separate them from the pyramidal corticospinal system.

Cerebellum

The cerebellum is located at the back of the brain, inferior to the occipital and temporal lobes. It is comprised of 10 lobules, grouped as the anterior (lobules I-V), posterior(lobules VI through IX), and the flocculonodular (lobule X) lobe. The cerebellum receives afferent inputs from subcortical regions in the spinal cord and brainstem, conveying information for the control of reflexes involved in posture and eye position during head movements, and also from the sensorimotor cortical network. Output from the cerebellum terminates mostly in the red nucleus in the midbrain and the ventral lateral nucleus (VL) of the thalamus. In turn, this thalamic nucleus projects fibers to several motor cortices, building a close loop between the cerebellum and cortex.

The cerebellum has traditionally been viewed as a motor control structure, although research on cerebellar functions in the last decades has expanded its role both as a motor organ and as a higher-order cognitive function. In the context of hand motor control, the cerebellum plays a major role in the predictive timing and coordination of isometric grip forces when grasping and handling objects in the environment. (Manto et al., 2012) A handheld dynamometer, one main tool that is used in several parts of this thesis work to measure hand motor outcome after stroke, involves a participant squeezing the dynamometer with maximum isometric effort. This task involves motor control that relies on prediction and sensory feedback (Wolpert and Flanagan, 2001).

Basal ganglia and thalamus

The basal ganglia is a group of paired subcortical nuclei, including the caudate, lentiform, subthalamic, and accumbens nuclei, and the substantia nigra. The lentiform nucleus is further composed of the putamen and the globus pallidus. Basal ganglia can be divided into two

components, the dorsal striatum (caudate and putamen) and the ventral striatum. The dorsal striatum is associated with a variety of functions, which include motor control, procedural learning, and habit learning. The thalamus, on the other hand, is a part of the diencephalon that provides a key relay for sensorimotor information. The input and output of the basal ganglia and thalamus and their association with other motor areas will be detailed in the following sections (see chapter 1.2.2)

White matter tracts

Anatomical tract-tracing studies in nonhuman primates have evidenced the functional relevance of white matter tracts engaged in sensorimotor control (Schmahmann and Pandya, 2006). Motor control engages the descending motor pathways, including the corticospinal tract (CST) (Lemon, 1997) and, to a lesser extent, the corticoreticulospinal pathway (CRP) (Kuypers, 2011; Lemon, 2008; Riddle et al., 2009; Zaaïmi et al., 2012), the middle segments of the corpus callosum (CC3 and CC4), providing connections between the two sensorimotor cortices, the superior longitudinal fasciculus (SLF) for goal-directed actions along with visuomotor processing and grasping (Schmahmann and Pandya, 2006), and the cerebellar peduncles (Canedo, 1997; Kelly and Strick, 2003; Manto et al., 2012). A difference between neural correlates of the hand and upper limb is that the upper limb is innervated by multiple tracts, including the CST, the CRP, and the vestibulospinal tract (VST) (Markham, 1987), while muscles of the hand and finger are predominately innervated by only the CST.

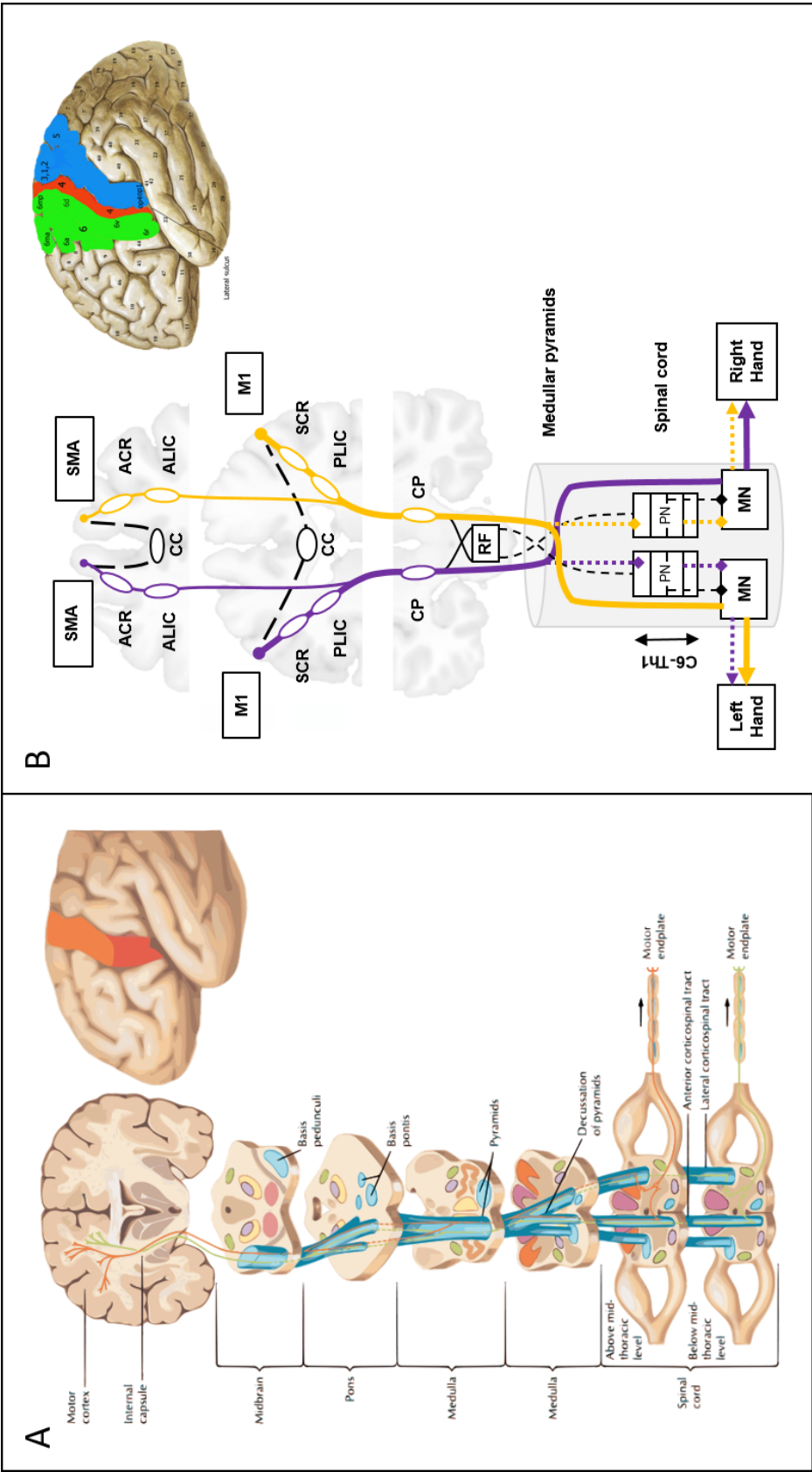


Fig. 1.7 A. Classical representation of the corticospinal tract (CST), descend via the posterior limb of the internal capsule, branch upon entering the basis pontis, rejoin to enter pyramids of the medulla, some cross median plane forming lateral CST while some continue ipsilaterally to lateral CST, form synapses at the spinal level. Adapted from (Hansen et al., 2002). B. Detailed schematic representation of CST and its cortical origins (CST includes fibers not only from the primary motor cortex but also from the somatosensory cortex (BA1,2,3), and superior parietal lobule (BA5), and related white matter tracts leading to the hand. M1: primary motor cortex, SMA: supplementary motor area, RF: reticular formation, MN: motor neurons, ACR/SCR: Anterior/Posterior limb of the internal capsule, ALIC/PLIC: Anterior/Posterior limb of the internal capsule, CP: Cerebral peduncle, PN: Proprioceptive neurons

Additional tracts include the anterior corona radiata (ACR), anterior limb of the internal capsule (ALIC), and corpus callosum genu (genu-CC), carrying descending fibers from the SMA, anterior cingulate motor areas and prefrontal and orbitofrontal cortices (Fries et al., 1993; Morecraft et al., 2002; Schmahmann and Pandya, 2006), and orbito- and pre-frontal projections to the motor areas providing emotional, motivational and cognitive components of motor function (Morecraft et al., 2002) through the cingulate fasciculus (Yeterian et al., 2012). A schematic representation of these white matter tracts is provided in figure 1.7.

1.2.2 Functional organization of the motor system

An organization of the motor system can be viewed in a simplified diagram of the motor system provided in Figure 1.9.

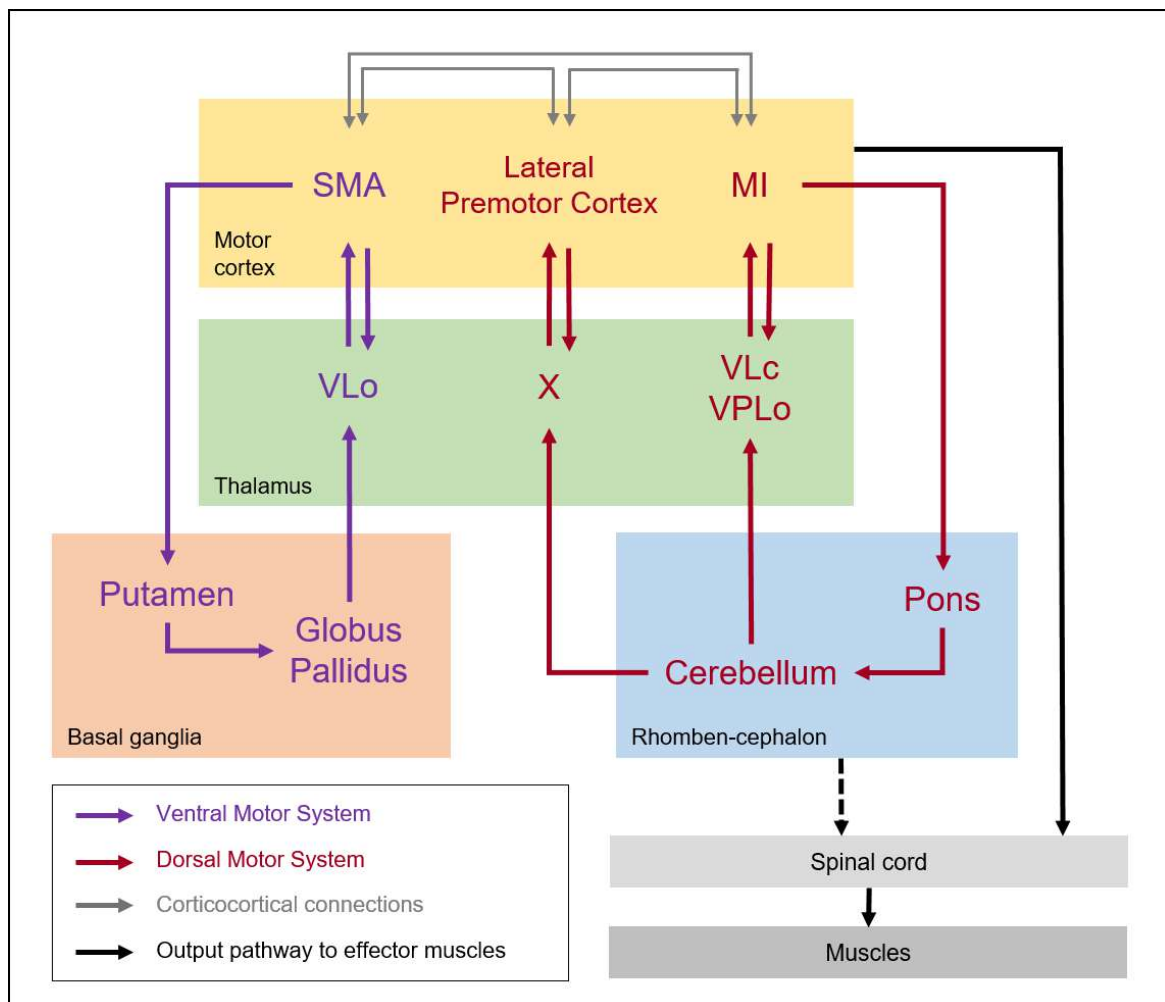


Fig. 1.8 Functional organization of the motor system. Adapted from(Doyon et al., 2003)

As seen above, there is a variety of descending pathways originating from the cerebral cortex that could convey information into the final common pathway to the effector muscles. These pathways include the corticospinal path and other paths involving the subcortical areas (the cerebellum and the basal ganglia). Despite not being involved in the main pathway, these are important components of the motor system, as not only do they have descending inputs into the brainstem, but also, they are part of closed loops from and to the cerebral cortex. It is also important to note that both closed loops pass through different thalamic regions toward the cerebral cortex. More specifically, the cortico-striato-thalamo-cortical loop (ventral motor system), and the cortico-cerebello-thalamo-cortical loop (dorsal motor system), together with interconnectivity between the major cortical structures (M1, SMA, PMC), involved in motor learning and motor adaptation.

1.2.3 Lateral grasping network in macaque and its putative human homolog

Effortless human hand movement, especially when interacting with different objects in different ways and for different purposes, has been a product of highly evolved neural mechanisms involving other areas in the parietal, temporal, and frontal areas in conjunction with those described above, called the lateral grasping network. In this context, most of the studies were carried out in non-human primates. However, it is largely agreed that the monkey and human brains share a common anatomical and functional organization of cortical areas. The following paragraph summarizes the areas involved in the lateral grasping network in the macaque and its putative human homolog, extracted from a detailed review article of Borra et al. (2017).

First, area F5 in the macaque is a major hub of the lateral grasping network, with the subdivision F5p being the hand-related part. It is involved in putting hand motor acts into action once selected and is associated with the dorsal part of human vPMC and the caudal part of BA44. Macaque area AIP, hosting neurons active during the execution of object-oriented hand actions, is homologous to the rostral part of the lateral bank of the intraparietal sulcus (AIPS). Area PFt has been considered a putative homolog of the macaque area PF/PFG involved in fine control of object grasping and manipulation. PV and SII regions in the macaque play a role in somatomotor transformations for object-oriented hand actions and for haptic processing of object shape and is a clear putative homolog of OP1 and OP4, respectively, in human. The lateral occipital complex (LOC) in the human is considered with the neighboring fusiform gyrus as the putative homolog of inferotemporal cortex in macaque,

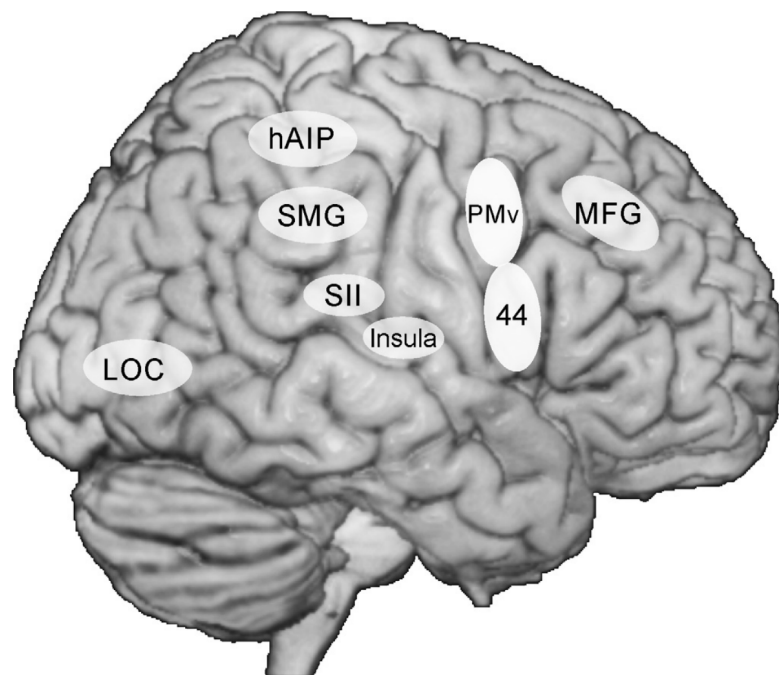


Fig. 1.9 Possible human counterparts of the nodes of the macaque lateral grasping network (Borra et al., 2017)

necessary for fast generation of new motor plans based on spatial and pictorial cues, and activates when grasping requires the processing of volumetric information. Regarding the prefrontal nodes of the lateral grasping network, there is clear evidence for the involvement of the human middle frontal gyrus (MFG) as the putative homolog of ventral area 46 in macaques. Lastly, the dorsoventral part of the insula is a human homolog of the macaque insula, activated in the execution of object-oriented hand actions performed (or imagined) with a vitality form (either gently or rudely).

1.2.4 Two visual streams theory - a brief history and its development

The influence of visual input in hand motor actions was formulated 40 years ago. It was Ungerleider and Mishkin, in 1982, who came up with the notion that the perception of the quality ("what") and space ("where") of an object is processed in the inferior temporal (ventral stream) and posterior parietal cortex (dorsal stream), respectively. (Mishkin and Ungerleider, 1982) This theory was mainly based on electrophysiological, anatomical, and behavioral studies. In 1992, Goodale and Milner challenged this idea and proposed an alternative perspective, placing less emphasis on input distinctions and taking more into account output requirements. (Goodale and Milner, 1992) Based on behavioral data in

humans, they proposed that the two streams were more about "what" versus "how" instead of "what" versus "where".

Despite the different perspectives between the two in terms of the detailed role of the two streams, both models proposed that the dorsal visuomotor stream is engaged in motor actions, either to process the spatial location of the object or to implement hand action and online control of the movements. According to this model, the dorsal stream projects from the visual areas to the posterior parietal cortex (SPL and IPS). From here, the information from visual areas is sent to the PMC and SMI.

This model was later developed more by Rizzolatti and Matelli (Rizzolatti and Matelli, 2003), supported by several other studies (Cavina-Pratesi et al., 2018, 2010; Culham et al., 2006), positing that the dorsal visual stream is further divided into two substreams: (1) the dorsomedial stream, circuits linking superior parieto-occipital cortex (SPOC), and SPL with dPMC, implementing the reach processing, and (2) the dorsolateral stream, connecting aIPS and IPL with the vPMC, for grasping. Putting this theory into perspective, it is expected that motor tasks requiring visual control, such as reaching an object or a target, would engage visuomotor connectivity. However, whether this is also the case for simple motor grasping tasks remains to be investigated. If it is, the type of visuomotor stream (either dorsomedial, dorsolateral, ventral, all, or none) that is involved in motor tasks would be further explored.

1.3 MRI Neuroimaging modalities and prognostic models in stroke

Among all neuroimaging modalities, magnetic resonance imaging (MRI) is a noninvasive tool providing high spatial resolution. In recent years, the neuroimaging field has developed very rapidly and become a powerful tool for both clinical and research use, with many new techniques providing more detailed organization of the brain. Brain MRI is often divided into structural and functional MRI. After the development of functional MRI (fMRI) in 1990 (Ogawa and Lee, 1990; Ogawa et al., 1990a,b), the definition of structural MRI has shifted to refer to those that are "not functional" MRI.

In the context of stroke, neurological deficits result not only from focal damage to cortical areas and white matter tracts at the site of the stroke but also from subsequent effects on remote areas that are directly or indirectly, structurally or functionally, connected to the primary lesion (Carrera and Tononi, 2014; Cheng et al., 2014; Seitz et al., 1998). Moreover, a more recent view of neuroscience has shifted from the traditional brain localization theory

1.3 MRI Neuroimaging modalities and prognostic models in stroke

- that any given behavior or process is carried out by some specifically dedicated brain structure - towards a network-based framework in which neurological function depends on the balanced orchestration of activity in multiple interconnected populations of neurons (Fornito and Bullmore, 2015; Griffa et al., 2013). The exploration of brain plasticity, in terms of structural and functional organizational changes after stroke, and more specifically, its association with hand motor recovery, is still relatively scarce and is mostly provided by studies with small sample sizes.

Although this thesis does not cover all of the MRI modalities currently used in MRI stroke research, several MRI modalities will be explored, including Surface-based morphometry (SBM), Voxel-based lesion-symptom mapping (VLSM), Diffusion MRI (dMRI), resting state fMRI, and task fMRI.

1.3.1 Structural MRI

Surface-based morphometry (SBM)

Basic principles

Surface-based morphometry is a brain morphometric technique used to construct and analyze brain structural properties at the level of the cortical surface level. As such, it differs from voxel-based morphometric approaches, which analyze image properties at the level of voxels. SBM metrics mainly include the cortical thickness, gyrification index, fractal dimension, and sulcal depth. Among these SBM metrics, cortical thickness has been widely used for the assessment of subtle cortical changes in the human brain and has been shown to be highly reliable (Han et al., 2006). As the name implies, cortical thickness is a measure of the width of the gray matter: the distance between the white matter-gray matter surface and the gray matter-cerebrospinal fluid surface (see figure 1.10) (Carey et al., 2013; Fischl and Dale, 2000) .

One of the advantages of any SBM metrics is that it can be calculated from T1-weighted MRI, a sequence that is routinely used in clinical settings, using automated freely available software like CAT12 (Gaser et al., 2022) or FreeSurfer (<https://surfer.nmr.mgh.harvard.edu>). Since its development, cortical thickness has been subject to studies of a wide range of neurological and psychiatric disorders, in which cortical thinning is reported to be associated with the diagnosis or progression of Alzheimer's Disease (Shaw et al., 2016), Huntington's disease (Rosas et al., 2002), Parkinson's Disease (Zarei et al., 2013), multiple sclerosis (Sailer et al., 2003), depression (Li et al., 2020), and schizophrenia (Kuperberg et al., 2003). In this work, most of the analysis will be focused on cortical thickness, among other SBM metrics.

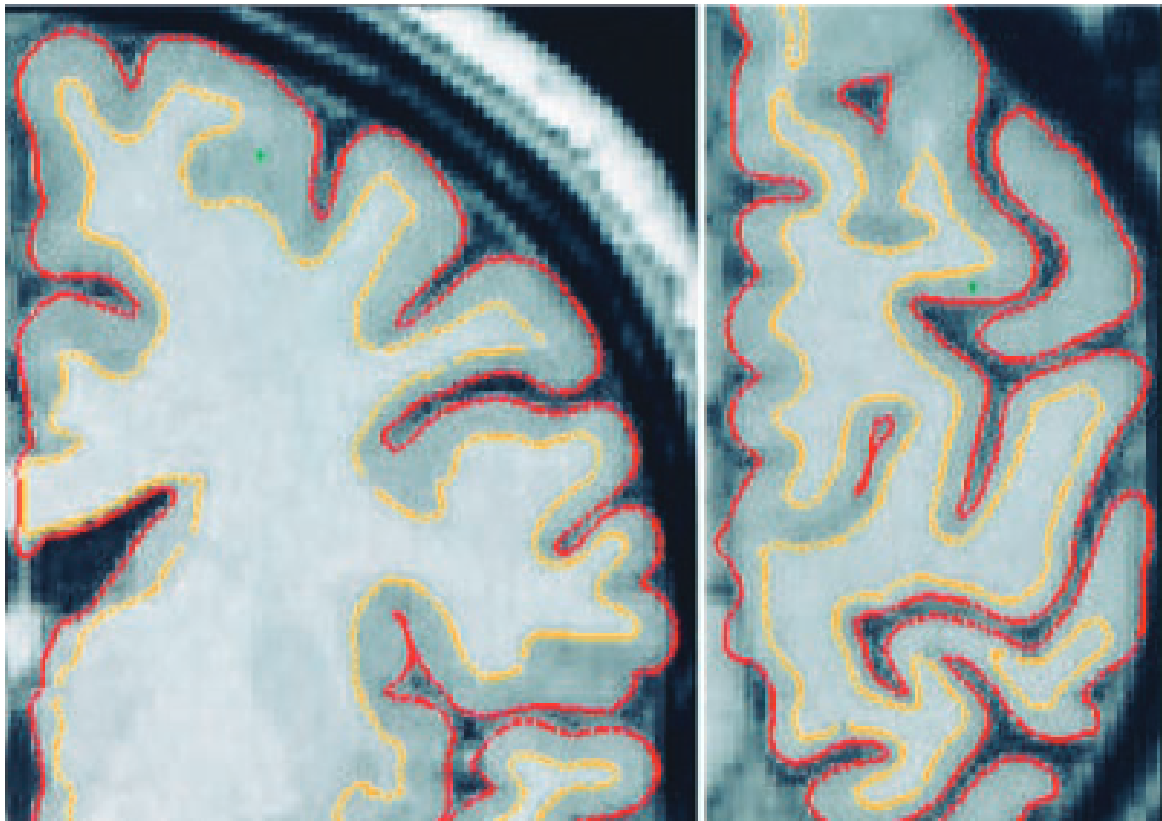


Fig. 1.10 Cortical thickness is defined as the distance between the white matter-gray matter surface (yellow line) and the gray matter-cerebrospinal fluid surface (red line). Image is taken from Fischl and Dale (2000)

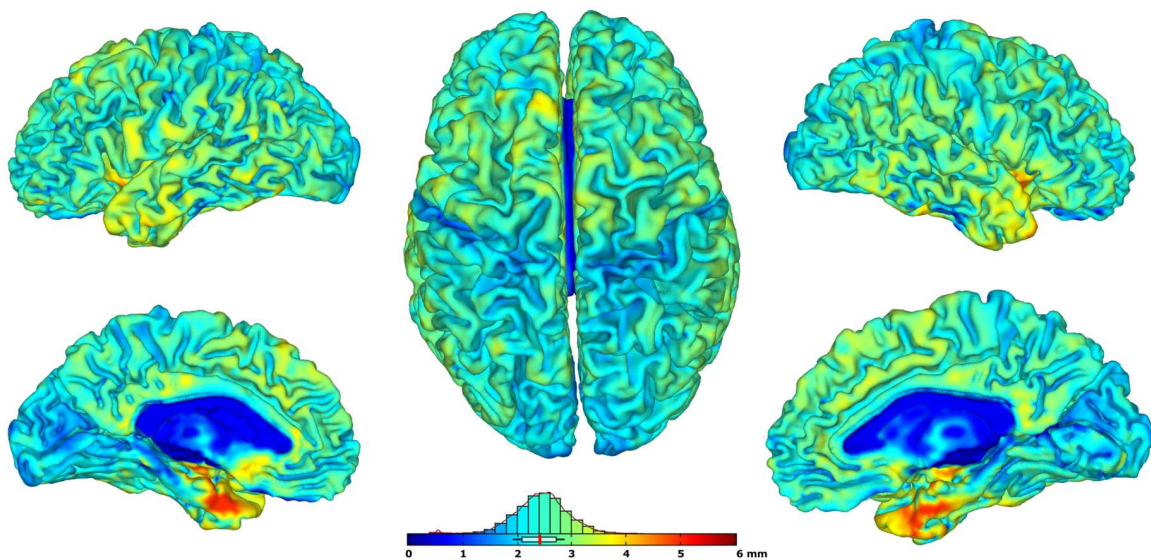


Fig. 1.11 Cortical thickness estimation using CAT12 in one of healthy controls

1.3 MRI Neuroimaging modalities and prognostic models in stroke

Cortical thickness in stroke

In the context of a stroke, there is neuroimaging evidence that structural neural reorganization can occur in brain regions following stroke, both inside and outside of the lesion (Fregni and Pascual-Leone, 2006; Ward et al., 2003). The decrease of cortical thickness in the ipsilesional hemisphere following stroke is well documented in acute (Chen et al., 2021; Duering et al., 2015; Liu et al., 2015a), subacute (Cheng et al., 2015), and chronic (Buetefisch et al., 2018; Jones et al., 2016; Ueda et al., 2019; Zhang et al., 2014) strokes. This cortical thinning is thought to be caused by cortical atrophy due to neuronal loss caused either directly by the lesion or indirectly by disconnection from a damaged region (Carrera and Tononi, 2014; Di Pino et al., 2014). Two different concepts have been long introduced in neurology through clinical, experimental, and imaging studies to explain post-stroke remote changes in the brain. First, diaschisis is a term applied to describe the dysfunction in anatomically separate but functionally related regions of the brain, first described by von Monakow (1914). Another concept is Wallerian degeneration (Waller, 1850), a secondary retrograde degeneration of white matter tracts after ischemic stroke, which, unlike diaschisis, is considered a pure structural phenomenon (van Niftrik et al., 2021). Indeed, Duering et al. (2015) and Cheng et al. (2015) reported degenerative changes in cortical regions that are structurally connected to the infarct regions. Moreover, Chen et al. (2021) and Liu et al. (2020) reported changes in cortical thickness following a brainstem and basal ganglia stroke, respectively. Studies reporting changes in the contralesional hemisphere, often termed "transcallosal diaschisis", however, are inconclusive. When compared to healthy controls, some studies showed an increase, (Brodtmann et al., 2012; Liu et al., 2015a) while some others reported a decrease (Chen et al., 2021), or no significant changes of cortical thickness (Cheng et al., 2015; Zhang et al., 2014). Previous studies reporting cortical thickness in stroke are listed and summarized in table 1.1.

There are challenges and considerations to bear in mind when analyzing the cortical thickness in stroke. First, changes in morphology are affected by other factors, such as the presence of edema and damage to the cortical structure, in which the impact of these factors on the measurements of cortical thickness has not been fully resolved (Carey et al., 2013). Second, is to take into account the effect of age, as patients with stroke tend to be older. Several studies have reported evidence for the effect of age on the cortical thickness, in this case, thinning of the cortical thickness along with older age. (Dotson et al., 2015; Fjell et al., 2009; Hurtz et al., 2014; Lemaitre et al., 2012; Preul et al., 2006; Salat et al., 2004) Of note, most of these studies reported that cortical thinning was prominent in the prefrontal cortex (Dotson et al., 2015; Hurtz et al., 2014; Lemaitre et al., 2012; Salat et al., 2004).

Literature Review

Association with motor clinical scores

Among the 8 identified studies assessing the association between cortical thickness and motor scores after stroke, the majority (n=6) studies reported no association, (Buetefisch et al., 2018; Cheng et al., 2020, 2015; Jones et al., 2016; Liu et al., 2020; Schaechter et al., 2006) and the remaining 2 studies (Liu et al., 2015a; Ueda et al., 2019) reported a positive correlation. In a more recent study, Rojas Albert et al. (2022) also observed a correlation but with stroke global outcome (modified Rankin Scale) instead of specific motor scores. In 4 studies using assessment of motor performance specific to the hand, (Buetefisch et al., 2018; Cheng et al., 2020, 2015; Schaechter et al., 2006) all reported no correlation with the absolute value or change in cortical thickness.

As an important note, most of the cited studies investigating cortical thickness and its association with motor scores were conducted using a relatively small sample size, with $n < 50$ in all and $n < 20$ in half of the studies. Further studies with a larger sample size are necessary to confirm the association between cortical thickness and hand motor outcome following stroke. In addition, very few studies (Chen et al., 2021; Zhang et al., 2008) explored this association using SBM metrics other than cortical thickness, such as fractal dimension or gyrification index.

Voxel-based lesion-symptom mapping (VLSM)

Basic principles

Understanding the relationship between the brain and behavior has been one of the most important quests in neuroscience. For more than 200 years, studies have used several methods, mainly experimental design in an animal model, to derive brain-behavior relationships from lesion-symptom mapping. (Godefroy et al., 1998) Recently, voxel-based lesion-symptom mapping (VLSM) has been developed to use lesion information in a more continuous manner (Baldo and Dronkers, 2007; Rorden et al., 2009). Previously, two types of approaches were used for lesion-symptom mapping: a lesion-defined, and a behavior-defined approach. A lesion-defined approach uses the behavioral performance of a group of patients with a common area of injury (a predefined ROI) compared to that of a control group. However, in contrast to experimental studies where a detailed surgery can be made specific to the area of interest, stroke lesions usually do not impact the area of interest exclusively, and therefore any conclusion should be taken carefully. Similarly, a behavior-defined approach grouped the patients by the presence of specific behavior and then constructed the corresponding lesions. As both approaches categorize the patients either by a lesion or by behavior in a unidimensional way, they risk losing valuable information. VLSM approach, in contrast, use

Table 1.1 Studies reporting cortical thickness in stroke

No	Author (year)	N	Time points	Behavioral metrics	Cortical thickness		Correlation
					Ipsilesional	Contralateral	
1	Brodthmann (2012)	12	acute	-	no change	increase	NA
2	Cheng (2015)	12	subacute	NIHSS, ARAT, FMS, Grip	decrease	no change	no correlation
3	Duering (2015)	32	acute	-	decrease	NA	NA
4	Zhang (2014)	26	chronic	-	decrease	no change	NA
5	Albert (2022)	38	acute	Modified Rankin Scale	NA	NA	positive correlation
6	Liu (2020)	33	acute	FMS	decrease		no correlation
7	Ueda (2019)	25	chronic	WMFT	decrease	NR	positive correlation
8	Schaechter (2006)	9	chronic	FMS, dynamometer, JHFT	increase	increase	no correlation
9	Jones (2016)	17	chronic	WMFT	decrease	NA	no correlation
10	Bueteifisch (2018)	18	chronic	Modified ashworth scale, JHFT, WMFT, MAL	decrease	NA	no correlation
11	Chen (2021)	48	acute	-	decrease	decrease	NA
12	Liu (2015)	22	acute	FMS	decrease	increase	positive correlation
13	Cheng (2020)	18	acute	NIHSS, UE-FMS, grip	decrease	decrease	no correlation

NA: Not applicable, NR: Not reported, NIHSS: National Institute of Health Stroke Scale, ARAT: Action Research Arm Test, FMS: Fugl-Meyer Scale, JHFT: Jebsen Hand Function Test, WMFT: Wolf Motor Function Test, MAL: Motor Activity Log, UE: Upper-extremity

Literature Review

the binarization concept (lesioned or not lesioned) at the level of the voxel, and therefore the resulting behavior-related map is not limited to a specified ROI but could be a subregion of the ROI, a larger ROI, multiple ROI, or any combination of significant voxels that survive thresholding cut-off.

A VLSM approach typically starts from lesion delineation on raw anatomical images and normalization, even though these two steps can be done in reverse (lesion delineation performed in normalized images). After quality control of the image and the mask, lesion overlap can be provided, followed by the VLSM statistical analysis (Figure 1.12). These steps can be done using several freely available software, such as non-parametric mapping (NPM) under MRICron (<https://www.nitrc.org/projects/mricron>), or niistat (<https://www.nitrc.org/projects/niistat/>).

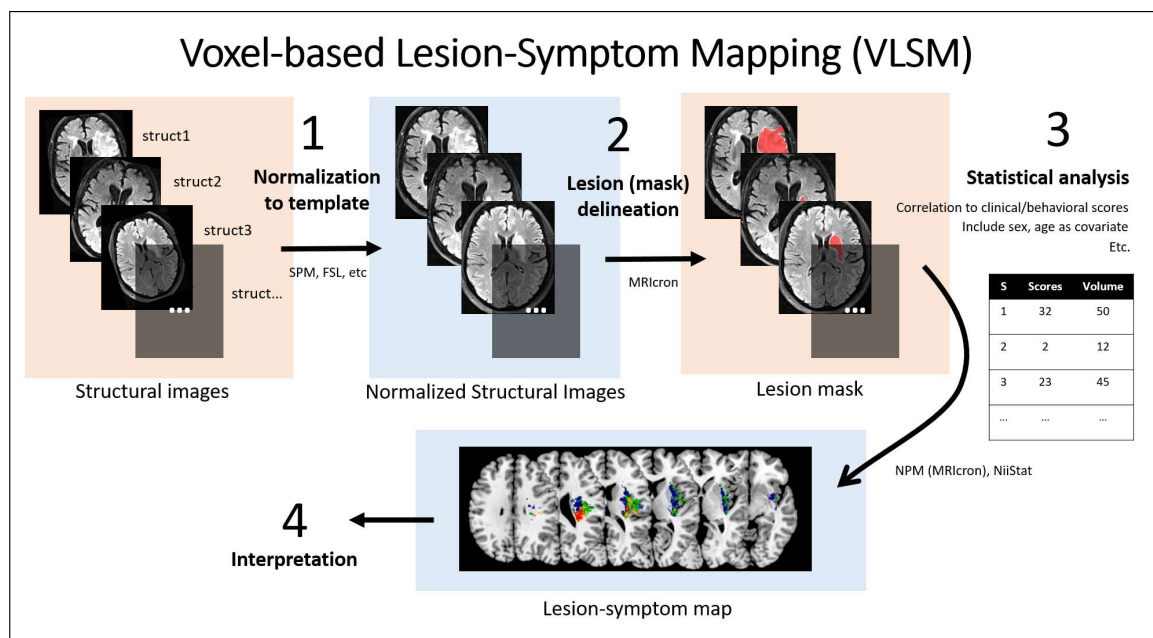


Fig. 1.12 Steps in VLSM analysis. VLSM statistical map was adapted from Meyer et al. (2015)

A major advantage of VLSM analysis compared to other advanced MRI analyses is that it is a conceptually simple yet useful tool to analyze lesion-symptom associations in any voxel of the brain (both grey and white matter or any deep subcortical part). As compared to functional MRI, for example, VLSM provides a better lesion-symptom relationship as fMRI results typically show brain response to damage due to a stroke rather than the representation of the damage itself. On the other hand, using diffusion tensor imaging (DTI), one can estimate several measures of a fiber tract but is limited only to the white matter.

Nevertheless, VLSM has some limitations. First, VLSM reflects a localizationist approach, in which any hypothesis used in VLSM is based on a premise that one symptom

1.3 MRI Neuroimaging modalities and prognostic models in stroke

corresponds to one specific lesion of the brain. In contrast, from a network-based perspective, it is possible that a motor symptom does result from one stroke lesion (for example, damaging the corticospinal tract) or from the combination of lesions in several areas engaged in motor control (for example, basal ganglia and motor and premotor cortex). This is even more frequent in cognitive deficits. As VLSM uses a statistical approach based on the voxel level, the possibility of the latter concept is not taken into account. A second limitation is related to the number of confounding factors that need to be controlled. For example, Rajashekar et al. (2020) found that age, volume, and follow-up time have distinct regional importance and, therefore, that they should be included as covariates when performing VLSM analyses.

VLSM in stroke

VLSM has been used in stroke patients to map several behaviors, such as language impairments (Baldo and Dronkers, 2007; Bates et al., 2003; Borovsky et al., 2007; Geva et al., 2012; Moore et al., 2021; Saygin et al., 2004), cognitive impairments (Molenberghs et al., 2008; Moore et al., 2021; Ploner et al., 2005), somatosensory deficits (Baier et al., 2014; Meyer et al., 2015; Preusser et al., 2015), and motor deficits (Lo et al., 2010; Moon et al., 2016; Plantin et al., 2019; Reynolds et al., 2014; Schoch et al., 2006).

Lesion map associated with motor deficits

Several studies examined motor impairments using VLSM. Motor deficit of the upper limb is reported to be associated with a lesion at the corona radiata (either superior [SCR] or posterior [PCR] part), anterior or posterior limb of the internal capsule (ALIC/PLIC), insula, basal ganglia, cerebellum, and white matter tracts other than the corticospinal tract (CST), such as the superior longitudinal fasciculus (SLF), external capsule (EC), and superior fronto-occipital fasciculus (SFO). (Frenkel-Toledo et al., 2019, 2022, 2020; Schoch et al., 2006) With regards to lesions associated to hand motor outcome, lesions in the corona radiata (Frenkel-Toledo et al., 2019, 2020; Lo et al., 2010; Plantin et al., 2019) and or posterior limb of the internal capsule (Frenkel-Toledo et al., 2019; Park et al., 2016; Schiemanck et al., 2008) are the most cited to correlate with worse outcomes. Taking all these results together, it can be inferred that most motor deficit is associated with lesions at the corona radiata or corticospinal tract (at any level). However, a larger sample size study assessing motor performance at the level of the hand would be necessary to confirm the lesion associated specifically to hand motor deficit.

Table 1.2 Studies reporting the association between lesion location and hand and upper limb motor deficit in stroke

Author (year)	N	Method	Phase	Motor score	Associated brain area(s)
Lo (2010)	41	VLSM	chronic	AMAT, BBT	CR within the CST
Plantin (2019)	61	VLSM	subacute	Neural resistance	White matter below cortical hand knob
Reynolds (2014)	16	VLSM	chronic	TUG, BBS, Gait velocity	Corona radiata, caudate nucleus, and putamen
Schoch (2006)	43	VLSM	acute	ICARS	Paravermal lobule V and VI, vermal lobule IV and V, hemispherical lobule V and VI
Frenkel-Toledo (2019)	130	VLSM	subacute, chronic	FMS, BBT	LHD (subacute and chronic): NS, RHD (subacute): Putamen, SCR (proximal and distal), Insula, EC, SLF, ALIC, Caudate, SFO (proximal), RHD (chronic): Putamen, SCR, Insula, SLF, SCR, EC, PLIC, RLIC and PCR
Frenkel-Toledo (2022)	41	VLSM	subacute	FMS, TSRT	Insula, superior and middle temporal gyri, Rolandic operculum), the CST (in CR and PLIC), IFO, SLF and UF, putamen and pallidum
Feys (2000)	45	LC	subacute, chronic	The Brunnstrom FM test	CR, IC, basal ganglia
Frenkel-Toledo (2020)	77	VLSM	chronic	FM-SAFE	For left stroke, only CST. For right stroke, CST, white matter association tracts, the putamen, and the insular cortex
Schiemanck (2008)	75	LC	chronic	FMS hand score	Internal capsule
Park (2015)	33	MVPA	chronic	ARAT, NHPT, MI, grip	CST

VLSM: Voxel-based lesion-symptom mapping, AMAT: Arm Motor Ability Test, BBT: Box and Block Test, CR: Corona radiata, CST: Corticospinal tract, LHD/RHD: Left/Right hemisphere damage, FMS: Fugl-Meyer Scale, SAFE: Shoulder abduction finger extension, JHFT: Jebsen Hand Function Test, ARAT: Action Research Arm Test, NHPT: Nine-hole Pegboard Test, MI: Motricity Index, MVPA: Multi-voxel pattern analysis, TSRT: Tonic Stretch Reflex Threshold, ICARS: International Cooperative Ataxia Rating Scale

Diffusion MRI

Basic principles

Diffusion MRI (dMRI) is an MRI modality that provides structural information at the level of the white matter microstructure. It provides an estimation of brain fiber structure by using the diffusion properties of water in the brain. The basic principle of dMRI is an adaptation of a conventional spin-echo sequence by adding a pair of dephasing and rephasing gradients in a certain direction in such a way that it is sensitive to capture information about the diffusion of water molecules in the corresponding direction. This is due to the Brownian movement of water molecules between the dephasing and rephasing gradient pulses, leading to imperfect rephasing and thus local signal loss (as opposed to fixed molecules that lead to perfect rephasing). The resulting signal is attenuated in the area where water molecules diffuse along the direction where the diffusion gradient was applied. In this way, the image is sensitized to diffusion and thus called "diffusion-weighted".

In a medium with no physical restriction, water molecules diffusion is isotropic, *i.e.*, diffusion occurs in all directions with the same amount. This random motion, called Brownian motion or passive diffusion, was first observed by Robert Brown (1827) and later formalized by Einstein (1905) in mathematical terms. This technique is currently widely used in neuroscience for the exploration of the white matter of the brain since the water tends to diffuse along the axonal tracts, producing anisotropic water diffusion. This anisotropy, when measured using dMRI, brings quantitative information on the axonal architecture and integrity.

Several models have been developed to represent the diffusion processes within the white matter. First, the estimation of the apparent diffusion coefficient (ADC) can be derived when assuming that the water diffusion follows the Gaussian model and Einstein's equation. The signal loss (the ratio between signal intensities with and without diffusion-encoding gradients) can be represented as:

$$\frac{I_2}{I_1} = \exp(-b \cdot ADC) \quad (1.1)$$

where b , or b -values, is the degree of diffusion weighting, I_1 and I_2 are the signal intensities measured with the lower (typically $b=0$) and higher b -values (typically $b=1000$), respectively, and ADC is the apparent diffusion coefficient (Le Bihan et al., 1986; Stejskal and Tanner, 1965). Based on this equation, the ADC can be estimated with at least two signal measurements with a known difference (b -values), and quantitative maps of ADC can be generated (Le Bihan et al., 1986). In general, ADC represents the magnitude of water diffusion, given

Literature Review

the local microstructure environment. In the case of brain dMRI, the water diffusion inside the brain captured by ADC reflects the complex architecture of intra- and extra-cellular restriction of water molecules, including the axons, cell bodies, glial cells, and capillary walls.

Diffusion-weighted Imaging is currently widely used in clinical settings for the diagnosis of acute ischemic stroke. The ischemic lesion due to cytotoxic edema results in restricted diffusion of water molecules per unit time, leading to decreased ADC (less signal attenuation on ADC maps) and a hyperintense signal on a diffusion-weighted sequence (Moseley et al., 1990). This is particularly useful because this diffusion-related information is not captured by the more conventional scans (T1-, T2-weighted, or even FLAIR) in the first few hours following a stroke, corresponding to the therapeutic window of thrombolytic therapies. In the same period, as the ADC reduction in ischemia was found, it was also observed that the ADC was strongly dependent on the direction of the diffusion-encoding gradients. This fact is illustrated in Figure 1.4, showing the diffusion-weighted images of a (human) brain in which the diffusion-encoding gradient is applied along one of three orthogonal axes.

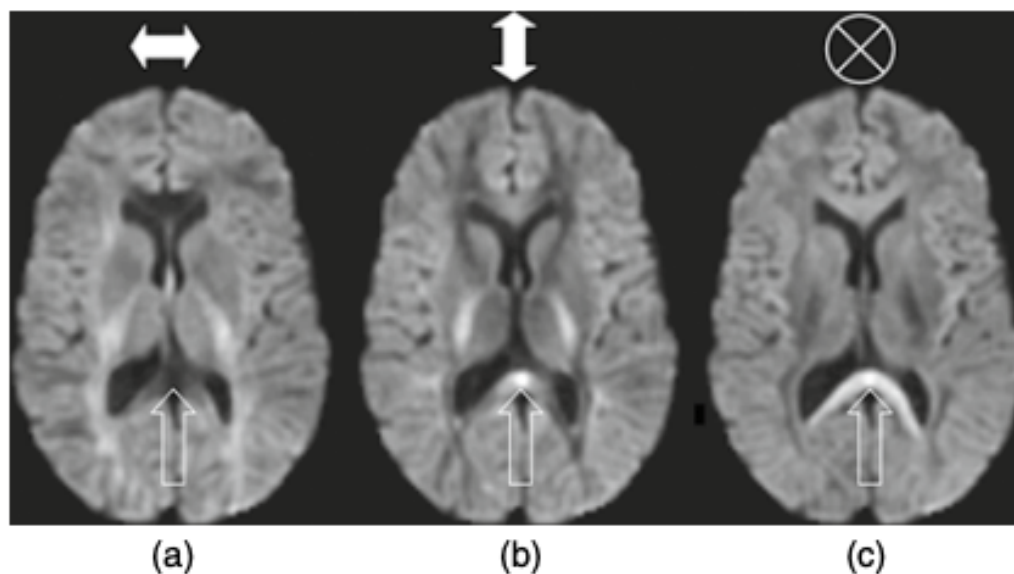


Fig. 1.13 Signal intensity change as an effect of changing the axis of the diffusion-encoding gradients (Johansen-Berg and Behrens, 2009)

While in certain regions of the brain, the diffusion-weighted intensity is relatively similar in all three images (*i.e.*, isotropic diffusion), like the cortical areas, in some areas such as the splenium of the corpus callosum (the one pointed by the arrow in Figure 1.13) the intensity is low (high ADC) only in the direction matching callosal fiber direction (left-right), and high in the other perpendicular directions. Therefore, the anisotropic diffusion (diffusion that

1.3 MRI Neuroimaging modalities and prognostic models in stroke

is not the same in all directions) among brain areas is required to capture the information about the directions of diffusion.

The second yet one of the most used models of dMRI is diffusion tensor imaging (DTI). With the same Gaussian assumption as that of ADC, DTI is useful for characterizing anisotropic diffusion. DTI uses a mathematical and physical interpretation of geometric quantities of tensor to model the rate and preferred direction of water diffusion in three-dimensional space. The displacement of water molecules can be represented in a 3x3 symmetric matrix of numbers:

$$\mathbf{D} = \begin{bmatrix} D_{xx} & D_{xy} & D_{xz} \\ D_{xy} & D_{yy} & D_{yz} \\ D_{xz} & D_{yz} & D_{zz} \end{bmatrix} \quad (1.2)$$

with the diagonal elements of the matrix referring to diffusivities along three orthogonal axes and the other elements to the correlation (not the ADC itself) between diffusivities along the indicated orthogonal axes. As there are six unknown parameters in \mathbf{D} , at least six noncollinear diffusion-encoding directions are acquired in addition to the non-diffusion-weighted ($b=0$) to estimate each element of the diffusion tensor. The detailed computation, derivation, and estimation of the diffusion tensor are beyond the scope of this thesis, and therefore interested readers should refer to Johansen-Berg and Behrens (2009), or even Mattiello et al. (1997) for a full explanation.

From the diffusion matrix, several metrics can be derived. These metrics were computed from the eigenvalues ($\lambda_1, \lambda_2, \lambda_3$; given $\lambda_1 > \lambda_2 > \lambda_3$), which refer to the diffusivities along the principal axes of the diffusion tensor, and the associated eigenvectors ($\mathbf{e}_1, \mathbf{e}_2, \mathbf{e}_3$), which refer to the three orthogonally orientation of the principal axes. First, the axial diffusivity (AD) is the λ_1 , representing the values of the main axis, *i.e.*, the axonal fibers. The radial diffusivity (RD), in contrast, is the average of the remaining eigenvalues (λ_2 and λ_3). As RD is the ADC in the direction perpendicular to the axonal fibers, it is commonly interpreted as a representation of demyelination or glial cell impairment (Basser et al., 1994). Mean diffusivity (MD), a self-explanatory term, is the average between the three eigenvalues and is basically the ADC. Then, the most commonly used metric is the Fractional anisotropy (FA), which represents the fraction of the tensor assigned to the anisotropic diffusion and is calculated by the variance of the eigenvalues normalized by their sum of squares, or:

$$FA = \sqrt{\frac{3}{2} \frac{(\lambda_1 - \langle \lambda \rangle)^2 + (\lambda_2 - \langle \lambda \rangle)^2 + (\lambda_3 - \langle \lambda \rangle)^2}{\lambda_1^2 + \lambda_2^2 + \lambda_3^2}} \quad (1.3)$$

Literature Review

One conceptual limitation of the diffusion tensor model is that it assumes Gaussian diffusion processes, which has been found to be inadequate to accurately represent the true diffusion process in the human brain. Another main limitation is related to the interpretation of DTI that any given voxel represents a single main fiber direction, while in fact, parts of the white matter contain different fibers with different direction crosses. This poses a problem because fractional anisotropy would be used as a term to represent "white matter integrity", while changes in these measures could also reflect fiber coherence. Indeed, it was suggested that between 70% and 90% of the entire white matter in the human brain involved at least two or more crossing fiber populations within the same area. (Behrens et al., 2007; Dell'Acqua et al., 2013; Descoteaux et al., 2009; Jeurissen et al., 2013) In order to solve these problems, higher-order models accounting for the crossing fibers have been used.

Among many recent new techniques addressing the crossing-fibers, (multi-tensor fitting, (Tuch et al., 2002) PAS-MRI, (Jansons and Alexander, 2003) Q-ball imaging(Tuch, 2004), ball, and sticks, (Behrens et al., 2007)), constrained spherical deconvolution (CSD) (Tournier et al., 2007) is one of few that provide a direct estimate of the fiber orientation and are reported to be practically useful in tractography and clinical use. (Dell'Acqua and Tournier, 2019) In general, any spherical deconvolution method assumes that the acquired diffusion signal in each voxel can be modeled as a spherical convolution between the fiber orientation distribution function (fODF, or FOD)-the fraction of total fibers within a sample that are aligned along a given direction-, and the fiber response function (FRF)-signal profile of single fiber orientation. Under this assumption, if the FRF can be estimated, the FOD can be estimated as a deconvolution problem by solving a system of linear equations. CSD applies a non-negativity constraint in the reconstructed FOD. Nevertheless, as the main target of the white matter tract in this thesis is the corticospinal tract, one that is known to have a minimal problem related to crossing fibers, analysis of the diffusion-weighted imaging will be based on diffusion tensor metrics (*i.e.*, the FA). The result regarding other tracts, therefore, would be interpreted more cautiously. Consequently, in the final analysis, using a multimodal approach, the CSD method is used as a step before tract segmentation.

Another step following the estimation of tensors or FOD is tractography, a 3D modeling method to reconstruct the fiber bundles in the brain. Generally, tractography is used to segment each white matter tract by virtually dissecting the streamlines based on combinations of inclusion and exclusion of ROIs based on neuroanatomical a priori. Two common approaches to performing tractography are deterministic and probabilistic. The deterministic model assumes one principal fiber orientation for each voxel (*i.e.*, the primary eigenvector, λ_1 , or peak of FOD), while the probabilistic model uses the probability distribution of

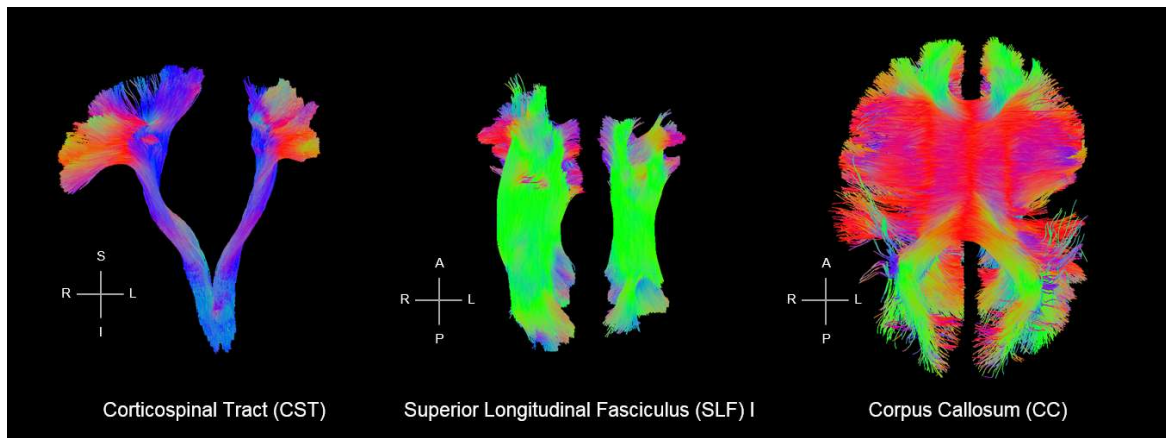


Fig. 1.14 White matter tract segmentation using deep learning approach (TractSeg) in one of ISIS-HERMES patients with left hemispheric stroke, showing the corticospinal tract (CST), superior longitudinal fasciculus (SLF) I, and corpus callosum (CC)

fiber orientation to reconstruct each bundle. Even though the deterministic approach is still predominantly used in the literature, the trends are moving toward the probabilistic approach, as it has been reported to be more accurate in reconstructing fiber bundles in the brain, particularly in white matter tracts known to have multiple fiber crossings. (Tournier et al., 2009) However, a pitfall of the probabilistic approach is that it is more computationally demanding and time-consuming.

dMRI in stroke

Diffusion-weighted imaging has been a very useful tool in the context of stroke diagnosis, as it provides a highly sensitive and specific biomarker within minutes of the stroke onset: a reduction of ADC and hyperintense DWI. On top of that, using DTI-derived metrics, a more detailed evaluation of white matter changes after stroke can be performed. Indeed, there are plenty of studies reporting results of DTI in stroke patients, either to characterize the progression of the ischemia (Bhagat et al., 2006; Harris et al., 2004; Schaefer et al., 2003) or to associate metrics with stroke severity or outcome (Moulton et al., 2019).

A common way to report the FA in the stroke model is as ratios between the ipsilesional and contralesional FA of the same tract ($rFA = \text{ipsiFA}/\text{contraFA}$). This relative measure is useful as it could remove the effect of confounding factors, however, it suffers from some inaccuracy as it assumes that the contralesional white matter is undamaged, while in fact, it is still not yet clear that it is always the case.

Association with motor clinical scores

Literature Review

Using DTI, a convergence result was reported regarding the association between FA and motor recovery in patients scanned at the subacute phase of stroke. A recent meta-analysis of 11 studies using different methods showed strong correlations (Correlation Coefficient=0.82; 95% Confidence Interval-0.66 to 0.90, P value<0.001) between FA measures and upper-limb performances (Kumar et al., 2016). Within the CST, FA estimated from DWI at the subacute phase has been consistently reported to be a predictor of motor outcome, both for the upper limb (Buch et al., 2016; Byblow et al., 2015; Puig et al., 2013, 2010; Radlinska et al., 2010; Yu et al., 2009; Zhang et al., 2014) and for the hand (Imura et al., 2015; Koyama et al., 2014; Schaechter et al., 2009; Song et al., 2012). In addition to the CST, these predictive values were also reported for other white matter tracts, including corticocortical intrahemispheric tracts such as SLF (Koyama and Domen, 2017; Rodríguez-Herreros et al., 2015), interhemispheric tracts (CC) (Li et al., 2015; Sisti et al., 2012; Stewart et al., 2017), and alternate corticofugal pathway (Jang et al., 2013). For a comprehensive review, see (Koch et al., 2016).

Among studies with MRI acquisition done at the acute phase of the stroke, the results were more heterogeneous. Radlinska et al. (2010) reported a positive correlation between rFA and motor outcome at 90 days. In contrast, Doughty et al. (2016) found no correlation between rFA at cerebral peduncle level and upper-limb Fugl-Meyer scores. Similarly, Groisser et al. (2014), who studied the hand motor outcome assessed using the hand dynamometer and Purdue pegboard test, reported that rFA at acute period did not correlate with hand motor outcome at 6 months and that rAD was a better predictor. Indeed, in the hyperacute or acute phase of the stroke, during which the process of early neural changes is still taking place, they argued that FA values would not provide a reliable predictor of outcome and that AD would serve as a better predictor than FA. This is supported by their findings that all of their patients had a decrease in AD in the first week after stroke, whereas the change of RD and FA was still variable (some decreased, but others increased).

While a large number of studies explored the association between DWI metrics and the motor outcome of the paretic hand, no study, as far as we are concerned, explored this relationship for the ipsilateral hand.

1.3.2 Functional MRI (fMRI)

While the anatomical and diffusion MRI modalities provide useful information about the structural features of the brain, they do not bring information about the dynamics of the MRI signal that are associated with neuronal activity. The notion that neuronal activity can be mapped by making use of the reflected effect on cerebral blood flow began in 1890 (Roy and

1.3 MRI Neuroimaging modalities and prognostic models in stroke

Sherrington, 1890) and then continued in 1990 when blood oxygenation level-dependent (BOLD) contrast imaging was introduced. (Ogawa and Lee, 1990; Ogawa et al., 1990a,b)

Briefly, BOLD contrast imaging sensitizes the MRI signal to the relative levels of oxyhemoglobin and deoxyhemoglobin in specific areas of the brain due to their different magnetic properties. As active neurons consume more oxygen and are therefore supplied with more oxygen than inactive neurons, the variability in the resulting MRI signal is assumed to indirectly mirror the neuronal function. Since then, the fMRI method using BOLD contrast was developed not long after and became the tool of choice in mapping the neural activity of the human brain. The main advantages of fMRI are that it is non-invasive (requires no contrast substance injected intravenously) and it possesses a quite high spatial resolution despite the low temporal resolution.

fMRI data consists of 4D data: a time series of 3D brain volume. The signal intensity of each voxel of the brain, therefore, can be plotted against time to observe whether or not the pattern relates to a specific function, for example, hemodynamic response function (HRF) for task-based fMRI, or to the time-series signal pattern of other voxels/ROIs in the brain during resting-state (resting-state functional connectivity).

Task-based fMRI

Basic principles

As fMRI measures the hemodynamic response induced by increased neural activity, the first paradigm of the fMRI is based on a task, or a stimulus, whose hemodynamic effects on the brain would be mapped from the acquired MRI signal. The task can be in form of visual, verbal, audio, sensory, motor, or any. Brain activity induced by these stimuli causes a canonical change in the MR signal known as the hemodynamic response function (HRF, figure 1.15).

Then, a task paradigm is designed. In general, two types of task-fMRI design are mainly used in the literature, blocked and event-related. In blocked design, a type of stimulation or task was performed within some short period of time (usually around 20-30 seconds), alternating with “off” or control stimulation/task blocks. This alternation of conditions was necessary because the resulting values at each voxel are in arbitrary units, and therefore brain activity is defined by the difference in BOLD signal within a voxel between different conditions. Conversely, in event-related design, the stimuli are in discrete events, separated by a random interval, as represented in the figure 1.16. This randomness minimizes the subject’s habituation and expectation of the incoming tasks. However, it requires more

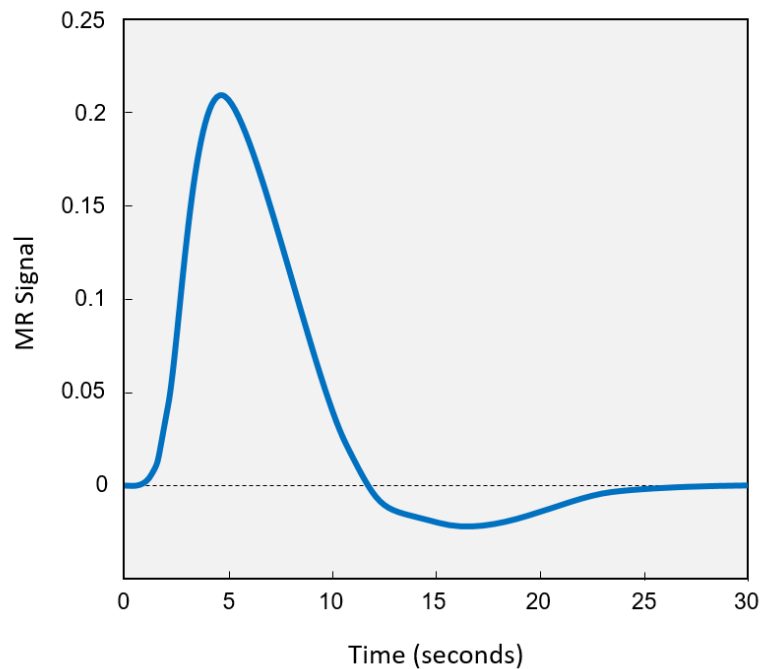


Fig. 1.15 The hemodynamic response function (HRF)

complex analysis, and it suffers from a lower Signal-to-Noise Ratio (SNR) when compared to the blocked design. (Huettel, 2012)

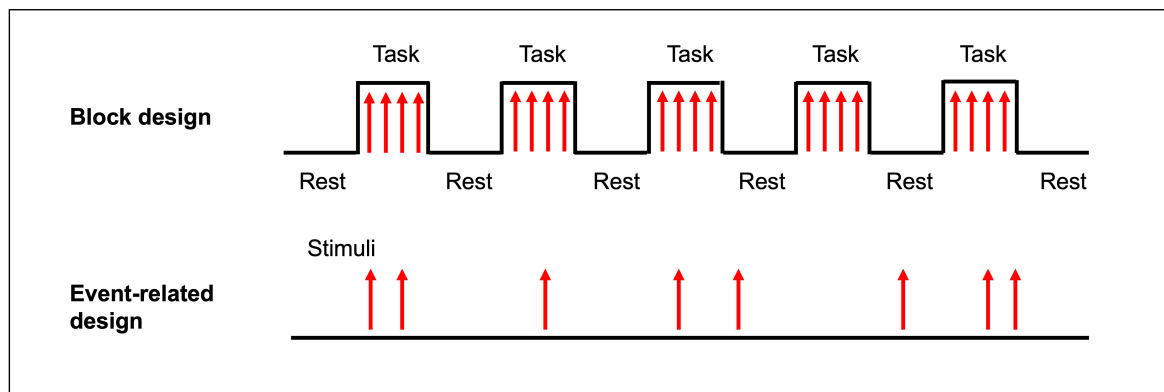


Fig. 1.16 Block and event-related task-fMRI design

Based on the knowledge of the generic HRF and the task design, the predicted task-paradigm-induced signal can be modeled by convolving the HRF with the task-paradigm. Ultimately, time-series correlation or linear regression between the observed signal and the predicted signal at each voxel is performed. One commonly used statistical method in this analysis is the general linear model (GLM), by assigning the signal time series as the

1.3 MRI Neuroimaging modalities and prognostic models in stroke

dependent variable and the expected BOLD stimulus time course as the independent variable. The formula of the GLM is

$$Y = X\beta + \epsilon \quad (1.4)$$

where Y is a matrix of observed time-series MR signal at each voxel, X is a matrix of basis functions, ϵ is an error term, and β is a vector of parameters to be estimated. To control the effect of random noise, the significance of the estimate β can be tested by calculating the test statistic T and comparing the T -values with a known distribution.

In practice, fMRI analysis is generally composed of several steps. These steps are to make sure that a number of factors, such as artifacts due to head movement, interindividual variability, and spatial and temporal artifacts, are taken into account. They include quality control, distortion correction, motion correction (realignment), slice-timing correction, spatial normalization, spatial smoothing, temporal filtering, statistical modeling, statistical inference, and finally, visualization. These preprocessing and processing steps are usually performed using software currently available, such as SPM (<https://www.fil.ion.ucl.ac.uk/spm/>), FSL (<https://fsl.fmrib.ox.ac.uk/fsl/fslwiki/>), AFNI (<https://afni.nimh.nih.gov/>), or Brain Voyager (<https://www.brainvoyager.com/>).

Passive motor task-fMRI in stroke

In healthy participants, the passive task of the hand has been reported to activate several regions of the brain, such as the contralateral primary sensorimotor cortex (SM1), dorsal premotor cortex (dPMC), supplementary motor area (SMA), and ipsilateral cerebellum. (Blatow et al., 2011; Boscolo Galazzo et al., 2014; Carel et al., 2000; Hannanu et al., 2017; Loubinoux et al., 2003) In addition, some studies also reported activity in the parietal cortex, (Boscolo Galazzo et al., 2014; Carel et al., 2000; Loubinoux et al., 2003) the contralateral cerebellum (Hannanu et al., 2017; Loubinoux et al., 2003), and the parietal operculum. (Hannanu et al., 2017) Of note, task-related brain activity during active and passive motor tasks was reported to show no difference in terms of brain activity pattern (Guzzetta et al., 2007; Jaeger et al., 2014; Loubinoux et al., 2001; Zhavoronkova et al., 2017), although some reported higher activity and extent during active than in passive task (Jaeger et al., 2014; Zhavoronkova et al., 2017).

In patients with stroke, fMRI activity related to movements of the paretic hand has been observed in ipsilesional SM1, dPMC, and SMA, similar to those in healthy controls but in different intensities. (Lotze et al., 2012; Loubinoux et al., 2003; Marshall et al., 2000; Rehme et al., 2015) Furthermore, some studies observed a change in brain activity patterns, such as

Literature Review

the recruitment of secondary sensorimotor areas (Carey et al., 2006; Hannanu et al., 2017), mirror areas in the contralesional hemisphere (Schaechter and Perdue, 2008), or activity in the perilesional areas (Cramer et al., 2006). The pattern of brain activity during passive task-fMRI in healthy controls and in stroke patients can be seen in Figure 1.17

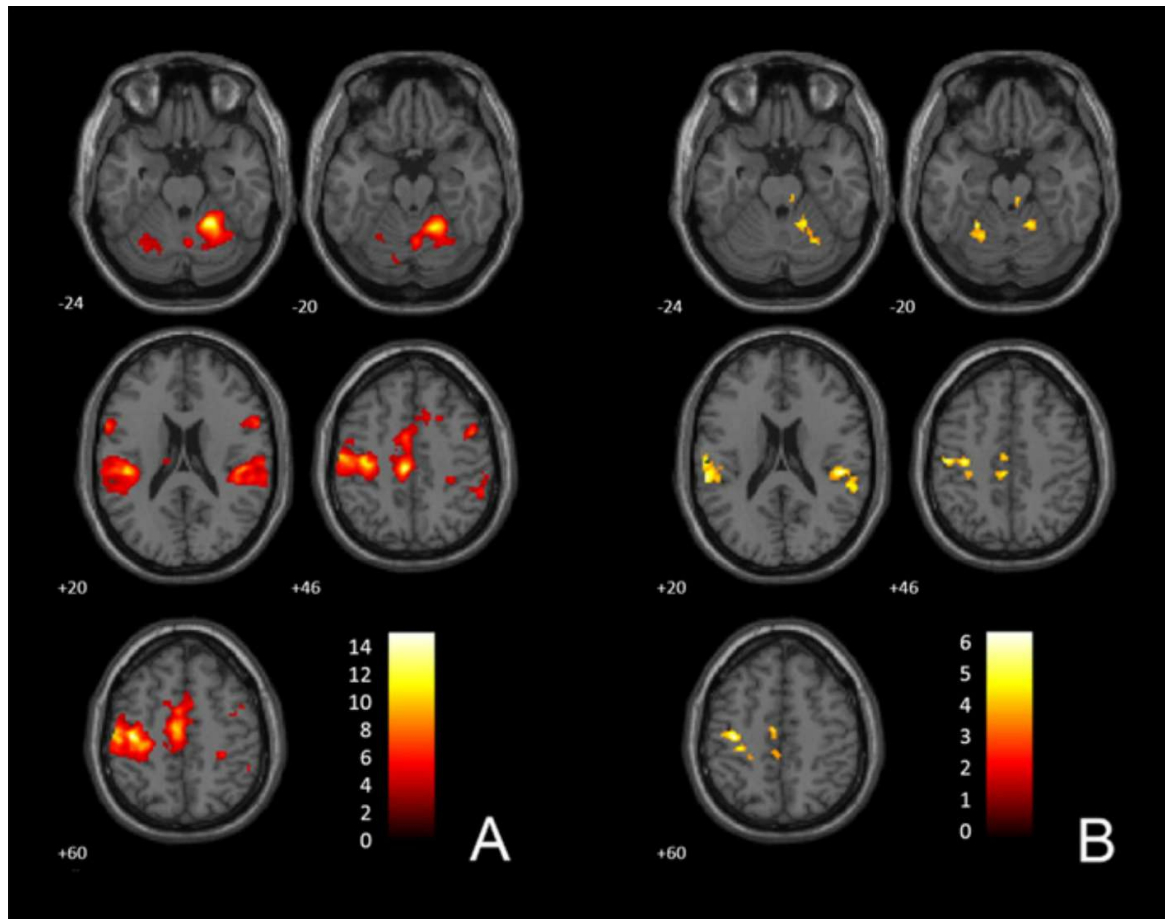


Fig. 1.17 Passive task-fMRI brain activity in healthy controls (A) and in stroke patients (B). (Hannanu et al., 2017)

Association with motor clinical scores

Generally, better motor outcome is associated with the restoration of a normal motor pattern (as shown in healthy controls) (Favre et al., 2014; Rehme et al., 2015), *i.e.*, higher activity in the ipsilesional SM1, SMA, contralesional dPMC, and cerebellum, whereas a poorer motor outcome is associated with persistent contralesional brain activity (Buma et al., 2010). Furthermore, there is increasing evidence that measures of motor-related fMRI activity in the sensorimotor network correlate with motor behavioral performance (Hannanu et al., 2017; Loubinoux et al., 2003; Rehme et al., 2012) and can predict motor recovery (Favre

1.3 MRI Neuroimaging modalities and prognostic models in stroke

et al., 2014; Hannanu et al., 2017; Loubinoux et al., 2007; Rehme et al., 2015; Richards et al., 2008).

Resting-state fMRI (RS-fMRI)

Basic principles

Resting-state fMRI (RS-fMRI) is based on the same basic principle as that of task-based fMRI, the BOLD response. However, as the name suggests, RS-fMRI is acquired without any stimulus or a task administered or performed by the subjects. This implies that the participant is lying still inside the MRI scanner either with eyes closed or fixed on a specific point on a screen, remains awake without doing anything, and is instructed not to think about anything in particular. This method was first described by Biswal et al. (1995) where they reported a temporal correlation between the left and right sensorimotor cortex (and with some other regions) that can be associated with hand motor function and that it was a manifestation of functional connectivity of the brain. Since then, researchers have replicated this finding (Cordes et al., 2000; Hampson et al., 2002; Lowe et al., 1998) and applied this method to study different brain networks (Fox et al., 2005; Raichle et al., 2001) and functional connectivity both in healthy (Damoiseaux et al., 2006) and neurological diseases, such as Alzheimer's disease (Li et al., 2013), schizophrenia (Venkataraman et al., 2012), Parkinson's disease (Tessitore et al., 2012), and many others (Li et al., 2012; Otti et al., 2013; Uddin et al., 2008).

Several methods have been used to analyze rs-fMRI data. One of the most popular methods is seed-based analysis, as used in several founding studies of rs-fMRI (Biswal et al., 1995; Fox et al., 2005; Raichle et al., 2001). In this method, a seed is defined as a selected voxel or ROIs, and then the time-series correlation between this seed and other voxels or areas of the brain is estimated. Functional connectivity is defined as the temporal correlation between the BOLD signal between two seeds in terms of voxel or regions of interest (See figure 1.18). As a set of ROIs needs to be selected, this method is suitable for a study with determined a priori. Another method is the independent component analysis (ICA), (Beckmann et al., 2005; Damoiseaux et al., 2006) which is based on a mathematical technique for separating a multivariate signal into additive subcomponents by assuming that the subcomponents are statistically independent of each other. Although ICA enables us to have fewer a priori when compared to the seed-based analysis, the ICA network components need to be identified by prior knowledge or experience. Graph theory, on the other hand, has been used (Power et al., 2011; van den Heuvel et al., 2008) to model the brain's complex network as a set of nodes and their corresponding edges. Several parameters can be derived

Literature Review

using the graph method, such as the average path length, clustering coefficient, degree of a node, centrality measures, global efficiency, and local efficiency. While the seed-based analysis gives the strength of correlation between one particular ROI to another, these graph theory metrics provide the properties of one ROI within the whole brain related to one specific function. Another method is called clustering algorithms. (Pereira et al., 2009) In this method, a collection of voxels or ROIs are grouped based on their similarities to some determined distance metric.

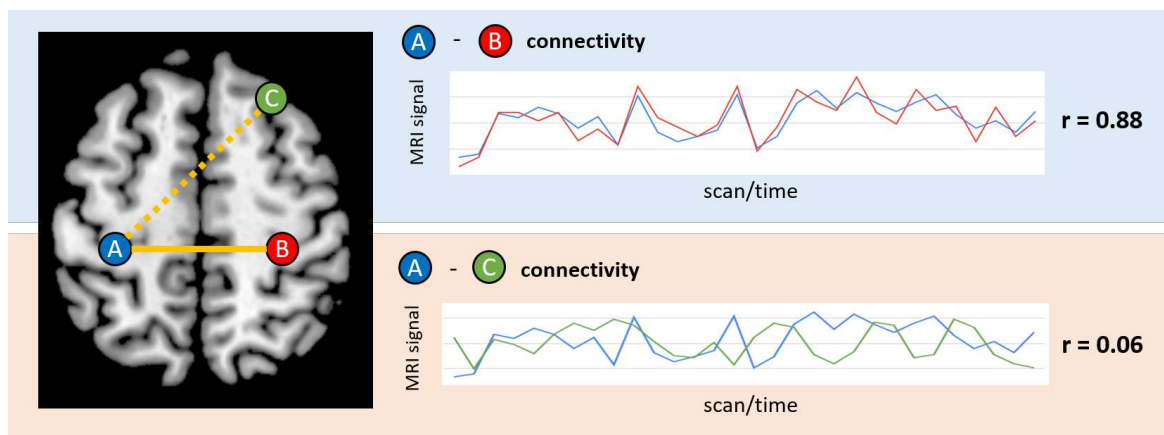


Fig. 1.18 Functional connectivity as temporal correlation of BOLD signal. Area "A" and "B" is interpreted as functionally connected, while area "A" and "C" is not.

In this thesis, functional connectivity related to hand motor outcome after stroke is hypothesized to include regions belonging to the sensorimotor network, including the posterior parietal cortex and the visual areas involved in the visuomotor streams. Based on this hypothesis, a seed-based approach is mainly used. Furthermore, in the multimodal approach, graph theory metrics will be used to limit the number of variables to be considered in the model.

Resting-state functional connectivity in stroke

Changes in the resting-state functional connectivity following stroke have been consistently reported. Among all, the most consistent result was the decrease in interhemispheric connectivity between homotopic areas, such as connectivity between ipsilesional and contralesional M1, followed by changes in the frontal, parietal, occipital, thalamus, and cerebellum. (Brihmat et al., 2020; Carter et al., 2010; Park et al., 2011; Wang et al., 2010) Some of the RSFC reduction is also specifically associated with a behavioral deficit, such as decreased RSFC in the dorsal attention network in patients with neglect, (Carter et al., 2010; He et al., 2007) between the anterior temporal lobe in patients with aphasia, (Warren et al., 2009) between somatosensory areas in patients with sensory loss, (Bannister et al., 2015) and between motor areas in patients with a motor deficit. (Brihmat et al., 2020; Carter et al., 2010)

1.3 MRI Neuroimaging modalities and prognostic models in stroke

Furthermore, this decrease in RSFC was observed early after stroke and then over time returned to normal level along with the recovery. (Carter et al., 2010)

Association with motor clinical scores

There is growing evidence in the literature that resting-state functional connectivity within the motor networks correlates with motor outcome.(Brihmat et al., 2020; Chi et al., 2018) The motor outcome of the upper limb has been diversely associated with increased or decreased functional connectivity between ipsilesional primary sensorimotor areas (SM1) and contralesional SM1 (Brihmat et al., 2020; Carter et al., 2010; Chen and Schlaug, 2013; Hong et al., 2019; Zhang et al., 2016b), SMA (Chen and Schlaug, 2013; Park et al., 2011; Zhang et al., 2016b), and dPMC (Brihmat et al., 2020; Chi et al., 2018; Grefkes et al., 2008). However, these studies focused on the connectivities within the sensorimotor network, whereas the influence of non-motor regions on motor recovery has been sparsely explored. A recent chronic stroke study suggested that better hand motor scores correlate with increased connectivity between the ipsilesional sensorimotor and ventral visual networks (Hong et al., 2019). Other studies have also reported extrinsic connectivity alterations between the motor and visual networks, but their design was based on comparisons between stroke and healthy participants rather than on the association between functional connectivity and hand behavior (Tang et al., 2016).

1.3.3 Predictive models of hand motor outcome using multimodal MRI

Each of the MRI modalities discussed above brings some degree of predictive value for hand motor outcomes. This raised the next question of whether these predictive values are complementary or rather redundant to each other. In this notion, some studies have included multiple modalities to predict the motor outcomes of stroke patients, in which a common practice is to combine two modalities that bring different features of the brain: one from structural and another from functional MRI modality. Diffusion-weighted imaging, or more specifically FA, is almost always used in these MRI multimodal approaches, either together with resting-state fMRI (Carter et al., 2012; Chen and Schlaug, 2013; Lam et al., 2018; Lee and van Donkelaar, 2006; Lin et al., 2018; Lindow et al., 2016; Liu et al., 2015b, 2022; Rosso et al., 2013; Xia et al., 2021) or with task-fMRI (Qiu et al., 2011; Song et al., 2014; Wang et al., 2012). This may come unsurprisingly, considering the reported predictive value of FA to hand motor outcome in a large body of neuroimaging studies. Indeed, FA is reported in all of these multimodal MRI studies to be highly associated with or predicts upper-limb motor performance. Functional features, on the other hand, were also found to be also associated

Literature Review

with motor performance but with lower coefficients or to improve prediction accuracy but with lower contributions to the explained outcome variance. In other studies, DWI and RS-fMRI were reported to be independently correlated with the motor outcomes but were not simultaneously analyzed. (Lee et al., 2019; Zhang et al., 2016a) Moreover, no study has explored the use of SBM metrics together with DWI or fMRI modality to predict motor outcomes. From these previous multimodal MRI studies, there is an indication that DWI would bring better predictive value when compared to fMRI. However, direct comparison between MRI modalities is rare, and the heterogeneity of the studies in terms of time when the patients were scanned makes it difficult to draw a clear conclusion.

From a clinical perspective, multimodal MRI analysis requires extensive resources in terms of MRI acquisition time and data processing that may be unsuitable for the nature of stroke management at the acute phase of stroke, when time is considered very valuable. During the hyperacute or acute period, anatomical images allowing simple yet useful analysis such as stroke location, lesion volume, and SBM should be sufficient. However, in the later stage, when a wider time window is available, additional assessments with high predictive value would be of interest. It is therefore important to be able to determine the best strategy and modality of choice to be used according to the need of patients that can be efficiently implemented in clinical settings.

Chapter 2

Materials and Methods

Chapter contents

2.1	Materials	46
2.1.1	Participants	47
2.1.2	Clinical and behavioral scores	49
2.1.3	MRI acquisition	50
2.2	Methods	53
2.2.1	MRI Data Processing	53
2.2.2	Statistical analysis	56

2.1 Materials



























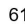
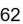
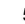

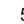


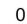




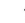

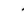


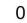


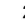






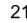



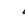




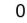


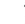




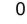










The materials of all studies in this thesis work is mainly based on three different cohorts performed in two different center: Grenoble (Centre Hospitalier Universitaire Grenoble Alpes, CHUGA) and Paris (APHP-Urgences Cérébro-Vasculaires Hôpitaux Universitaires Pitié-Salpêtrière). The three cohorts are:

1. The ISIS-HERMES study (Intravenous Stem cells after Ischemic Stroke and HEuristic value of multimodal MRI to assess MEsenchymal stem cell therapy in Stroke) has been carried out in the CHU of Grenoble Alpes from 2010 to 2018 and is a prospective randomized controlled trial. The primary objective was to assess the feasibility and tolerance of intravenous autologous mesenchymal stem cells in 31 patients with subacute anterior ischemic stroke using longitudinal clinical and multimodal MRI measurements. ISIS-HERMES study was approved by the local ethics committee (Comité de Protection des Personnes) and registered on ClinicalTrial.gov, number NCT00875654.
2. The IRMAS Study (Récupération après un Accident Ischémique Cérébrale: Mécanismes et Prédiction en IRM) was carried out in the CHU of Pitié Salpêtrière (Paris) from 2010 to 2012 to find predictive factors of motor recovery in 76 patients with a subacute hemispheric stroke. The study was approved by the institutional Ethics Committee. The use of this dataset for this thesis has been approved by the principal investigator of the IRMAS study, Charlotte Rosso, thanks to the fruitful collaboration between the two centers.
3. The RESSTORE study (REgenerative Stem cell therapy for STroke in Europe) is a European multicentre randomized clinical trial (H2020 European Project) that aimed to explore the efficacy and safety of intravenous infusion of allogeneic adipose tissue-derived mesenchymal stem cells (ADMSCs) in patients with an acute stroke. Phase IA of the project was carried out in 15 patients with an acute anterior ischemic stroke admitted at the CHU of Grenoble Alpes. All patients received various doses of intravenous stem cells and had a 2-year follow-up based on clinical rating scales, multimodal MRI, and blood biomarkers. MRI data were acquired from 2018 to 2020.

The use of the three cohorts is based on the similarities between their study design, including a longitudinal design with an assessment of clinical scores, hand motor performance, and multimodal MRI (anatomical, diffusion-weighted imaging, task-fMRI, and resting-state

2.1 Materials

fMRI) performed at one and six months follow-up. The thesis work is composed of 6 studies, using each MRI modality independently (Study I-V), and jointly (Study VI). Accordingly, each work in this thesis used a different subset of the merged dataset from these three cohorts, represented in figure 2.1 with the sample size available for each study and each MRI modality. The detailed further sample selection flow of each study is detailed in the methods section of the corresponding study.

Cohorts		MRI					Clinical/Behavioral			
		Lesion volume	SBM	DWI	Task-Fmri	Resting-state fMRI	NIHSS	mRS	Handgrip strength	PPT
Controls	HERMES	N/A	76 	29 	32 	77 	N/A	N/A	0	0
	IRMAS	N/A	62 	61 	61 	61 	N/A	N/A	0	0
	RESSTORE	N/A	31 	25 	31 	31 	N/A	N/A	0	0
Patients at M0	HERMES	31 	29 	29 	23 	25 	30   	30 	   	23
	IRMAS	64 	61 	62 	56 	61 	56 	0	   	0
	RESSTORE	16 	16 	14 	16 	15 	16 	0	  	0
Patients at M6	HERMES	31	28 	22 	25 	25 	31  	31 	   	21
	IRMAS	np	46 	52 	45 	45 	45 	0	  	0
	RESSTORE	np	9 	7 	13 	9 	14 	0	  	0
Patients at M24	HERMES				18 		28 	31 	24 	24
Data used in:		 Study I	 Study II	 Study III	 Study IV	 Study V	 Study VI			




Data used in:  Study I  Study II  Study III  Study IV  Study V  Study VI

Fig. 2.1 Number of data available for each cohort for each MRI modalities and clinical variables, and sub datasets used in each study. N/A: not applicable; np: not processed

2.1.1 Participants

ISIS-HERMES study

Healthy participants

Eighty-one healthy participants aged 18-84 years (40 males) were included in the ISIS-HERMES study and underwent multimodal MRI. Of note, 25 participants performed the behavioral tasks and completed the whole multimodal MRI protocole.

Materials and Methods

Patients

ISIS-HERMES study enrolled 31 patients aged 18-70 years (21 males, 10 right lesions) with a first-ever ischemic stroke within the anterior circulation territory, a delay less than 14 days after stroke onset, and with a persistent neurological deficit (NIHSS ≥ 7). Patients with severe, extensive stroke, severe persistent neurological deficit, serious psychiatric disease, and severe comorbid medical disease were not included. Detailed inclusion and exclusion criteria are provided in Appendix A.1. After inclusion, patients were randomized to receive either an IV injection of mesenchymal stem cells (MSCs) or rehabilitation alone.

IRMAS study

Healthy participants

Sixty-two healthy subjects aged 21-81 years (23 males) participated in the IRMAS study, performed behavioral tasks, and underwent the multimodal MRI protocols.

Patients

The IRMAS study enrolled 76 patients with a first-ever ischemic stroke with mild-severe stroke severity (NIHSS > 0). Detailed inclusion and exclusion criteria are provided in Appendix A.1.

RESSTORE study

Healthy participants

Thirty-two healthy subjects aged 19-55 years (17 males) participated in the RESSTORE study, performed behavioral tasks, and underwent the multimodal MRI protocols.

Patients

Sixteen patients aged 22-76 years (12 males, 8 right lesions) with a first-ever carotid ischemic stroke, admitted to the stroke unit within the first 24 hours after stroke onset, with $NIHSS \geq 7$ were enrolled in the RESSTORE study. All patients were treated by intravenous Adipose derived Mesenchymal Stem Cells (ADMSCs). Detailed inclusion and exclusion criteria are provided in Appendix A.1

In the 3 cohorts, intravenous administration with recombinant tissue plasminogen activator (rtPA) and/or thrombectomy was allowed in accordance with routine clinical procedures at the corresponding institution.

2.1.2 Clinical and behavioral scores

Clinical scores

National Institute of Health Stroke Scale (NIHSS)

Stroke severity was assessed with the National Institute of Health Stroke Scale (NIHSS) (Brott et al., 1989). The NIHSS is composed of 11 items: level of consciousness, eye movement, visual field, facial palsy, motor, ataxia, sensory, language, and speech. Each item is scored, with a score of 0 indicating normal function, while a higher score indicates some level of impairment. Then the total score is summed, with a maximum possible score of 42 and a minimum of 0. The motor subscale of the NIHSS (mNIHSS) can be computed by the summation of the motor arm and motor leg items (without facial or hand paresis). In patients with a unilateral stroke, a score of 0 indicates normal proximal motor function and a score of 8 indicates hemiplegia. A complete form is provided in Appendix A.2.1.

modified Rankin Scale (mRS)

The functional (global) outcome was measured using the modified Rankin Scale (mRS) (van Swieten et al., 1988), with a scale ranging from 0 to 6. A score of 0 refers to no symptoms at all, a higher score indicates some degree of disability and independence, and a score of 6 indicates death. The mRS form is provided in Appendix A.2.2

Behavioral scores

Handgrip strength

Hand motor performance represented by handgrip strength was measured using a handgrip dynamometer (Lafayette Instrument Company, Indiana; <https://www.prohealthcareproducts.com/100-kg-220lb-hand-grip-dynamometer-lafayette-instruments/>) (Sunderland et al., 1989). Patients held the dynamometer in the hand, with the arm at right angles and the elbow by the side of the body. They were asked to squeeze the dynamometer with maximum isometric effort (<https://www.topendsports.com/testing/tests/handgrip.htm>). The grip force score was obtained by computing the average of 3 trials.

Purdue Pegboard Test (PPT)

Patients in the ISIS-HERMES population underwent the Purdue Pegboard Test (PPT) (<http://www.equipement-ergotherapie.com/8-dexterite-manipulation.html>) (Rapin et al., 1966), to test fine manual dexterity and reaching and grasping components of motor action. During the PPT test, patients were seated with the Purdue Pegboard on a table in front of

Materials and Methods

him/her. The testing board consisted of a board with 2 cups across the top containing 25 pins each and two vertical rows of 25 small holes down the center. Patients were asked to place as many pins as possible down the row within 30 seconds with the paretic hand. The total number of pins placed in the allocated time was recorded. The trial was repeated 3 times, and a PPT score was calculated based on the average score across the 3 trials. A score of 0 was given when the participant could not perform the task due to upper limb paresis.

2.1.3 MRI acquisition

ISIS-HERMES study

MRI was performed using 3T (Achieva 3.0T TX, Philips, The Netherlands) at the IRMaGe MRI facility with a 32-channel head coil.

Anatomical sequences

Sagittal 3D-T1-weighted with TR 7.75 ms, TE 3.62, flip angle 9° , FOV: $252 \times 192 \times 252$, 192 slices, voxel size = $0.98 \times 0.98 \times 1 \text{ mm}^3$, thickness = 1 mm, gap = 0 mm, duration = 339 s. 3D-FLAIR images with TR 8 sec, TE 342 ms, flip angle = 90° , FOV: $241 \times 192 \times 250$, 274 slices, voxel size = $0.434 \times 0.434 \times 0.7 \text{ mm}^3$, thickness = 1.4 mm, gap = -0.7 mm, duration = 424 s.

Diffusion-weighted sequence

Echo planar images (EPI) with TR 11 ms, TE 72 ms, FOV 240 mm, slice thickness 2.0 mm, 70 axial slices, SENSE factor 2, fold-over direction anteroposterior, fat shift direction P, fat suppression, and voxel size $1.67 \times 1.67 \times 2 \text{ mm}$, 60 noncollinear directions with $b=1000 \text{ s/mm}^2$, and 10 directions with $b = 0 \text{ s/mm}^2$ that were averaged to give 1 average direction.

Task-fMRI sequence

EPI with TR 3000 ms, TE 30 ms, FOV $220 \times 220 \times 147 \text{ mm}^3$, 59 axial slices, 113 volumes, flip angle = 80° , voxel size $2.3 \times 2.3 \times 2.3 \text{ mm}^3$, gap = 0.25 mm, duration 348 s. Passive wrist flexion-extension task of the paretic hand of the patients and matched hand for controls was performed inside the MRI machine by an investigator, with alternating 20 s of task (1 Hz) and rest during 8 cycles (total time 5 min 40 s). During the scan, a white dot that could be seen by the examiner inside the room was flashed at 1 Hz on a screen as a cue to perform the task. A small supporting board strapped to the subject's hand was used to constrain the passive movements (horizontal position to a maximum of 40°). All subjects were instructed

to remain still and relaxed during the scan, and care was taken to observe mirror movements of the opposite hand or foot.

Resting-state fMRI sequence

EPI, TE 30 ms, TR 2000 ms, voxel size $3 \times 3 \times 3.5 \text{ mm}^3$, gap 0.25 mm, 400 volumes, duration 13 min 40 s. Participants were instructed to remain still and relaxed during the scan with eyes open while looking at a white "X" sign in the middle of the black background screen, without thinking anything in particular, and to avoid falling asleep.

IRMAS study

Images were acquired using a 3T Siemens Trio MRI Scanner with 12-channel head matrix coil at the CENIR facility (www.cenir.org).

Anatomical sequences

3D-T1 TR 2.3 sec, TE 4.18 ms; flip angle 9° , TI 900 ms, FOV $240 \times 256 \times 176$, voxel size $1 \times 1 \times 1 \text{ mm}^3$, 176 slices. Axial T2 FLAIR, with TR 9.5 s; TE 103 ms, flip angle 120° , TI 2.4 sec.

Diffusion-weighted sequence

EPI sequence of TR 10 sec, TE 87 msec, FOV $256 \times 256 \text{ mm}$, slice thickness 2 mm, number of acquisitions 60, with a 35 gradient encoded direction and a b-value of 1000 s/mm^2

Task-fMRI sequence

EPI pulse sequence, with TR 3 sec, TE 25 msec, flip angle 90° , matrix 100×100 , voxel size $2 \times 2 \times 2.5 \text{ mm}^3$, 53 volumes. The motor paradigm consists of a self-paced squeeze-release action on a grip device connected to a pressure transducer to record performance and control the task during the scan. Auditory cue instructions were given with words as follows: "action" to start the alternating squeeze and release of the gripping device until the command "stop" was given. All subjects were trained to perform the motor task before entering the scanner. The paradigm consists of three blocks of task activation and four rest blocks, starting with the rest block. Each block lasted 20 seconds, with a total duration of 2 minutes and 20 seconds.

Resting-state fMRI sequence

Two RS-fMRI sequences of 7 minutes each were acquired: EPI, 173 volumes, 41 slices, TR 2460 ms, TE 30 ms, flip angle 90° , voxel size $= 3 \times 3 \times 3 \text{ mm}^3$, gap = 0. Participants were instructed to keep their eyes closed and to avoid moving or falling asleep.

Materials and Methods

RESSTORE study

Similar to the ISIS-HERMES study, PHILIPS MRI was performed at 3T (Achieva 3.0T TX, Philips, NL) at the IRMaGe MRI facility (Grenoble, France) with a 32-channel head coil.

Anatomical sequences

T1-weighted structural images were acquired using TR: 7.7 ms, TE: 3.6 ms, voxels: $1 \times 1 \times 1 \text{ mm}^3$, FOV: $255 \times 255 \times 192$, flip angle 9° , 192 slices, acquisition time 5m 39 seconds. 3D-FLAIR sagittal images were acquired using TR: 4800 ms, TE: 390 ms, voxels: $0.49 \times 0.49 \times 1 \text{ mm}^3$, no gap, FOV: $256 \times 256 \times 192$, and 192 slices, TI 1650 s, reconstruction 0.49×0.49 , acquisition time 6 minutes 10 seconds.

Diffusion-weighted sequence

EPI with TR 5520, TE 89.5 ms, flip angle 79° , matrix 168×144 , 60 non-collinear gradient directions and 10 $b=0$ images, FOV $=240 \times 240 \times 140$; slice thickness 2 mm, 70 slices; voxels size $=1.6 \times 1.6 \times 2.0 \text{ mm}^3$; b-value = 1000 s/mm^2

Task-fMRI sequence

EPI sequence, with TR 1.8 s, TE 30 ms, flip angle 75° , FOV $216 \times 216 \times 153$, voxel size $2.261 \times 2.261 \times 3 \text{ mm}^3$, 166 volumes, 60 axial slices, duration 311 s, a multiband factor of 2 (parallel) sense 2.5, matrix $88 \times 86 \times 60$. Passive wrist flexion-extension task of the paretic hand of the patients and matched hand for controls was performed inside the MRI machine by an investigator, with alternating 20 s of task (1 Hz) and rest during 8 cycles (total time 5 min 40 s). During the scan, a white dot that could be seen by the examiner inside the room was flashed at 1 Hz on a screen as a cue to perform the task. A small supporting board strapped to the subject's hand was used to constrain the passive movements (horizontal position to a maximum of 40°). All subjects were instructed to remain still and relaxed during the scan, and care was taken to observe mirror movements of the opposite hand or foot.

Resting-state fMRI sequence

EPI was acquired with TR 1.5 s, TE 30 ms, voxel size $2.261 \times 2.261 \times 3 \text{ mm}^3$, 400 volumes, matrix 88×86 , flip angle 75° , slice thickness 3 mm, 48 slices, FOV $217 \times 217 \times 144$ with a total duration of 10 min 10 s, a multiband factor of 2 (parallel) sense 2.5. Participants were instructed to remain still and relaxed during the scan with eyes open while looking at a white "X" sign in the middle of the black background screen, without thinking anything in particular and to avoid falling asleep.

2.2 Methods

2.2.1 MRI Data Processing

Lesion volume and VLSM

T1 and FLAIR images were normalized to the MNI template using Statistical Parametric Mapping (<https://www.fil.ion.ucl.ac.uk/spm/>). Manual lesion delineation in all participants was performed on the normalized FLAIR images by a stroke neurologist and a stroke neuroradiologist. Lesion volumes were calculated from the lesion binary mask using MRIcron software. Images from patients with right lesions were flipped along the x-axis, and thus all lesions were on the left. This way, all patients were included in the analysis without having to divide into subgroups based on the lesion side, and analysis can be performed only in voxels of the left hemisphere in order to decrease the number of multiple comparisons. The effect of age, sex, center, and lesion volume were regressed. In the ISIS-HERMES study, stem-cell treatments were administered to some randomly assigned patients one day after the M0 assessment, and thus the effect of stem cell treatment was regressed only when predicting scores at M6. VLSM analysis was performed using niistat software (<https://www.nitrc.org/projects/niistat/>). Fredman-Lane with -5000 permutation was used to correct for multiple comparisons. The resulting nifti file corresponding to the significant voxels associated with the clinical scores was used to calculate the number of significant voxels in the JHU-white-matter atlas and AAL-grey-matter atlas.

Surface-based Morphometry

T1 images were segmented and normalized to the MNI template using a segmentation pipeline integrated into Computational Anatomy Toolbox (CAT12), an extension to SPM12 (Gaser et al., 2022). More specifically, CAT12 includes denoising, interpolation, affine preprocessing, local adaptive segmentation, AMAP (Adaptive Maximum A Posterior) segmentation, partial volume segmentation, skull-stripping and cleanup, spatial normalization, white matter hyper-intensity correction, and stroke lesion correction. Then, three SBM metrics were estimated: cortical thickness (CT), fractal dimension (FD), and gyrification index (GI). These metrics were then extracted using an ROI-based approach, using the HCP (Human Connectome Project) atlas (Glasser et al., 2016) (See Figure 2.2), to be used for further statistical analysis.

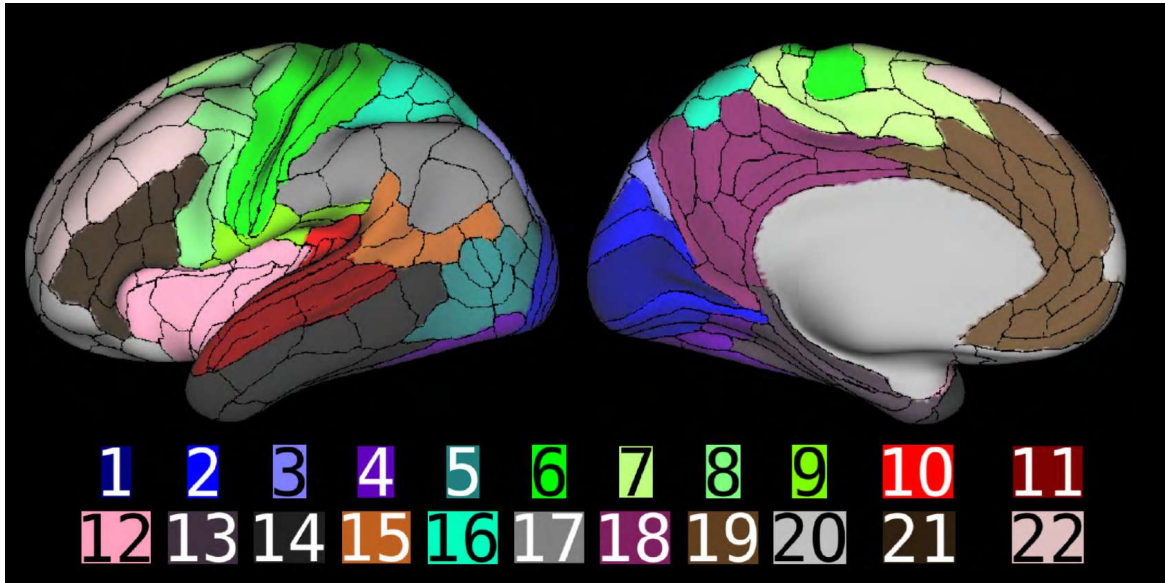


Fig. 2.2 HCP atlas. Representation of the multi-modal parcellation of 180 areas spanning the entire cerebral neocortex and divided into the following 22 numbered sections. The first five regions cover the early and intermediate visual cortex, including sections on V1 (1), the early visual cortex (2), the dorsal stream (3), the ventral stream (4), and the MT+ Complex (5), and its neighbors. The next four regions cover the primary somatosensory and motor cortex (6), the sensorimotor-associated paracentral lobular and mid-cingulate cortex (7), the premotor cortex (8), and the parietal opercular cortex (9). Next are the regions covering the early auditory (10) and association auditory cortex (11), the insular and frontal opercular cortex (12), and the medial (13) and lateral temporal cortex (14). Then there are four regions covering the rest of the posterior cortex, including the sensory “bridge” regions of the temporal-parietal-occipital junction (15) and the superior parietal and IPS cortex (16), the inferior parietal cortex (17), and the posterior cingulate cortex (18). The final four regions cover the rest of the anterior cortex, including the anterior cingulate and medial prefrontal cortex (19), orbital and polar frontal cortex (20), inferior frontal cortex (21), and dorsolateral prefrontal cortex (22). (Glasser et al., 2016)

Diffusion-weighted imaging

We used two different preprocessing pipelines. For study II (Hannanu 2022), preprocessing was done by the DTI approach using the Diffusionist toolkit (related documentation can be found in mri-diffusionist.com/). The preprocessing included quality assurance that was visually performed for each diffusion-weighted image, in which corrupted images were removed. Then, after correction of eddy-current distortions, the diffusion tensor was estimated. Linear and nonlinear registration transformations were applied to an FA map in order to get the FA maps in the MNI space. From these FA maps, an atlas-based ROI

approach was used to extract the average FA in each ROI from the white matter atlas of the JHU-ICBM-DTI (JHU) atlas25.

For the multimodal analysis, the constrained spherical deconvolution (CSD) approach was performed using MRTrix software. The general pipelines used were as follows: denoising, removal of Gibbs artifact, preprocessing, upsampling, estimation of response function (FRF), the estimation of fractional anisotropy (FA), linear registration of FA and DWI images, and then the estimation of the fiber orientation density (FOD) using CSD. Using the peak of the FOD, fiber bundles in 72 anatomically well-described tracts were reconstructed using the deep-learning method applied in the TractSeg tool (Wasserthal et al., 2018). Finally, the average FA value was calculated in each fiber bundle mask and used for further analysis.

Resting-state fMRI

Data preprocessing and processing were performed using CONN Toolbox (<http://www.nitrc.org/projects/conn>). Preprocessing pipeline for volume-based analysis with direct normalization to MNI-space was performed in CONN Toolbox, including realignment, slice-timing correction, outlier detection, coregistration, direct segmentation, and normalization of functional ($2 \times 2 \times 2 \text{ mm}^3$) and structural images ($1 \times 1 \times 1 \text{ mm}^3$), and smoothing of functional images. Images from patients with lesions on the right side were flipped about the x-axis prior to the pipeline to perform group analyses without dividing participants into smaller groups based on the lesion side. Thus, all lesions are located in the left hemisphere. We used the Artifacts Detection Tool (ART) to detect outliers, with thresholds for signal intensity outliers set at 5 standard deviations (SD) above or below the mean and a motion limit of 0.9 mm in any direction. During the denoising step, white matter, CSF, and the outliers detected by the ART toolbox were used as confounding effects in the linear regression. Then, a bandpass filter of 0.09 to 0.008 was applied. For IRMAS dataset, the two sessions of rs-fMRI were preprocessed separately and then merged for group analyses.

We performed a First-Level analysis (FLA) using ROI-to-ROI-based analysis resulting in ROI-to-ROI connectivity values that were then transformed into Fisher Z scores. In study III, we used 78 ROIs from the Juelich atlas that was relevant to the research question. However, in the multimodal analysis, to be able to analyze across modalities, we used the same atlas as in the SBM analysis, *i.e.*, 360 ROIs (180 at each hemisphere) from the HCP atlas (Glasser et al., 2016), and 38 (19 at each hemisphere) subcortical and cerebellar ROIs from the Julich-Brain cytoarchitectonic atlas (Amunts et al., 2020). In addition to the ROI to ROI connectivity z-score values, 7 graph theory metrics (Global efficiency, local efficiency,

Materials and Methods

betweenness centrality, degree, clustering coefficient, and cost) were estimated and extracted using CONN Toolbox. These values were then used for further statistical analysis.

Task fMRI

Data preprocessing and processing was performed using SPM12. Following visual inspection for spatial artifacts, EPI time series were checked for temporal artifacts and realigned. Next, the T1-weighted and FLAIR images were coregistered and aligned to the mean of the EPI time series. Segmentation of the structural images (T1 and FLAIR) resulted in a deformation field that was used to spatially normalize the EPI data in Montreal Neurological Institute (MNI) space. Finally, the EPI images in MNI space were smoothed using a full-width at half maximum (FWHM) Gaussian kernel of 5*5*5 mm³. The structural T1-weighted and FLAIR images were also normalized to MNI space at 1 mm³ resolution. Intensity outliers were detected using ART (<https://www.nitrc.org/projects/artifact-detect>), with an interscan movement threshold of 1 mm, and a global interscan signal intensity threshold of 3 SD relative to the session means. The data preprocessing pipeline is represented in the figure 2.3

The first level voxel-wise analysis was performed in SPM12 using a general linear model including passive movement conditions, outliers and head motion estimates as regressors, and a high-pass (128hz) filter. The task regressors were convolved with a canonical HRF. Contrasts of the movement-related parameter estimates were generated for subsequent ROI analyses. The resulting t maps (spmT) were converted to Cohen's d effect size maps (some), and then the peak value of each ROI was extracted using the REX tool (<https://www.nitrc.org/projects/rex/>). For Study I, 72 ROIs (36 at each hemisphere) from the Anatomy Toolbox (Eickhoff et al., 2007) and from AAL atlas (Tzourio-Mazoyer et al., 2002) were used. For multimodal analysis (Study VI), for between-studies compatibility reason, 360 ROIs (180 at each hemisphere) from the HCP atlas (Glasser et al., 2016), plus 38 (19 at each hemisphere) subcortical and cerebellar ROIs from the Julich atlas were used. These values were then used for further statistical analysis.

2.2.2 Statistical analysis

Statistical analysis was performed using SPSS version 23 and Python version 3.5.

Univariate analysis

Descriptives of the data are presented using the mean, standard deviation (SD), median, and interquartile range (IQR) for continuous variables and in absolute count and frequency

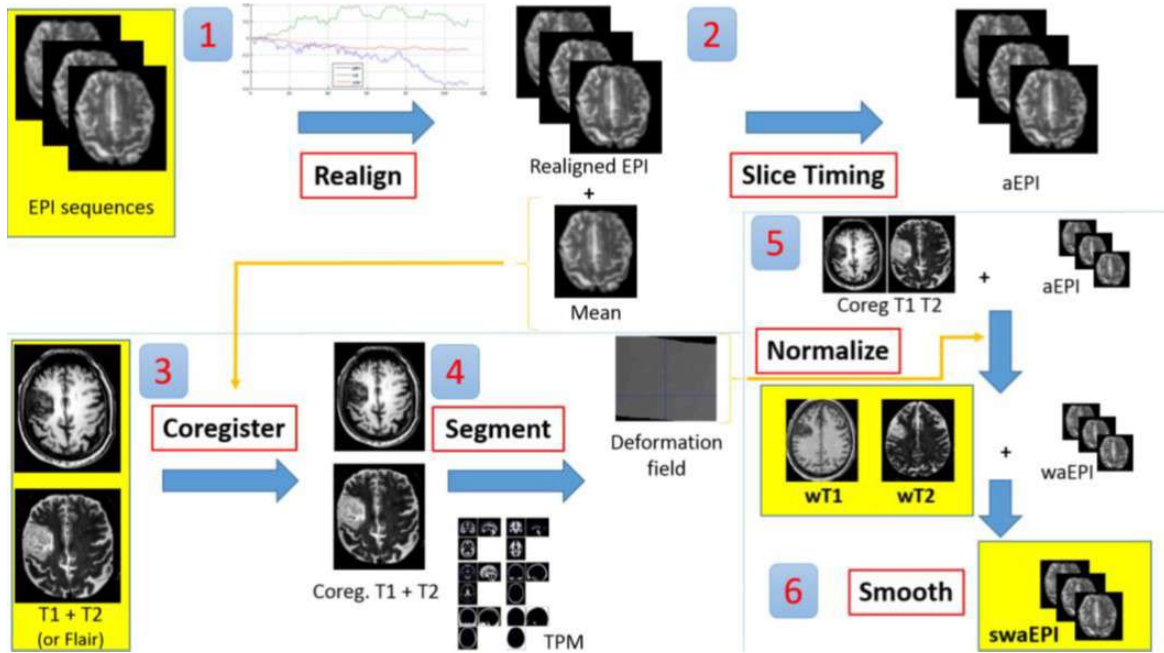


Fig. 2.3 Preprocessing steps performed for task-fMRI modality

for categorical variables. Maximum and minimum values by each variable (column) and by each participant (row) for each modality are plotted to expose any outliers in the data. Outliers related to preprocessing failure or due to excessive head movements in the scanner were removed from the analysis. The normality of the distribution was visually inspected using histograms, and significant differences to the normal distribution were tested using the one-sample Kolmogorov-Smirnov test.

Bivariate analysis

Group comparisons were performed using independent t-tests for comparisons between controls and patients and paired t-tests for comparisons between patients at different time points (M0 and M6). Correlations between two variables were performed using Spearman correlations for non-normally distributed variables and Pearson correlations for normally distributed variables. Since a clear effect of sex and age has been consistently documented on handgrip strength, the association between grip strength and MRI-derived metrics was tested using partial correlation adjusting for age, sex, and study. For resting-state functional connectivity measures, correlation coefficient matrices of ROI-to-ROI connectivity and behavioral scores were plotted into a heatmap.

Materials and Methods

Regression and machine learning analysis

Predictive models in study I were built using linear mixed models (LMMs) to account for the repeated measure design used in the analysis, the random effect at the subject level, and to handle missing data. In studies II and III, we used multiple linear regression to model the behavioral measures using MRI-derived metrics, adjusting for relevant covariates. We used R-squared measures of goodness of fit (R^2 , coefficient of determination), the Durbin-Watson test, and residual statistics (plots, descriptives, and Cook's distance) to assess the overall performance of the models. In study VI (multimodal MRI analysis), several machine learning algorithms were used and compared: Logistic regression (LR) with L1 and L2 penalty, Random Forest (RF), and Support Vector Machine (SVM). Regularization methods were used to decrease the effect of overfitting in non-penalized LR. In addition, RF and SVM algorithms were used to handle the limitation of LR in terms of correlation between covariates, nonlinearity, and potential complex interactions among covariates, as it produces a more flexible relationship between the predictors (alone or in combination) and the outcome (Scrutinio et al., 2020).

In Study IV, V, and VI, hand motor performance (grip strength) and motor severity (mNIHSS) were binarized using a threshold of 0 and 1, respectively. In this context, the algorithm was trained to classify patients into no hand motor function (grip = 0) and any degree of hand motor function (grip > 0). Similarly, the mNIHSS was categorized into severe motor deficit (mNIHSS > 1) and no motor deficit (mNIHSS 0 or 1). The motivation behind the categorization, in addition to the linear regression, is that it may be more clinically useful to provide a dichotomous outcome. Indeed, almost half (45%) of the patients in the merged dataset had a grip strength of 0 kg at M0 and one-third (35%) at M6. Finally, we evaluated the model using the prediction accuracy (in percentage), specificity, sensitivity, ROC curve, and the area under the curve (AUC).

The general pipeline of the analysis is as follows. The data from stroke patients was first standardized into z-scores against data from healthy control of the each cohort. Then, the patient data was randomly splitted into training and test dataset with 70:30 proportion. The model was built on the training dataset and was applied to the test dataset to determine the accuracy. To test which modality best predicts the hand motor outcome, features was first selected from each modality separately, and then used in combination.

Chapter 3

Thesis Work

Chapter contents

3.1	Study I. Task-fMRI	61
3.1.1	Overview	61
3.1.2	Article	62
3.1.3	Methodological considerations	82
3.2	Study II. DTI	83
3.2.1	Overview	83
3.2.2	Article	83
3.3	Study III. Resting-state fMRI	95
3.3.1	Overview	95
3.3.2	Article	96
3.4	Study IV (Surface-based morphometry)	126
3.4.1	Introduction	126
3.4.2	Methods	127
3.4.3	Results	128
3.4.4	Discussion	130
3.5	Study V (VLSM)	135
3.5.1	Introduction	135
3.5.2	Methods	137
3.5.3	Results	137
3.5.4	Discussion	141
3.6	Study VI (Multimodal MRI)	145
3.6.1	Introduction	145

Thesis Work

3.6.2	Methods	146
3.6.3	Results	147
3.6.4	Discussion	147

3.1 Study I. Spatiotemporal patterns of sensorimotor fMRI activity influence hand motor recovery in subacute stroke: A longitudinal task-related fMRI study

3.1.1 Overview

The first work of this thesis explored hand motor recovery using passive wrist flexion-extension task fMRI in 27 patients with stroke (from the ISIS-HERMES study participants). Two hand behavioral scores were used, the handgrip strength and the Purdue Pegboard test (PPT). Task-fMRI and behavioral scores were assessed at three time points: 1 month following stroke, and then 6 months and 24 months later. Correlation and linear mixed model (LMM) analysis were used to determine the effects of sensorimotor activity on hand recovery.

The hypothesis of this study is based on the dual visuomotor stream model Goodale and Milner (1992); Rizzolatti and Matelli (2003) positing that two segregated dorsomedial and dorsolateral cerebral networks control reach and grasp movements. The notion that the two streams act independently has been much challenged, (Cavina-Pratesi et al., 2010; Davare et al., 2006) with more views suggesting that dorsolateral and dorsomedial circuits interact to achieve appropriate grasping behaviors. (Grafton, 2010) In this study, by using a purely grasp task without a reaching component (handgrip strength) and a more complex task including both reach and grasp components, we aimed to disentangle this theory in the context of hand motor recovery following stroke. More specifically, we hypothesized that the handgrip is expected to be associated with brain activity in the dorsolateral stream, while the PPT task would be associated with brain activity in both the dorsolateral and dorsomedial stream. In addition, we were also interested in exploring whether there was a functional dissociation between the subregions of the primary motor cortex (M1), namely BA4a and BA4p.

We found a dissociation between the two tasks in terms of task-related brain activity: while both PPT and handgrip force led to activate the sensorimotor and parietal areas, PPT recovery was modeled by fMRI activity in the ipsilesional primary motor cortex (M1-4p), superior parietal lobule (SPL-7M) and parietal operculum OP1, and lesion side, and handgrip force by activity in the ipsilesional M1-4a, OP1, and contralesional inferior parietal lobule (IPL-PFt). Moreover, the relationship between fMRI activity and hand recovery was time-dependent, occurring in the early recovery period in SPL-BA-7M and later in M1.

In conclusion, our results confirmed our hypothesis, suggesting that brain areas of both dorsolateral and dorsomedial networks participate to visuomotor reach and grasp tasks (PPT), while only the dorsolateral network areas may control recovery of simple grasp (handgrip

force). These findings support the notion that the type of movement modulates network recruitment. We also found that BA4a is more related to a simple grasp task and BA4p to PPT, a task that requires independent finger movements. The article was published in Cortex Journal on 17 April 2020.

3.1.2 Article

This part was intentionally left blank. The article starts on the next page.

Available online at www.sciencedirect.com

ScienceDirect

Journal homepage: www.elsevier.com/locate/cortex

Research Report

Spatiotemporal patterns of sensorimotor fMRI activity influence hand motor recovery in subacute stroke: A longitudinal task-related fMRI study



Fabrice F. Hannanu^a, Issa Goundous^a, Olivier Detante^b,
Bernadette Naegele^b and Assia Jaillard^{a,c,d,*}

^a AGEIS, EA 7407, Université Grenoble Alpes, Grenoble, France

^b Stroke Unit, Neurologie, Centre Hospitalier Universitaire Grenoble Alpes (CHUGA), Grenoble, France

^c Unité IRM 3T Recherche - IRMaGe, Inserm US 17 CNRS - UMS 3552 UGA, CHUGA, Grenoble, France

^d Pôle Recherche, CHUGA, Grenoble, France

ARTICLE INFO

Article history:

Received 9 July 2019

Revised 27 November 2019

Accepted 13 March 2020

Published online 17 April 2020

Keywords:

Dexterity

Stroke

fMRI

Recovery

Primary motor cortex

ABSTRACT

Motor hand deficits impact autonomy in everyday life, and neuroplasticity processes of motor recovery can be explored using functional MRI (fMRI). However, few studies have used fMRI to explore the mechanisms underlying hand recovery following stroke. Based on the dual visuomotor model positing that two segregated dorsomedial and dorsolateral cerebral networks control reach and grasp movements, we explored the relationship between motor task-related activity in the sensorimotor network and hand recovery following stroke.

Behavioral recovery was explored with a handgrip force task assessing simple grasp, and a visuomotor reaching and precise grasping task, the Purdue Pegboard Test (PPT). We used a passive wrist flexion-extension task to measure fMRI activity in 36 sensorimotor brain areas. Behavioral and fMRI measurements were performed in 27 patients (53.2 ± 9.5 years) 1-month following stroke, and then 6-month and 24-month later. The effects of sensorimotor activity on hand recovery were analyzed using correlations and linear mixed models (LMMs).

PPT and handgrip force correlated with fMRI activity measures in the sensorimotor and parietal areas. PPT recovery was modeled by fMRI measures in the ipsilesional primary motor cortex (MI-4p), superior parietal lobule (SPL-7M) and parietal operculum OP1, and lesion side. Handgrip force was modeled by ipsilesional MI-4a, OP1, and contralesional inferior parietal lobule (IPL-PFt). Moreover, the relationship between fMRI activity and hand recovery was time-dependent, occurring in the early recovery period in SPL-BA-7M, and later in MI.

These results suggest that areas of both dorsolateral and dorsomedial networks participate to visuomotor reach and grasp tasks (PPT), while dorsolateral network areas may control recovery of simple grasp (handgrip force), suggesting that the type of movement modulates network recruitment. We also found functional dissociations between MI-

* Corresponding author. Unité IRM 3T - Recherche CHU Grenoble Alpes, CS 10217 38043 Grenoble Cedex 9, France.

E-mail address: Assia.Jaillard@univ-grenoble-alpes.fr (A. Jaillard).

<https://doi.org/10.1016/j.cortex.2020.03.024>

0010-9452/© 2020 Elsevier Ltd. All rights reserved.

4p related to PPT that required independent finger movements and MI-4a related to simple grasp without independent finger movements. These findings need to be replicated in further studies.

© 2020 Elsevier Ltd. All rights reserved.

1. Introduction

Stroke remains a leading cause of acquired motor disability in adults, with manual dexterity being often impaired following stroke (Horn, Grothe, & Lotze, 2016). As new therapies are emerging in stroke, approaches to identify mechanisms and biomarkers of motor recovery of the paretic hand using MRI are needed. Furthermore, prognostic measures to assess the individual potential for improvement are also an important step in developing more targeted interventions. To this end, functional neuroimaging techniques may provide an insight into neuroplasticity processes involved in motor recovery to develop tailored programs of rehabilitation following stroke (Horn et al., 2016). Among the currently available MRI techniques, functional MRI (fMRI) using motor task paradigms is considered as a potential tool in stroke recovery studies because of its ability to allow dynamic representation of motor activity. Typical patterns related to hand motor tasks in healthy participants are characterized by increased activity in the canonical sensorimotor areas, comprising the contralateral premotor cortex (PMC), primary sensorimotor cortex (SI, MI), Supplementary Motor Area (SMA), and ipsilateral cerebellum (anterior cerebellum or IV, V, VI lobules and posterior cerebellum or VIII lobules) (Keisker, Hepp-Reymond, Blickenstorfer, Meyer, & Kollias, 2009). Of note, both passive and active motor tasks activate the sensorimotor cortex (Berlot, Prichard, O'Reilly, Ejaz, & Diedrichsen, 2019; Blatow et al., 2011; Weiller et al., 1996), as well as the other areas of the sensorimotor network such as the posterior parietal regions (Estevez et al., 2014; Loubinoux et al., 2001). In stroke, fMRI activity related to movements of the paretic hand has been observed in both ipsilesional and contralesional frontoparietal regions (Lotze et al., 2012; Marshall et al., 2000; Rehme et al., 2015). Typically, the restoration of a normal motor pattern is typically associated with good motor outcomes (Favre et al., 2014; Rehme, Eickhoff, Rottschy, Fink, & Grefkes, 2012). Furthermore, there is increasing evidence that measures of motor related fMRI activity in the sensorimotor network correlate with motor performance assessed outside the scanner (Hannanu et al., 2017; Loubinoux et al., 2003; Rehme et al., 2012), and can predict motor recovery (Favre et al., 2014; Hannanu et al., 2017; Loubinoux et al., 2007; Rehme et al., 2015; Richards, Stewart, Woodbury, Senesac, & Cauraugh, 2008).

Prehension is a basic and pivotal component of daily-life functional tasks for the manipulation of objects (Frey, 2008). Manual prehension consists of two temporally integrated movements, reach and grasp, each mediated by different neural pathways from the visual to motor cortex (Goodale & Milner, 1992; Jeannerod, Arbib, Rizzolatti, & Sakata, 1995;

Pandya, 2015a). First, Milner (Milner & Goodale, 2008) and Goodale (Goodale & Milner, 1992) proposed the coexistence of a ventral circuit for object identification, and a dorsal circuit from the visual cortex via the posterior parietal to premotor and motor regions for visually guided actions directed at objects. A more recent view (Culham & Valyear, 2006) based on the macaque model (Borra, Gerbella, Rozzi, & Luppino, 2017) and neuroimaging studies in humans (Cavina-Pratesi et al., 2010) posits that two specialized dorso-parietofrontal circuits control prehension, both of which include projections to MI. In humans, the dorsolateral circuit connects the anterior bank of the intraparietal sulcus (aIPS) and inferior parietal lobule (IPL) to the ventral premotor cortex (PMv) for generating purposeful hand actions such as grasping, including hand pre-shaping as well as some programming aspects of grasping and manipulation of objects that require precision (Culham & Valyear, 2006; Davare, Andres, Clerget, Thonnard, & Olivier, 2007).

The dorsomedial circuit connects the superior parieto-occipital cortex (SPOC) and superior parietal lobule (SPL = BA5 and BA7) to the dorsolateral premotor cortex (PMd = dorsolateral BA6), where visuospatial processing can combine appropriate sensorimotor information to monitor the different phases of reaching (Cavina-Pratesi et al., 2010; Filimon, Nelson, Hagler, & Sereno, 2007; Filimon, Nelson, Huang, & Sereno, 2009; Vesia et al., 2017). However this dual visuomotor circuit model has been challenged with recent evidence of a more complex arrangement in both human (Grol et al., 2007) and nonhuman primates (Nelissen, Fiave, & Vanduffel, 2018). First, functional neuroimaging and TMS studies have shown that grasping tasks may involve both dorsomedial and dorsolateral circuits, although with different timings, according to the type and the degree of precision required by the movement (Davare, Andres, Cosnard, Thonnard, & Olivier, 2006; Grol et al., 2007). Second, fMRI studies have revealed that PMd and SMA were activated for grasp movements without reach component (Cavina-Pratesi et al., 2010). Third, TMS (Vesia et al., 2017) and fMRI (Cavina-Pratesi et al., 2010) studies have shown that the anterior SPOC, which includes the putative human homologue of V6A (Pitzalis, Fattori, & Galletti, 2015) and belongs to the dorso-medial circuit, controls grip components that might be integrated in goal directed actions. These findings are in line with nonhuman primate works showing that the dorsomedial reaching circuit, and more specifically V6Ad, conveyed aspects of grasp-specific information (Nelissen et al., 2018).

Along these lines (Budisavljevic et al., 2017), have correlated diffusion tractography with kinematic data in 30 healthy participants to explore the selectivity of fronto-parietal connections of the three branches of superior longitudinal

fasciculus (SLF, including SLFI, SLFII and SLFIII) for different components of a hand reach and grasp paradigm. The authors found that bilateral SLFII and SLF III were associated with the kinematic markers of both reaching and grasping components of action (Budisavljevic et al., 2017), suggesting that a common network supports visuomotor processing to generate and control reaching and reach and grasp movements (Budisavljevic et al., 2017; Howells et al., 2018).

Nevertheless, there is some agreement in the literature that reach and grasp movements are to some extent subserved by segregated visuomotor frontoparietal pathways, with a dissociation between the dorsomedial/reach circuit and the dorsolateral/grasp circuit (Cavina-Pratesi et al., 2018; Grafton, 2010; Karl & Whishaw, 2013; Vesia et al., 2017). The human dorsolateral/grasp circuit, similarly to the grasping lateral network in the macaque (Borra et al., 2017), comprises SMI, PMd and PMv, SMA, aIPS, SII (human OP1 and OP4), thalamus, and cerebellum (Cavina-Pratesi et al., 2018; Ehrsson et al., 2000). Moreover, while there are multiple actions that can be combined to generate grasp behaviors, two main components, grip force and precision grasping, have emerged (Ehrsson et al., 2000; Grafton, 2010). The pattern of activity for grip tasks in which fingers need to generate an appropriate grip force includes the IPL, pallidum, anterior insula, and cingulate motor area (CMA) in addition to the common grasp-related pattern (Cramer et al., 2002; Dettmers et al., 1995; Keisker et al., 2009). Moreover, the degree of force exerted was directly proportional to the amplitude of the brain signal determined by fMRI in the sensorimotor cortex and the anterior cerebellum (Keisker et al., 2009). A relationship between force and fMRI signal was also observed for PMv and IPL (Dai, Liu, Sahgal, Brown, & Yue, 2001; Keisker et al., 2009), with more controversial findings for SMA and CMA (Dai et al., 2001; Dettmers et al., 1995; Keisker et al., 2009). This suggests that network activity in areas of the dorsolateral circuit (MI, PMv, IPL) is necessary for controlling static force of finger muscles (Dai et al., 2001). For precision grasp, such as the grasp used in reach to grasp tasks, the key hubs include the aIPS and PMv in the dorsolateral network, and V6A, PMd, and SMA in the dorsomedial network (Cavina-Pratesi et al., 2010, 2018; Culham & Valyear, 2006; Vesia et al., 2017).

Taken together, these studies suggest that dorsolateral and dorsomedial circuits interact to achieve appropriate grasping behaviors, arguing against the dual visuomotor model viewing two independent fronto-parietal pathways to be responsible for reaching (dorsomedial network) and grasp movements (dorsolateral network). As previously suggested by (Grafton, 2010; Milner & Goodale, 2008), one approach to address some of the issues raised in the literature would be to account for the type of the task, as many paradigms engage some degree of both reach and grasp components. Accordingly, we hypothesized that a prototypical grasping task (without reach movement) would be subserved by the dorsolateral circuit, while tasks combining reach and fine grasp movements would engage both circuits.

We were also interested to explore the visuomotor model in the primary motor cortex (MI), which is the common output of the dorsolateral and dorsomedial circuits (Karl & Whishaw, 2013). In both human (Geyer et al., 1996) and nonhuman primates (He, Dum, & Strick, 1993), MI area can be divided into

two subregions. In the human brain, MI-4a and MI-4p differ in terms of cyto-, myelo- and chemoarchitectony: MI-4a is lying in the rostral part of MI located caudally to the dorsal premotor cortex, and MI-4p is the caudal part lying in the depth of the central sulcus next to SI-3a (Geyer et al., 1996). Rathelot et al. (Rathelot & Strick, 2009) showed a differential distribution of the cortico-motoneuronal cells for MI-4a and MI-4p in the macaque brain, resulting in a new view of MI organization, with monosynaptic connections from MI-4a to interneurons in the intermediate zone of the spinal cord, and monosynaptic connections from MI-4p directly to motoneurons in the ventral horn of the spinal cord. Monosynaptic input from the cerebral cortex to motoneurons is a relatively new phylogenetic feature (Kuypers, 1981), providing the ability to produce independent movements of the fingers and thus skilled movements such as precise grasp and tool manipulation. As a result, MI-4p is considered as the new MI, as compared to the phylogenetically older MI-4a, which is associated with less complex motor patterns (Rathelot & Strick, 2009). In humans, the functional role of MI-4a and MI-4p in human studies remains debated. On one hand, an fMRI study in healthy participants has observed a functional dissociation between MI-4a and MI-4p, with higher fMRI activity related to a flexion-extension task of the fingers in MI-4a than in MI-4p, while the reverse was observed for a sequential finger tapping requiring to move the fingers independently (Jaillard, Martin, Garambois, Lebas, & Hommel, 2005). Similar dissociations were also found in other stroke studies. The anatomo-functional subdivision of MI hand area has been related to subregions subserving different roles in motor control with MI-4p recruited by tasks engaging cognitive (Sharma, Jones, Carpenter, & Baron, 2008), attentional (Binkofski et al., 2002) or distal components (Vigano et al., 2019). In contrast, a meta-analysis showed that MI-4a activity was related to precision (versus force) handgrip, and MI-4p was related to dynamic (versus static) handgrip (King, Rauch, Stein, & Brooks, 2014). Here, we explored MI-4a and MI-4p separately, based on the assumption that MI-4p may be the output of precise grip tasks requiring independent finger movements, while MI-4a would drive simple motor tasks without independent finger movements, such as handgrip.

The main goal of this study was to determine using fMRI the neural structures engaged in motor hand recovery, in relation with the dorsolateral and dorsolateral frontoparietal circuits and the dual visuomotor model.

We first characterized motor hand recovery in patients with moderate to severe ischemic hemispheric stroke with two types of grasping tasks: a handgrip force task measuring the maximum force grip using a dynamometer, and a reach and grasp task requiring manual dexterity (i.e. precision grip) using the Purdue pegboard Task (PPT). Second, we measured fMRI activity elicited by a passive sensorimotor task of the paretic hand as described in Hannanu et al. (2017). As the regional fMRI BOLD-contrast signal is monotonically related to underlying neural activity in the frontoparietal cortex, it is possible, by comparing movement and rest periods, to measure changes in sensorimotor system activity reflecting motor behavioral performances following stroke. Therefore, to assess the neural correlates of handgrip force and PPT, we correlated behavioral performances

with fMRI activity measures from the sensorimotor network including the dorsolateral and dorsomedial regions during stroke recovery. We used a passive sensorimotor task because most patients were not able to perform active hand movements due to upper limb motor paresis at the subacute period of stroke. During the passive task, an examiner standing in the scanner room during the fMRI scan performed the flexion extension of the patient's paretic wrist. As both motor behavioral performances and fMRI activity patterns change during motor recovery (Favre et al., 2014; Marshall et al., 2000), we performed a longitudinal study combining behavioral and fMRI measurements at one month following stroke (M0), and six months (M6) and 24 months (M24) later.

Third, to determine the neural structures engaged in recovery of handgrip force and PPT, we modeled handgrip and PPT recovery using linear mixed models (LMMs) testing the effects of fMRI activity of ROIs spanning the frontoparietal networks on motor recovery. We also tested the effects of stroke features in the LMMs, including the hemispheric side of the lesion due to frontoparietal pathway asymmetry (Sainburg, 2002; Thiebaut de Schotten et al., 2011). Of note, patients were enrolled in a clinical trial assessing stem cell therapy (Jaillard et al., 2020). They were included at one month following stroke (M0) and were followed until the late chronic period of stroke (M24).

2. Material and methods

We report how we determined our sample size, all data exclusions, all inclusion/exclusion criteria, whether inclusion/exclusion criteria were established prior to data analysis, all manipulations, and all measures in the study.

2.1. Participants

We performed the ISIS-HERMES study, a monocenter (Grenoble Alpes University Hospital (CHUGA), France), prospective, randomized, open-label, controlled trial with blind outcome evaluation. Patients were randomized to receive IV injection of MSCs (Treatment group) or rehabilitation alone (Control group). Both ISIS (Intravenous Stem cells after Ischemic Stroke) and HERMES (HEuristic value of multimodal MRI to assess MEsenchymal stem cell therapy in Stroke) studies were approved by the ethics committee (Comité de Protection des Personnes). The trial is registered with [ClinicalTrials.gov](https://clinicaltrials.gov), number NCT00875654.

We enrolled 31 patients aged 18–70 years with an ischemic stroke within the anterior circulation territory, less than two weeks post-onset, with persistent neurological deficits (NIHSS ≥ 7), assessed just before cell injection. We did not include patients with brainstem or minor stroke, previous neurological or psychiatric disease, or severe comorbid medical disease. All patients were admitted to the CHUGA Stroke Unit for inclusion and follow-up visits. They received standard medical and rehabilitation care. The baseline visit (M0) was performed just before the MSC injection. Follow-up visits were performed after six months (M6) and 24 months (M24) following M0.

Thirty two healthy participants aged 18–70 years were also included in the ISIS-HERMES study to undergo the experimental motor tasks and the MRI protocol.

All patients and healthy participants gave written informed consent.

2.2. Behavioral tests

Patients underwent the Purdue Pegboard Test [PPT] (<http://www.equipement-ergotherapie.com/8-dextérité-manipulation.html>) (Rapin, Tourk, & Costa, 1966) and the LaFayette Dynamometer (<https://www.prohealthcareproducts.com/100-kg-220lb-hand-grip-dynamometer-lafayette-instruments/>) (Sunderland, Tinson, Bradley, & Hewer, 1989) that were used as the main outcome measures at M0, M6, and M24.

The purpose of the PPT was to test fine manual dexterity comprising reaching and grasping components. Features of the measure are described online: https://www.strokengine.ca/en/indepth/ppt_indepth. During the test, patients were seated with the Purdue Pegboard on a table in front of him/her. The testing board consisted of a board with 2 cups across the top containing 25 pins each and two vertical rows of 25 small holes down the center. Patients were asked to place as many pins as possible down the row within 30 s, first with the paretic hand. We measured the total number of pins placed in the assigned row using the paretic hand in the allotted time. The trial was repeated 3 times and a PPT score was calculated based on the number of pins placed down averaged across the 3 trials. A score of 0 was given when the participant could not perform the task due to upper limb paresis.

The dynamometer by measuring grip force involves mainly grasping components. The purpose of the handgrip force test was to measure the maximum isometric force of the hand and forearm muscles. Patients held the dynamometer in the hand, with the arm at right angles and the elbow by the side of the body. They were asked to squeeze the dynamometer with maximum isometric effort, which is maintained for about 5 s, without other body movements (<https://www.topendsports.com/testing/tests/handgrip.htm>). The grip force score was obtained by computing the average of 3 trials. Both PPT and dynamometer provide reliable and valid evaluation for hand motor function (Heller et al., 1987), and force (Sunderland et al., 1989) respectively.

In addition, we assessed stroke severity using the National Institutes of Health Stroke Scale (NIHSS) (Brott et al., 1989), functional independence using the Barthel Index of activities of daily living (Mahoney & Barthel, 1965), and neurological disability using the Modified Rankin Score (mRS) (van Swieten, Koudstaal, Visser, Schouten, & van Gijn, 1988). Motor impairment was assessed with the motor-Fugl Meyer Score (FMS, range 0–100) (Sullivan et al., 2011). The motor-FMS is a validated and reliable scale assessing motor function based on reflex activity, volitional movements and coordination of the upper and lower limbs, widely used for post-stroke motor assessment in RCTs (Chollet et al., 2011).

Behavioral assessment was performed by a neuropsychologist (dynamometer, PPT), a stroke neurologist (neurological examination, NIHSS, Barthel, mRS) and a physiotherapist (FMS), all blind to treatment allocation, at baseline (one month after stroke) and at six and 24-month

follow-up. The behavioral and fMRI assessment time points are shown in Table 1.

2.3. MRI data acquisition

Passive task paradigm. We used a passive sensorimotor task for the paretic hand rather than an active task because most patients could not perform voluntary movements of the hand at baseline (M0), since they had hemiparesis due to stroke. Moreover, passive tasks have higher reproducibility because of lower associated neural activity variability related to the patient's degree of motor impairment, range, and speed of motion, and required effort. Test-retest reproducibility studies of passive limb movements have shown good reliability for both within and between sessions in healthy participants and stroke patients (Gountouna et al., 2010; Loubinoux et al., 2001; Quiton, Keaser, Zhuo, Gullapalli, & Greenspan, 2014). The task paradigm consisted of 8 cycles alternating 20 sec epochs of rest and 45° passive wrist flexion and extension at 1 Hz (Fig. 1). We studied the passive-FE for the paretic hand in patients and the right hand in healthy participants, as described in (Loubinoux et al., 2001) and (Hannanu et al., 2017). All participants were instructed to remain still and relaxed during the scan. One examiner standing inside the room administered movements by moving a forearm splint with an axis of rotation through the wrist. Movements were visually cued using a screen placed in front of the examiner. While care was taken to observe mirror movements of both hands and feet, none were observed.

MRI protocol. MRI was performed at 3T (Achieva 3.0T TX, Philips, The Netherlands) at the IRMaGe MRI facility (Grenoble, France) with a 32 channel head coil. We acquired high resolution structural images including sagittal 3D-T1-weighted (TR 7.75 ms, TE 3.62 ms, flip angle 9°, FOV: 252*192*252, 192 slices, voxel size = .98*0.98*1 mm, thickness = 1 mm, gap = 0 mm, duration = 339 sec) and 3D-FLAIR images (TR 8 sec, TE 342 ms, flip angle = 90°, FOV: 241*192*250, 274 slices, voxel size = .434*.434*.7 mm, thickness = 1.4 mm, gap = -.7 mm, duration = 424 sec). Then, we acquired 113 Echo planar images (EPI) for the passive task of the paretic hand using the following parameters: TR 3000 ms, TE 30 ms, field of view (FOV): 220*220*147 mm, 59 axial slices. Flip angle = 80°, voxels 2.3*2.3*2.3 mm³, gap = .25 mm, run duration = 348 s. Total acquisition time was 20 min. These sequences were part of the study MRI protocol including in the following order: T1, FLAIR, resting state, passive motor task, tactile sensory task, diffusion, and perfusion sequences. The total duration was one hour.

2.4. MRI data analysis

Lesion volumes were determined by manual delineation of FLAIR images (Kuhn et al., 1989) using MRIcron (<https://www.nitrc.org/projects/mricron>).

Data preprocessing and processing, was performed using Statistical Parametric Mapping (SPM12: <http://www.fil.ion.ucl.ac.uk/spm>), as described in (Hannanu et al., 2017). Of note, T1, FLAIR, and EPI images were not flipped. Following visual inspection for spatial artifacts, EPI time series were checked for temporal artifacts and realigned. Next, the T1-weighted and FLAIR images were coregistered and aligned to the mean of the EPI time series. Segmentation of the structural images (T1 and FLAIR) resulted in a deformation field that was used to spatially normalize the EPI data to Montreal Neurological Institute (MNI) space. Finally, the EPI images in MNI space were smoothed using a full-width at half maximum (FWHM) Gaussian kernel of 5*5*5 mm³. The structural T1-weighted and FLAIR images were also normalized to MNI space at 1 mm³ resolution. Intensity outliers were detected using ART (https://www.nitrc.org/projects/artifact_detect), with an interscan movement threshold of 1 mm, and a global interscan signal intensity threshold of 3 SD relative to the session mean. In 6 patients with significant head motions, the movement thresholds were adjusted to limit the number of outliers to 20% of the total volumes.

The first level voxel-wise analysis was performed in SPM12 using a general linear model including passive movement conditions, outliers and head motion estimates as regressors, and a high-pass (128hz) filter. The task regressors were convolved with a canonical HRF. Contrasts of the movement related parameter estimates were generated for subsequent ROI analyses.

To explore the relationship between the sensorimotor network and outcome, we selected a priori ROIs that are reported as part of the sensorimotor network, and the parietal areas of the dorsolateral and dorsomedial networks, resulting in 36 left and 36 right ROIs listed in Table 2. For more information on these ROIs, see (Borra et al., 2017; Doyon, Penhune, & Ungerleider, 2003; Eickhoff et al., 2010; Hannanu et al., 2017; Pandya, 2015b). Prefrontal, occipital and temporal areas were not included because they were not activated by the passive sensorimotor task (Fig. 2), and thus could not be sensitive to task effects. The 36*2 ROIs were extracted from the SPM Anatomy Toolbox (Eickhoff, Paus, et al., 2007) and from the AAL atlas (Tzourio-Mazoyer et al., 2002). Using these ROIs, we

Table 1 – Hand motor task including Purdue Pegboard Test (PPT) and Grip Force (Grip) and fMRI assessment time points.

Study time points	Mean Delay from stroke onset	Hand motor tasks	MRI	Clinical assessment
Stroke onset	Day 0	–	–	NIHSS
Inclusion	Day 4–15	–	–	NIHSS + MRS + BI
Baseline visit (M0)	Day 31 (27–35)	PPT + Grip	fMRI	NIHSS + MRS + BI
Cell therapy	Day 32 (28–35)	–	–	NIHSS
Six-month follow-up (M6)	Day 210 (±15)	PPT + Grip	fMRI	NIHSS + MRS + BI
Two-year follow-up (M24)	Day 760 (±30)	PPT + Grip	fMRI	NIHSS + MRS + BI
NIHSS indicates the National Institutes of Health Stroke Scale, mRS the modified Rankin Score, and BI the Barthel Index.				

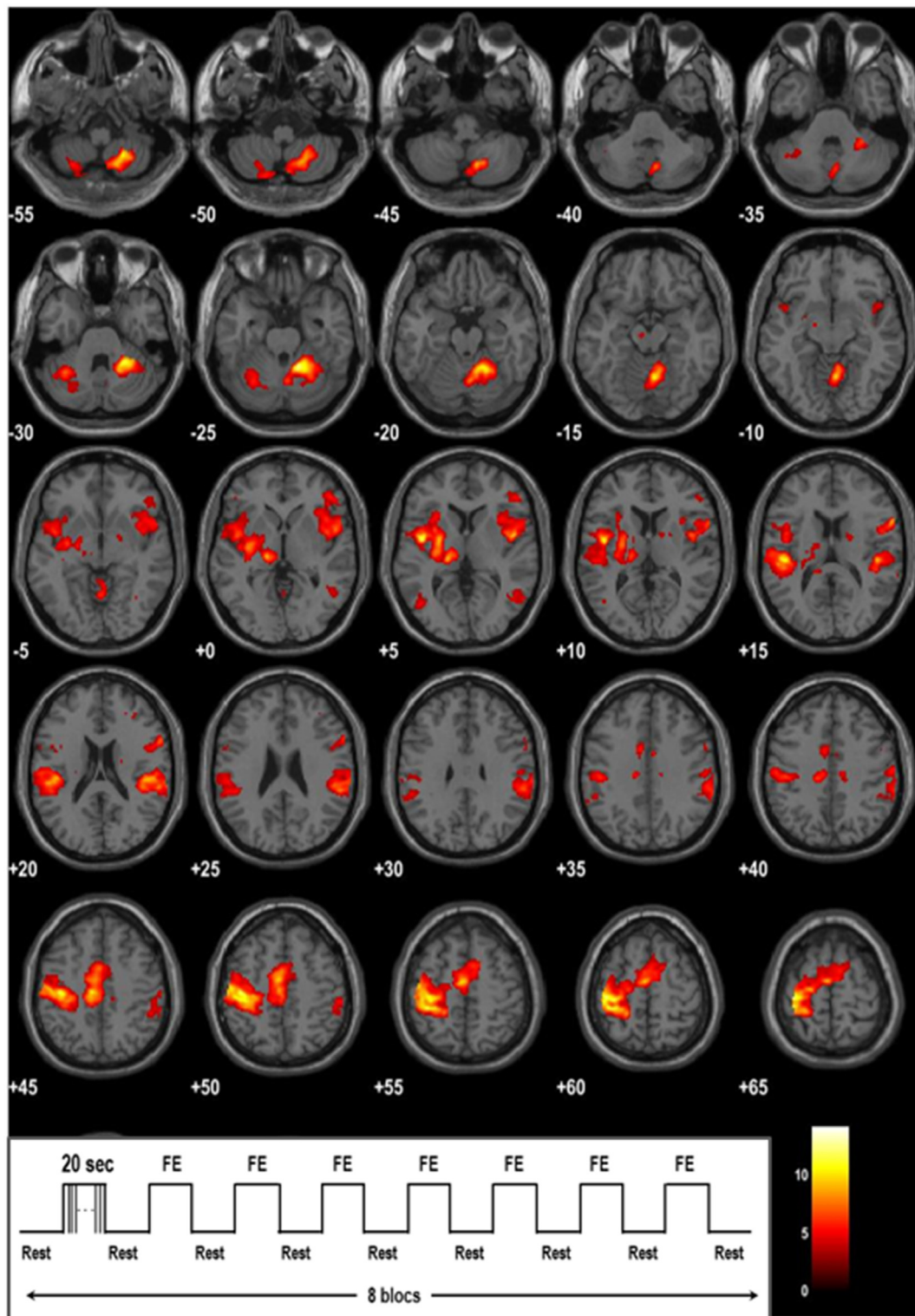


Fig. 1 – T1-rendered montage of brain activity during passive movement of the right hand in 32 healthy participants. Axial slices are displayed with for z MNI coordinates indicated in the bottom left corner in mm. A threshold of $p < .05$ corrected for multiple comparisons is used to allow visualization of the spatial distribution of activity. The color of the bar indicates the intensity of brain activity (t-statistic). The right hand is the referent hand. The left hemisphere is represented on the left side of picture (neurological convention).

Table 2 – Abbreviations for the 36 brain regions included in the analysis. In the text, i-indicates ipsilesional and c-contralesional ROIs. BA indicates Brodmann area and IPL inferior parietal lobule.

No.	Abbreviation	Full ROI Name
1.	MI-4a	Primary Motor cortex (MI) BA 4a
2.	MI-4p	Primary Motor cortex (MI) BA 4p
3.	SI-3a	Primary Somatosensory cortex (SI) BA 3a
4.	SI-3b	Primary Somatosensory cortex (SI) BA 3b
5.	SI-1	Primary Somatosensory cortex (SI) BA 1
6.	SI-2	Primary Somatosensory cortex (SI) BA 2
7.	dPMC	dorsal PreMotor Cortex BA6
8.	vPMC	ventral PreMotor Cortex BA6
9.	SMA	Supplementary Motor Area BA6
10.	Cereb V	Cerebellum lobule V
11.	Cereb VI	Cerebellum lobule VI
12.	Cereb VIIa	Cerebellum lobule VIIa
13.	Cereb VIIb	Cerebellum lobule VIIb
14.	MCA	Motor Cingulate Area
15.	BA44	BA44
16.	Insula	Anterior Insula
17.	Lenticular	Lenticular nucleus
18.	Thal-M	Motor Thalamus
19.	Thal-M	Somatosensory Thalamus
20.	OP1	Parietal operculum OP1 (S2)
21.	OP4	Parietal operculum OP4 (PV)
22.	IPL PF	Inferior Parietal Lobule (IPL) Supramarginal gyrus (SMG) BA 40 F
23.	IPL PFCm	IPL SMG BA 40
24.	IPL PFCm	IPL SMG BA 40
25.	IPL PFop	IPL SMG BA 40
26.	IPL PFCt	IPL SMG BA 40
27.	AIPS IPL1	Ventral anterior intraparietal sulcus (vAIPS) hIP1 (Scheperjans 2008a, b)
28.	AIPS IPL2	Lateral anterior intraparietal sulcus (lAIPS) hIP2 (Choi 2006)
29.	AIPS IPL3	Anterior medial intraparietal sulcus (amIPS) (Scheperjans 2008a, b)
30.	SPL 5ci	Superior Parietal Lobule (SPL) BA 5ci
31.	SPL 5L	SPL BA 5L
32.	SPL 5M	SPL BA 5M
33.	SPL 7A	Superior Parietal Lobule (SPL) BA 7A
34.	SPL 7M	SPL BA 7M (Posterior precuneus, hypothetic V6Ad)
35.	SPL 7P	SPL BA 7P
36.	SPL 7 PC	SPL BA 7 PC

computed peak ROI Cohen's *d* effect sizes (*d* values) that were derived from *t* maps for each participant using the 'Volumes toolbox' SPM extension (Volkmar Glaucher <http://sourceforge.net/projects/spmtools>). Cohen's *d* values were used to assess the relationship between passive-FE related brain activity and behavioral scores.

2.5. Statistical analysis

Clinical characteristics and behavioral scores are reported using: 1) median with percentiles and mean with standard deviations for continuous data and 2) absolute counts and percentages for categorical data. PPT and handgrip tests were scored 0 when patients could not perform the tasks due to hand paresis. Comparisons of PPT and handgrip performances between healthy participants and patients at each session were performed using univariate analyses of variance (ANOVA) after adjusting for the effects of age and sex and bootstrapping with 1000 replications. The influence of time and sensorimotor activity on hand motor recovery was analyzed using a linear mixed model (LMM)

accommodating repeated measures and including patient as a random effect (Cheng, Edwards, Maldonado-Molina, Komro, & Muller, 2010; Maas & Snijders, 2003). The dependent variables were the behavioral scores measured 3 times per patient. For both PPT and grip force scores, we first modeled the fixed effects of time from M0 (baseline), M6, and M24 (end of follow-up), adjusting for cell therapy and lesion side. Bonferroni correction was applied for adjustment for multiple comparisons of sessions. Then, we tested the effects of sensorimotor activity on PPT and handgrip over time, after adjustment for cell therapy. The effects of demographic and stroke characteristics including age, sex, lesion side, and volume were also tested and kept in the model if significant. Statistical significance was determined with the *F*-test ($p < .05$) and model fit was estimated with the $-2 \log$ likelihood ($-2LL$), Akaike Information Criterion (AIC), calibration and discrimination (Steyerberg et al., 2001). Calibration was examined by plotting adjusted predicted versus observed values for the behavioral scores. Discrimination assessed prediction accuracy by examining the distribution of the Pearson residuals and plotting residuals

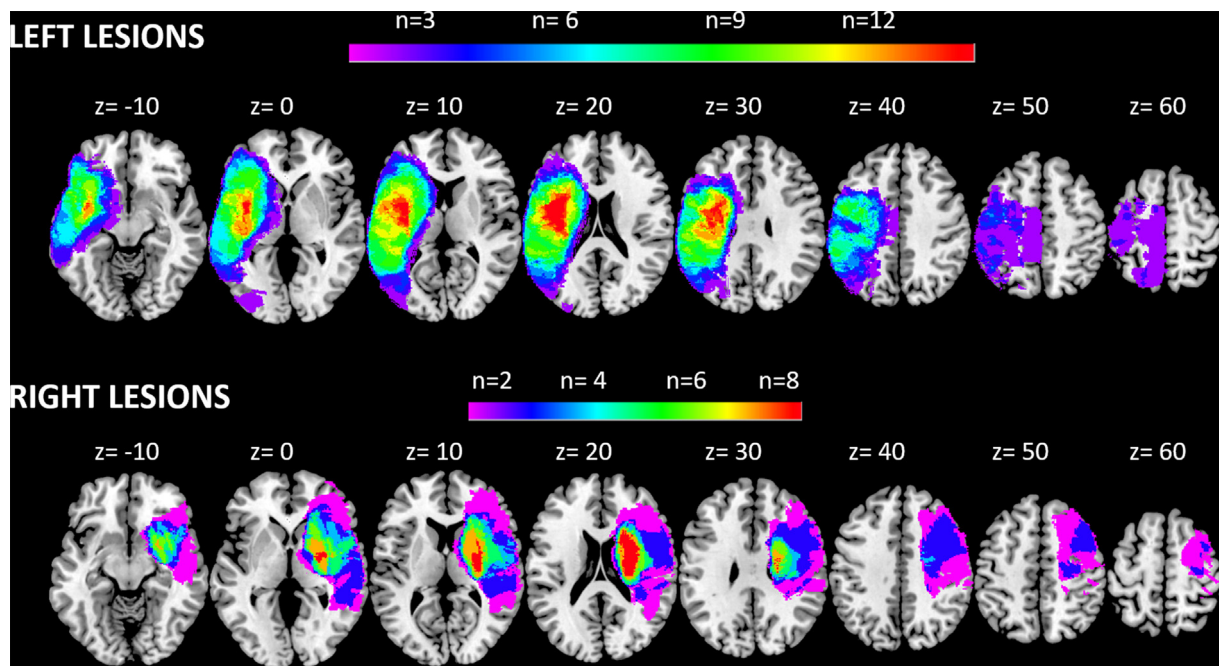


Fig. 2 – Overlay lesion plots of the 27 patients with left and right hemispheric stroke lesions. The number of overlapping lesions (n) is shown by different colors coding increasing frequencies from violet to red.

versus observed values. SPSS 20.0 was used for data analysis.

3. Results

3.1. Participants

Thirty-one patients (mean age = 52 ± 10 years; 22 males; 21 left-sided) were recruited between Aug 31, 2010 and Aug 31, 2015. Five patients could not undergo hand motor evaluation because of stroke severity resulting in severe neglect ($N = 1$), anosognosia ($N = 1$), head movements ($N=1$), or refusal ($N = 1$).

Therefore, twenty-seven patients remained in the study (mean age = 52.69 ± 10 years; 19 males; 17 left-sided lesions). Mean baseline NIHSS = 13.74 ± 4.63 , and motor-FMS 36.41 ± 28.21 , indicating moderate to severe neurological deficits. Among the 27 patients, 13 received intravenous stem cell therapy at baseline (Jaillard et al., 2020). Patient characteristics at baseline are presented in Table 3. The left and right hemispheric overlapping lesions plots are presented in Fig. 2. In addition, Thirty two healthy participants were included in the study and underwent both behavioral and fMRI assessment (mean age = 25 ± 6 years; 15 males).

Behavioral measures: Descriptive statistics are presented in Table 4 for the 32 healthy participants and 27 patients.

Table 3 – Patients' characteristics at baseline (one month following stroke onset) for left and right lesion subgroup. N = 27.

Variables	All (n = 27)		Left Lesion (n = 17)		Right Lesion (n = 10)		p values*
Numerical	Mean (SD)	Median (IQR)	Mean (SD)	Median (IQR)	Mean (SD)	Median (IQR)	
Age, years	53.15 (9.54)	53 (13)	55 (8.79)	57 (16)	50 (10.40)	51 (13)	.204
Lesion volume, cm ³	100.67 (63.51)	83 (103)	105.65 (55.23)	112 (83)	92.20 (78.13)	57.50 (143)	.41
Motor FMS	36.41 (28.21)	31 (34)	43.53 (32.88)	34 (62)	24.30 (10.90)	20.50 (10)	.188
Motor NIHSS	6.38 (2.64)	6.50 (4)	6.19 (3.23)	6 (5)	6.70 (1.33)	7 (1)	.787
NIHSS	13.74 (4.63)	12 (5)	14.88 (5.46)	12 (10)	11.80 (1.48)	12 (2)	.376
Barthel Index	45 (31.89)	45 (55)	42.06 (35.97)	45 (63)	50 (24.38)	47.50 (31)	.606
Rankin	3.78 (.51)	4 (0)	3.71 (.59)	4 (1)	3.90 (.32)	4 (0)	.572
PPT - Paretic Hand	1.3 (3.28)	0 (0)	2.06 (3.98)	0 (3)	0 (0)	0 (0)	.24
Grip - Paretic Hand	3.93 (9.95)	0 (0)	6.24 (12.06)	0 (8)	0 (0)	0 (0)	.127
Categorical	n	%	n	%	n	%	
Male	19	70.4	11	64.7	8	80	.666
Cell therapy	13	48.1	9	52.9	4	40	.695

SD, standard deviation; IQR, interquartile range; FMS, Fugl–Meyer Scale; NIHSS, National Institutes of Health Stroke Scale. *Comparison of left and right lesion subgroup, Mann–Whitney U test was used for numerical variables, and Chi-square/Fisher test for categorical variables, comparing data from left and right side lesion subgroups.

Table 4 – Descriptive statistics (Mean, Standard Deviation (SD), Median, Interquartile Range (IQR)) for Purdue Pegboard Test (PPT) and grip force (Grip) performed with the dominant hand in 32 controls and the paretic hand in 27 patients assessed at baseline (M0), six month (M6) and two-year (M24) follow-up.

Group/Session		Performance	Mean	SD	Median	IQR
Healthy Participants (n = 32)		PPT	16.75	1.64	16.67	2.67
		Grip	30.44	11.77	26.585	14.92
Patients	M0 (n = 27)	PPT	1.3	3.279	0	0
		Grip	3.93	9.95	0	0
	M6 (n = 25)	PPT	2.84	4.58	0	7
		Grip	7	11.712	0	11
	M24 (n = 25)	PPT	3.48	5.144	0	9
		Grip	9.62	14.688	0	21

Stroke patients had significantly lower scores than healthy participants at each session in the PPT ($p = .001$) and handgrip ($p = .001$). There was no significant effect of age for PPT ($p = .852$) and handgrip ($p = .733$). In patients with stroke, men performed significantly better than women in the handgrip force ($p = .002$), but not in the PPT ($p = .125$). LMM analyses showed that PPT and grip force improved significantly over time, after adjusting for lesion side, and cell therapy, indicating significant recovery of hand motor function over time (Table 5; Fig. 3). For PPT, there was a significant effect of time from baseline to M24 (mean difference = 1.65, $p = .010$) and from baseline to M6 (mean difference = 1.42, $p = .029$), but not between M6 and M24 (mean difference = .23, $p = 1.00$), with a significant effect of lesion side (mean difference 'left – right lesion' = 3.14, $p = .038$). For handgrip force, there was a significant effect of time from baseline to M24 (mean difference = 5.16, $p < .001$), with a trend from baseline to M6 (mean difference = 2.68, $p = .072$) and no difference between M6 and M24 (mean difference = 2.47, $p = .127$). There was a trend for the lesion side (mean difference 'left – right lesion' = 7.53, $p = .092$). Of note, age, gender, and lesion volume had no significant effect on recovery in these models.

3.2. MRI measures

The fMRI activity map related to the passive flexion extension (FE) of the right wrist in 32 healthy participants showed a typical activity in the sensorimotor network, and in posterior parietal areas (Fig. 1). To explore hand motor recovery using fMRI, we analyzed fMRI sessions in the 27 patients. Among the 81 scheduled sessions (3 time points for 27 patients), 13 fMRI sessions were not performed because of wrist spasticity and three additional sessions were excluded from analysis because

Table 5 – Linear mixed model of PPT and grip force showing the effects of time over time (2 years follow-up), lesion side and cell therapy, with F test and p values.

Factors	PPT		Handgrip force	
	F	p value	F	p value
Intercept	7.56	.011	7.02	.014
Time	5.74	.006	9.78	<.001
Lesion side	4.83	.038	3.08	.092
Cell therapy	2.05	.165	1.14	.296

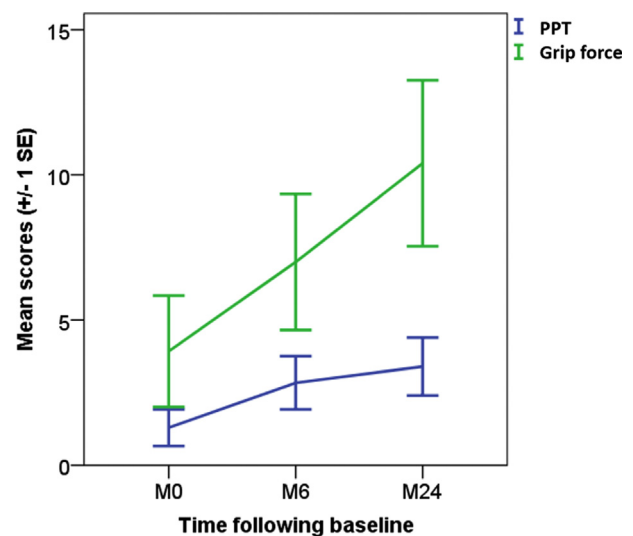


Fig. 3 – Performances of the Purdue Pegboard Test (PPT) and the handgrip force over time in 27 patients.

of excessive head movements (two sessions). The remaining 66 sessions (23 at M0, 25 at M6, and 18 at M24) were included for further analysis. Correlations between hand dexterity, grip force, and the sensorimotor regions are presented for each session (M0, M6 and M24) in Table 6 for the sensorimotor network and Table 7 for the posterior parietal cortex. Broadly, the correlations between most of the canonical motor ROIs and motor tasks were not significant at baseline (M0). Then, at M6, the ipsilesional canonical motor ROIs (except i-PMv), c-PMV, c-SMA, and contralesional cerebellar ROIs became significant. The other sensorimotor ROIs were not correlated with PPT and grip force at M0, except for c-MCA, c-BA44, and c-lenticular nucleus. In the posterior parietal network, IPL and OP ROIs at M0 were not correlated with PPT and grip force at M0, while the contralesional ROIs showed significant correlations with PPT and grip force at M6 and M24. By contrast, contralesional AIPs, and ipsilesional posterior/caudal SPL including BA 5M, 7A, 7M, and 7P showed significant correlations with motor tasks at M0 that faded over time. Of note, correlations were significant at M6 for ipsilesional BA 5L, 5M and 7A, and at M24 for ipsilesional BA 5L and 5M.

Hand motor recovery was explored using a LMM analysis including time and lesion side. Cell therapy was included in the model to account for any effect on the outcome. The best

Table 6 – Correlations between motor scores and fMRI activity in the sensorimotor network at M0, M6 and M24. *p* values are provided with bootstrapping (1000 replications). ROI correlations included in the LMM models are bold.

	M0				M6				M24			
	PPT		GRIP		PPT		GRIP		PPT		GRIP	
	<i>r</i>	<i>p</i>	<i>r</i>	<i>p</i>	<i>r</i>	<i>p</i>	<i>r</i>	<i>p</i>	<i>r</i>	<i>p</i>	<i>r</i>	<i>p</i>
Canonical sensorimotor regions												
i-MI-4a	.332	.141	.294	.195	.552	.006	.606	.002	.653	.006	.597	.015
c-MI-4a	.295	.195	.341	.131	.646	.001	.599	.003	.333	.207	.598	.014
i-MI-4p	.327	.148	.411	.064	.444	.034	.452	.031	.508	.045	.439	.089
c-MI-4p	.208	.367	.366	.102	.217	.319	.185	.398	.273	.307	.287	.282
i-SI-3a	.406	.067	.441	.046	.532	.009	.464	.026	.718	.002	.454	.078
c-SI-3a	.247	.28	.377	.092	.342	.110	.176	.421	.232	.388	.256	.339
i-SI-3b	.297	.191	.294	.196	.537	.008	.570	.004	.569	.021	.514	.042
c-SI-3b	.29	.203	.38	.089	.629	.001	.507	.014	.238	.375	.384	.142
i-SI-1	.254	.266	.236	.303	.595	.003	.685	.000	.627	.009	.644	.007
c-SI-1	.381	.088	.412	.064	.615	.002	.485	.019	.227	.397	.379	.148
i-SI-2	.448	.042	.507	.019	.535	.008	.538	.008	.456	.088	.548	.034
c-SI-2	.416	.061	.474	.03	.593	.003	.495	.016	.13	.645	.24	.389
i-dPMC	.332	.141	.03	.187	.511	.013	.621	.002	.595	.015	.575	.02
c-dPMC	.253	.269	.241	.293	.486	.019	.452	.031	.188	.486	.29	.276
i-vPMC	-.069	.766	-.037	.873	.048	.829	-.034	.877	.135	.617	.022	.935
c-vPMC	.396	.075	.418	.06	.532	.009	.506	.014	.496	.051	.532	.034
i-SMA	.287	.207	.315	.164	.411	.052	.373	.080	.364	.166	.543	.03
c-SMA	.337	.135	.404	.069	.494	.017	.424	.044	.354	.178	.583	.018
Cerebellar network (cerebellar lobules)												
i-V	.035	.879	.07	.762	.284	.189	.217	.321	.573	.020	.464	.07
c-V	.217	.345	.105	.65	.643	.001	.544	.007	.771	.000	.610	.012
i-VI	-.12	.605	-.069	.767	.271	.211	.184	.400	.122	.653	.275	.303
c-VI	.338	.134	.428	.053	.63	.001	.492	.017	.779	.000	.583	.018
i-VIIIa	-.012	.96	-.046	.844	.309	.151	.185	.398	.385	.141	.413	.112
c-VIIIa	.275	.228	.27	.236	.495	.016	.312	.148	.579	.019	.444	.085
i-VIIIb	.066	.775	.169	.464	.403	.056	.216	.322	.31	.243	.349	.186
c-VIIIb	.402	.071	.372	.097	.47	.024	.275	.204	.612	.012	.399	.126
Sensorimotor related regions												
i-MCA	.147	.525	.268	.241	.351	.101	.308	.153	.229	.394	.376	.152
c-MCA	.294	.196	.449	.041	.361	.09	.208	.341	.295	.267	.325	.22
i-BA44	-.037	.875	-.06	.795	.002	.993	-.05	.822	.314	.237	.209	.437
c-BA44	.442	.045	.462	.035	.25	.25	.229	.294	.323	.222	.314	.236
i-ant Insula	.204	.376	.167	.469	-.07	.768	-.077	.727	.377	.149	.395	.13
c-ant Insula	.236	.302	.264	.247	.292	.177	.275	.205	.226	.399	.379	.148
i-lenticular	.088	.704	.002	.993	.201	.358	.009	.969	-.07	.804	.087	.748
c-lenticular	.411	.064	.454	.039	-.23	.301	-.262	.227	.03	.913	.114	.674
i-M-thal.	-.062	.789	-.171	.458	-.16	.461	-.161	.462	.085	.756	.128	.637
c-M-thal.	.222	.334	.261	.253	-.11	.625	-.227	.298	.004	.988	.123	.651
i-S-thal.	.095	.682	-.023	.921	-.17	.436	-.09	.682	.051	.85	.154	.568
c-S-thal.	.19	.41	.169	.463	.232	.287	.106	.632	.046	.866	.161	.552
<i>r</i> indicates Pearson's coefficient, i-for ipsilesional, and c-for contralesional. See Table 2 for the list of ROIs.												

linear mixed model for dexterity recovery of the paretic hand assessed with PPT [-2LL = 255; AIC = 259; $R^2 = .93$] was obtained with a set of sensorimotor regions including ipsilesional MI-4p by time interaction [$F(3, 33) = 3.82, p = .019$], ipsilesional superior parietal lobule (SPL) 7M by time interaction [$F(3, 31) = 4.79, p = .007$], ipsilesional parietal operculum (OP1) [$F(1, 39) = 9.1, p = .004$], lesion side [$F(1, 20) = 6.01, p = .024$], and cell therapy [$F(1, 22) = 1.32, p = .26$]. Coefficient estimates are reported in Table 8. Significant ROIs are represented in Fig. 3A.

The LMM for grip force of the paretic hand [-2LL = 358; AIC = 362; $R^2 = .96$] included ipsilesional MI-4a by time interaction [$F(1, 41) = 9.0, p < .001$], ipsilesional OP1 [$F(1,$

42) = 7.32, $p = .011$], and contralesional IPL-PFt by lesion side [$F(1, 37) = 8.95, p = .001$], and cell therapy [$F(1, 25) = .76, p = .391$]. Coefficient estimates are reported in Table 9. Significant ROIs are represented in Fig. 4.

4. Discussion

This longitudinal study explored 27 patients with moderate to severe subacute stroke using concomitant sensorimotor hand behavioral and fMRI measurements with a passive FE task from the subacute to the chronic period of stroke. We assessed the relationship between manual dexterity and

Table 7 – Correlations between motor scores and fMRI activity in the posterior parietal cortex at M0, M6 and M24 (See Table 2 for ROI list). *p* values are provided with bootstrapping (1000 replications). ROI correlations included in the LMM models are bold.

	M0				M6				M24			
	PPT		GRIP		PPT		GRIP		PPT		GRIP	
	<i>r</i>	<i>p</i>	<i>r</i>	<i>p</i>	<i>r</i>	<i>p</i>	<i>r</i>	<i>p</i>	<i>r</i>	<i>p</i>	<i>r</i>	<i>p</i>
Parietal operculum												
i- OP1	.122	.597	.181	.432	.527	.010	.590	.003	.454	.077	.534	.033
c-OP1	.068	.769	.096	.678	.593	.003	.599	.003	.334	.207	.483	.058
i-OP4	.148	.523	.134	.561	.331	.123	.194	.375	.449	.081	.318	.231
c-OP4	.394	.078	.327	.148	.574	.004	.604	.002	.317	.231	.522	.038
Inferior parietal lobule												
i-IPL-PF	.043	.854	.113	.626	.231	.288	.283	.191	.341	.196	.35	.184
c-IPL-PF	.346	.124	.349	.120	.641	.001	.543	.007	.571	.021	.616	.011
i-IPL-PFcm	.052	.822	.125	.589	.408	.054	.514	.012	.474	.064	.473	.064
c-IPL-PFcm	.173	.453	.171	.459	.463	.026	.309	.151	.339	.200	.411	.114
i-IPL-PFm	.055	.812	.015	.948	.262	.228	.288	.182	.168	.534	.276	.300
c-IPL-PFm	.297	.19	.41	.065	.481	.02	.355	.096	.478	.061	.572	.021
i-IPL-PFop	.097	.674	.19	.411	.418	.047	.576	.004	.381	.145	.472	.065
c-IPL-PFop	.147	.525	.15	.517	.677	.000	.634	.001	.512	.043	.642	.007
i-IPL-PFt	.021	.927	.063	.788	.184	.401	.13	.554	.191	.479	.261	.329
c-IPL-PFt	.306	.177	.342	.129	.738	.000	.645	.001	.549	.028	.634	.008
Anterior bank of intraparietal sulcus												
i-IPL-AIPS1	.221	.336	.139	.547	–.003	.99	.0740	.739	.642	.007	.553	.026
c-IPL-AIPS1	.432	.050	.553	.009	.226	.299	.193	.377	–.038	.89	.142	.599
i-IPL-AIPS2	.37	.098	.34	.132	.296	.170	.401	.058	.329	.213	.420	.105
c-IPL-AIPS2	.468	.032	.576	.006	.211	.333	–.008	.97	–.061	.824	–.022	.935
i-IPL-AIPS3	.414	.062	.355	.115	.183	.404	.118	.593	.210	.435	.24	.372
c-IPL-AIPS3	.515	.017	.571	.007	.257	.237	.235	.28	.147	.586	.188	.487
Superior parietal Lobule												
i-SPL-5ci	.028	.905	.095	.682	.197	.368	.11	.616	–.127	.64	.003	.991
c-SPL-5ci	.08	.73	.085	.714	.277	.201	.167	.447	.276	.301	.184	.496
i-SPL 5L	.216	.347	.224	.33	.63	.001	.649	.001	.592	.016	.656	.006
c- SPL 5L	.37	.099	.279	.221	.367	.085	.427	.042	.185	.494	.388	.137
i-SPL 5M	.516	.017	.634	.002	.477	.021	.418	.047	.428	.098	.633	.009
c- SPL 5M	.278	.223	.166	.472	.204	.35	.276	.203	–.005	.985	.136	.617
i-SPL 7A	.63	.002	.587	.005	.55	.007	.612	.002	.383	.143	.401	.124
c- SPL 7A	.278	.222	.232	.311	.068	.759	.036	.87	.064	.813	.081	.767
i-SPL 7M	.537	.012	.633	.002	.235	.280	.022	.919	.454	.077	.264	.322
c- SPL 7M	.415	.062	.481	.027	.197	.369	–.007	.975	.283	.289	.139	.607
i-SPL 7P	.509	.018	.452	.040	.219	.315	.022	.92	.151	.577	.044	.870
c- SPL 7P	.298	.190	.254	.266	.136	.535	.008	.971	–.043	.875	–.081	.766
i-SPL 7 PC	.310	.172	.351	.119	.348	.104	.237	.276	.268	.316	.351	.183
c- SPL 7 PC	.225	.328	.23	.315	.328	.126	.34	.113	.234	.383	.242	.367

r indicates Pearson's coefficient, i-for ipsilesional, and c-for contralesional. See Table 2 for the list of ROIs.

handgrip force and sensorimotor region activity at one month following stroke (M0) and then six months (M6) and two years later (M24). Then, using a linear mixed model analysis, we assessed the role of regional sensorimotor activity on hand motor recovery as a function of time. Our findings showed an association between fMRI activity patterns and hand motor recovery with a spatiotemporal pattern. Hand performance was correlated with fMRI activity in (1) AIPS and SPL ROIs at the early phase of recovery (M0); (2) bilateral regions of the sensorimotor network and the parietal operculum, IPL, and SPL at the early chronic phase of recovery (M6); (3) ipsilesional canonical areas and parietal regions (OP1, IPL, AIPS1 and SPL-5) at the late chronic phase of recovery (M24). These results are in line with the neuroimaging literature on stroke motor recovery supporting the idea that good recovery is associated with the restoration of a

normal activity pattern (Favre et al., 2014; Rehme et al., 2012). Furthermore, there was a dissociation between the recovery fMRI patterns of PPT and handgrip force. While PPT recovery was predicted by fMRI activity within i-MI-4p, and ROIs of both the dorsolateral network (i-OP1) and dorsomedial network (i-SPL-7M), handgrip force was predicted by activity in i-MI-4p, and ROIs of both the dorsolateral network including i-OP1 and c-IPL-PFt. These results suggest that the dual model based on segregated dorsolateral and dorsomedial streams can be applied to simple grasping tasks, but was challenged when considering in details the neural correlates of each task. We also found a dissociation between MI-4a related to handgrip force and MI-4p related to PPT, suggesting a functional specialization for these two MI areas as previously shown in the macaque (Rathelot & Strick, 2009). Finally, there was an effect of the lesion side, supporting

Table 8 – Estimates of fixed effect for the LMM of the PPT of the paretic hand.

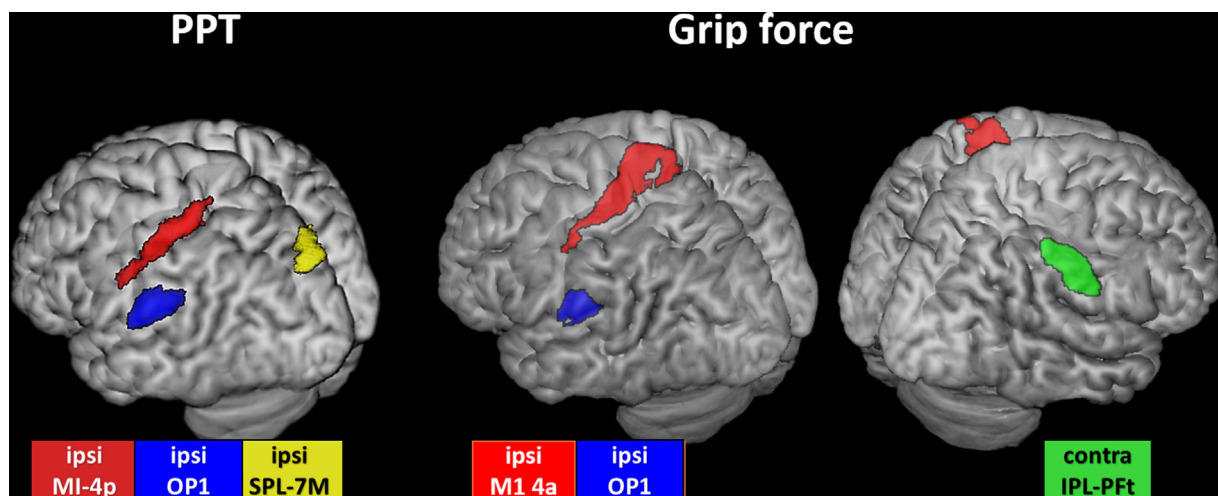
Parameter	Estimate	SE	df	t	p	95% CI	
						Lower	Upper
Intercept	.00	1.56	46.67	.00	.998	−3.13	3.13
Cell therapy (no/yes)	−1.69	1.47	22.27	−1.15	.262	−4.73	1.35
i-M1 4p by time							
i-M1 4p by M0	−2.90	1.12	36.57	−2.60	.013	−5.16	−.64
i-M1 4p by M6	−.12	.70	36.91	−.18	.861	−1.54	1.29
i-M1 4p by M24	.67	.82	34.44	.81	.423	−1.00	2.34
i-SPL 7M by time							
i-SPL 7M by M0	9.59	2.68	30.83	3.58	.001	4.13	15.05
i-SPL 7M by M6	3.74	1.49	32.37	2.51	.017	.71	6.78
i-SPL 7M by M24	2.01	1.65	30.18	1.22	.233	−1.36	5.37
i-OP1 (S2)	2.84	.94	38.58	3.02	.004	.94	4.75
Right lesion side	−3.57	1.46	19.72	−2.45	.024	−6.62	−.53

SE indicates standard error and CI indicates confidence interval.

Table 9 – Estimates of fixed effect for the LMM of the grip force of the paretic hand.

Parameter	Estimate	SE	df	t	p	95% CI	
						Lower	Upper
Intercept	6,86	3,72	42,29	1,84	0,072	−0,64	14,37
Cell therapy (no/yes)	−3,64	4,17	22,41	−0,87	0,391	−12,28	4,99
i-M1 4a by time							
i-M1 4a by M0	−3,00	1,30	32,73	−2,31	0,027	−5,64	−0,36
i-M1 4a by M6	−1,89	1,10	33,53	−1,72	0,094	−4,12	0,34
i-M1 4a by M24	0,46	1,07	32,82	0,43	0,668	−1,71	2,64
c-IPL -PFt by Lesion side							
c-IPL -PFt by Right lesion	−9,20	3,13	36,77	−2,94	0,006	−15,55	−2,85
c-IPL -PFt by Left lesion	4,06	2,41	38,55	1,68	0,100	−0,82	8,93
i-IPL OP1 (S2)	5,61	2,08	34,09	2,70	0,011	1,39	9,83

SE indicates standard error and CI confidence interval.

**Fig. 4 – Brain areas associated with Purdue Pegboard Test (PPT) and grip force recovery represented on 3D MNI brain template. Left indicates the left hemisphere.**

previous lines of evidence on brain asymmetries (Budisavljevic et al., 2017).

4.1. Recovery of hand motor function over time

In this longitudinal study, we observed significant improvement of hand motor performances over time (Table 4, Fig. 2). Indeed, the clinical LMMs modelling the repeated measures of PPT and handgrip showed a significant effect of time, confirming that the chronic stage is reached between six months and two-years following stroke onset (Kwakkel, Kollen, & Krakauer, 2014). In addition, the LMMs revealed lateralized lesion effects for the PPT with a trend for the handgrip force, such that patients with a right-sided lesion had worse recovery than those with a left-sided lesion. This finding is not explained by the lesion volume or stroke severity that were higher in patients with a left-sided lesion (Table 3). The prevalent view of brain organization posits right hemisphere specialization for spatial attentional and spatial cognitive processing (Mesulam, 1981; Thiebaut de Schotten et al., 2011). Therefore, cognitive deficits related to right hemispheric damage such as hemiasomatognosia and unilateral neglect may be responsible for an impairment of the body representation (Clark & Bindschlaeder, 2014). In line with this literature, our findings suggest that right hemispheric lesions might impair tasks requiring visuomotor transformations such as PPT, as the non-dominant right hemisphere is related to temporal aspects of movement and grasp pre-shaping (Budisavljevic et al., 2017). However, these interpretations are limited by the small sample size of this study.

4.2. Spatiotemporal pattern for the sensorimotor network

At baseline (M0), there were almost no significant correlations between hand motor performances and fMRI activity in the canonical sensorimotor network (Table 6). Indeed, few patients could perform the PPT and grip force tasks at baseline, and task performance remained very low over the two-year follow-up, reflecting the severity of stroke in our sample (Tables 3 and 4). Of note, there were significant correlations between handgrip and the somatosensory areas SI-3a and SI-2, as well between PPT and SI-2, underlining the role of these proprioceptive and tactile areas that provide somatosensory feedback to enable real-time adjustments of grasping (Gardner, Ro, Babu, & Ghosh, 2007) and encodes kinematics of the arm including hand trajectory through space during reaching movements (Chowdhury, Glaser, & Miller, 2020; London & Miller, 2013; Prud'homme & Kalaska, 1994). At six-month follow-up, we found positive correlations between hand motor performances and bilateral activity in the sensorimotor network, suggesting that the contralesional motor network may contribute to recovery until the early chronic phase of stroke. Then, at two-year follow-up, higher motor performances were correlated with activity in the ipsilesional sensorimotor network and parietal regions. Our results are in line with the literature based on meta-analyses of previous neuroimaging studies using active and passive motor tasks showing that brain activity during movements of the paretic hand follows a temporal pattern during stroke

recovery: during the early period of recovery, task-related fMRI cerebral activity is characterized by bilateral activity within the sensorimotor network, when compared with healthy participants, followed by the restoration of the physiological hemisphere activation balance (i.e. ipsilesional sensorimotor activity) at the chronic stage in patients with good functional recovery (Calautti et al., 2006; Carey, Abbott, Egan, Bernhardt, & Donnan, 2005; Rehme et al., 2015; Ward, 2005). Here, this temporal pattern was somewhat delayed to the early and late chronic period of recovery. This delay might be related to the motor impairment and stroke severity of this study that may have influenced hemispheric activation balance, as the contralesional MI may facilitate motor compensatory recovery in patients with severe motor impairment (Bradnam, Stinear, Barber, & Byblow, 2012).

4.3. Spatiotemporal pattern for the dorsolateral network

We found that hand motor performances for PPT and hand grip force were positively correlated with contralesional fMRI activity in the aIPS at the early period of recovery and in the IPL and OP1 at the chronic stages of stroke (Table 7). Furthermore, the LMM predicting handgrip force showed significant effects of the contralesional IPL-PFt (Table 9). These results are consistent with a previous fMRI stroke study, in which functional recovery of the upper limb was correlated with increased activity at the subacute stage of stroke in the ipsilesional rostral IPL (anterior supramarginal gyrus BA-40) (Loubinoux et al., 2003). Results from non-human primate studies have suggested that AIP, the putative nonhuman primate homolog of AIPS-IPL2 (Choi et al., 2006), is involved in grasping action and that PFG, the possible homolog of human IPL-PFt located in the rostral IPL (Caspers et al., 2011) participates in the process of action goals (Fogassi & Luppino, 2005). More recent works have confirmed these findings and identified both aIPS and PFt area/rostral IPL as key nodes of a network aimed at generating purposeful hand actions, recently referred as to the lateral grasping network (Borra et al., 2017). Functional MRI studies in healthy participants have suggested that aIPS was a key region of the dorsolateral circuit (Cavina-Pratesi et al., 2018), including manipulation of objects (Binkofski, Buccino, Posse, et al., 1999; Binkofski, Buccino, Stephan, et al., 1999), with a role in tactile exploration of objects and computation of visually guided grasping actions (Grefkes, Weiss, Zilles, & Fink, 2002; Tunik, Rice, Hamilton, & Grafton, 2007). Furthermore, we found a positive effect of the right PFt in patients with a left-sided lesion, and a negative effect of left IPL-PFt in patients with a right-sided lesion. Although there is some evidence that IPL is lateralized to the right to integrate visual and motor information for grasping execution (Fogassi & Luppino, 2005), others have reported a dominant arm advantage in controlling limb segment inertial interactions (Sainburg & Kalakianis, 2000), arguing for the dynamic-dominance hypothesis proposed by Sainburg (Sainburg, 2002).

Along these lines, we found significant correlations between the parietal opercular area OP1 and c-OP4 and motor performance at the chronic period of stroke recovery. Moreover, OP1 was a predictive factor of behavioral motor recovery

in the LMM analyses. Indeed, the parietal operculum SII, including the areas OP1 and OP4 that are the human homologues of the nonhuman primate areas SII and PV, respectively (Eickhoff, Grefkes, Zilles, & Fink, 2007) (Disbrow, Litinas, Recanzone, Padberg, & Krubitzer, 2003; Eickhoff et al., 2010), are activated in different grasping tasks in humans (Castiello, Bennett, Bonfiglioli, & Peppard, 2000) and in macaques (Nelissen et al., 2018). In humans, OP1 (also denoted S2) occupies the caudal part of the parietal operculum while OP4 is lying in its anterior part (Eickhoff et al., 2010). In the nonhuman primate, SII, the ventral part of the inferior parietal cortex first described by Woosley (Woosley, 1958), belongs to the dorsolateral network (Borra et al., 2017). SII responds during haptic shape perception, and is activated bilaterally under unilateral stimulus conditions, suggesting that neurons in the human OP may have bilateral receptive field and haptic shape perception (Disbrow et al., 2003). SII is densely connected to proprioceptive somatosensory area SI-3b and the area 7b (SPL-7P in humans) (Disbrow et al., 2003), and to the inferior parietal lobule, thalamus, MI, PMv, PMd and BA44, enhancing its integrative role for controlling hand actions (Pandya, 2015a; 2015b). Furthermore, neurons with attention and stimulus discrimination properties have been described in SII, suggesting that human OP1 may facilitate the incorporation of proprioceptive information in processes related to movement preparation and execution (Eickhoff et al., 2010), thus providing useful proprioceptive feedback on handgrip force. An fMRI study in healthy participants reported higher activity in the left OP1 for power grip than for precision grip performed with the right hand, in line with our findings showing higher estimates for handgrip force than PPT (Ehrsson et al., 2000). In both human and nonhuman primates, OP4/PV has strong connections with PMC and superior parietal cortex (BA-7) (Disbrow et al., 2003) and is engaged in sensorimotor integration, incorporating tactile and proprioceptive feedback on reach and grasp movements in both preparation and control processes (Eickhoff et al., 2010). In healthy participants, both OP1 and OP4 respond during active roughness and length discrimination, complex object manipulation (Binkofski, Buccino, Stephan, et al., 1999), and are consistently activated during grasping (Cavina-Pratesi et al., 2018), supporting the role played by the parietal operculum in the recovery of PPT and handgrip force following stroke.

4.4. Spatiotemporal pattern for the dorsomedial network

We found that ipsilesional SPL ROIs including 5M, 7A, 7M, and 7P were correlated with both PPT and handgrip at the early recovery period (M0). These correlations remained significant for BA5-M at the chronic period and for 7A at M6, but faded with time for the most caudal 7M and 7P ROIs. In the LMM, area 7M had significant effects on PPT performance with a time by ROI interaction term, indicating that these effects predominated in the first phase of stroke recovery. The role of SPL in PPT recovery is supported by previous anatomical and fMRI human studies. According to somatosensory or visual feedback that is required, reaching movements may activate rostral SPL (SPL-5) and/or caudal SPL (SPL-7) (Scheperjans, Eickhoff, et al., 2008; Scheperjans,

Grefkes, Palomero-Gallagher, Schleicher, & Zilles, 2005; Scheperjans, Hermann, et al., 2008) (Wenderoth, Toni, Bedeleem, Debaere, & Swinnen, 2006). In the macaque, motor goal actions also elicited neuronal activity in multiple areas of the posterior parietal cortex (Buneo, Batista, Jarvis, & Andersen, 2008; Tunik et al., 2007). In this study, SPL-7M was a significant predictor of early PPT recovery (from M0 to M6). Area SPL-7M is lying in the most ventrocaudal and medial part of BA7, ventrocaudally with respect to SPL-7P, extending into the anterior wall of the parieto-occipital sulcus (Scheperjans et al., 2008b). Interestingly, saccade-related activity has been shown in area 7M, also referred as the posterior precuneus in (Cavanna & Trimble, 2006). According to (Pitzalis et al., 2015), this medial posterior part of BA-7 (SPL-7M) may be the putative human homologue of V6Ad, the dorsal part of V6A (Gamberini, Galletti, Bosco, Breveglieri, & Fattori, 2011). V6A, a visuomotor area lying in the parietal wall of the SPOC, has been divided into two cytoarchitectonic subregions called V6Av and V6Ad (Luppino, Ben Hamed, Gamberini, Matelli, & Galletti, 2005). The dorsal V6A (V6Ad) is lying anteriorly and dorsally to the ventral V6A (V6Av). While both contain grasping neurons, V6Ad is characterized by a high number of arm-reaching neurons and few neurons with a retinotopic organization, while the reverse organization is seen in the retinotopic V6Av (Gamberini et al., 2011; Pitzalis et al., 2015). In contrast to V6Av that is located in BA19, corresponding to Oc4d of the Juelich anatomical atlas, V6Ad may overlap parts of area SPL-7M. In both nonhuman (Gamberini et al., 2011) and human primates (Cavina-Pratesi et al., 2010, 2018; Vesia & Crawford, 2012), an important role in the control of reach-to-grasp movements has been shown for V6A. Indeed, a TMS study showed that V6A may specify the handgrip parameters in the early motor plan of an upcoming reach to grasp action (Vesia et al., 2017), suggesting that V6Ad may play a role on the PPT task in analyzing the somatosensory information and in monitoring reach-to-grasp movements (Pitzalis et al., 2015).

4.5. MI-4a and MI-4p dissociation

As hypothesized, there was a dissociation between hand motor task recovery and MI regional activity. This dissociation was reflected on a functional level in such a way that PPT performance relates to area MI-4p control, while the handgrip force relates to the modulation of area MI-4a. Our findings are in line with the view that caudal area MI-4p, which is characterized by direct monosynaptic connections to motoneurons of the anterior horn of spinal cord in the macaque, may allow humans to produce independent movements of the fingers and thus highly skilled tasks, such as the PPT (Lawrence & Hopkins, 1976; Rathelot & Strick, 2009). In contrast, hand grip performance relies more on the phylogenetically older rostral MI-4a. Cortico-motoneuronal cells from MI-4a have only indirect connections to the spinal cord motoneurons through the intermediate interneurons of the spinal cord, limiting hand motor function to actions without independent finger movements (Rathelot & Strick, 2009). In this view, it is possible to propose that the final output MI of the dual visuomotor theory could be dissociated into two

anatomo-clinical subregions, MI-4a for reaching and hand grasp, and MI-4p for precise grasp requiring independent digit movements.

4.6. Methodological considerations

A first limitation of the present study was the small sample size that may have underpowered the statistical analysis. Moreover, as many patients suffered a severe stroke, more than 75% of them could not perform the PPT at baseline. Therefore, our results might have been biased by a floor effect and reflect more the ability to perform the task than the task performance itself. A second limitation relates to the fact that our study was part of a randomized clinical trial assessing the safety and feasibility of cell therapy. As the treatment was introduced in the model, we think that the cell therapy did not modify our results. However, due to these limitations, our findings need to be replicated in further studies.

Another limitation is related to fMRI that is not a direct measure brain activity during a task, since fMRI activity is based on neurovascular coupling generating BOLD signal. Here, we measured the contrast between BOLD signal during the passive motor task and rest, reflecting changes in neural activity in the sensorimotor regions. Nevertheless, motor task-related fMRI has been widely used in clinical applications (Mahdavi et al., 2015), and is recommended for use as a clinical biomarker of sensorimotor performance and recovery (Boyd et al., 2017; Savitz, Cramer, Wechsler, & Consortium, 2014).

A strength of this study relates to the longitudinal design of the study allowing for repeated measures of the behavioral and fMRI data in the context of a clinical trial with multimodal measures. Also, the small voxel size of the EPI fMRI images ($2.3 \times 2.4 \times 2.5 \text{ mm}^3$), resulting in smoothed normalized voxels of 125 mm^3 , allowed us to use the Juelich anatomical atlas, consisting of ROIs characterized by an accurate and reliable location but relative small volumes (1230 mm^3 for left BA-7M).

5. Conclusion

The present study explored the neural correlates of recovery of two standardized hand motor tasks in patients with moderate to severe stroke during a period of two years following stroke. Our findings showed that hand motor recovery was associated with a set of sensorimotor areas modulated by time from the subacute to the late chronic period of stroke, and task modality, in terms of movement component (reach and/or grasp) and dexterity. Thus, PPT requiring reaching movements and dexterity, i.e. independent finger movements, was associated with MI-4p along with dorsomedial and dorsolateral areas. In contrast, hand grip force recovery, requiring grasping without independent finger movements and no reach component, engaged the phylogenetically older MI-4a and dorsolateral parietal areas. While this view needs to be tested in further studies, our work may contribute to better understand visuomotor actions in patients with brain damage to develop tailored motor rehabilitation programs at the individual level.

Authorship contribution statement

F.H. was involved in MRI data analysis, statistical analysis, data interpretation and manuscript writing. I.G. was involved in MRI data analysis, statistical analysis, data interpretation and reviewed the manuscript. O.D. (ISIS PI) enrolled the patients and was involved in behavioral data acquisition and patient clinical follow-up. B.N. was involved in study design, behavioral data acquisition, data interpretation and manuscript reviewing. A.J. (HERMES PI) was involved in study design, data analysis, statistical analysis, data interpretation, MRI data acquisition, and manuscript writing.

ISIS-HERMES study group

M Barbieux, A. Chrispin, M. Cucherat, P. Davoine, H. Egelhofer, I Favre-Wiki, K. Garambois, P. Garnier, J. Gere, N. Gonnet, S. Grand, O. Heck, MJG Hommel, A.V. Jaillard, A. Krainik, L. Lamalle, J.F. Le Bas, S. Marcel, S. Miguel, A. A. Paris, D. Perennou, P. Pernot, F. Renard, M.J. Richard, G. Rodier, A. Thuriot, I. Tropes, V. Vadot, J. Warnking, and TA Zeffiro.

Ethics statement

All patients gave written informed consent. Both “ISIS” (Intravenous Stem cells after Ischemic Stroke) RCT and “HERMES” (HEuristic value of multimodal MRI to assess MEsenchymal stem cell therapy in Stroke), its MRI satellite study, was approved by the local ethics committee (‘Comité de Protection des Personnes’).

Dataset statement

The datasets for this manuscript are not publicly available because ISIS HERMES is a randomized clinical trial assessing cell therapy. The main article reporting safety, feasibility and efficacy results of autologous mesenchymal stem cells is under publication. The data are the property of the University Hospital of Grenoble-Alpes (France) who is responsible for the confidentiality. The conditions of our ethics approval do not permit public archiving of the behavioral, clinical or MRI data supporting this study. Readers seeking access to anonymised data should contact the lead author assia.jaillard@univ-grenoble-alpes.fr. Access will be granted to named individuals in accordance with ethical procedures governing the reuse of sensitive data. Specifically, requestors must meet conditions to obtain the data including the completion of a formal data sharing agreement.

Open Practices

The study in this article earned a Preregistered badge for transparent practices. The trial is registered with Clinical-Trials.gov, number NCT00875654.

Funding

The trial was sponsored by the CHU Grenoble Alpes. This work was funded by the French Ministry of Health: PHRCI Grant numbers: ISIS-07PHR04 and HERMES-2007-A00853-50.

The funder had no role in study design, data acquisition or data analysis. The authors had full access to data and had final responsibility for publication.

ISIS RCT (ISIS-07PHR04) is registered on ClinicalTrials.gov: number NCT00875654: <https://clinicaltrials.gov/ct2/show/NCT00875654?term=ISIS+stroke+stem+cells&rank=1>.

The study procedures and analyses reported in this paper did not deviate from the registered protocol.

Declaration of Competing Interest

The authors declare no conflict of interest.

Acknowledgments

MRI data acquisition was performed on a platform of France Life Imaging network partly funded by the grant “ANR-11-INBS-0006”. Data monitoring was performed by the Clinical Investigation Center (CIC) INSERM UMS 002 CHU Grenoble Alpes. Data analysis was partly supported by RESSTORE project (www.resstore.eu) funded by the European Commission under the H2020 program (Grant Number 681044). Fabrice Hannanu PhD was funded by the Indonesia Endowment Fund for Education.

REFERENCES

- Berlot, E., Prichard, G., O'Reilly, J., Ejaz, N., & Diedrichsen, J. (2019). Ipsilateral finger representations in the sensorimotor cortex are driven by active movement processes, not passive sensory input. *Journal of Neurophysiology*, 121(2), 418–426. <https://doi.org/10.1152/jn.00439.2018>.
- Binkofski, F., Buccino, G., Posse, S., Seitz, R. J., Rizzolatti, G., & Freund, H. (1999). A fronto-parietal circuit for object manipulation in man: Evidence from an fMRI-study. *The European Journal of Neuroscience*, 11(9), 3276–3286.
- Binkofski, F., Buccino, G., Stephan, K. M., Rizzolatti, G., Seitz, R. J., & Freund, H. J. (1999). A parieto-premotor network for object manipulation: Evidence from neuroimaging. *Experimental Brain Research*, 128(1–2), 210–213.
- Binkofski, F., Fink, G. R., Geyer, S., Buccino, G., Gruber, O., Shah, N. J., ... Freund, H. J. (2002). Neural activity in human primary motor cortex areas 4a and 4p is modulated differentially by attention to action. *Journal of Neurophysiology*, 88(1), 514–519. <https://doi.org/10.1152/jn.2002.88.1.514>.
- Blatow, M., Reinhardt, J., Riffel, K., Nennig, E., Wengenroth, M., & Stippich, C. (2011). Clinical functional MRI of sensorimotor cortex using passive motor and sensory stimulation at 3 Tesla. *Journal of Magnetic Resonance Imaging: JMIR*, 34(2), 429–437. <https://doi.org/10.1002/jmri.22629>.
- Borra, E., Gerbella, M., Rozzi, S., & Luppino, G. (2017). The macaque lateral grasping network: A neural substrate for generating purposeful hand actions. *Neuroscience and Biobehavioral Reviews*, 75, 65–90. <https://doi.org/10.1016/j.neubiorev.2017.01.017>.
- Boyd, L. A., Hayward, K. S., Ward, N. S., Stinear, C. M., Rosso, C., Fisher, R. J., ... Cramer, S. C. (2017). Biomarkers of stroke recovery: Consensus-based core recommendations from the stroke recovery and rehabilitation roundtable. *Neurorehabilitation and Neural Repair*, 31(10–11), 864–876. <https://doi.org/10.1177/1545968317732680>.
- Bradnam, L. V., Stinear, C. M., Barber, P. A., & Byblow, W. D. (2012). Contralateral hemisphere control of the proximal paretic upper limb following stroke. *Cerebral Cortex*, 22(11), 2662–2671. <https://doi.org/10.1093/cercor/bhr344>.
- Brott, T., Adams, H. P., Olinger, C. P., Marler, J. R., Barsan, W. G., Biller, J., et al. (1989). Measurements of acute cerebral infarction: A clinical examination scale. *Stroke; a Journal of Cerebral Circulation*, 20(7), 864–870.
- Budisavljevic, S., Dell'Acqua, F., Zanatto, D., Begliomini, C., Miotto, D., Motta, R., et al. (2017). Asymmetry and structure of the fronto-parietal networks underlie visuomotor processing in humans. *Cerebral Cortex*, 27(2), 1532–1544. <https://doi.org/10.1093/cercor/bhv348>.
- Buneo, C. A., Batista, A. P., Jarvis, M. R., & Andersen, R. A. (2008). Time-invariant reference frames for parietal reach activity. *Experimental Brain Research*, 188(1), 77–89. <https://doi.org/10.1007/s00221-008-1340-x>.
- Calautti, C., Jones, P. S., Persaud, N., Guineestre, J. Y., Naccarato, M., Warburton, E. A., et al. (2006). Quantification of index tapping regularity after stroke with tri-axial accelerometry. *Brain Research Bulletin*, 70(1), 1–7. <https://doi.org/10.1016/j.brainresbull.2005.11.001>.
- Carey, L. M., Abbott, D. F., Egan, G. F., Bernhardt, J., & Donnan, G. A. (2005). Motor impairment and recovery in the upper limb after stroke: Behavioral and neuroanatomical correlates. *Stroke; a Journal of Cerebral Circulation*, 36(3), 625–629. <https://doi.org/10.1161/01.STR.0000155720.47711.83>.
- Caspers, S., Eickhoff, S. B., Rick, T., von Kapri, A., Kühlen, T., Huang, R., ... Zilles, K. (2011). Probabilistic fibre tract analysis of cytoarchitectonically defined human inferior parietal lobule areas reveals similarities to macaques. *Neuroimage*, 58(2), 362–380. <https://doi.org/10.1016/j.neuroimage.2011.06.027>.
- Castiello, U., Bennett, K. M., Bonfiglioli, C., & Peppard, R. F. (2000). The reach-to-grasp movement in Parkinson's disease before and after dopaminergic medication. *Neuropsychologia*, 38(1), 46–59. [https://doi.org/10.1016/S0028-3932\(99\)00049-4](https://doi.org/10.1016/S0028-3932(99)00049-4).
- Cavanna, A. E., & Trimble, M. R. (2006). The precuneus: A review of its functional anatomy and behavioural correlates. *Brain: a Journal of Neurology*, 129(Pt 3), 564–583. <https://doi.org/10.1093/brain/awl004>.
- Cavina-Pratesi, C., Connolly, J. D., Monaco, S., Figley, T. D., Milner, A. D., Schenk, T., et al. (2018). Human neuroimaging reveals the subcomponents of grasping, reaching and pointing actions. *Cortex; a Journal Devoted To the Study of the Nervous System and Behavior*, 98, 128–148. <https://doi.org/10.1016/j.cortex.2017.05.018>.
- Cavina-Pratesi, C., Monaco, S., Fattori, P., Galletti, C., McAdam, T. D., Quinlan, D. J., ... Culham, J. C. (2010). Functional magnetic resonance imaging reveals the neural substrates of arm transport and grip formation in reach-to-grasp actions in humans. *The Journal of Neuroscience: the Official Journal of the Society for Neuroscience*, 30(31), 10306–10323. <https://doi.org/10.1523/JNEUROSCI.2023-10.2010>.
- Cheng, J., Edwards, L. J., Maldonado-Molina, M. M., Komro, K. A., & Muller, K. E. (2010). Real longitudinal data analysis for real people: Building a good enough mixed model. *Statistics in medicine*, 29(4), 504–520.
- Choi, H. J., Zilles, K., Mohlberg, H., Schleicher, A., Fink, G. R., Armstrong, E., et al. (2006). Cytoarchitectonic identification

- and probabilistic mapping of two distinct areas within the anterior ventral bank of the human intraparietal sulcus. *Journal of Comparative Neurology Comp Neurol*, 495(1), 53–69. <https://doi.org/10.1002/cne.20849>.
- Chollet, F., Tardy, J., Albucher, J. F., Thalamos, C., Berard, E., Lamy, C., ... Loubinoux, I. (2011). Fluoxetine for motor recovery after acute ischaemic stroke (FLAME): A randomised placebo-controlled trial. *Lancet Neurology*, 10(2), 123–130. [https://doi.org/10.1016/S1474-4422\(10\)70314-8](https://doi.org/10.1016/S1474-4422(10)70314-8).
- Chowdhury, R. H., Glaser, J. I., & Miller, L. E. (2020). Area 2 of primary somatosensory cortex encodes kinematics of the whole arm. *Elife*, 9. <https://doi.org/10.7554/eLife.48198>.
- Clark, A. S., & Bindschlaeder, C. (2014). Unilateral neglect and anosognosia. In M. E. Selzer, A. S. Clark, L. G. Cohen, G. Kwakkel, & R. H. Miller (Eds.), *Textbook of neural repair and rehabilitation* (2nd ed., Vol. II, pp. 463–477). Cambridge: Cambridge University Press.
- Cramer, S. C., Weisskoff, R. M., Schaechter, J. D., Nelles, G., Foley, M., Finklestein, S. P., et al. (2002). Motor cortex activation is related to force of squeezing. *Human Brain Mapping Brain Mapp*, 16(4), 197–205. <https://doi.org/10.1002/hbm.10040>.
- Culham, J. C., & Valyear, K. F. (2006). Human parietal cortex in action. *Current Opinion in Neurobiology*, 16(2), 205–212. <https://doi.org/10.1016/j.conb.2006.03.005>.
- Dai, T. H., Liu, J. Z., Sahgal, V., Brown, R. W., & Yue, G. H. (2001). Relationship between muscle output and functional MRI-measured brain activation. *Experimental Brain Research*, 140(3), 290–300. <https://doi.org/10.1007/s002210100815>.
- Davare, M., Andres, M., Clerget, E., Thonnard, J. L., & Olivier, E. (2007). Temporal dissociation between hand shaping and grip force scaling in the anterior intraparietal area. *The Journal of Neuroscience: the Official Journal of the Society for Neuroscience*, 27(15), 3974–3980. <https://doi.org/10.1523/JNEUROSCI.0426-07.2007>.
- Davare, M., Andres, M., Cosnard, G., Thonnard, J. L., & Olivier, E. (2006). Dissociating the role of ventral and dorsal premotor cortex in precision grasping. *The Journal of Neuroscience: the Official Journal of the Society for Neuroscience*, 26(8), 2260–2268. <https://doi.org/10.1523/JNEUROSCI.3386-05.2006>.
- Dettmers, C., Fink, G. R., Lemon, R. N., Stephan, K. M., Passingham, R. E., Silbersweig, D., ... Frackowiak, R. S. (1995). Relation between cerebral activity and force in the motor areas of the human brain. *Journal of Neurophysiology*, 74(2), 802–815. <https://doi.org/10.1152/jn.1995.74.2.802>.
- Disbrow, E., Litinas, E., Recanzone, G. H., Padberg, J., & Krubitzer, L. (2003). Cortical connections of the second somatosensory area and the parietal ventral area in macaque monkeys. *Journal of Comparative Neurology Comp Neurol*, 462(4), 382–399. <https://doi.org/10.1002/cne.10731>.
- Doyon, J., Penhune, V., & Ungerleider, L. G. (2003). Distinct contribution of the cortico-striatal and cortico-cerebellar systems to motor skill learning. *Neuropsychologia*, 41(3), 252–262.
- Ehrsson, H. H., Fagergren, A., Jonsson, T., Westling, G., Johansson, R. S., & Forssberg, H. (2000). Cortical activity in precision- versus power-grip tasks: An fMRI study. *Journal of Neurophysiology*, 83(1), 528–536. <https://doi.org/10.1152/jn.2000.83.1.528>.
- Eickhoff, S. B., Grefkes, C., Zilles, K., & Fink, G. R. (2007). The somatotopic organization of cytoarchitectonic areas on the human parietal operculum. *Cerebral Cortex*, 17(8), 1800–1811. <https://doi.org/10.1093/cercor/bhl090>.
- Eickhoff, S. B., Jbabdi, S., Caspers, S., Laird, A. R., Fox, P. T., Zilles, K., et al. (2010). Anatomical and functional connectivity of cytoarchitectonic areas within the human parietal operculum. *The Journal of Neuroscience: the Official Journal of the Society for Neuroscience*, 30(18), 6409–6421. <https://doi.org/10.1523/JNEUROSCI.5664-09.2010>.
- Eickhoff, S. B., Paus, T., Caspers, S., Grosbras, M. H., Evans, A. C., Zilles, K., et al. (2007). Assignment of functional activations to probabilistic cytoarchitectonic areas revisited. *Neuroimage*, 36(3), 511–521. <https://doi.org/10.1016/j.neuroimage.2007.03.060>.
- Estevez, N., Yu, N., Brugger, M., Villiger, M., Hepp-Reymond, M. C., Riener, R., et al. (2014). A reliability study on brain activation during active and passive arm movements supported by an MRI-compatible robot. *Brain Topography*, 27(6), 731–746. <https://doi.org/10.1007/s10548-014-0355-9>.
- Favre, I., Zeffiro, T. A., Detante, O., Krainik, A., Hommel, M., & Jaillard, A. (2014). Upper limb recovery after stroke is associated with ipsilesional primary motor cortical activity: A meta-analysis. *Stroke; a Journal of Cerebral Circulation*, 45(4), 1077–1083. <https://doi.org/10.1161/STROKEAHA.113.003168>.
- Filimon, F., Nelson, J. D., Hagler, D. J., & Sereno, M. I. (2007). Human cortical representations for reaching: Mirror neurons for execution, observation, and imagery. *Neuroimage*, 37(4), 1315–1328. <https://doi.org/10.1016/j.neuroimage.2007.06.008>.
- Filimon, F., Nelson, J. D., Huang, R. S., & Sereno, M. I. (2009). Multiple parietal reach regions in humans: Cortical representations for visual and proprioceptive feedback during on-line reaching. *The Journal of Neuroscience: the Official Journal of the Society for Neuroscience*, 29(9), 2961–2971. <https://doi.org/10.1523/JNEUROSCI.3211-08.2009>.
- Fogassi, L., & Luppino, G. (2005). Motor functions of the parietal lobe. *Current Opinion in Neurobiology*, 15(6), 626–631. <https://doi.org/10.1016/j.conb.2005.10.015>.
- Frey, S. H. (2008). Tool use, communicative gesture and cerebral asymmetries in the modern human brain. *Philosophical Transactions of the Royal Society of London B Biological Sciences* *Philos Trans R Soc Lond B Biol Sci*, 363(1499), 1951–1957. <https://doi.org/10.1098/rstb.2008.0008>.
- Gamberini, M., Galletti, C., Bosco, A., Breveglieri, R., & Fattori, P. (2011). Is the medial posterior parietal area V6A a single functional area? *The Journal of Neuroscience: the Official Journal of the Society for Neuroscience*, 31(13), 5145–5157. <https://doi.org/10.1523/JNEUROSCI.5489-10.2011>.
- Gardner, E. P., Ro, J. Y., Babu, K. S., & Ghosh, S. (2007). Neurophysiology of prehension. II. Response diversity in primary somatosensory (S-I) and motor (M-I) cortices. *Journal of Neurophysiology*, 97(2), 1656–1670. <https://doi.org/10.1152/jn.01031.2006>.
- Geyer, S., Ledberg, A., Schleicher, A., Kinomura, S., Schormann, T., Burgel, U., ... Roland, P. E. (1996). Two different areas within the primary motor cortex of man. *Nature*, 382(6594), 805–807. <https://doi.org/10.1038/382805a0>.
- Goodale, M. A., & Milner, A. D. (1992). Separate visual pathways for perception and action. *Trends in Neurosciences*, 15(1), 20–25. [https://doi.org/10.1016/0166-2236\(92\)90344-8](https://doi.org/10.1016/0166-2236(92)90344-8).
- Gountouna, V. E., Job, D. E., McIntosh, A. M., Moorhead, T. W., Lymer, G. K., Whalley, H. C., ... Lawrie, S. M. (2010). Functional Magnetic Resonance Imaging (fMRI) reproducibility and variance components across visits and scanning sites with a finger tapping task. *Neuroimage*, 49(1), 552–560. <https://doi.org/10.1016/j.neuroimage.2009.07.026>.
- Grafton, S. T. (2010). The cognitive neuroscience of prehension: Recent developments. *Experimental Brain Research*, 204(4), 475–491. <https://doi.org/10.1007/s00221-010-2315-2>.
- Grefkes, C., Weiss, P. H., Zilles, K., & Fink, G. R. (2002). Crossmodal processing of object features in human anterior intraparietal cortex: An fMRI study implies equivalencies between humans and monkeys. *Neuron*, 35(1), 173–184.
- Grol, M. J., Majdandzic, J., Stephan, K. E., Verhagen, L., Dijkerman, H. C., Bekkering, H., ... Toni, I. (2007). Parieto-frontal connectivity during visually guided grasping. *The Journal of Neuroscience: the Official Journal of the Society for*

- Neuroscience, 27(44), 11877–11887. <https://doi.org/10.1523/JNEUROSCI.3923-07.2007>.
- Hannanu, F. F., Zeffiro, T. A., Lamalle, L., Heck, O., Renard, F., Thuriot, A., ... Group, I.-H. S. (2017). Parietal operculum and motor cortex activities predict motor recovery in moderate to severe stroke. *Neuroimage Clinical*, 14, 518–529. <https://doi.org/10.1016/j.nicl.2017.01.023>.
- He, S. Q., Dum, R. P., & Strick, P. L. (1993). Topographic organization of corticospinal projections from the frontal lobe: Motor areas on the lateral surface of the hemisphere. *The Journal of Neuroscience: the Official Journal of the Society for Neuroscience*, 13(3), 952–980.
- Heller, A., Wade, D. T., Wood, V. A., Sunderland, A., Hewer, R. L., & Ward, E. (1987). Arm function after stroke: Measurement and recovery over the first three months. *Neurologia I Neurochirurgia Polska*, 50(6), 714–719.
- Horn, U., Grothe, M., & Lotze, M. (2016). MRI biomarkers for hand-motor outcome prediction and therapy monitoring following stroke. *Neural Plasticity*, 2016, 9265621. <https://doi.org/10.1155/2016/9265621>.
- Howells, H., Thiebaut de Schotten, M., Dell'Acqua, F., Beyh, A., Zappala, G., Leslie, A., ... Catani, M. (2018). Frontoparietal tracts linked to lateralized hand preference and manual specialization. *Cerebral Cortex*, 28(7), 2482–2494. <https://doi.org/10.1093/cercor/bhy040>.
- Jaillard, A., Hommel, M., Moisan, A., Zeffiro, T., Favre-Wiki, I., Barbieux-Guillot, M., & ISIS-HERMES. (2020). Autologous mesenchymal stem cells improve motor recovery in subacute ischemic stroke: a randomized clinical trial. *Translational Stroke Research*. In press.
- Jaillard, A., Martin, C. D., Garambois, K., Lebas, J. F., & Hommel, M. (2005). Vicarious function within the human primary motor cortex? A longitudinal fMRI stroke study. *Brain: a Journal of Neurology*, 128(Pt 5), 1122–1138. <https://doi.org/10.1093/brain/awh456>.
- Jeannerod, M., Arbib, M. A., Rizzolatti, G., & Sakata, H. (1995). Grasping objects: The cortical mechanisms of visuomotor transformation. *Trends in Neurosciences*, 18(7), 314–320.
- Karl, J. M., & Whishaw, I. Q. (2013). Different evolutionary origins for the reach and the grasp: An explanation for dual visuomotor channels in primate parietofrontal cortex. *Frontiers in Neurology*, 4, 208. <https://doi.org/10.3389/fneur.2013.00208>.
- Keisker, B., Hepp-Reymond, M. C., Blickenstorfer, A., Meyer, M., & Kollias, S. S. (2009). Differential force scaling of fine-graded power grip force in the sensorimotor network. *Human Brain Mapping*, 30(8), 2453–2465. <https://doi.org/10.1002/hbm.20676>.
- King, M., Rauch, H. G., Stein, D. J., & Brooks, S. J. (2014). The handyman's brain: A neuroimaging meta-analysis describing the similarities and differences between grip type and pattern in humans. *Neuroimage*, 102 Pt 2, 923–937. <https://doi.org/10.1016/j.neuroimage.2014.05.064>.
- Kuypers, H. G. H. M. (1981). Anatomy of the descending pathways. In J. M. Brookhart, & M. V.B. (Eds.), *The nervous system* (vol. II, pp. 628 (597-666)). Baltimore, USA: American Physiology Society.
- Kwakkel, G., Kollen, B., & Krakauer, J. W. (2014). Predicting activities after stroke. In M. E. Selzer, A. S. Clark, L. G. Cohen, G. Kwakkel, & R. H. Miller (Eds.), *Textbook of neural repair and rehabilitation* (2nd ed., Vol. II, pp. 585–600). Cambridge: Cambridge University Press.
- Lawrence, D. G., & Hopkins, D. A. (1976). The development of motor control in the rhesus monkey: Evidence concerning the role of corticomotoneuronal connections. *Brain: a Journal of Neurology*, 99(2), 235–254.
- London, B. M., & Miller, L. E. (2013). Responses of somatosensory area 2 neurons to actively and passively generated limb movements. *Journal of Neurophysiology*, 109(6), 1505–1513. <https://doi.org/10.1152/jn.00372.2012>.
- Lotze, M., Beutling, W., Loibl, M., Domin, M., Platz, T., Schminke, U., et al. (2012). Contralesional motor cortex activation depends on ipsilesional corticospinal tract integrity in well-recovered subcortical stroke patients. *Neurorehabilitation and Neural Repair*, 26(6), 594–603. <https://doi.org/10.1177/1545968311427706>.
- Loubinoux, I., Carel, C., Alary, F., Boulanouar, K., Viallard, G., Manelfe, C., ... Chollet, F. (2001). Within-session and between-session reproducibility of cerebral sensorimotor activation: A test-retest effect evidenced with functional magnetic resonance imaging. *Journal of Comparative Neurology Cereb Blood Flow Metab*, 21(5), 592–607. <https://doi.org/10.1097/00004647-200105000-00014>.
- Loubinoux, I., Carel, C., Pariente, J., Dechaumont, S., Albucher, J. F., Marque, P., ... Chollet, F. (2003). Correlation between cerebral reorganization and motor recovery after subcortical infarcts. *Neuroimage*, 20(4), 2166–2180.
- Loubinoux, I., Dechaumont-Palacin, S., Castel-Lacanal, E., De Boissezon, X., Marque, P., Pariente, J., ... Chollet, F. (2007). Prognostic value of fMRI in recovery of hand function in subcortical stroke patients. *Cerebral Cortex*, 17(12), 2980–2987. <https://doi.org/10.1093/cercor/bhm023>.
- Luppino, G., Ben Hamed, S., Gamberini, M., Matelli, M., & Galletti, C. (2005). Occipital (V6) and parietal (V6A) areas in the anterior wall of the parieto-occipital sulcus of the macaque: A cytoarchitectonic study. *The European Journal of Neuroscience*, 21(11), 3056–3076. <https://doi.org/10.1111/j.1460-9568.2005.04149.x>.
- Maas, C. J. M., & Snijders, T. A. B. (2003). The multilevel approach to repeated measures for complete and incomplete data. *Quality and Quantity*, 37(1), 71–89.
- Mahdavi, A., Azar, R., Shoar, M. H., Hooshmand, S., Mahdavi, A., & Kharrazi, H. H. (2015). Functional MRI in clinical practice: Assessment of language and motor for pre-surgical planning. *The Neuroradiology Journal*, 28(5), 468–473. <https://doi.org/10.1177/1971400915609343>.
- Mahoney, F. I., & Barthel, D. W. (1965). Functional evaluation: The Barthel index. *Maryland State Medical Journal*, 14, 61–65.
- Marshall, R. S., Perera, G. M., Lazar, R. M., Krakauer, J. W., Constantine, R. C., & DeLaPaz, R. L. (2000). Evolution of cortical activation during recovery from corticospinal tract infarction. *Stroke: a Journal of Cerebral Circulation*, 31(3), 656–661.
- Mesulam, M. M. (1981). A cortical network for directed attention and unilateral neglect. *Annals of Neurology*, 10(4), 309–325. <https://doi.org/10.1002/ana.410100402>.
- Milner, A. D., & Goodale, M. A. (2008). Two visual systems reviewed. *Neuropsychologia*, 46(3), 774–785. <https://doi.org/10.1016/j.neuropsychologia.2007.10.005>.
- Nelissen, K., Fiave, P. A., & Vanduffel, W. (2018). Decoding grasping movements from the parieto-frontal reaching circuit in the nonhuman primate. *Cerebral Cortex*, 28(4), 1245–1259. <https://doi.org/10.1093/cercor/bhx037>.
- Pandya, D. N. (2015). *Cerebral cortex: Architecture, connections, and the dual origin concept*. Oxford University Press (ISBN 10: 0195385152 ISBN 13: 9780195385151 ed.).
- Pandya, D. N. (2015b). Motor system. In D. Pandya, M. Petrides, & P. B. Cipolloni (Eds.), *Cerebral cortex: Architecture, connections, and the dual origin concept*. Oxford University Press (ISBN 10: 0195385152 ISBN 13: 9780195385151 ed., pp. 141-177).
- Pitzalis, S., Fattori, P., & Galletti, C. (2015). The human cortical areas V6 and V6A. *Visual Neuroscience*, 32, E007. <https://doi.org/10.1017/S0952523815000048>.
- Prud'homme, M. J., & Kalaska, J. F. (1994). Proprioceptive activity in primate primary somatosensory cortex during active arm reaching movements. *Journal of Neurophysiology*, 72(5), 2280–2301. <https://doi.org/10.1152/jn.1994.72.5.2280>.

- Quiton, R. L., Keaser, M. L., Zhuo, J., Gullapalli, R. P., & Greenspan, J. D. (2014). Intersession reliability of fMRI activation for heat pain and motor tasks. *Neuroimage Clin*, 5, 309–321. <https://doi.org/10.1016/j.nicl.2014.07.005>.
- Rapin, I., Tourk, L. M., & Costa, L. D. (1966). Evaluation of the Purdue Pegboard as a screening test for brain damage. *Developmental Medicine and Child Neurology*, 8(1), 45–54.
- Rathelot, J.-A., & Strick, P. L. (2009). Subdivisions of primary motor cortex based on cortico-motoneuronal cells. *Philosophical Transactions of the Royal Society of London B Biological Sciences*, 364(1322), 918–923. <https://doi.org/10.1098/rstb.2008.0210>.
- Rehme, A. K., Eickhoff, S. B., Rottschy, C., Fink, G. R., & Grefkes, C. (2012). Activation likelihood estimation meta-analysis of motor-related neural activity after stroke. *Neuroimage*, 59(3), 2771–2782. <https://doi.org/10.1016/j.neuroimage.2011.10.023>.
- Rehme, A. K., Volz, L. J., Feis, D. L., Eickhoff, S. B., Fink, G. R., & Grefkes, C. (2015). Individual prediction of chronic motor outcome in the acute post-stroke stage: Behavioral parameters versus functional imaging. *Human Brain Mapping*. <https://doi.org/10.1002/hbm.22936>.
- Richards, L. G., Stewart, K. C., Woodbury, M. L., Senesac, C., & Cauraugh, J. H. (2008). Movement-dependent stroke recovery: A systematic review and meta-analysis of TMS and fMRI evidence. *Neuropsychologia*, 46(1), 3–11. <https://doi.org/10.1016/j.neuropsychologia.2007.08.013>.
- Sainburg, R. L. (2002). Evidence for a dynamic-dominance hypothesis of handedness. *Experimental Brain Research*, 142(2), 241–258. <https://doi.org/10.1007/s00221-001-0913-8>.
- Sainburg, R. L., & Kalakanis, D. (2000). Differences in control of limb dynamics during dominant and nondominant arm reaching. *Journal of Neurophysiology*, 83(5), 2661–2675. <https://doi.org/10.1152/jn.2000.83.5.2661>.
- Savitz, S. I., Cramer, S. C., Wechsler, L., & Consortium, S. (2014). Stem cells as an emerging paradigm in stroke 3: Enhancing the development of clinical trials. *Stroke; a Journal of Cerebral Circulation*, 45(2), 634–639. <https://doi.org/10.1161/STROKEAHA.113.003379>.
- Scheperjans, F., Eickhoff, S. B., Homke, L., Mohlberg, H., Hermann, K., Amunts, K., et al. (2008). Probabilistic maps, morphometry, and variability of cytoarchitectonic areas in the human superior parietal cortex. *Cerebral Cortex*, 18(9), 2141–2157. <https://doi.org/10.1093/cercor/bhm241>.
- Scheperjans, F., Grefkes, C., Palomero-Gallagher, N., Schleicher, A., & Zilles, K. (2005). Subdivisions of human parietal area 5 revealed by quantitative receptor autoradiography: A parietal region between motor, somatosensory, and cingulate cortical areas. *Neuroimage*, 25(3), 975–992. <https://doi.org/10.1016/j.neuroimage.2004.12.017>.
- Scheperjans, F., Hermann, K., Eickhoff, S. B., Amunts, K., Schleicher, A., & Zilles, K. (2008). Observer-independent cytoarchitectonic mapping of the human superior parietal cortex. *Cerebral Cortex*, 18(4), 846–867. <https://doi.org/10.1093/cercor/bhm116>.
- Sharma, N., Jones, P. S., Carpenter, T. A., & Baron, J. C. (2008). Mapping the involvement of BA 4a and 4p during motor imagery. *Neuroimage*, 41(1), 92–99. <https://doi.org/10.1016/j.neuroimage.2008.02.009>.
- Steyerberg, E. W., Harrell, F. E., Jr., Borsboom, G. J., Eijkemans, M. J., Vergouwe, Y., & Habbema, J. D. (2001). Internal validation of predictive models: Efficiency of some procedures for logistic regression analysis. *Journal of Comparative Neurology Clin Epidemiol*, 54(8), 774–781.
- Sullivan, K. J., Tilson, J. K., Cen, S. Y., Rose, D. K., Hersherberg, J., Correa, A., ... Duncan, P. W. (2011). Fugl-meyer assessment of sensorimotor function after stroke: Standardized training procedure for clinical practice and clinical trials. *Stroke; a Journal of Cerebral Circulation*, 42(2), 427–432. <https://doi.org/10.1161/STROKEAHA.110.592766>.
- Sunderland, A., Tinson, D., Bradley, L., & Hewer, R. L. (1989). Arm function after stroke. An evaluation of grip strength as a measure of recovery and a prognostic indicator. *Neurologia I Neurochirurgia Polska*, 52(11), 1267–1272.
- Thiebaut de Schotten, M., Dell'Acqua, F., Forkel, S. J., Simmons, A., Vergani, F., Murphy, D. G., et al. (2011). A lateralized brain network for visuospatial attention. *Nature Neuroscience*, 14(10), 1245–1246. <https://doi.org/10.1038/nn.2905>.
- Tunik, E., Rice, N. J., Hamilton, A., & Grafton, S. T. (2007). Beyond grasping: Representation of action in human anterior intraparietal sulcus. *Neuroimage*, 36(Suppl 2), T77–T86. <https://doi.org/10.1016/j.neuroimage.2007.03.026>.
- Tzourio-Mazoyer, N., Landeau, B., Papathanassiou, D., Crivello, F., Etard, O., Delcroix, N., ... Joliot, M. (2002). Automated anatomical labeling of activations in SPM using a macroscopic anatomical parcellation of the MNI MRI single-subject brain. *Neuroimage*, 15(1), 273–289. <https://doi.org/10.1006/nimg.2001.0978>.
- van Swieten, J. C., Koudstaal, P. J., Visser, M. C., Schouten, H. J., & van Gijn, J. (1988). Interobserver agreement for the assessment of handicap in stroke patients. *Stroke*, 19(5), 604–607. <https://doi.org/10.1161/01.str.19.5.604>.
- Vesia, M., Barnett-Cowan, M., Elahi, B., Jegatheeswaran, G., Isayama, R., Neva, J. L., ... Chen, R. (2017). Human dorsomedial parieto-motor circuit specifies grasp during the planning of goal-directed hand actions. *Cortex; a Journal Devoted To the Study of the Nervous System and Behavior*, 92, 175–186. <https://doi.org/10.1016/j.cortex.2017.04.007>.
- Vesia, M., & Crawford, J. D. (2012). Specialization of reach function in human posterior parietal cortex. *Experimental Brain Research*, 221(1), 1–18. <https://doi.org/10.1007/s00221-012-3158-9>.
- Vigano, L., Fonia, L., Rossi, M., Howells, H., Leonetti, A., Puglisi, G., ... Cerri, G. (2019). Anatomical-functional characterisation of the human "hand-knob": A direct electrophysiological study. *Cortex; a Journal Devoted To the Study of the Nervous System and Behavior*, 113, 239–254. <https://doi.org/10.1016/j.cortex.2018.12.011>.
- Ward, N. S. (2005). Mechanisms underlying recovery of motor function after stroke. *Postgraduate Medical Journal*, 81(958), 510–514. <https://doi.org/10.1136/pgmj.2004.030809>.
- Weiller, C., Juptner, M., Fellows, S., Rijntjes, M., Leonhardt, G., Kiebel, S., ... Thilmann, A. F. (1996). Brain representation of active and passive movements. *Neuroimage*, 4(2), 105–110. <https://doi.org/10.1006/nimg.1996.0034>.
- Wenderoth, N., Toni, I., Bedeleem, S., Debaere, F., & Swinnen, S. P. (2006). Information processing in human parieto-frontal circuits during goal-directed bimanual movements. *Neuroimage*, 31(1), 264–278. <https://doi.org/10.1016/j.neuroimage.2005.11.033>.
- Woosley, C. N. (1958). Organization of somatic sensory and motor areas of the cerebral cortex. In H. F. Harlow, & C. N. Woosley (Eds.), *Biological and biochemical bases of behavior* (pp. 63–81). Madison: University of Wisconsin Press.

3.1.3 Methodological considerations

A common practice in task-fMRI preprocessing pipeline is to perform image reorientation (flip along the x-axis) so that all images can be assumed to have the same-sided lesion. This step is usually performed in order to increase the statistical power, as the participants do not have to be divided into smaller subgroups based on the lesion side. Considering the small sample size of the ISIS-HERMES population, the first version of this article included the flip step and was consequently questioned by the reviewer. The concern was about brain asymmetry, and it was suggested that flipping would cause inaccuracy in the images that were flipped. Following the reviewer's recommendation, we redid the analysis without flipping the images (published version). Interestingly, although the detailed results (values) were different, the main results remained the same. Interestingly, the effect sizes in the relevant sensorimotor-related ROIs of the flipped and unflipped images were not significantly different. However, we think that image flipping should be avoided whenever possible.

3.2 Study II. White matter tract disruption is associated with ipsilateral hand impairment in subacute stroke: a diffusion MRI study

3.2.1 Overview

The second work of this thesis explored the mechanisms underlying the ipsilateral hand motor impairment using Diffusion Tensor Imaging (DTI). To this aim, we tested the association between tract white matter integrity assessed with the Fractional Anisotropy (FA) and hand behavioral scores using the grip strength and Purdue Pegboard test (PPT). While many studies have explored the association between FA and motor outcome after stroke, few studies have reported results regarding the ipsilateral hand. In fact, patients with stroke rely a lot on the ipsilateral hand to perform daily life activities, while the ipsilateral hand may show some degree of sensorimotor deficits from acute to chronic periods of stroke. (Colebatch and Gandevia, 1989; Gowers WR, 1887; Jones et al., 1989; Varghese and Winstein, 2019) Meanwhile, no consensus about the mechanisms to account for post-stroke ipsilateral hand impairment.

In this study, we aimed to determine the white matter tract disruptions associated with ipsilateral hand impairment in 29 patients with an ischemic anterior stroke. We used three behavioral tasks, the PPT, handgrip strength, and movement time. Diffusion MRI and behavioral scores were assessed at the same time, 1-month post-stroke. Fractional anisotropy was estimated in 33 white matter regions of the motor system from JHU atlas, and the resulting values were introduced in linear regression models to determine the white matter regions that are associated with ipsilateral hand impairment.

We found that PPT was predicted by the ipsilesional corticospinal tract (CST), and superior longitudinal fasciculus, handgrip by ipsilesional CST and anterior corona radiata, and movement time by the corpus callosum, contralesional CST at the pons level, and ipsilesional corticoreticulospinal pathway. In summary, impairment of the ipsilateral hand may result from not one but the summation of several white matter disruptions, supporting the concept of the degeneracy of the motor network. The article was published in *Neuroradiology Journal* on 28 March 2022.

3.2.2 Article

This part was intentionally left blank. The article starts on the next page.



White matter tract disruption is associated with ipsilateral hand impairment in subacute stroke: a diffusion MRI study

Firdaus Fabrice Hannanu^{1,2,3} · Bernadette Naegele⁴ · Marc Hommel¹ · Alexandre Krainik^{2,5} · Olivier Detante³ · Assia Jaillard^{1,2,6}

Received: 4 January 2022 / Accepted: 1 March 2022

© The Author(s), under exclusive licence to Springer-Verlag GmbH Germany, part of Springer Nature 2022

Abstract

Purpose The ipsilateral hand (ILH) is impaired after unilateral stroke, but the underlying mechanisms remain unresolved. Based on the degeneracy theory of network connectivity that many connectivity patterns are functionally equivalent, we hypothesized that ILH impairment would result from the summation of microstructural white matter (WM) disruption in the motor network, with a task-related profile. We aimed to determine the WM disruption patterns associated with ILH impairment.

Methods This was a cross-sectional analysis of patients in the ISIS-HERMES Study with ILH and diffusion-MRI data collected 1 month post-stroke. Patients performed three tasks, the Purdue Pegboard Test (PPT), handgrip strength, and movement time. Fractional anisotropy (FA) derived from diffusion MRI was measured in 33 WM regions. We used linear regression models controlling for age, sex, and education to determine WM regions associated with ILH impairment.

Results PPT was impaired in 42%, grip in 59%, and movement time in 24% of 29 included patients (mean age, 51.9 ± 10.5 years; 21 men). PPT was predicted by ipsilesional corticospinal tract (i-CST) ($B = 17.95$; $p = 0.002$) and superior longitudinal Fasciculus (i-SLF) ($B = 20.52$; $p = 0.008$); handgrip by i-CST ($B = 109.58$; $p = 0.016$) and contralesional anterior corona radiata ($B = 42.69$; $p = 0.039$); and movement time by the corpus callosum ($B = -1810.03$; $p = 0.003$) i-SLF ($B = -917.45$; $p = 0.015$), contralesional pons-CST ($B = 1744.31$; $p = 0.016$), and i-corticoreticulospinal pathway ($B = -380.54$; $p = 0.037$).

Conclusion ILH impairment was associated with WM disruption to a combination of ipsilateral and contralesional tracts with a pattern influenced by task-related processes, supporting the degeneracy theory. We propose to integrate ILH assessment in rehabilitation programs and treatment interventions such as neuromodulation.

Keywords Less-affected hand · Ipsilateral pyramidal tract · Contralesional hemisphere · Sensorimotor systems · Structural Connectivity

Glossary

FA	fraction of Anisotropy (diffusion MRI measure of white matter integrity)
FMS	Fugl-Meyer Score (Total score ranging 0 to 226, upper limb motor score subscore 0-66, sensory score 0-24 and coordination score 0-6)
JHU atlas	Johns Hopkins University atlas based on the MNI-ICBM labels 2-mm template
ILH	Ipsilateral Hand
MST	Movement Screening Test = movement time
NIHSS	National Institute of Health Stroke Scale (neurological severity)
PPT	Purdue Pegboard Test

✉ Assia Jaillard
Assia.Jaillard@univ-grenoble-alpes.fr

¹ AGEIS, EA 7407 Université Grenoble Alpes, Grenoble, France

² Unité IRM 3T Recherche - IRMaGe, Inserm US 17 CNRS - UMS 3552 UGA, CHUGA, Grenoble, France

³ Medical Faculty of Hasanuddin University, Makassar, Indonesia

⁴ Centre Hospitalier Universitaire Grenoble Alpes (CHUGA), Stroke Unit Neurology, Grenoble, France

⁵ Neuroradiologie, Pôle Imagerie, CHUGA, Grenoble, France

⁶ Pôle Recherche, CHUGA, Grenoble, France

RBANS	Repeatable Battery for the Assessment of Neuropsychological Status (global assessment of cognitive functions with a mean of 100 in healthy participants)
SD	Standard deviation

White matter tracts and Regions of Interest (ROIs)

ACR	Anterior Corona Radiata
ALIC	Anterior Limb of Internal Capsule
body-CC	body or middle segment of the Corpus Callosum (CC3 and CC4)
CST	Corticospinal tract
SCR	Superior Corona Radiata
PLIC	Posterior Limb of Internal Capsule
CP	Cerebral Peduncle
CRP	Cortico Reticulospinal Pathway
genu-CC	genu of the Corpus Callosum
ICP	inferior cerebellar peduncle
MCP	middle cerebellar peduncle
SCP	superior cerebellar peduncle
SLF	superior longitudinal fasciculus
i	ipsilesional
c	contralesional

Introduction

Hand movements represent a specific and essential function in humans required for everyday life activities. Following stroke, loss of hand functionality is one of the main factors affecting disability and remains a major target of rehabilitation interventions [1, 2]. Parallel to sensorimotor deficits of the paretic hand contralateral to the lesion, the ipsilateral hand (ILH) may show sensorimotor deficits for a large variety of sensorimotor tasks from the acute to chronic periods of stroke [3–8]. ILH impairment is frequent in subacute stroke [8] and may compound functional disability since patients require both hands to perform daily life activities [9].

Although several mechanisms have been postulated to account for post-stroke ILH deficits, no consensus has been reached and many aspects remain unresolved [10]. Anatomically, ILH impairment may result from ipsilateral descending motor pathways (i.e., fibers emerging from the damaged hemisphere and descending in the spinal cord without decussating), transcallosal fibers interacting with the undamaged hemisphere, and altered sensorimotor information through fibers crossing in the brainstem such as cerebellar peduncles. Accordingly, a first theory implicates the “uncrossed” ipsilateral corticospinal tract (CST) [11], as 3–15% of the corticospinal fibers descend in the ipsilateral spinal lateral funiculus without decussating in the medullary pyramids [12, 13] (Fig. 1). ILH impairment may also relate to the

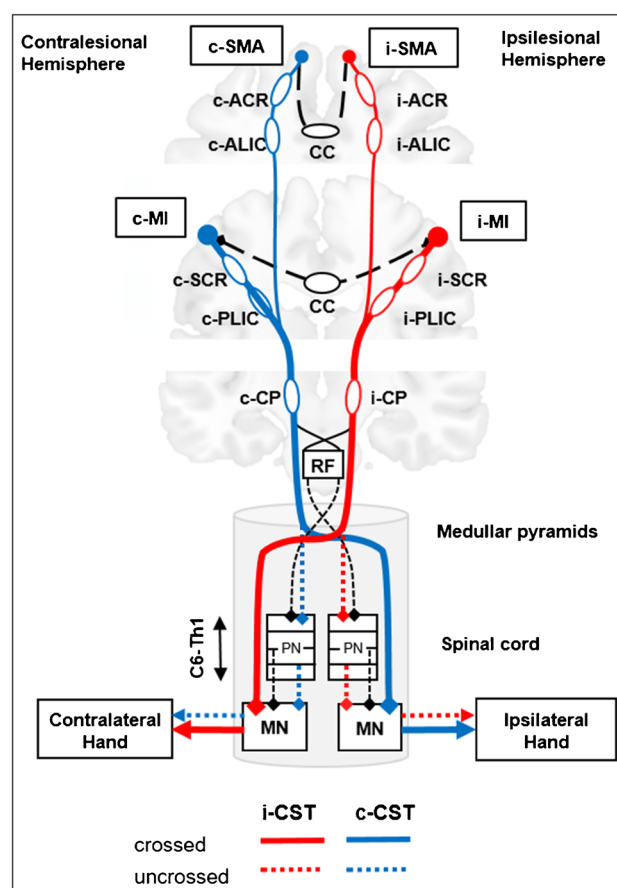


Fig. 1 Schematic representation of crossed and uncrossed fibers of the corticospinal tract (CST). ACR and ALIC fibers emerging from the SMA and PMC and SCR-PLIC fibers emerging from PMC and MI merge in the CP to form the CST, which continue in the pons and medulla. Then, the CST is divided into 2 parts. (1) Crossed CST (solid red and blue lines): most CST fibers decussate in the medullary pyramids to descend in the contralateral spinal cord and terminate in the contralateral anterior spinal horn to distal extremity muscles (direct cortico-motoneurons). (2) Uncrossed CST (dotted red and blue lines): a small proportion of the CST descends in the ipsilateral spinal lateral funiculus without decussating and terminates bilaterally in the ventromedial intermediate zone to propriospinal neurons. In addition, information is shared between the ipsilesional and contralesional hemispheres through transcallosal fibers (CC, dashed dark lines), before travelling through the CST. *Abbreviations:* CST=corticospinal tract, SCR=superior corona radiata; PLIC=posterior limb of internal capsule, CP=cerebral peduncle. Other ROIs are ACR=anterior corona radiata; ALIC=anterior limb of internal capsule; CC=corpus callosum; RF=reticular formation; PN=propriospinal neurons; MN= motoneurons; i=ipsilesional; and c=contralesional tracts

cerebellar peduncles via the fronto-cerebellar loops and the corticoreticulospinal pathway (CRP) that has bilateral spinal outputs. Another theory relies on bilateral parietal hemispheric control of unilateral movements [6, 10, 14, 15]. The lateralization of motor control has been recently revisited to enhance the role of the contralesional hemisphere, based on increased contralesional activity in the sensorimotor network

[16–18], and bilateral motor control supported by the posterior parietal cortex [19]. ILH impairment may also relate to interhemispheric transcallosal disconnections [20] as the corpus callosum (CC) coordinates motor function through the balance of excitatory and inhibitory interhemispheric interactions [14]. Finally, the impact of neuropsychological deficits such as apraxia and neglect has also been reported as a factor of ILH impairment [21–23].

Such a large variety of mechanisms can be put in perspective with the theory about degeneracy of the connectivity in neural networks [24] proposing that many patterns of neural architecture are functionally equivalent. Indeed, the connectivity pattern for a specified task arises during development in part by a process involving exuberant extension of neuronal processes that compete for targets. In this view, degenerate mechanisms would allow for sensorimotor plasticity and behavioral adaptation [25].

Based on the degeneracy theory, we hypothesized that ILH impairment would result from the summation of several disruptions to the sensorimotor network, with a pattern determined by the motor and visuomotor processes engaged in the ILH tasks. Since diffusion MRI provides reliable measures of white matter microstructure such as fractional anisotropy (FA) reflecting the neural changes related to the stroke lesion and its remote effects [26–30], we aimed to determine microstructure white matter (WM) disruption patterns associated with ILH impairment. WM disruption was assessed with FA measures in the motor WM network and ILH with three behavioral tasks engaging distinct motor and visuomotor processes. To this extent, we performed a cross-sectional analysis of patients in the ISIS-HERMES Study [31] with concomitant ILH and FA measures collected 1 month post-stroke.

Materials and methods

Participants

Patients

We enrolled 31 patients in the randomized controlled stem cell trial (ISIS-HERMES) at the stroke unit of the hospital from October 2010 to 2014 (ClinicalTrials.gov NCT00875654) [31]. In this study, we used the clinical, behavioral, and MRI data collected 1 month post-stroke, corresponding to the baseline visit performed before cell therapy administration. Patients received standard medical care including thrombolysis and thrombectomy when indicated. The ISIS-HERMES study was approved by the Institutional Review Board (CPP: 07-CHUG-25). Written informed consent was obtained from all patients before they participated in the study. The main inclusion criteria were

age 18–70 years, first-ever unilateral infarct in the internal carotid artery territory, moderate to severe neurological deficit defined as a NIH stroke scale (NIHSS) [32] score ≥ 7 , and the ability to follow a rehabilitation program. In addition to the inclusion–exclusion criteria listed in Table S1, we excluded patients with apraxia, or neglect diagnosed with an extinction NIHSS subscore > 1 .

Healthy participants

In addition, we included 31 healthy participants matched for age (± 5 years) and sex to the patients. Exclusion criteria are listed in Table S1.

Demographic and clinical measures

Age, sex, education level, handedness [33], height, weight, and stroke risk factors were collected. Of note, all participants were right-handed. Neurological severity was assessed using NIHSS and sensorimotor deficit using the Fugl-Meyer Score (FMS) [34], with upper limb motor, sensory, and coordination subscores (Table 1). A global cognitive assessment was performed with the Mini-Mental State Exam and the RBANS, exploring five domains (spatial, attention/executive, immediate and delayed memory, language) [35]. Assessments were performed by a stroke neurologist (NIHSS, neuropsychologists (RBANS, behavioral measures), and physiotherapists (FMS).

Behavioral measures

We explored ILH impairment using three behavioral tests. The Purdue Pegboard Test (PPT) (Lafayette Instrument Company, Indiana) [36] was performed as described in <http://www.equipement-ergotherapie.com/8-dexterité-manipulation.html>, as a standardized quantitative test requiring motor (for grasping) and visuomotor (for reaching) components. The hand dynamometer (Lafayette Instrument Company, Indiana; <https://www.prohealthcareproducts.com/100-kg-220lb-hand-grip-dynamometer-lafayette-instruments/>) is a validated test to measure handgrip force (Grip). The Motor Screening Task (MST) measures movement time to assess sensorimotor deficits in CANTAB (<https://www.cambridgecognition.com/cantab/cognitive-tests/attention/motor-screening-task-mot/>). Raw scores were converted to percentiles to adjust for age and sex using published norms [37] and CANTAB norms. Scores below the 5th percentile were considered as impaired. The frequency of ILH impairment was also assessed in patients without cognitive deficit, defined as RBANS > 40 .

Table 1 Patients' clinical and behavioral data ($n = 29$)

Variables	Mean	SD	Median	Percentile 25	Percentile 75
Age (years)	52.14	9.84	53.00	59.00	46.50
Education (years)	10.90	3.53	10.00	14.00	8.00
Lesion volume (ml)	102.66	63.99	97.00	141.50	49.50
Barthel Index	44.48	32.39	45.00	12.50	72.50
NIHSS	13.90	4.72	12.00	17.50	11.00
FMS total score/226	136.86	38.97	130.00	166.50	106.00
FMS motor score /66	36.45	27.91	31.00	52.00	15.00
FMS sensory score /24	11.31	7.92	14.00	17.00	0
FMS hand coordination /6	0.93	1.98	0	0	0
MMSE	25.15	6.20	27.00	29.00	24.50
Paretic PPT performance	1.25	3.23	0	0	0
Paretic Grip performance	3.79	9.79	0	0	0
Paretic MST (s)	634	284	441	942	423
ILH PPT performance	10.84	4.41	12.00	14.33	9.17
ILH Grip performance	23.90	12.34	21.66	34.83	16.50
ILH MST (s)	561	223	502	593	409

See glossary for abbreviations

MRI data acquisition

The MRI protocol included structural and diffusion sequences. All participants were scanned on a 3 T Philips magnet (Achieva 3.0 TTX; Philips, the Netherlands) with a 32-channel head coil. High-resolution (1 mm^3) sagittal 3D-T1-weighted (TR 9.9 ms, TE 4.6 ms, flip angle 8° , TI 920 ms, inter shot time 1792 ms) and fluid-attenuated inversion recovery (FLAIR) images (TR 8 s, TE 342 ms) were acquired. Diffusion-weighted images were acquired using single-shot echo-planar imaging (EPI) sequence (TR 11 ms, TE 72 ms, FOV 240 mm, slice thickness 2.0 mm, 70 axial slices, SENSE factor 2, fold-over direction anteroposterior, fat shift direction P, fat suppression, and voxel size $1.67 \times 1.67 \times 2 \text{ mm}$). We acquired 60 noncollinear directions with a b value of 1000 s/mm^2 and 10 directions with a b value of 0 s/mm^2 that were averaged to give 1 average direction.

MRI data analysis

Structural images were used to manually delineate lesion masks and compute lesion volumes using MRIcron (<https://www.nitrc.org/projects/mricron>). Diffusion-weighted images were processed with the *Diffusionist* toolkit derived from FSL software, as previously described [38]. Each DWI image was visually checked and removed if corrupted. Then, after correction of eddy-current distortions, the diffusion tensor was estimated.

We used FA to assess WM disruptions. Voxel-wise FA images were constructed from the resulting tensors. Linear and nonlinear registration transformations were applied to

the FSL FA template in the MNI-152 space by incorporating the knowledge of each brain lesion using manually delineated lesion masks [39]. FA was estimated only in the template's skeleton and outside the lesion mask. We estimated average FA values with atlas-based regions of interest (ROI) approach using the human brain WM JHU atlas [40]. As FA values vary along the CST tract, we selected the JHU atlas that includes 4 ROIs for the CST. FA was estimated in a set of 33 ROIs listed in Table 2 and represented in Fig. S1. *Diffusionist* toolkit and related documentation can be found at <http://mri-diffusionist.com/>.

Statistical analysis

ILH impairment was explored using descriptive statistics. First, we explored the relationship between behavioral tasks (PPT, handgrip, and MST percentiles) and clinical scores using Spearman correlations. As both ILH scores and FA measures showed a normal distribution, we tested the linear associations between ROI-derived FA and ILH raw scores using partial Pearson's correlations controlling for education, age, and sex, with 95% confidence intervals obtained with bootstrapping based on 1000 samples. In addition, FA values were compared between stroke patients and healthy participants using a t -test with bootstrapping based on 1000 samples to provide robust 95% confidence intervals.

We used linear regression models to determine the WM ROIs and thus the tracts associated with ILH impairment. The effects of ROIs, lesion side, volume, BMI, height, and weight were tested and included in the model only if significant. All models were adjusted for the effects of education, age, and sex. The best model was determined with

Table 2 Partial correlations between ILH tasks and JHU tracts controlling for education, age, and sex, with bootstrapping based on 1000 samples

Tracts	PPT				Grip				MST			
	r	p	95% CI		r	p	95% CI		r	p	95% CI	
			Lower	Upper			Lower	Upper			Lower	Upper
Vol tot	−0.38	0.058	−0.76	0.08	−0.34	0.093	−0.68	0.06	0.44	0.025	0.17	0.69
Corticospinal tract (CST)												
i-Pons	0.30	0.137	−0.14	0.64	0.30	0.141	−0.08	0.60	−0.18	0.387	−0.53	0.28
c-Pons	0.05	0.814	−0.47	0.41	0.12	0.564	−0.48	0.48	0.05	0.820	−0.20	0.38
i-CP	0.48	0.014	0.10	0.79	0.51	0.008	0.19	0.75	−0.26	0.192	−0.62	0.11
c-CP	0.42	0.031	0.03	0.71	0.44	0.024	0.08	0.68	−0.29	0.149	−0.68	0.06
i-PLIC	0.57	0.002	0.32	0.80	0.40	0.044	0.09	0.69	−0.32	0.108	−0.66	0.04
c-PLIC	0.16	0.423	−0.22	0.54	0.09	0.662	−0.28	0.49	−0.02	0.913	−0.44	0.28
i-SCR	0.41	0.038	−0.02	0.70	0.37	0.061	−0.06	0.68	−0.27	0.175	−0.60	0.21
c-SCR	0.20	0.337	−0.16	0.49	0.08	0.691	−0.36	0.52	−0.11	0.601	−0.42	0.22
Hemispheric tracts												
i-ACR	0.50	0.009	0.16	0.77	0.42	0.034	0.08	0.73	−0.50	0.009	−0.73	−0.22
c-ACR	0.54	0.005	0.27	0.76	0.59	0.002	0.23	0.78	−0.56	0.003	−0.77	−0.25
i-ALIC	0.42	0.032	0.04	0.72	0.22	0.271	−0.14	0.54	−0.18	0.368	−0.54	0.25
c-ALIC	0.48	0.012	0.16	0.74	0.44	0.024	0.11	0.72	−0.43	0.029	−0.71	−0.08
i-SLF	0.54	0.005	0.15	0.79	0.39	0.049	−0.04	0.78	−0.57	0.002	−0.80	−0.26
c-SLF	0.49	0.011	0.05	0.79	0.52	0.007	0.24	0.77	−0.49	0.010	−0.73	−0.16
i-PCR	0.63	0.001	0.26	0.83	0.61	0.001	0.33	0.81	−0.40	0.046	−0.63	−0.14
c-PCR	0.44	0.026	0.04	0.70	0.50	0.010	0.14	0.75	−0.52	0.007	−0.77	−0.16
Commissural tracts (corpus callosum)												
Genu	0.62	0.001	0.33	0.85	0.61	0.001	0.31	0.79	−0.61	0.001	−0.83	−0.36
Body	0.42	0.032	0.08	0.70	0.46	0.017	0.06	0.72	−0.31	0.118	−0.58	0.01
Splenium	0.54	0.004	0.18	0.77	0.60	0.001	0.21	0.86	−0.47	0.015	−0.69	−0.17
Cerebellar peduncles												
i-SCP	0.31	0.119	−0.08	0.64	0.38	0.053	−0.01	0.64	−0.23	0.263	−0.52	0.09
c-SCP	0.47	0.016	0.12	0.73	0.45	0.020	0.11	0.68	−0.32	0.113	−0.62	0.01
i-ICP	0.35	0.077	−0.09	0.67	0.41	0.038	0.06	0.64	−0.34	0.093	−0.59	−0.09
c-ICP	0.17	0.405	−0.29	0.64	0.18	0.374	−0.20	0.55	−0.20	0.319	−0.57	0.15
i-MCP	0.11	0.587	−0.30	0.46	0.20	0.335	−0.32	0.55	−0.05	0.798	−0.31	0.24
c-MCP	0.26	0.205	−0.16	0.58	0.16	0.436	−0.24	0.50	−0.10	0.615	−0.47	0.33
Cortico Reticulospinal Pathway (CRP)												
i-Pons-CRP	0.34	0.092	0.11	0.59	0.31	0.130	0.03	0.64	−0.35	0.084	−0.67	0.06
i-CP-CRP	0.24	0.244	−0.08	0.52	0.24	0.242	−0.05	0.56	−0.25	0.216	−0.59	0.19
i-PLIC-CRP	0.30	0.143	−0.07	0.61	0.20	0.326	−0.16	0.56	−0.32	0.109	−0.64	0.06
i-CR-CRP	0.02	0.922	−0.33	0.31	0.07	0.747	−0.31	0.41	−0.22	0.271	−0.55	0.06
c-Pons-CRP	0.06	0.783	−0.35	0.38	0.08	0.696	−0.30	0.48	−0.03	0.900	−0.43	0.37
c-CP-CRP	0.07	0.733	−0.28	0.48	0.14	0.510	−0.24	0.50	−0.04	0.848	−0.47	0.37
c-PLIC-CRP	−0.05	0.829	−0.42	0.37	0.10	0.632	−0.27	0.48	−0.02	0.910	−0.29	0.22
c-CR-CRP	−0.02	0.925	−0.35	0.37	−0.13	0.515	−0.45	0.20	0.08	0.717	−0.21	0.33

Abbreviations: *r* indicates Pearson correlation coefficient; *p* significance (2-tailed); 95% *CI* 95% confidence interval. Tracts: ipsilesional (i-) and contralesional (c-). ROIs: *SCR* superior corona radiata; *PLIC* posterior limb of the internal capsule; *CP* cerebral peduncle; *PCR* posterior corona radiata; *SCP* superior, *MCP* middle, and *ICP* inferior cerebellar peduncles; *SLF* superior longitudinal fasciculus, *CC* genu body and splenium of the corpus callosum, *ACR* anterior corona radiata, *ALIC* anterior limb of the internal capsular

the statistical significance of the factors with the *F*-test ($p < 0.05$), model fit estimated with Durbin-Watson test and distribution of residuals, and model accuracy assessed with

adjusted R^2 . Internal validation was performed with bootstrapping based on 1000 samples. Statistical data analyses were performed using SPSS 23.0.

Results

Twenty-nine patients (21 males, 10 right lesions, all right-handed) completed clinical, behavioral, and MRI assessments at 1 month post-stroke (Fig. S2). We also included 29 age- and sex-matched healthy participants (21 males, mean age 51.1 ± 12.2 years, all right-handed). Clinical data are presented in Table 1. Lesion overlap (Fig. 2) highlights that the middle cerebral artery territory was infarcted in all patients.

ILH assessment

Behavioral measures are presented in Table 1. ILH was impaired in 12 patients for PPT (41.4%, 95% CI = 24.1–62.1), 17 for grip (58.6%, 95% CI = 41.4–75.9) and 7 for MST (24.1%, 95% CI = 10.3–41.4). In the subgroup of 24 patients without cognitive deficit, rates were not significantly different from the whole group, with PPT impaired in 10 patients (41.7%, 95% CI = 21.7–62.5), grip in 16 patients (66.7%, 95% CI = 47.6–86.4), and MST in 7 patients (29.2%, 95% CI = 10.0–47.6).

Factors associated with ILH impairment

PPT, Grip, and MST significantly correlated with clinical but cognitive scores (Table S2). ILH correlated with the paretic hand for PPT, with a trend for grip and MST (Table S3). There was no significant effect of lesion side on ILH performances. FA values were significantly lower in the patients than in the healthy participants for all ROIs but the contralesional pons-CST, PLIC-CST, and PLIC-CRT, and bilateral SCR-CRT (Table S4).

Table 2 reports ILH and FA correlations. PPT correlated with the ipsilesional (i-) CST (CP-, PLIC, and SCR ROIs), contralesional (c-) CP-CST, bilateral SLF, ALIC, ACR, and PCR, CC, and c-SCP. Grip correlated with the same ROIs but i-SCR and i-ALIC, and with i-ICP. MST correlated with bilateral SLF, ACR, PCR, c-ALIC, CC genu and splenium, and lesion volume.

Linear regression models are presented in Table 3. PPT was predicted by ipsilesional PLIC-CST ($B = 17.95$; $p = 0.002$) and SLF ($B = 20.52$; $p = 0.008$) with no significant effect of education, age, and sex; $r^2 = 0.696$, indicating good model accuracy. Handgrip strength was predicted by ipsilesional CP-CST ($B = 109.58$; $p = 0.016$) and contralesional ACR ($B = 42.69$; $p = 0.039$), with an effect of male sex, but no education and age; $r^2 = 0.571$, indicating moderate accuracy. Movement time was predicted by CC genu ($B = -1810.03$; $p = 0.003$) ipsilesional-SLF ($B = -917.45$; $p = 0.015$), contralesional pons-CST ($B = 1744.31$; $p = 0.016$), and ipsilesional PLIC-CRT ($B = -380.54$; $p = 0.037$), with male sex and high education supporting better performance; $r^2 = 0.755$, indicating good accuracy.

Discussion

Clinical assessment of ILH

We assessed behavioral performances of the less-affected hand (ILH) in 29 patients at 1 month post-stroke. Since the degree of ILH impairment may depend on the type of task that is tested [10], we used three tasks with different motor and visuomotor processes. PPT, grip, and movement time were impaired in 41.4%, 58.6%, and 24.1%, respectively, highlighting that ILH impairment is frequent, in line with

Fig. 2 Overlap of stroke lesions in the 29 patients. Axial slices are displayed with for z MNI coordinates. Left lesions are represented on the left side and right lesions on the right side of each slice (neurologic convention). Note that ipsilesional SCR and SLF were damaged in all patients, and PLIC, ALIC, and ACR in 70% of them

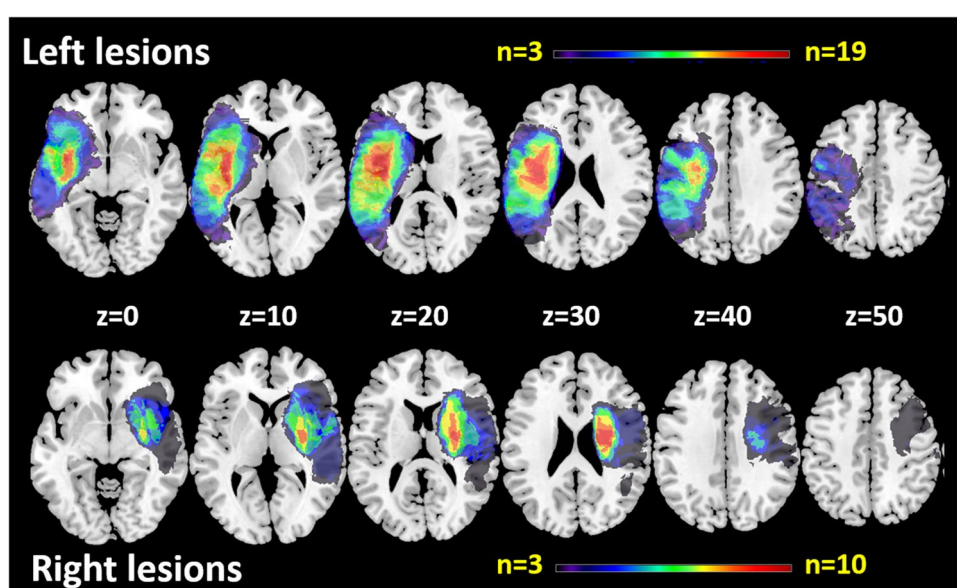


Table 3 Linear regression models for ILH PPT, GRIP, and MST, with bootstrapping based on 1000 samples

PPT	$r^2=0.696$	B	Bootstrap				
			Bias	SE	p	95% CI	
Variables	r^2 change					Lower	Upper
(Constant)		− 1.69	− 0.16	4.79	0.696	− 12.30	7.02
Education		0.32	− 0.01	0.17	0.065	− 0.02	0.65
Age	0.450	− 0.08	0.00	0.05	0.067	− 0.17	0.02
Sex		− 1.16	− 0.22	1.04	0.251	− 3.57	0.63
i-PLIC	0.182	17.95	0.82	5.22	0.002	8.24	29.15
i-SLF	0.120	20.52	0.46	6.78	0.008	8.80	36.36
GRIP	$r^2=0.571$	B	Bootstrap				
			Bias	SE	p	95% CI	
Variables	r^2 change					Lower	Upper
Constant		− 18.10	− 1.98	21.03	0.329	− 66.47	17.71
Sex		− 14.89	− 0.66	3.79	0.001	− 24.01	− 8.54
Age	0.327	− 0.12	0.01	0.14	0.318	− 0.38	0.18
Education		0.35	0.02	0.50	0.484	− 0.55	1.38
c-ACR	0.233	109.58	5.48	42.65	0.016	36.52	206.99
i-CP-CST	0.088	42.69	0.02	18.67	0.039	4.09	78.76
MST	$r^2=0.755$	B	Bootstrap				
			Bias	SE	p	95% CI	
Variables	r^2 change					Lower	Upper
Constant		1172.19	52.11	431.26	0.008	398.01	2202.31
Education		− 17.66	0.00	6.36	0.009	− 29.74	− 3.14
Age	0.351	− 1.83	− 0.26	3.57	0.612	− 9.02	5.39
Sex		135.87	0.83	58.95	0.035	24.22	261.94
genu -CC	0.243	− 1810.03	− 47.30	419.95	0.003	− 2632.43	− 925.48
i-SLF	0.103	− 917.45	− 18.63	308.59	0.015	− 1539.04	− 323.94
c-pons-CST	0.074	1744.31	− 5.22	672.29	0.016	260.57	2947.88
i-PLIC-CRT	0.045	− 380.54	− 5.18	170.54	0.037	− 719.31	− 75.81

SE indicates standard error; 95% CI, 95% confidence interval; Tracts: ipsilesional (i-) and contralesional (c-). ROIs: *PLIC* posterior limb of the internal capsule, *CP* cerebral peduncle, *SLF* superior longitudinal fasciculus, *genu-CC* genu body of the corpus callosum, *ACR* anterior corona radiata

previous studies [6, 8, 10, 15, 41]. Among the multiple tasks described in the literature exploring post-stroke ILH impairment, PPT impairment is the most commonly described, while more heterogeneous results are reported for handgrip strength [6, 15] and movement time [42]. Here, the low frequency of MST suggests that this test may be an insensitive measure compared to kinematic measures, [42, 43], and that visuomotor components of ILH impairment may have been underestimated.

We measured FA in the main tracts related to hand motor function [29, 30, 44] and found that all ROIs but pons and PLIC ROIs of the contralesional CST had lower FA values in patients than in healthy participants, indicating microstructural damage to contralesional and interhemispheric white matter tracts following stroke that may compound ILH function.

ILH performances correlated with clinical motor and sensory scores highlighting that ILH impairment scales with

sensorimotor stroke severity and Barthel index. The effect of stroke severity was particularly strong for ILH PPT that correlated with the paretic PPT and lesion volume, while trends were observed for grip and MST.

Correlation analyses between ILH and FA in ROIs of the motor network also revealed task dissociations. PPT (including reach movements requiring visuomotor processes and precise grasp requiring motor processes), MST (visuomotor reaching task), and grip strength (pure motor task) were predicted by a combination of different tracts of the motor network. This argues against the idea that a single mechanism may account for ILH impairment that varies in terms of modality and degree.

Mechanisms of ILH impairment

Our findings showed that, depending on the task, several tracts including the CST, c-ACR, CC, i-SLF, and to a lesser extent i-CRP, were associated with ILH impairment.

We found moderate to strong correlations between the three ILH scores and i-CST, while no significant correlation was observed with contralesional CST-CR and CST-PLIC, suggesting that motor processes of ILH impairment are driven by the ipsilesional CST. Furthermore, i-CST predicted ILH impairment, explaining 18.2 and 8.8% of the PPT and grip variance, respectively. Anatomically, the uncrossed fibers of the ipsilesional CST (Fig. 1-S3A) descending in the dorsal funiculus terminate in the ventromedial intermediate zone to propriospinal neurons connected to distal motoneurons through intersegment spinal interneurons. Although the ventromedial intermediate zone is related to the motor function of the trunk and arms [45], propriospinal neurons may connect with distal motoneurons through intersegment spinal interneurons and thus be involved in the motor control of dexterous hand movements [46]. Moreover, other corticospinal pathways projecting to the reticular formation such as the CRP terminate bilaterally to the propriospinal neurons of the ventral and lateral intermediate zone and contribute to motor performance [47]. Our findings, showing that i-PLIC-CRP was a factor of MST performance, strengthen the hypothesis that ipsilesional descending pathways participate in ILH impairment.

ILH scores were also correlated with FA in the bilateral ALIC, ACR, and CC. Linear models showed that c-ACR was a significant factor of handgrip impairment, explaining 23.3% of the variance. ACR has been linked to cognition and particularly to attention in adults with brain injury [48]. Moreover, a part of ACR fibers originate in the SMA, descend through the ALIC [49], and then merge with the CST in the CP [13], which continues in the pons and medulla to decussate at the pyramid caudal end [13, 50]. The involvement of SMA in simple motor tasks is documented by stroke studies, with SMA lesions leading to mild motor deficits [50], and i-SMA fMRI-related activity supporting motor recovery [17, 51]. Therefore, motor control components of ILH impairment may also implicate the contralesional CST through transcallosal and c-ACR fibers from premotor and/or prefrontal areas (Fig. 1-S3.B).

We found that all ILH scores strongly correlated with the CC including the genu, which predicted MST and explained 24.3% of the variance. A role of the CC is motor coordination of bimanual [52] and unilateral hand motor movements through the balance of excitatory and inhibitory interhemispheric interactions [14]. The ipsi- and contralesional motor areas exert a reciprocal influence through transcallosal fibers [53], as evidenced in tracer studies showing reciprocal transcallosal connections for both MI and SMA [54]. In

nonhuman primates, SMA lesions impaired the ILH motor program through transcallosal connections to contralesional SMA [55]. Taken together, our findings concur with previous stroke studies [6, 56], suggesting that the information is shared with the contralesional hemisphere through transcallosal fibers, before travelling through the descending motor pathways. This is consistent with the recent literature proposing an active and specific role of the ipsilateral hemisphere in the planning and execution of voluntary movements [19].

ILH impairment also correlated with decreased FA in bilateral SLF and i-SLF predicted PPT and MST explaining 12.0 and 10.3% of the variance, respectively. These findings support the theory that ILH impairment relates to the bilateral hemispheric control of unilateral movement [6, 10, 14, 15]. In this view, the damaged hemisphere would alter movements of both ILH and paretic hands. In the literature, unimanual motor tasks implicating visuomotor components yield bilateral activity in the frontoparietal network [14, 57–59]. In our study, PPT and MST that require visuomotor control (in contrast to handgrip) were associated with the SLF, a key structure of the frontoparietal network connecting parietal, premotor, and motor frontal areas in both human [60–62] and nonhuman primates [13]. Furthermore, our findings that i-SLF disruptions alter ILH with visuomotor processing are supported by previous works showing an essential role for the SLF in motor planning and kinematic components of movement execution in 30 right-handed healthy participants [44].

Interestingly, ILH impairment did not correlate with cognitive deficits and was not significantly improved in patients without cognitive deficit, suggesting that cognitive impairment did not influence ILH impairment in this study. Nevertheless, as patients with severe apraxia or neglect were excluded from our study, we may have underestimated the effects of cognitive impairment related to apraxia and neglect on ILH impairment [22].

There were significant correlations between lesion volume and MST, with a trend for PPT and grip. Surprisingly, few studies, if any, have explored the relationships between lesion volume and ILH impairment in humans. Our findings are consistent with nonhuman macaque experiments [63] reporting that reaching ILH tasks were compounded by lesion volume.

Limitations

The small sample size is the main limitation of this study. However, this is the first study exploring the microstructural WM disruptions to understand the underlying mechanisms of ILH impairment following stroke. Also, the homogeneity of our population in terms of age, absence of leukoaraiosis, and stroke severity and territory may

have compensated, at least for a part, for this limitation. Nevertheless, the small sample may explain why we did not observe any effect of the lesion side, in contrast with others [7]. Another limitation relates to ILH impairment patients' perception. When patients with impaired ILH were asked if they noticed that their ILH was impaired, most of them answered that their ILH function was worse than before stroke, but much better than the contralateral hand. However, we did not record all patients' answers.

Conclusion

This study showed that motor-related tract disruptions predict ILH impairment, with a pattern related to the processes engaged in each task: tasks with motor processing were associated with the ipsilateral CST suggesting the involvement of uncrossed CST fibers, while tasks with visuomotor processing were related to i-SLF supporting hand motor control. In addition, our findings revealed a role for the contralesional hemisphere that may modulate the planning and execution of hand movements through prefrontal/premotor areas and transcallosal interactions. Taken together, ILH impairment may result from the summation of several WM disruptions, supporting the concept of degeneracy of the motor network. Our results provide a theoretical basis for integrating ILH impairment in rehabilitation programs to improve functional recovery and for research interventions, such as neuromodulation.

Supplementary Information The online version contains supplementary material available at <https://doi.org/10.1007/s00234-022-02927-8>.

Acknowledgements We thank the platform of France Life Imaging network for partly supporting MRI data acquisition through the grant "ANR-11-INBS-0006, the Clinical Investigation Center (CIC) INSERM UMS 002 CHU Grenoble Alpes for data monitoring, and Felix Renard and Bérengère Aubert-Broche for the Diffusionist software (Diffusion MRI processing).

Funding This work was supported by: Ministère des Solidarités et de la Santé. Programme hospitalier de recherche clinique – PHRC: ISIS-2007PHR04 (NCT00875654) and HERMES-2007-A00853-50 for patient inclusion and clinical and multimodal MRI data acquisition; IRMaGE platform partly funded by the French program "investissement d'avenir" run by the agence nationale pour la recherche, grant « infrastructure d'avenir en Biologie Santé »—ANR – 11 – INBS-0006 m; and the Indonesia Endowment Fund for Education (LPDP) for F. F. Hannanu PhD.

Data availability The data that support the findings of this study are available from the corresponding author upon reasonable request criteria.

Declarations

Ethics approval Institutional review board approval by the Institutional Review Board (CPP: 07-CHUG-25).

Consent to participate A written informed consent from all patients or relatives was obtained before their participation in the study.

Consent to publish All the authors have read and approved the submission.

Competing interest The authors have no conflict of interest to declare.

References

1. Pennati GV et al (2020) Recovery and prediction of dynamic precision grip force control after stroke. *Stroke* 51(3):944–951
2. Stinear C (2010) Prediction of recovery of motor function after stroke. *Lancet Neurol* 9(12):1228–1232
3. Carey LM, Matyas TA (2011) Frequency of discriminative sensory loss in the hand after stroke in a rehabilitation setting. *J Rehabil Med* 43(3):257–263
4. Colebatch JG, Gandevia SC (1989) The distribution of muscular weakness in upper motor neuron lesions affecting the arm. *Brain* 112(Pt 3):749–763
5. Gowers, W.R., *A manual of diseases of the nervous system. Motor Symptoms*. Vol. II. 1886, London UK: Churchill. 988.
6. Jones RD, Donaldson IM, Parkin PJ (1989) Impairment and recovery of ipsilateral sensory-motor function following unilateral cerebral infarction. *Brain* 112(Pt 1):113–132
7. Varghese R, Winstein CJ (2019) Relationship between motor capacity of the contralesional and ipsilesional hand depends on the side of stroke in chronic stroke survivors with mild-to-moderate impairment. *Front Neurol* 10:1340
8. Semrau JA et al (2017) Robotic Characterization of ipsilesional motor function in subacute stroke. *Neurorehabil Neural Repair* 31(6):571–582
9. Plantin J et al (2021) Recovery and prediction of bimanual hand use after stroke. *Neurology* 97(7):e706–e719
10. Kitsos GH et al (2013) The ipsilesional upper limb can be affected following stroke. *ScientificWorldJournal* 2013:684860
11. Ziemann U et al (1999) Dissociation of the pathways mediating ipsilateral and contralateral motor-evoked potentials in human hand and arm muscles. *J Physiol* 518(Pt 3):895–906
12. Nyberg-Hansen R (1968) "The pyramidal tract syndrome" in man in the light of experimental investigations. *Tidsskr Nor Laegeforen* 88(1):8–14
13. Schmähmann JD, Pandya DN (2006) Fiber pathways of the brain. Oxford University Press, Oxford, p 654
14. Chettouf S et al (2020) Are unimanual movements bilateral? *Neurosci Biobehav Rev* 113:39–50
15. Noskin O et al (2008) Ipsilateral motor dysfunction from unilateral stroke: implications for the functional neuroanatomy of hemiparesis. *J Neurol Neurosurg Psychiatry* 79(4):401–406
16. Dechaumont-Palacin S et al (2008) Neural correlates of proprioceptive integration in the contralesional hemisphere of very impaired patients shortly after a subcortical stroke: an FMRI study. *Neurorehabil Neural Repair* 22(2):154–165
17. Favre I et al (2014) Upper limb recovery after stroke is associated with ipsilesional primary motor cortical activity: a meta-analysis. *Stroke* 45(4):1077–1083

18. Rehme AK et al (2011) The role of the contralesional motor cortex for motor recovery in the early days after stroke assessed with longitudinal FMRI. *Cereb Cortex* 21(4):756–768
19. Bundy DT, Leuthardt EC (2019) The cortical physiology of ipsilateral limb movements. *Trends Neurosci* 42(11):825–839
20. Jung HY, Yoon JS, Park BS (2002) Recovery of proximal and distal arm weakness in the ipsilateral upper limb after stroke. *NeuroRehabilitation* 17(2):153–159
21. Chestnut C, Haaland KY (2008) Functional significance of ipsilesional motor deficits after unilateral stroke. *Arch Phys Med Rehabil* 89(1):62–68
22. Sunderland A et al (1999) Impaired dexterity of the ipsilateral hand after stroke and the relationship to cognitive deficit. *Stroke* 30(5):949–955
23. Wetter S, Poole JL, Haaland KY (2005) Functional implications of ipsilesional motor deficits after unilateral stroke. *Arch Phys Med Rehabil* 86(4):776–781
24. Edelman GM, Gally JA (2001) Degeneracy and complexity in biological systems. *Proc Natl Acad Sci U S A* 98(24):13763–13768
25. Price CJ, Friston KJ (2002) Degeneracy and cognitive anatomy. *Trends Cogn Sci* 6(10):416–421
26. Auriat AM et al (2015) A review of transcranial magnetic stimulation and multimodal neuroimaging to characterize post-stroke neuroplasticity. *Front Neurol* 6:226–226
27. Kumar P et al (2016) Prediction of upper limb motor recovery after subacute ischemic stroke using diffusion tensor imaging: a systematic review and meta-analysis. *J Stroke* 18(1):50–59
28. Lindenberg R et al (2012) Predicting functional motor potential in chronic stroke patients using diffusion tensor imaging. *Hum Brain Mapp* 33(5):1040–1051
29. Lindow J et al (2016) Connectivity-based predictions of hand motor outcome for patients at the subacute stage after stroke. *Front Hum Neurosci* 10:101
30. Puig J et al (2017) Diffusion tensor imaging as a prognostic biomarker for motor recovery and rehabilitation after stroke. *Neuroradiology* 59(4):343–351
31. Jaillard A, et al. (2020) Autologous mesenchymal stem cells improve motor recovery in subacute ischemic stroke: a randomized clinical trial. *Transl Stroke Res*
32. Brott T et al (1989) Measurements of acute cerebral infarction: a clinical examination scale. *Stroke* 20(7):864–870
33. Oldfield RC (1971) The assessment and analysis of handedness: the Edinburgh inventory. *Neuropsychologia* 9(1):97–113
34. Fugl-Meyer AR et al (1975) The post-stroke hemiplegic patient. 1. a method for evaluation of physical performance. *Scand J Rehabil Med* 7(1):13–31
35. Randolph C et al (1998) The repeatable battery for the assessment of neuropsychological status (RBANS): preliminary clinical validity. *J Clin Exp Neuropsychol* 20(3):310–319
36. Rapin I, Tourk LM, Costa LD (1966) Evaluation of the Purdue Pegboard as a screening test for brain damage. *Dev Med Child Neurol* 8(1):45–54
37. Spreen O, Strauss E, A compendium of neuropsychological test. Second, (eds) (1998) New York. Oxford University Press, USA
38. Soulard J et al (2020) Motor tract integrity predicts walking recovery: a diffusion MRI study in subacute stroke. *Neurology* 94(6):e583–e593
39. Renard F, Urvoy M, Jaillard A (2015) Bayesian stroke lesion estimation for automatic registration of DTI images. 91–103
40. Oishi K et al (2008) Human brain white matter atlas: identification and assignment of common anatomical structures in superficial white matter. *Neuroimage* 43(3):447–457
41. Marque P et al (1997) Impairment and recovery of left motor function in patients with right hemiplegia. *J Neurol Neurosurg Psychiatry* 62(1):77–81
42. Metrot J et al (2013) Motor recovery of the ipsilesional upper limb in subacute stroke. *Arch Phys Med Rehabil* 94(11):2283–2290
43. Bustren EL, Sunnerhagen KS, Alt Murphy M (2017) Movement kinematics of the ipsilesional upper extremity in persons with moderate or mild stroke. *Neurorehabil Neural Repair* 31(4):376–386
44. Budisavljevic S et al (2017) Asymmetry and structure of the fronto-parietal networks underlie visuomotor processing in humans. *Cereb Cortex* 27(2):1532–1544
45. Kuypers H (2011) Anatomy of the descending pathways
46. Tohyama T et al (2017) Contribution of propriospinal neurons to recovery of hand dexterity after corticospinal tract lesions in monkeys. *Proc Natl Acad Sci U S A* 114(3):604–609
47. Bradnam LV, Stinear CM, Byblow WD (2013) Ipsilateral motor pathways after stroke: implications for non-invasive brain stimulation. *Front Hum Neurosci* 7:184
48. Niogi SN et al (2008) Structural dissociation of attentional control and memory in adults with and without mild traumatic brain injury. *Brain* 131(Pt 12):3209–3221
49. Morecraft RJ et al (2002) Localization of arm representation in the corona radiata and internal capsule in the non-human primate. *Brain* 125(Pt 1):176–198
50. Fries W et al (1993) Motor recovery following capsular stroke. Role of descending pathways from multiple motor areas. *Brain* 116(Pt 2):369–382
51. Grefkes C et al (2008) Cortical connectivity after subcortical stroke assessed with functional magnetic resonance imaging. *Ann Neurol* 63(2):236–246
52. Andres FG et al (1999) Functional coupling of human cortical sensorimotor areas during bimanual skill acquisition. *Brain* 122(Pt 5):855–870
53. Leichnetz GR (1986) Afferent and efferent connections of the dorsolateral precentral gyrus (area 4, hand/arm region) in the macaque monkey, with comparisons to area 8. *J Comp Neurol* 254(4):460–492
54. Gould HJ 3rd et al (1986) The relationship of corpus callosum connections to electrical stimulation maps of motor, supplementary motor, and the frontal eye fields in owl monkeys. *J Comp Neurol* 247(3):297–325
55. Brinkman C (1984) Supplementary motor area of the monkey's cerebral cortex: short- and long-term deficits after unilateral ablation and the effects of subsequent callosal section. *J Neurosci* 4(4):918–929
56. Nowak DA et al (2007) Dexterity is impaired at both hands following unilateral subcortical middle cerebral artery stroke. *Eur J Neurosci* 25(10):3173–3184
57. Cavina-Pratesi C et al (2018) Human neuroimaging reveals the subcomponents of grasping, reaching and pointing actions. *Cortex* 98:128–148
58. Cavina-Pratesi C et al (2010) Functional magnetic resonance imaging reveals the neural substrates of arm transport and grip formation in reach-to-grasp actions in humans. *J Neurosci* 30(31):10306–10323
59. Begliomini C et al (2014) An investigation of the neural circuits underlying reaching and reach-to-grasp movements: from planning to execution. *Front Hum Neurosci* 8:676
60. Makris N et al (2005) Segmentation of subcomponents within the superior longitudinal fascicle in humans: a quantitative, in vivo, *DT-MRI* study. *Cereb Cortex* 15(6):854–869

61. Thiebaut de Schotten M et al (2011) A lateralized brain network for visuospatial attention. *Nat Neurosci* 14(10):1245–1246
62. Wang X et al (2016) Subcomponents and connectivity of the superior longitudinal fasciculus in the human brain. *Brain Struct Funct* 221(4):2075–2092
63. Darling WG et al (2011) Volumetric effects of motor cortex injury on recovery of ipsilesional dexterous movements. *Exp Neurol* 231(1):56–71

Publisher's Note Springer Nature remains neutral with regard to jurisdictional claims in published maps and institutional affiliations.

3.3 Study III. Visuomotor resting-state functional MRI connectivity predicts hand motor outcome following stroke

3.3.1 Overview

The third work of this thesis explored the resting-state fMRI functional connectivity associated with hand motor outcome following stroke. In Study I, using the task-fMRI, we found a dissociation between simple grasp task and reach-to-grasp task in terms of brain activity within the sensorimotor network. However, we could not explore the influence of visual components on motor recovery and test the dual visual theory since our analysis was limited to the sensorimotor regions activated during the passive motor task performed in the task-fMRI scan. As no task is performed during the scan, resting-state fMRI allows the exploration of both motor and non-motor functional connectivity associated with motor performance and motor outcome after stroke.

This study aimed to explore the influence of visual regions on hand motor outcomes following stroke. Similar to Study I, our hypothesis was mainly based on the dual visuomotor stream theory (Goodale and Milner, 1992). For a visuomotor task, it can be expected to find an association between visuomotor connectivity and the performance of a task involving online visuomotor feedback, such as the PPT. In contrast, such an association is not certain with regard to a pure motor task, such as the handgrip. Although the handgrip task does not require a continuous visual input to be performed, the visual system may have an influence on the preparation and execution of any motor actions. Based on this, we hypothesized that in addition to the intrinsic motor connections (*i.e.*, connectivities within the sensorimotor network), visuomotor connectivity (*i.e.*, connectivity between occipital areas and motor areas) is engaged in any motor action, regardless of whether or not it requires online visual control.

In this study, we used handgrip strength to assess the hand motor performance and outcome. RS-fMRI was assessed at one-month post-stroke, and handgrip scores were assessed at one-month post-stroke (M0), and six months later (M6). Correlation analysis and linear regression modeling were used. Internal validation was performed using bootstrapping based on 1000 samples. To validate our model, we used the IRMAS dataset as the training dataset (n=54) and validated it using the ISIS-HERMES dataset (n=25).

We found that at M0, handgrip was associated with connectivity between the ipsilesional primary motor (BA4a) and visual cortices and between the ipsilesional parietal (SPL-7M) and lateral occipital cortex (OC). At M6, grip predictors included connectivity between ipsilesional BA4a and dorsal OC, between ipsilesional primary sensory (BA3b) and contralesional

premotor (BA6 ma) cortices, and between ipsilesional SPL-7M and lateral OC. The models were adjusted for age, sex, and baseline motor-NIHSS.

In summary, in addition to interhemispheric sensorimotor connectivity, visuomotor connectivity (*i.e.*, connectivity between primary sensorimotor areas and occipital areas) was associated with hand motor outcome at M0 and at M6. The article was submitted to Neurology Journal on 11 May 2022 and is currently under review.

3.3.2 Article

This part was intentionally left blank. The article starts on the next page.

Visuomotor resting-state functional MRI connectivity predicts hand motor outcome following stroke

Firdaus Fabrice HANNANU MD,^{1,2} Flore BARONNET MDPH,³ Bernadette NAEGELE PhD,⁴ Aliénor JAILLARD, MSc,^{1,5} Alexandre KRAINIK, MD-PhD,^{2,6,7} Olivier DETANTE, MD-PhD,^{3,7} Charlotte ROSSO, MDPH,^{3,8} and Assia JAILLARD MD PhD.^{1,5,9}

1. AGEIS, Université Grenoble Alpes (UGA), France
2. IRM 3T Recherche, IRMaGe, Centre Hospitalier Universitaire Grenoble Alpes (CHUGA) France
3. APHP-Urgences Cérébro-Vasculaires, Hôpital Pitié-Salpêtrière, Paris, France
4. Stroke Unit, Neurologie, CHUGA France
5. Faculté de Médecine, Université Paris-Saclay
6. Unité IRM, Pole Imagerie, CHUGA France
7. Inserm U1216, Grenoble Institut Neurosciences, UGA, France
8. Inserm U 1127, CNRS UMR 7225, Sorbonne Université, UPMC Univ Paris 06 UMR S 1127, Institut du Cerveau et de la Moelle épinière, ICM, F-75013, Paris, France
9. Pôle Recherche, CHUGA France

Corresponding author: Assia Jaillard

Email: Assia.Jaillard@univ-grenoble-alpes.fr

Address: Unité IRM 3T - Recherche

CHU Grenoble Alpes CS 10217 38043 Grenoble Cedex 9 France

Tel : [+33 \(0\)4 76 76 93 06](tel:+330476769306)

Fax: [+33 \(0\)4 76 76 93 05](tel:+330476769305)

Running title: visuomotor connectivity following stroke

Abstract: 344 words

Manuscript: 4497 words

3 Tables and 4 Figures

References: 40

Supplemental: TRIPOD Checklist Prediction Model Development and Validation

CONTRIBUTIONS:

Fabrice Firdaus Hannanu: Drafting/revision of the manuscript for content, including medical writing for content. MRI data acquisition (Validation Dataset) and analysis. Data interpretation.

Bernadette Naegele. Study concept. Data acquisition (Validation Dataset). Revision of the manuscript for content.

Flore BARONNET. Clinical, behavioral, and MRI data acquisition (Training Dataset). Revision of the manuscript for content.

Aliénor Jaillard. MRI data acquisition (Validation Dataset). MRI Data processing. Revision of the manuscript for content.

Alexandre Krainik, MRI data acquisition (Validation Dataset). Revision of the manuscript for content.

Olivier Detante. Study supervision and coordination. Obtaining funding. Data acquisition (Validation Dataset). Revision of the manuscript for content.

Charlotte Rosso. Study concept and design. Clinical and MRI data acquisition (Training Dataset). Revision of the manuscript for content.

Assia Jaillard: Drafting/revision of the manuscript for content, including medical writing for content. Study supervision and coordination. Obtaining funding. Study concept and design. MRI data acquisition. Data analysis and interpretation.

FUNDING

This work was supported by:

- Ministère des Affaires Sociales et de la Santé, PHRC: ISIS-2007PHR04 (NCT00875654) and HERMES-2007-A00853-50 for patient inclusion and clinical and multimodal MRI data acquisition.
- The IRMAS study has received funding from “Investissements d’avenir” ANR-10-IAIHU-06.
- IRMaGE platform partly funded by the french program « investissement Agence Nationale de la Recherche: grant « infrastructure d’avenir en Biologie Santé » - ANR – 11 – INBS-0006.»
- The Indonesia Endowment Fund for Education, LPPD (F. Hannanu PhD)

DISCLOSURES

The authors report no disclosure relevant to the submitted manuscript

ACKNOWLEDGEMENTS

We thank the ISIS-HERMES study group.

We thank the platform of France Life Imaging network for partly supporting MRI data acquisition through the grant “ANR-11-INBS-0006.

We thank the Clinical Investigation Center (CIC) INSERM UMS 002 CHU Grenoble Alpes for data monitoring

SEARCH TERMS:

1. All Cerebrovascular disease/Stroke
2. MRI
3. Rehabilitation
4. Plasticity
5. fMRI

ABSTRACT

Background and Objectives. Hand motor deficit following stroke is a leading factor of long-term disability. Based on the two-visual-stream theory positing two separate streams for perception and action, we hypothesized that visuomotor connectivity may influence hand motor outcome. In this study, we investigated whether visuomotor connectivity assessed with resting-state functional MRI (rs-fMRI) predicts hand motor outcome following stroke.

Methods. This longitudinal study included patients with a first-ever ischemic stroke in the anterior circulation from two datasets. Handgrip strength was assessed one month following stroke (M0) and six months later (M6). Rs-fMRI data acquired at M0 was analyzed using Conn toolbox. The Fisher z-scores of the ROI-to-ROI correlation coefficients from the individual first-level analysis were correlated to grip after adjusting for age and sex. Then, we built a developmental model in dataset-I to determine the connectivity predictors of handgrip at M0 and M6. We used the second dataset for external validation.

Results. The developmental study included 54 patients (mean age 58.2; SD=15 years), and the validation study 25 patients (mean age 52.7; SD=9.3 years). There were significant differences between the two datasets in terms of motor severity and lesion volume.

At M0, handgrip was associated with connectivity between the ipsilesional primary motor (BA4a) and visual cortices and between ipsilesional parietal (SPL-7M) and lateral occipital cortex (OC) after adjusting for age, sex, and baseline motor-NIHSS. At M6, grip predictors included connectivity between ipsilesional BA4a and dorsal OC, between ipsilesional primary sensory (BA3b) and contralesional premotor (BA6 ma) cortices, and between ipsilesional SPL-7M and lateral OC after adjusting for age, sex, and baseline motor-NIHSS. Calibration plots of predicted against observed values for the training and validation models showed large overlaps of the 95% confidence intervals of the regression lines, with R^2 reaching 0.615 and 0.780 at M0 and 0.776 and 0.820 at M6, respectively.

Conclusions. This study, based on training-validation models, showed that visuomotor connectivity predicts hand motor outcome, consistently with the two-visual-stream theory. Hand motor outcome was also predicted by interhemispheric sensorimotor connectivity, confirming previous works. Visuomotor connectivity may be a target in developing rehabilitation interventions.

Glossary

NIHSS =National Institutes of Health Stroke Scale; **ROI**= Region of Interest; **rs-fc**; resting state functional connectivity; **rs-fMRI**= resting state functional MRI.

Brain areas are listed in Figure 2.

Introduction

Stroke is a leading cause of motor disability, with the hand being frequently impaired.¹ As hand movements are involved in most of the basic daily life activities, loss of functional hand movement is tremendously disabling. The extent of hand motor deficit and recovery varies across patients. While some patients fully regain hand motor function six months after stroke, recovery remains incomplete in 30-67% of the cases even with rehabilitative training programs.^{2, 3} In this context, accurate prediction of hand function could allow for more timely and targeted intervention, thereby improving recovery, and reducing post-stroke disability. Among the numerous neuroimaging techniques for exploring hand motor recovery,³⁻⁶ resting-state functional MRI (rs-fMRI) has emerged as a powerful and reliable tool to map the functional brain connectivity and reorganization following stroke.⁷⁻⁹ An advantage is that rs-fMRI can be performed in patients with severe motor deficit, as no movement is required during image acquisition. There is growing evidence in the stroke literature that resting-state functional connectivity within the motor networks correlates with neurological scores^{8, 10, 11} and motor outcome.^{12, 13} Motor outcome of the upper limb has been diversely associated with increased or decreased functional connectivity between ipsilesional primary sensorimotor areas (SMI) and contralesional SMI,^{8, 13-16} SMA,^{10, 15, 16} and dPMC.^{12, 13, 17} In contrast, the influence of non-motor regions on hand recovery has been sparsely explored. A recent chronic stroke study suggested that better hand motor scores correlate with increased connectivity between the ipsilesional sensorimotor and ventral visual networks.¹⁴ Several other studies have also reported extrinsic connectivity alterations between the motor and visual networks, but their design was based on comparisons between stroke and healthy participants rather than on the association between functional connectivity and hand behavior.^{18, 19} From a theoretical perspective, the influence of the occipital regions on hand motor recovery is supported by the two streams hypothesis, a model developed first by Ungerleider and Mishkin in nonhuman primates,²⁰ and then by Goodale and Milner in humans,²¹ positing two separate streams for perception and action. In this model, cortical visual processing is segregated between a dorsal stream in the parieto-occipital cortex engaged in hand motor actions and a ventral stream in the temporo-occipital cortex for object perception.²¹ The essential role of the dorsal (or dorsolateral) stream in grasping and hand movements has been confirmed by several studies in both macaques²² and humans using fMRI and TMS paradigms.^{23,}²⁴ In other words, the different modalities of grip, such as strength and goal-related actions, may

3.3 Study III. Resting-state fMRI

be influenced by visual inputs, depending on context-related cues about, for example, weight and temperature.²²

Furthermore, we have shown using task-fMRI that hand motor recovery following stroke is associated with motor task-related activity in a set of sensorimotor and parietal regions of the dorsal stream.⁶ Given the evidence that the dorsal stream originates in the dorsal visual cortex and may interact with the ventral visual cortex,²⁵ we hypothesized that the visual cortex may promote hand recovery following stroke through visuomotor connections in addition to intrinsic motor connections. In the present study, we sought to identify resting state connectivity predictors that independently contribute to the prediction of hand motor outcome following ischemic stroke. To this aim, we applied a longitudinal design assessing handgrip one month following stroke and six months later. We used rs-fMRI with a seed-based approach to study rs-fc between the different regions of the visuomotor network. Hand motor outcome was assessed with handgrip strength since it is a reliable measure of motor impairment^{3, 26} and rehabilitation outcome.²⁷ Furthermore it is a specific measure of the motor system while other measures such as hand dexterity may be compounded by additional visual, sensory and cognitive deficits. Following the current recommendations for predictive modeling,²⁸ we used a training dataset of 54 patients (IRMAS study) to develop our models, and tested their validity in a validation dataset including 25 patients from the ISIS-HERMES study.⁶

Methods

Participants

Training Dataset

The IRMAS study included 76 patients with a first-ever ischemic stroke, recruited between January 2010 and January 2012 confirmed with an MRI within 12 hours after onset, with mild-severe stroke severity (NIHSS ≥ 1) (IRMAS study, CHU Pitié-Salpêtrière, Paris, France).⁴ Inclusion and exclusion criteria are presented in Figure 1A. Then, only patients with anterior stroke circulation and with both MRI and behavioral assessment at one month (M0) and behavioral assessment at six months (M6) following stroke were included in training dataset, resulting in 54 patients (Figure 1B). IRMAS study was approved by the local ethic committee of the Pitié-Salpêtrière Hospital. All patients gave written informed consent.

Validation Dataset

The validation Dataset was part of ISIS-HERMES study, a monocentric (Grenoble Alpes University Hospital (CHUGA), France), prospective, randomized clinical controlled trial assessing the safety and tolerance of intravenous autologous mesenchymal stem cells (MSCs) in patients with a first-ever moderate to severe ischemic stroke within the anterior circulation territory.²⁹ Thirty-one patients aged 18-70 with a persistent neurological deficit (National Institutes of Health Stroke Scale (NIHSS)) were enrolled at two weeks post-onset between August 2010 and August 2015. The duration of the follow-up was 2 years and the study ended August 31, 2018. Inclusion and exclusion criteria are presented in Figure 1A and the details of the study elsewhere.²⁹ The present dataset included 25 patients who underwent the full MRI protocol one month following stroke (M0, just before the MSC injection) with a behavioral follow-up six months later (M6). ISIS-HERMES study was approved by the local ethic committee, and registered with ClinicalTrials.gov number NCT00875654. All patients gave written informed consent.

Clinical and behavioral scores

Stroke severity was assessed with the of NIHSS³⁰ that was used to compute a motor severity score summing the motor arm and motor leg items. The maximum score of 8 indicates hemiplegia. We assessed hand motor deficit with handgrip strength, a reliable and sensitive measure of stroke motor recovery,³¹ using the LaFayette dynamometer. (<https://www.prohealthcareproducts.com/100-kg-220lb-hand-grip-dynamometer-lafayette-instruments/>). Patients were seated with the paretic hand positioned at the side of the body holding the dynamometer. Then they were asked to squeeze the dynamometer as strong as possible without moving other parts of the body. The average of raw scores in 3 trials was used as the handgrip score. NIHSS and handgrip were assessed one month following stroke and 6 months later. Clinical assessment was performed by a stroke neurologist (OD, CR) and handgrip measurements by a stroke neurologist for training dataset (FBC) and a neuropsychologist for validation dataset (BN).

MRI

Training dataset

3.3 Study III. Resting-state fMRI

Images were acquired with 3T Siemens Trio MRI Scanner, with 12-channel head matrix coil at CENIR facility (www.cenir.org). Structural imaging involved a T1-weighted MP-RAGE (TR 2.3 s, TE 4.18 ms, voxel size $1 \times 1 \times 1 \text{ mm}^3$) and T2-FLAIR weighted (TR 9.5 s, TE 103 ms, voxel size $0.9 \times 0.9 \times 3 \text{ mm}^3$). Two rs-fMRI sequences of 7 minutes each were acquired for every participant: EPI, 173 volumes, 41 slices, TR 2460 ms, TE 30 ms, flip angle 90° , voxel size = $3 \times 3 \times 3 \text{ mm}^3$, gap = 0). Participants were instructed to keep their eyes closed and to avoid moving or falling asleep. MRI protocol and behavioral scores were acquired one month following stroke during the same session.

Validation dataset

MRI images were acquired on a Philips 3T scanner (Achieva 3.0T TX) with a 32-channel head coil at IRMaGe MRI facility (Grenoble, France). Two high-resolution structural and one rs-fMRI sequences were acquired with the following parameters. 3D-T1-weighted images: TR 7.75 ms, TE 3.62 ms, flip angle 90° , FOV: $255 \times 192 \times 255$, 192 slices, voxel size = $0.98 \times 0.98 \times 1 \text{ mm}$, thickness = 1 mm, gap = 0, duration = 339 s; 3D-FLAIR: $0.5 \times 0.5 \times 1 \text{ mm}$, TR 4800 ms, TE 342 ms, flip angle 9° , FOV: $256 \times 192 \times 256$, 192 slices, voxel size = 1 mm, thickness = 1.4 mm, gap = 0, duration = 370 s); rs-fMRI: echo planar images (EPI), TE = 30 ms, TR 2000 ms, voxel size $3 \times 3 \times 3.5 \text{ mm}$; gap = 0.25 mm, 400 volumes, duration 13 min 40 s. Participants were instructed to remain still and relaxed during the scan with eyes open while looking at a white “X” sign in the middle of the black background screen, without thinking anything in particular and to avoid falling asleep. These sequences were the first part of the ISIS-HERMES MRI protocol that was acquired one month following stroke at the same time as behavioral scores.

MRI data analysis

Stroke lesion volume was determined by manual delineation based on the FLAIR images using mricron (<https://www.nitrc.org/projects/mricron>). Data preprocessing and processing were performed using CONN Toolbox (<http://www.nitrc.org/projects/conn>). Preprocessing pipeline for volume-based analysis with direct normalization to MNI-space was performed in CONN Toolbox, including realignment, slice-timing correction, outlier detection, direct segmentation, and

normalization of functional ($2*2*2\text{ mm}^3$) and structural images ($1*1*1\text{ mm}^3$), and smoothing of functional images ($5*5*5\text{ mm}^3$). Images from patients with lesions on the right side were flipped about the y axis prior to the pipeline, and thus all lesions are located in the left hemisphere for group analyses, to perform the group analysis without having to divide participants into smaller groups based on lesion side. Of note, most stroke studies flip their data as only slight and non-significant asymmetry exists regarding the sensorimotor system.^{13,32} As hemispheric asymmetries have been reported for the occipital lobes in terms of surface area, cortical thickness, and local gyrification,³³ the 10 anatomical occipital regions extracted from the Julich atlas (brain.eu) were grouped into 3 ROIs based on the visual area subdivisions (See Figure 2).

We used the Artifacts Detection Tool (ART) to detect outliers, with thresholds for signal intensity outliers set at 5 standard deviations (SD) above or below the mean, and a motion limit of 0.9 mm in any direction. During the denoising step, white matter, CSF, and the outliers detected by the ART toolbox were used as confounding effects in the linear regression. Then, a bandpass filter of 0.09 to 0.008 was applied. For training dataset, the two sessions of rs-fMRI were preprocessed separately and then merged for group analyses.

Since the regions of interest (ROIs) were determined *a priori*, based on the hypothesis that visuomotor connectivity would predict handgrip at M0 and M6, we used an ROI-based approach, including 78 ROIs (39 ROIs for each hemisphere) provided by the sensorimotor, parietal and occipital areas of the Julich atlas (ebrains.eu). The ROI list is provided in Figure 2.

We performed a First-Level analysis (FLA) resulting in a seed-based connectivity (SBC) map for each patient *representing the level of functional connectivity between a ROI and every voxel in the brain*. We checked by visual inspection image quality of each SBC map. Then, we computed ROI-to-ROI connectivity (RRC) matrices to estimate the level of functional connectivity between each pair of ROIs in our set of 78 regions. Finally, we extracted the Z-scores that are the RRC matrices of Fisher-transformed correlation coefficients for each pair of ROIs. Then, we correlated the z-scores of each RRC (pair of ROIs) with the grip performance at M0 and M6 using partial correlations adjusted for age and sex, resulting in a matrix representing RRC associated to grip performance at each time point, M0 and M6, for each dataset. Of note, partial correlations were adjusted for cell treatment in addition to age and sex for the validation dataset at M6.

3.3 Study III. Resting-state fMRI

MRI data analysis was performed at IRMaGe by A.V.J. and F.F.H. who were blinded to clinical and behavioral outcomes.

Statistical analysis

First, we performed univariate analysis using descriptive statistics of means, standard deviations (*SD*), medians, interquartile ranges (*IQR*) for continuous data, and frequencies for categorical data. We assessed test normality using the One-sample Kolmogorov-Smirnov test. Bivariate analyses for dataset comparisons were performed with the Mann-Whitney-*U* test and chi-squared test. We also examined whether the connectivity measures (i.e. the RRC Z-scores) have a linear relationship with the outcome.

For model development, we sought to determine the connectivity measures associated with grip at M0 and M6 in the training dataset using multivariate linear regression. We built a model at each timepoint, with handgrip at M0 or M6 as the dependent variable. As we used grip raw scores, we entered age and gender to account for the effects of demographics influencing task performances. The effects of handedness, lesion volume and side, and stroke severity on the models were tested and kept if significant. Connectivity measures were preselected from RRC matrices using LASSO linear regression, and then introduced in the linear regression model using a stepwise forward method. Variables were kept in the model if significant ($p < 0.05$). We evaluated unadjusted correlations between predictors and handgrip using Spearman tests. We used R-squared measures of goodness of fit (R^2 , coefficient of determination), Durbin-Watson test, and residuals statistics (plots, descriptives, and Cook's distance) to assess the overall performance of the models. Collinearity statistics were performed to remove variables with high collinearity indicated by variance inflation factor (VIF) > 4 . In addition, to adjust the models for overfitting, we performed an internal validation using bootstrapping based on 1000 samples providing unbiased coefficients with 95% CIs. The contribution of connectivity measures on handgrip was assessed with the R^2 change, F significance, and significance of bootstrap coefficients.

For external validation, we first built a validation model at each timepoint in the validation dataset using the formula (intercept and predictor coefficients) provided by the training models. We estimated model performance with R^2 , Durbin-Watson test and residuals statistics. Calibration was

Thesis Work

assessed using the R^2 obtained from the plots of the predicted against observed values with 95% CIs.³⁴ Training and validation models were compared using the calibration plots. Second, we used the validation dataset to test the significance of the training model predictors, after adjusting for the effect of stem-cell treatment in the M6 model, resulting in a updated model with estimates and 95% confidence intervals (CIs) at each timepoint.

We performed statistical analyses using IBM SPSS Statistics-28.1 and Python-3.8.

Data availability

Data are available on-demand in accord with applicable French laws and regulations.

Results

Participants

Out of 76 and 31 patients with unilateral stroke that were enrolled, 54 had complete data eligible for analysis in training dataset and 25 in validation dataset. Figure 1B shows the study flowchart. Demographic, stroke, and behavioral data for each dataset with dataset comparisons are presented in Table 1. The datasets matched for age, sex, handedness, and lesion side. Lesion volume was larger and clinical scores were worse in the validation dataset. Grip was higher in men than in women in the training but not in the validation dataset. In both datasets, lesion volume and stroke severity correlated with grip but not age, handedness, and lesion side (table 1). Finally, stem cell treatment had no significant effect on handgrip at M6 in the validation dataset. The overlap of stroke lesions represented in Figure 3 shows a similar maximal extent of the lesions in both datasets with a higher proportion of subcortical lesions in the validation dataset.

Figure 1. Training and Validation datasets. A. Inclusion Criteria and B. Study Flow Chart

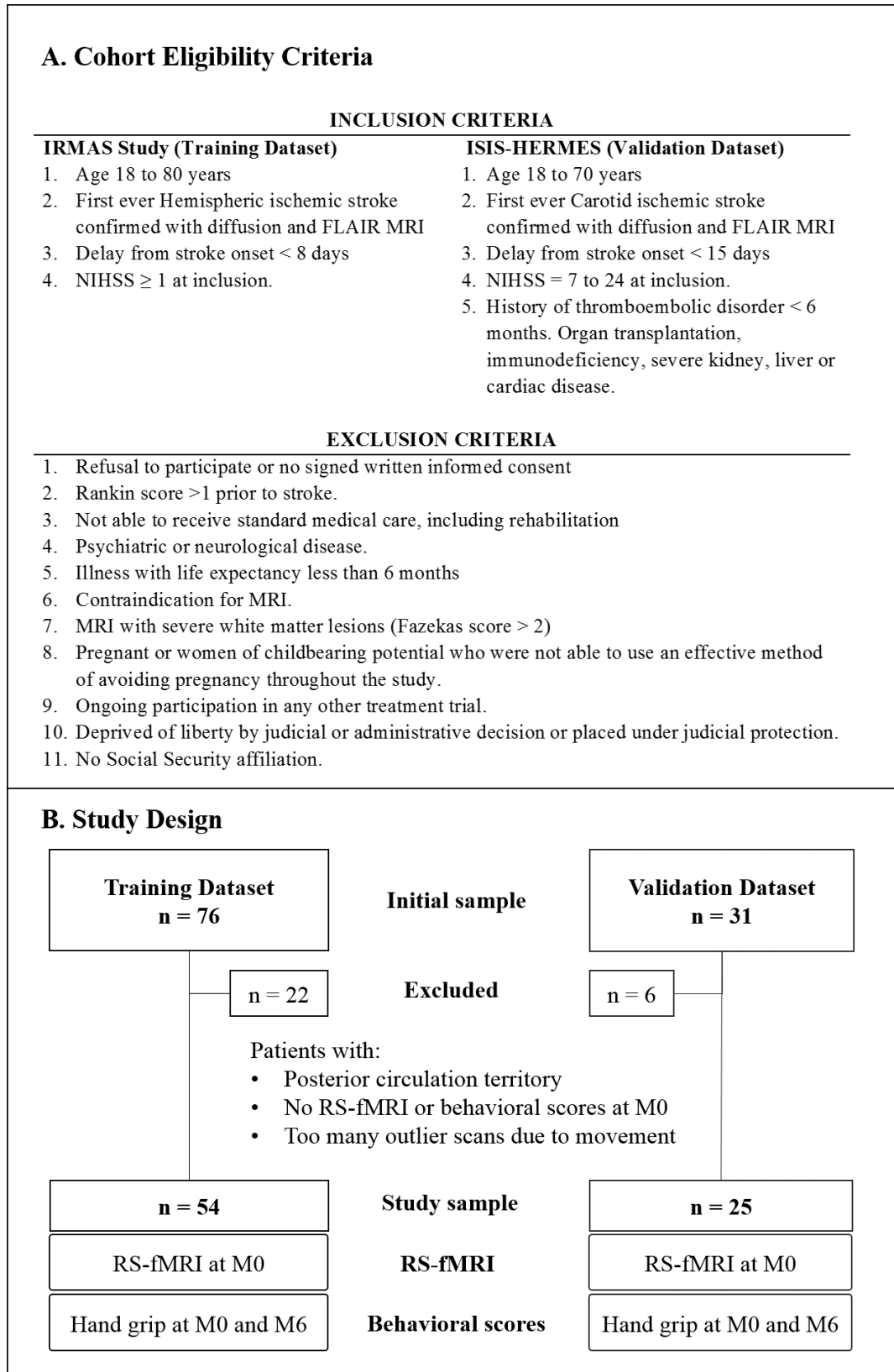
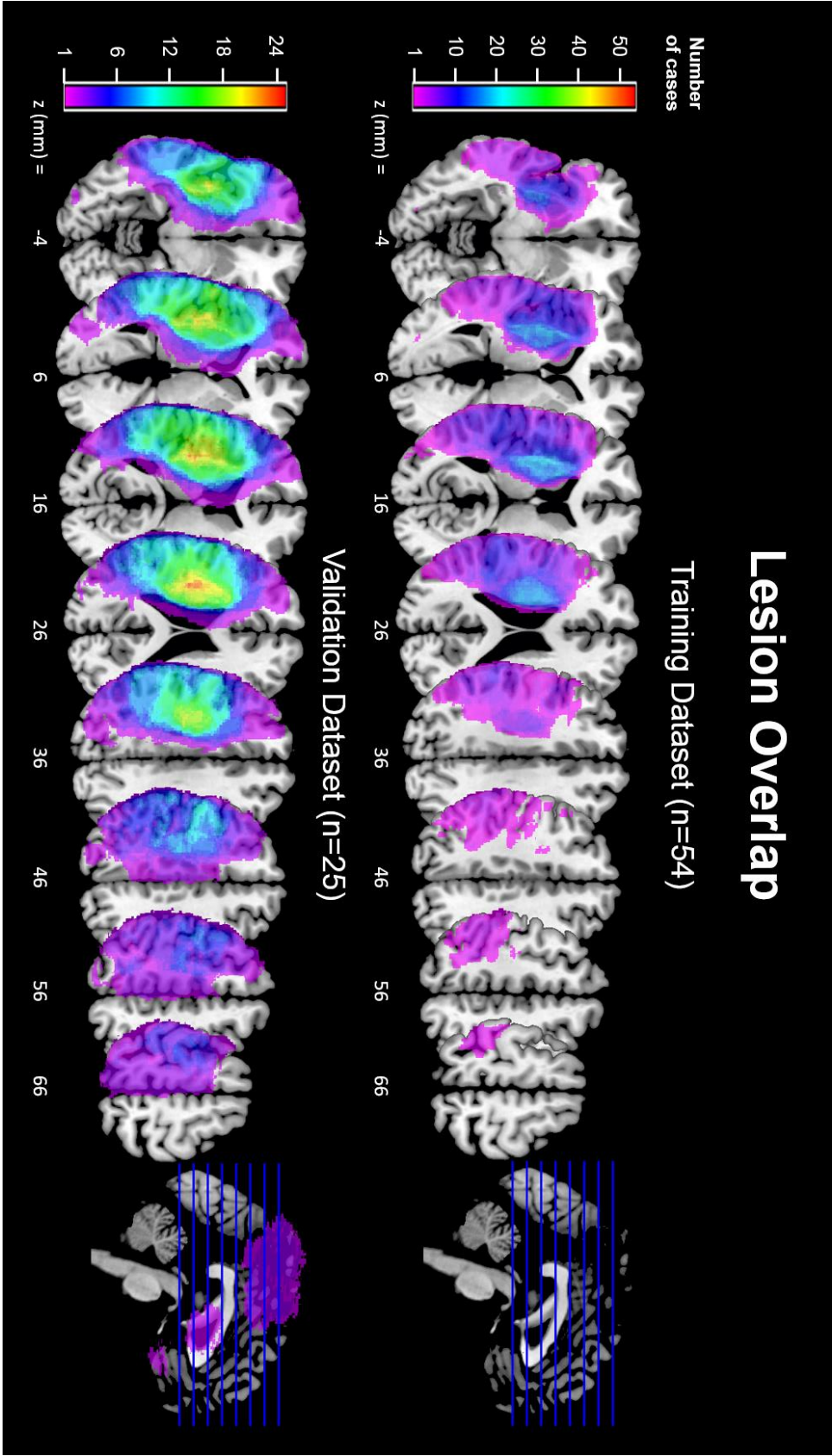


Table 1. Patient characteristics and behavioral scores in the training and validation datasets. Effects on outcome were analyzed using Mann-Whitney (MW) tests for categorical variables and using Spearman correlation tests for continuous variables. Datasets were compared with the chi-square (χ^2) test for categorical variables and MW test for continuous variables. * indicates statistical significance of the tests ($p < 0.05$).

Training Dataset (n = 54)					Validation Dataset (n = 25)					Dataset Comparison
Categorical variables	Descriptives		Effects on outcome			Descriptives		Effects on outcome		χ^2
	n	%	Grip M0 MW (Z)	Grip M6 MW (Z)	n	%	Grip M0 Z (p)	Grip M6 Z (p)		
Sex (M/F)	34/20	63/37	-2.237*	-3.248	18/7	72/28	-0.39	-0.352	0.620	
Handedness (R/L)	48/6	88.9/11.1	-0.887	-1.282	22/3	88/12	-0.897	-1.314	0.013	
Lesion side (L/R)	32/22	59.3/40.7	-1.17	-1.909	15/10	60/40	-1.984*	-1.485	0.004	
Stem Cell (Yes/No)	-	-	-	-	13/12	52/48	-1.206	-1.772	-	
Continuous variables	Mean (SD)	Median (IQR)	Grip M0 rho	Grip M6 rho	Mean (SD)	Median (IQR)	Grip M0 rho (p)	Grip M6 rho (p)	MW (Z)	
Age	58.19 (15)	59.5 (23.5)	0.134	0.119	52.72 (9.31)	53 (11.5)	0.138	-0.099	1.609	
Lesion volume	39.23 (55.53)	10.66 (78.69)	-0.406*	-0.517*	97.08 (63.98)	73.34 (96.64)	-0.302	-0.415*	-4.259*	
NIHSS at admission	8.58 (6.01)	6 (11.25)	-0.591*	-0.639*	15.72 (3.92)	15 (5)	-0.485*	-0.445*	-4.427*	
NIHSS at M0	3.25 (4.19)	1 (6)	-0.508*	-0.607*	13.24 (4.43)	12 (4.5)	-0.471*	-0.538*	-4.683*	
mNIHSS at M0	1.61 (2.55)	0 (3)	-0.710*	-0.731*	4.24 (2.5)	5 (4)	-0.673*	-0.569*	-3.924*	
Grip PH at M0	14 (12.03)	12.85 (25.39)	-	0.833*	3.85 (9.22)	0 (0)	-	0.785*	-4.116*	
NIHSS at M6	1.43 (2.72)	0 (2.25)	-0.672*	-0.737*	7.96 (4.26)	8 (6)	-0.424*	-0.751*	-5.985*	
mNIHSS at M6	0.88 (1.63)	0 (1.5)	-0.697*	-0.758*	2.6 (2.4)	3 (4)	-0.571*	-0.772*	-3.106*	
Grip PH at M6	20.1 (15)	20.09 (26.23)	0.833*	-	7.01 (12.23)	0 (10)	0.785*	-	-3.714*	

Figure 3. Lesion Overlap



rs-fMRI

RRC matrices

The RRC matrices representing the resting state functional connectivity associated with grip at M0 and M6 are provided in Figure 2 for each dataset. Globally, grip measures at M0 and M6 in both datasets were associated with connectivity between bilateral motor (SM1-PMC) and occipital areas. More specifically, handgrip was strongly associated with connectivity between i.SM1-PMC regions and bilateral OC including OC1, and in a lesser extent the dorsal, lateral and ventral OC regions. Grip was also strongly associated with connectivity from ipsilesional (i.) SM1 to contralesional (c.) SM1-PMC, c.IPS, and bilateral SPL. In addition, grip was associated with connectivity from occipital areas to i.SPL and interhemispheric occipital connectivity.

Model development

The linear regression model in the training dataset showed that grip at M0 was predicted by visuomotor connectivity, *i.e.* connectivity between the ipsilesional primary motor (Brodmann Area BA4a) and visual (OC1) cortices and between the ipsilesional parietal (SPL-7M) and visual (OC lateral) cortices after adjusting for age, sex, and baseline motor NIHSS. At M6, grip predictors included ipsilesional BA4a to OC-dorsal connectivity, sensorimotor connectivity, *i.e.* connectivity between the ipsilesional primary sensory cortex (BA3b) and contralesional premotor cortex (BA6 ma), and connectivity between ipsilesional SPL-7M and OC lateral areas after adjusting for age, sex, and baseline motor NIHSS. Of note, all connectivity predictors but i.7M to i.OC-lateral connectivity were correlated with grip. These results are illustrated in Figure 4. The fit of the models, R^2 , reached 0.615 at M0 and 0.776 at M6 (Figure 4B). Table 2 indicates the contribution of each predictor. Internal validation with bootstrap based on 1000 replications showed that all predictors remained statistically significant (Table 2).

Figure 2. List of ROIs and RRC matrices representing the resting state functional connectivity associated with grip at M0 and M6.

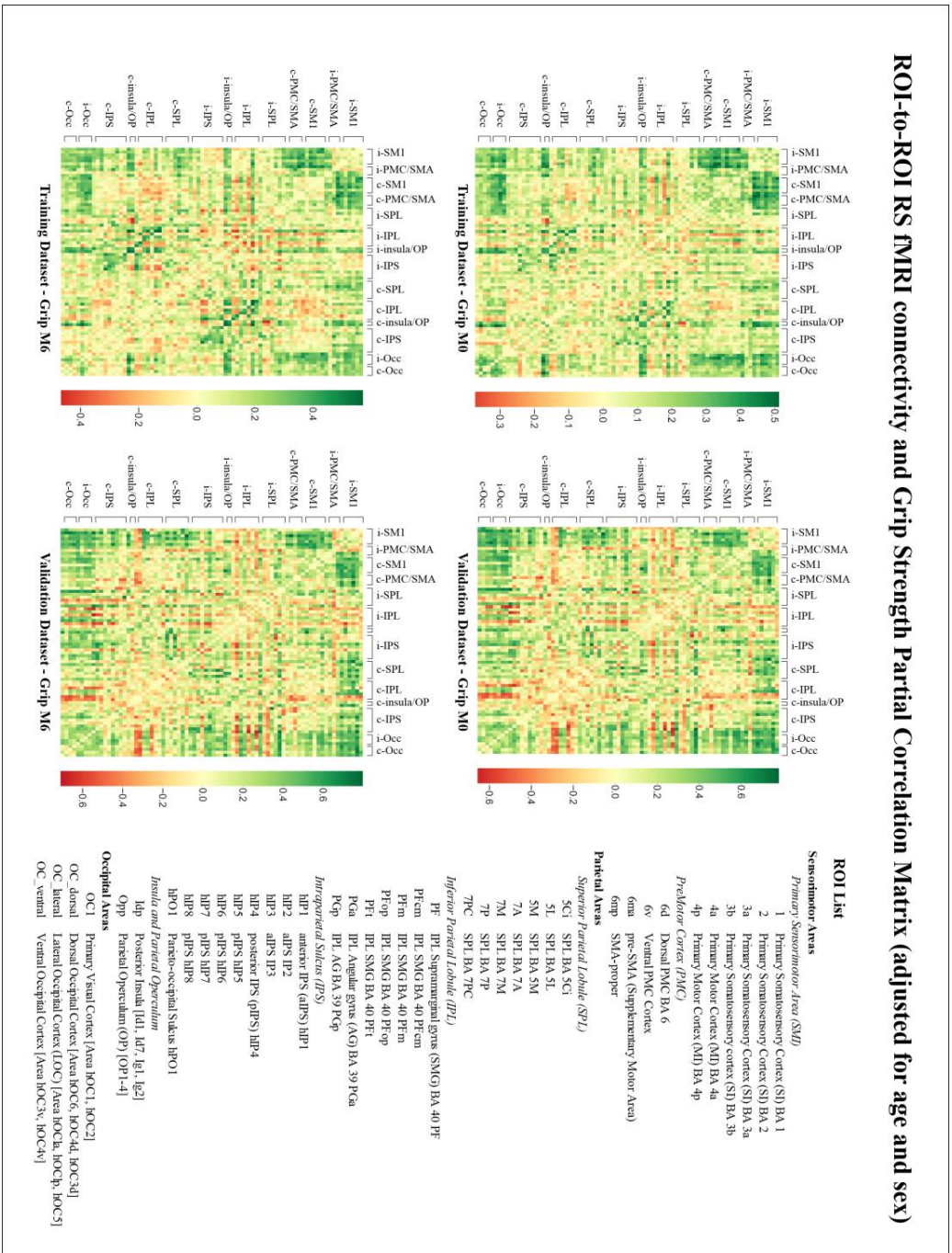


Table 2. Training Model based on bootstrap with predictor contribution (R^2 change) and unadjusted correlation with grip at M0 and M6.

Model Specification (Bootstrap)							Contribution to the model		Unadjusted Correlation to Dependent Variable	
Grip M0	B	Bias	SE	p	95% CI	R ² change	p	rho	p	
Intercept	10.022	0.025	6.600	0.128	-2.189 23.558					
Age	0.126	-0.002	0.081	0.130	-0.042 0.271	0.018	0.328	0.134	0.334	
Female/Male	-1.716	-0.036	2.055	0.406	-5.795 2.194	0.129	0.008	-0.307	0.024	
Motor NIHSS at M0	-2.468	-0.030	0.421	0.001	-3.361 -1.716	0.306	<0.001	-0.71	<0.001	
i.4a-i.OCI	30.047	0.040	5.622	0.001	17.221 40.204	0.109	0.001	0.374	0.005	
i.7M-i.OClateral	-17.128	-0.202	5.745	0.003	-28.447 -5.908	0.053	0.014	-0.041	0.769	
Grip M6	B	Bias	SE	p	95% CI	R ² change	p	rho	p	
Intercept	22.371	-0.061	7.976	0.011	6.759 39.211					
Age	0.097	0.004	0.087	0.260	-0.079 0.258	0.021	0.328	0.119	0.422	
Female/Male	-7.281	-0.207	2.264	0.007	-12.006 -2.755	0.224	0.001	-0.474	0.001	
Motor NIHSS at M0	-3.278	-0.027	0.537	0.001	-4.361 -2.253	0.394	<0.001	-0.731	<0.001	
i.3b-c.6ma	19.673	0.887	6.698	0.011	7.149 34.209	0.053	0.003	0.397	0.005	
i.4a-i.OCdorsal	20.561	-0.233	6.763	0.008	6.311 32.982	0.043	0.021	0.303	0.037	
i.7M-i.OClateral	-20.598	0.756	7.059	0.005	-33.607 -6.367	0.042	0.016	-0.168	0.253	

External validation

Calibration step

For external validation, we first calibrated the models in the validation dataset by applying the predictors and coefficients of the training dataset and computing R^2 . Calibration plots of predicted against observed values at M0 and M6 showed a large overlap of the 95% CIs of the regression lines of the two models, indicating that the training model was validated in the external dataset. (Figure 4A). Figure 4B shows similar R^2 (0.780 at M0 and 0.820 at M6) and adjusted R^2 values for the training and validation models, with residuals and Cook's distances showing no major bias.

Updated model

We tested the significance of the connectivity predictors in the validation dataset at M0 and M6 after adjusting for age, sex and motor NIHSS. We entered stem-cell treatment in the M6 model to account for a potential effect of stem-cells on grip outcome. The models showed statistically significant effects of the connectivity predictors with updated coefficients at both timepoints as shown in Table 3.

Demographic and stroke predictors. There was an effect of age on the grip at M0 in the validation model, and an effect of sex on the grip at M6 in the training model. We observed no effect of handedness or lesion side. While lesion volume and total NIHSS correlated with the grip at M0 and M6 (Table 1), they were not kept by the models. In contrast, motor severity indicated by the motor NIHSS was a strong predictor of grip at both M0 and M6 (Tables 2-3).

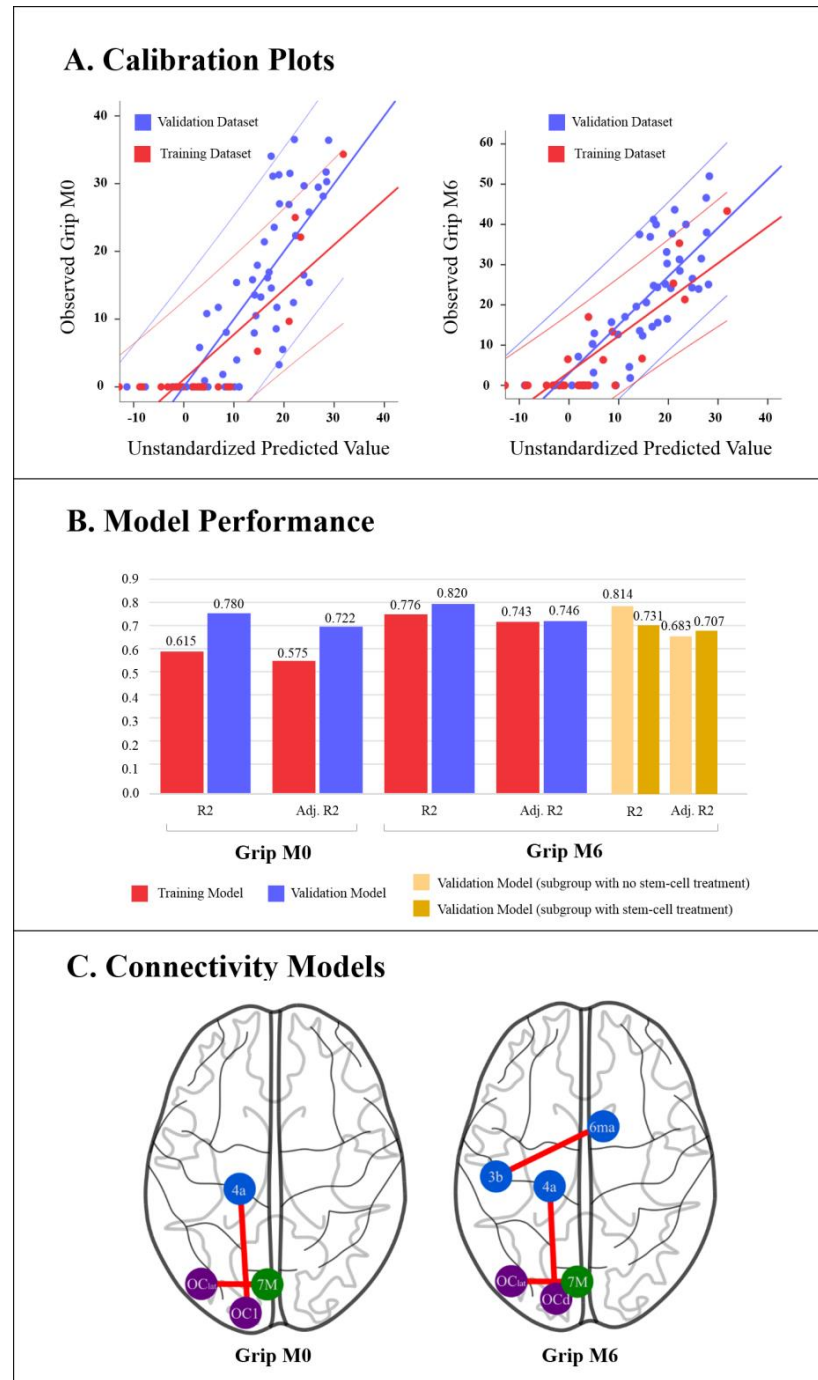
The effect of visuomotor connectivity on the difference of M6-M0 hand motor scores assessing hand motor recovery was not result.

Table 3. Validation Model with updated coefficients with predictor contribution (R^2 change) and unadjusted correlation with grip at M0 and M6.

Model Specification							Contribution to the model		Unadjusted Correlation to Dependent Variable	
Grip M0	B	SE	Beta	t	p	95% CI	R ² change	p	rho	p
Intercept	-3.853	7.816		-0.493	0.628	-20.211 12.505				
Age	0.366	0.118	0.369	3.111	0.006	0.120 0.612	0.082	0.164	-0.099	0.638
Female/Male	-1.666	2.317	-0.083	-0.719	0.481	-6.516 3.184	0.001	0.905	0.072	0.733
Motor NIHSS at M0	-2.153	0.415	-0.585	-5.184	0.000	-3.023 -1.284	0.514	<0.001	-0.569	0.003
i.4a-i.OCI	15.371	3.949	0.465	3.892	0.001	7.105 23.637	0.127	0.007	0.519	0.008
i.7M-i.OClateral	-12.003	5.462	-0.270	-2.198	0.041	-23.435 -0.571	0.056	0.041	-0.393	0.052
Grip M6	B	SE	Beta	t	p	95% CI	R ² change	p	rho	p
Intercept	3.823	10.793		0.354	0.728	-18.948 26.594				
Age	0.239	0.151	0.182	1.578	0.133	-0.080 0.558	0.001	0.908	-0.099	0.638
Female/Male	-1.528	3.267	-0.057	-0.468	0.646	-8.420 5.363	0.000	0.923	0.072	0.733
Motor NIHSS at M0	-2.472	0.549	-0.506	-4.499	0.000	-3.631 -1.313	0.490	<0.001	-0.569	0.003
i.3b-c.6ma	19.526	7.470	0.298	2.614	0.018	3.766 35.286	0.118	0.013	0.369	0.069
i.4a-i.OCdorsal	19.006	5.314	0.498	3.577	0.002	7.795 30.217	0.094	0.045	0.496	0.012
i.7M-i.OClateral	-23.592	7.842	-0.400	-3.009	0.008	-40.137 -7.048	0.116	0.003	-0.393	0.052
Stem cell (yes/no)	0.500	2.876	0.021	0.174	0.864	-5.568 6.569	<0.001	0.864	0.362	0.076

3.3 Study III. Resting-state fMRI

Figure 4. External validation. A) Model calibration plots of predicted against observed grip values at M0 and M6; B) Model performance for the training and validation datasets at M0 and M6 assessed with R^2 and adjusted R^2 ; C) Schematic representation of the connectivity predictors on an axial view of the brain.



Discussion

Main findings

Based on the two-visual-system theory, we hypothesized that the visuomotor connectivity and more specifically connectivity between dorsal occipital and sensorimotor areas was associated with hand motor outcome following stroke. To test our hypothesis, we assessed rs-fMRI connectivity at one month following stroke (M0) and hand motor performance at M0 and 6 months later (M6) in a training dataset of 54 patients and an external validation dataset of 25 patients. We found that hand motor performance at M0 was associated with connectivity between ipsilesional primary motor (i.4a) and occipital (i.OC1) cortices, and between ipsilateral SPL-7M and lateral occipital cortex. At M6, hand motor outcome was predicted by connectivity between ipsilateral 4a and dorsal occipital cortex, between i.SPL-7M and i.OC-lateral, and between ipsilesional primary somatosensory cortex (i.3b) and contralesional pre-SMA (c.6ma) (Figure 4C). Our findings highlight the influence of visuomotor connectivity assessed with resting fMRI data on hand motor performances measured at both subacute and chronic phases of stroke. Furthermore, the dorsal visuomotor stream was an independent predictor of hand motor outcome, in agreement with our hypothesis. In addition, ipsilesional and contralesional SMI-PMC connectivity were associated with handgrip scores at both timepoints, confirming the role of interhemispheric sensorimotor connectivity in motor recovery. We evaluated our models using internal and external validation to limit the overfitting that is usually observed in MRI studies. However, the generalizability of our findings is limited by the relative small sample size of the datasets and other features that are discussed in the sequel of the paper.

Visuomotor connectivity

We found that visuomotor connectivity at M0 was associated with grip at M0 and M6, suggesting a role for visuomotor influence on hand motor performance following stroke.

First, functional connectivity between ipsilesional primary motor cortex BA-4a and primary occipital cortex OC1 was associated with handgrip at M0. Handgrip is a manual task requiring distal upper limb sensorimotor control with a proprioceptive feedback to adjust the position of the hand and to apply the maximal grip force to a dynamometer. While there is no reaching movement and visual control is not essential, handgrip requires object manipulation and force evaluation. BA-4a is a motor area specifically involved in handgrip strength as shown in previous works.^{6, 35} OC1 is primarily involved in visual perception that is subsequently

processed in the dorsal, lateral and/or ventral visual extrastriate areas depending on the type of visual information. According to the two-visual-system theory, the visual ventral and dorsal streams originate from the primary occipital area OC1.²⁵ Interestingly, as shown in Figure 2, handgrip performance was associated with connectivity between OC1 and all sensorimotor areas, and not only BA4a. Overall, our findings highlight the influence of visual perception on motor actions, in agreement with Milner's theory proposing that perceptual systems participate in motor actions to move or manipulate objects.

Increased connectivity between the dorsal occipital and SMI cortex was a strong predictor of hand motor outcome at M6, confirming our main hypothesis. The role of the dorsal visuomotor stream in motor actions has been formulated since 1982 in nonhuman primates²⁰ and 1992 in humans.²¹ Despite conceptual differences between the two models in terms of the detailed role of the two streams ("what and where" versus "what and how", respectively), both models proposed that the dorsal visuomotor stream is engaged in motor actions, either to process the spatial location of the object or to implement hand action and online control of hand manipulation and movement. According to this model, the dorsal stream projects from the visual areas to the posterior parietal cortex to reach the PMC and then SMI.

While the dorsal visuomotor stream is engaged in visually guided movements, we found that dorsal visuomotor connectivity predicted handgrip strength, a task that does not integrate reach movements. As described above, handgrip requires perceptual information on object properties, fingers, wrist and arm orientation, and strength control related to static muscle contraction. Our findings are in line with the current literature proposing that the dorsal visuomotor network participates in generating and controlling hand actions, with or without reach movement.^{22, 23} In this view, dorsal visuomotor connectivity may be promoted by rehabilitation programs that integrate mirror therapy to improve hand motor stroke recovery.

Connectivity between the ipsilateral lateral occipital cortex and dorsomedial SPL (7M) was a predictor of hand motor performance at both timepoints. SPL-7m, lying in the medial posterior part of BA7, is strongly connected with the dorsal visual areas and plays an important role in the integration of visual and motor information.^{23, 36} SPL-7m is also involved in aspects of contextual attention and visuospatial perception, including the representation and manipulation of objects. The lateral occipital cortex belongs to the lateral grasping network dedicated to selecting and controlling purposeful hand actions.²² For example, it is activated when grasping requires the prediction of weight of an object.³⁷

Connectivity within the sensorimotor network

Our rs-fMRI data acquired at M0 showed that increased interhemispheric motor connectivity predicted better hand motor outcome at M6, suggesting a supportive role of ipsilesional and contralesional sensorimotor coupling at the subacute period of stroke. Our findings are in line with a large body of the literature showing that motor outcome is associated with interhemispheric connectivity including the primary sensorimotor,^{8, 13, 15, 16} SMA,^{10, 15, 16} and PMC regions.¹³

Regarding the respective contribution of connectivity predictors to the model, visuomotor connectivity reached 16.2% at M0 and 8.5% at M6 while interhemispheric motor connectivity contributed to 5.3% of the model at M6. The contribution of visuomotor and motor connectivity was even higher in the validation study reaching 18.3% at M0 and 21.0% at M6, and 11.8% at M6, respectively (Tables 2-3). Interhemispheric motor connectivity predicted hand outcome in the same amount (6.3%) as in another study.³⁸ Although a recent study in 52 patients with chronic subcortical stroke reported a trend for correlations between ventral visuomotor connectivity and hand-wrist motor scores of the Fugl-Meyer assessment,¹⁴ the role of subacute visuomotor connectivity on hand outcome has not been reported yet.

Methodological considerations and limitations

Following TRIPOD guidelines, we performed internal validation resulting in robust connectivity predictors and external validation showing similar performances for both models. At our knowledge, this is the first study assessing functional connectivity following stroke with internal and external validation. However, since a single external validation appears insufficient to understand the performance heterogeneity across different settings,³⁹ larger populations should be tested before our model can be used at individual level. Indeed, a first limitation of this study is the small sample size of the datasets decreasing the statistical power of our analysis. We partly compensated for this limitation by using long runs for the resting-state sequence.^{19,}
⁴⁰ Of note, most previous rs-fMRI studies were performed with a similar or smaller sample size and shorter scan duration.

A second limitation relates to the differences between the two datasets in terms of lesion volume, lesion location, and motor severity. Lesion volume, while lower in the training than in the validation dataset, had no effect on brain connectivity when tested in the models. The subcortical versus cortical location of stroke lesions may have influenced the connectivity

pattern supporting hand motor performance since cortical lesions may affect the motor network. Here, the proportion of subcortical lesions was higher in the validation dataset, which may explain some differences between the models. However, patients from both datasets had both cortical and/or subcortical lesions (Figure 3), which has probably limited the effect of stroke location in our study. Along the same lines, the higher motor severity observed in the validation dataset may have influenced the effects of visuomotor and motor connectivity on hand outcome. Higher contribution of both visuomotor and motor connectivity in the validation model suggests a compensatory process in patients with a more severe deficit. However, we found no significant interaction between motor severity and visuomotor or motor connectivity supporting this hypothesis. It is also possible that the higher homogeneity of the validation population that was included in a clinical trial accounted for better model performances.

Another limitation relates to the validation study that was part of a randomized clinical trial assessing cell-therapy safety,²⁹ as treatment may have influenced hand outcome. To compensate for this limitation, we entered the treatment in the M6 model. Interestingly, cell-therapy effect was weak and not significant.

Clinical Implications

Several clinical implications may benefit from this study. First, resting-state visuomotor connectivity at the subacute phase of stroke may serve as a biomarker to predict hand motor outcome. Second, stroke rehabilitation may implement programs integrating visual inputs to enhance motor re-learning processes in patients with hand motor deficit. Third, our results suggest a supportive role of the dorsal visual stream in hand motor recovery and that occipital areas may represent a relevant target for brain stimulation therapy such as TMS.

Conclusion

This study highlighted the influence of visuomotor connectivity on hand motor outcome following stroke, supporting the two visual stream model. The role of visuomotor connectivity along with interhemispheric sensorimotor connectivity in motor recovery needs to be confirmed in further studies before it can be used in clinical settings.

References

1. Raghavan P. The nature of hand motor impairment after stroke and its treatment. *Current treatment options in cardiovascular medicine* 2007;9:221-228.
2. Verheyden G, Nieuwboer A, De Wit L, et al. Time course of trunk, arm, leg, and functional recovery after ischemic stroke. *Neurorehabilitation and neural repair* 2008;22:173-179.
3. Pennati GV, Plantin J, Carment L, et al. Recovery and Prediction of Dynamic Precision Grip Force Control After Stroke. *Stroke* 2020;51:944-951.
4. Rosso C, Valabregue R, Attal Y, et al. Contribution of corticospinal tract and functional connectivity in hand motor impairment after stroke. *PloS one* 2013;8:e73164.
5. van Kuijk AA, Pasman JW, Hendricks HT, Zwarts MJ, Geurts AC. Predicting hand motor recovery in severe stroke: the role of motor evoked potentials in relation to early clinical assessment. *Neurorehabilitation and neural repair* 2009;23:45-51.
6. Hannanu FF, Goundous I, Detante O, Naegel B, Jaillard A. Spatiotemporal patterns of sensorimotor fMRI activity influence hand motor recovery in subacute stroke: A longitudinal task-related fMRI study. *Cortex; a journal devoted to the study of the nervous system and behavior* 2020;129:80-98.
7. Birn RM, Molloy EK, Patriat R, et al. The effect of scan length on the reliability of resting-state fMRI connectivity estimates. *NeuroImage* 2013;83:550-558.
8. Carter AR, Astafiev SV, Lang CE, et al. Resting interhemispheric functional magnetic resonance imaging connectivity predicts performance after stroke. *Annals of neurology* 2010;67:365-375.
9. Puig J, Blasco G, Alberich-Bayarri A, et al. Resting-State Functional Connectivity Magnetic Resonance Imaging and Outcome After Acute Stroke. *Stroke* 2018;49:2353-2360.
10. Park CH, Chang WH, Ohn SH, et al. Longitudinal changes of resting-state functional connectivity during motor recovery after stroke. *Stroke* 2011;42:1357-1362.
11. Baldassarre A, Ramsey L, Rengachary J, et al. Dissociated functional connectivity profiles for motor and attention deficits in acute right-hemisphere stroke. *Brain : a journal of neurology* 2016;139:2024-2038.
12. Chi NF, Ku HL, Chen DY, et al. Cerebral Motor Functional Connectivity at the Acute Stage: An Outcome Predictor of Ischemic Stroke. *Scientific reports* 2018;8:16803.

13. Brihmat N, Tarri M, Gasq D, Marque P, Castel-Lacanal E, Loubinoux I. Cross-Modal Functional Connectivity of the Premotor Cortex Reflects Residual Motor Output After Stroke. *Brain connectivity* 2020;10:236-249.
14. Hong W, Lin Q, Cui Z, Liu F, Xu R, Tang C. Diverse functional connectivity patterns of resting-state brain networks associated with good and poor hand outcomes following stroke. *NeuroImage Clinical* 2019;24:102065.
15. Chen JL, Schlaug G. Resting state interhemispheric motor connectivity and white matter integrity correlate with motor impairment in chronic stroke. *Frontiers in neurology* 2013;4:178.
16. Zhang Y, Liu H, Wang L, et al. Relationship between functional connectivity and motor function assessment in stroke patients with hemiplegia: a resting-state functional MRI study. *Neuroradiology* 2016;58:503-511.
17. Grefkes C, Nowak DA, Eickhoff SB, et al. Cortical connectivity after subcortical stroke assessed with functional magnetic resonance imaging. *Annals of neurology* 2008;63:236-246.
18. Tang C, Zhao Z, Chen C, et al. Decreased Functional Connectivity of Homotopic Brain Regions in Chronic Stroke Patients: A Resting State fMRI Study. *PloS one* 2016;11:e0152875.
19. Termenon M, Jaillard A, Delon-Martin C, Achard S. Reliability of graph analysis of resting state fMRI using test-retest dataset from the Human Connectome Project. *NeuroImage* 2016;142:172-187.
20. Ungerleider JT, Mishkin M. Two cortical visual systems. In: Ingle DJ, Goodale MA, Mansfield RJ, eds. *Analysis of Visual Behavior*. Cambridge, MA, USA: The MIT Press, 1982: 549-586.
21. Goodale MA, Milner AD. Separate visual pathways for perception and action. *Trends in neurosciences* 1992;15:20-25.
22. Borra E, Gerbella M, Rozzi S, Luppino G. The macaque lateral grasping network: A neural substrate for generating purposeful hand actions. *Neuroscience and biobehavioral reviews* 2017;75:65-90.
23. Cavina-Pratesi C, Connolly JD, Monaco S, et al. Human neuroimaging reveals the subcomponents of grasping, reaching and pointing actions. *Cortex; a journal devoted to the study of the nervous system and behavior* 2018;98:128-148.
24. Pitzalis S, Fattori P, Galletti C. The human cortical areas V6 and V6A. *Visual neuroscience* 2015;32:E007.
25. Milner AD, Goodale MA. *The visual brain in action*. Oxford: Oxford University Press., 1995.

26. Lindow J, Domin M, Grothe M, Horn U, Eickhoff SB, Lotze M. Connectivity-Based Predictions of Hand Motor Outcome for Patients at the Subacute Stage After Stroke. *Frontiers in human neuroscience* 2016;10:101.
27. HersHKovitz A, Yichayaou B, Ronen A, et al. The association between hand grip strength and rehabilitation outcome in post-acute hip fractured patients. *Aging clinical and experimental research* 2019;31:1509-1516.
28. Collins GS, Reitsma JB, Altman DG, Moons KG, Group T. Transparent reporting of a multivariable prediction model for individual prognosis or diagnosis (TRIPOD): the TRIPOD statement. The TRIPOD Group. *Circulation* 2015;131:211-219.
29. Jaillard A, Hommel M, Moisan A, et al. Autologous Mesenchymal Stem Cells Improve Motor Recovery in Subacute Ischemic Stroke: a Randomized Clinical Trial. *Translational stroke research* 2020;11:910-923.
30. Brott T, Adams HP, Jr., Olinger CP, et al. Measurements of acute cerebral infarction: a clinical examination scale. *Stroke* 1989;20:864-870.
31. Sunderland A, Tinson D, Bradley L, Hewer RL. Arm function after stroke. An evaluation of grip strength as a measure of recovery and a prognostic indicator. *Journal of neurology, neurosurgery, and psychiatry* 1989;52:1267-1272.
32. White LE, Andrews TJ, Hulette C, et al. Structure of the human sensorimotor system. I: Morphology and cytoarchitecture of the central sulcus. *Cerebral cortex* (New York, NY : 1991) 1997;7:18-30.
33. Chiarello C, Vazquez D, Felton A, McDowell A. Structural asymmetry of the human cerebral cortex: Regional and between-subject variability of surface area, cortical thickness, and local gyrification. *Neuropsychologia* 2016;93:365-379.
34. Altman DG, Vergouwe Y, Royston P, Moons KG. Prognosis and prognostic research: validating a prognostic model. *Bmj* 2009;338:b605.
35. Geyer S, Ledberg A, Schleicher A, et al. Two different areas within the primary motor cortex of man. *Nature* 1996;382:805-807.
36. Konen CS, Mruczek RE, Montoya JL, Kastner S. Functional organization of human posterior parietal cortex: grasping- and reaching-related activations relative to topographically organized cortex. *Journal of neurophysiology* 2013;109:2897-2908.
37. Gallivan JP, Cant JS, Goodale MA, Flanagan JR. Representation of object weight in human ventral visual cortex. *Current biology : CB* 2014;24:1866-1873.
38. Plantin J, Verneau M, Godbolt AK, et al. Recovery and Prediction of Bimanual Hand Use After Stroke. *Neurology* 2021;97:e706-e719.

3.3 Study III. Resting-state fMRI

39. Wessler BS, Nelson J, Park JG, et al. External Validations of Cardiovascular Clinical Prediction Models: A Large-Scale Review of the Literature. *Circulation Cardiovascular quality and outcomes* 2021;14:e007858.
40. Caparelli EC, Ross TJ, Gu H, Yang Y. Factors Affecting Detection Power of Blood Oxygen-Level Dependent Signal in Resting-State Functional Magnetic Resonance Imaging Using High-Resolution Echo-Planar Imaging. *Brain connectivity* 2019;9:638-648.

3.4 Study IV. Predictive value of Surface-based morphometry metrics on hand motor outcome after stroke

3.4.1 Introduction

There is neuroimaging evidence that structural neural reorganization can occur in brain regions following stroke, both inside and outside of the lesion. Decrease of cortical thickness in the ipsilesional hemisphere following stroke has been reported in acute (Chen et al., 2021; Duering et al., 2015; Liu et al., 2015a), subacute, (Cheng et al., 2015) and chronic (Buetefisch et al., 2018; Jones et al., 2016; Ueda et al., 2019; Zhang et al., 2014) stroke. Brain regions may undergo cortical atrophy due to neuronal loss caused either directly by the lesion or indirectly by disconnection from a damaged region (Carrera and Tononi, 2014; Di Pino et al., 2014). Indeed, Chen et al. (2021) and Liu et al. (2020) reported changes in cortical thickness following a brainstem and basal ganglia stroke, respectively. Studies have also reported changes in the contralesional hemisphere, termed "transcallosal diaschisis". When compared to healthy controls, some studies showed increased cortical thickness (Brodthmann et al., 2012; Liu et al., 2015a), while some others reported a decrease (Chen et al., 2021; Cheng et al., 2020), or no significant changes (Cheng et al., 2015; Zhang et al., 2014) of cortical thickness in the contralesional hemisphere. In this case, the increased cortical thickness can be interpreted as a result of a compensatory process in areas participating in the recovery. These changes were influenced by the time of assessment following stroke and stroke topography (cortical or subcortical strokes). Therefore, the first aim of this study was to explore the changes in the SBM metrics, including the cortical thickness, fractal dimension, and gyrification index both in damaged and undamaged hemispheres following stroke, and its evolution over time, from baseline to six-month follow-up.

The current literature about the relationship between morphological changes and hand motor performance after stroke remains inconclusive. While most studies did not show significant correlations, (Buetefisch et al., 2018; Cheng et al., 2020, 2015; Jones et al., 2016; Liu et al., 2020; Schaechter et al., 2006) others have reported a positive correlation between motor performance and cortical thickness changes in the primary sensorimotor cortex and supramarginal gyrus (Liu et al., 2015a; Ueda et al., 2019). Of note, the latter studies used motor scores assessing the upper limb but not the hand. In studies using a specific assessment of hand motor performance, (Buetefisch et al., 2018; Cheng et al., 2020, 2015; Schaechter et al., 2006) hand performance did not correlate with the absolute value or change in cortical thickness. This lack of correlation may be due to the relatively small

3.4 Study IV (Surface-based morphometry)

sample size ($n < 50$) in most of the cited studies. In addition, very few studies, (Chen et al., 2021; Zhang et al., 2008) explored more sophisticated surface-based morphometry metrics, such as the gyrification index or fractal dimension representing the cortical complexity of the brain regions. Therefore, our second aim was to investigate the association between surface-based morphometric measures, including cortical thickness, fractal dimension, gyrification index, and hand motor outcome following stroke.

3.4.2 Methods

In this study, we used data from patients and healthy controls of the ISIS-HERMES, IRMAS, and RESSTORE studies, with a total of 106 patients and 107 healthy participants that served as controls. The SBM metrics were derived from anatomical T1 images and processed using CAT12 (detailed in the chapter 2). In addition to the cortical thickness (CT), we extracted two other metrics: the fractal dimension (FD), representing the structural complexity of the cerebral cortex, and the gyrification index (GI), measuring a comparison of the amount of cortex within the sulcal folds and the outer visible cortex. We first compared the three metrics between groups (controls, patients at M0, and patients at M6) and then used these metrics to predict hand and global motor performance, respectively, assessed with the handgrip and the mNIHSS.

Comparisons between controls and patients at M0 and at M6 were performed using independent t-tests for each hemisphere (ipsilesional and contralesional hemispheres) and each ROI of the HCP atlas with Bonferroni correction for multiple comparisons. For the hemispheres, patients were grouped by lesion side so that the left ipsilesional hemisphere and left contralesional hemisphere of the patients was compared to the left hemisphere of the controls and similarly for the right side. Then, the three metrics (CT, FD, and GI) were extracted at the ROI level using the HCP atlas (Glasser et al., 2016), see figure 2.2. for controls-patients comparison. Binary lesion masks of each patient were used to calculate the percentage of patients having lesions at each ROI, but stroke lesions were not masked.

To assess the predictive value of SBM metrics on hand motor recovery, several statistical and machine learning methods were used to predict hand motor outcomes at M6 using each of the SBM metrics separately and in combination. The methods include linear regression with l1 and l2 penalty (separately), random forest (RF), and support vector machine (SVM). As baseline models, predictive models using either initial severity or lesion volume were built.

3.4.3 Results

Participants

To control for the effect of age on the SBM-derived metrics, we included healthy participants who were older than 30 years old (107 from 169 participants [63%]) so that the age of the selected control and stroke groups was comparable. One hundred and six patients with stroke were included, among which 83 have behavioral and clinical scores at M6. The flowchart of the sample selection is presented in figure3.1. Participants' characteristics are presented in table 3.1, and behavioral and clinical scores were provided in table3.2.

Fig. 3.1 Study flowchart

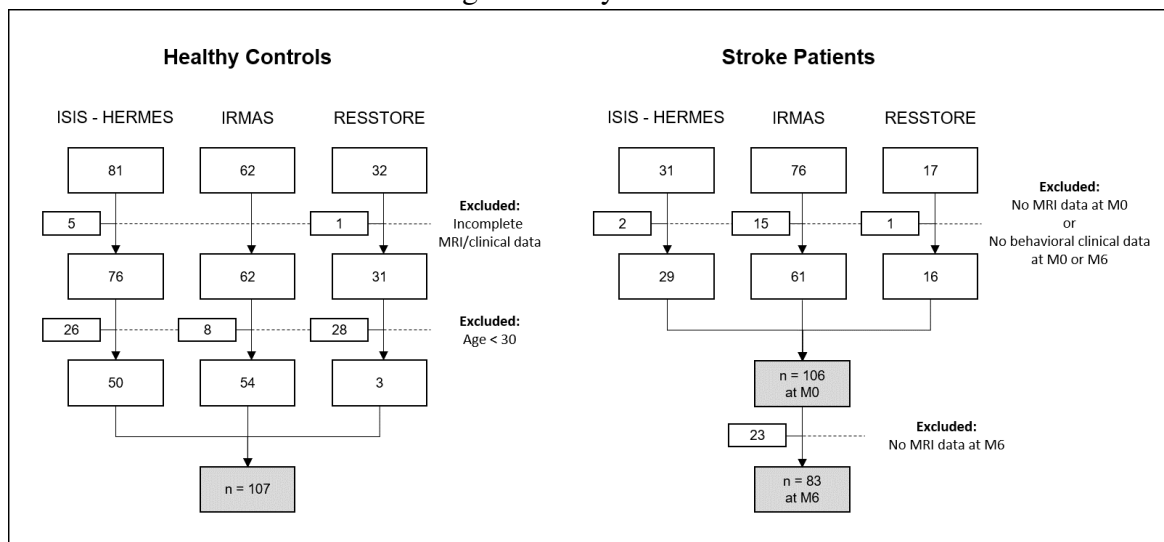


Table 3.1 Characteristics of participants

Variables	Patients	Controls
Age, mean(SD)	55.97 (13.99)	54.45 (15.34)
Male/Female, n(%)	67/36 (65.05/34.95)	50/57 (46.73/53.27)
Right/Left lesion, n(%)	53/53 (50/50)	N/A
Lesion volume, mean(SD)	63.57 (67.95)	N/A
Subcortical/Cortical/Both, n(%)	48/34/24 (45.28/32.08/22.64)	N/A
Stem-cell Treatment/Not, n(%)	30/76 (28.3/71.7)	N/A

3.4 Study IV (Surface-based morphometry)

Table 3.2 Behavioral and clinical scores of stroke group

Variables	mean	SD	median	IQR
Grip_PH_M0	8.72	11.44	1	14.99
Grip_PH_M6	14.16	14.35	12.8	24.28
mNIHSS_M0	3.04	3.07	2	5
mNIHSS_M6	1.72	2.25	0	4
NIHSS_M0	7.79	6.61	8	11
NIHSS_M6	4.5	4.84	3	8

Comparison between controls and patients

Mean, standard deviation (SD), median, and interquartile range (IQR) of the cortical thickness (CT), fractal dimension (FD), and gyrification index (GI) are presented for each group in Table B.1. When analyzed at the hemispheric level, CT at M0 was significantly lower in patients than in controls in the ipsilesional, contralesional, and both hemispheres, with a higher difference for the ipsilesional hemisphere. On the other hand, while FD in stroke patients was decreased in the ipsilesional hemisphere, the difference did not reach significance in the contralesional hemisphere. In contrast, we did not find any change in GI in the patients' group compared to the controls. Similar results were found at M6, with higher differences between CT and controls, suggesting a decrease in CT over time. Indeed, CT was significantly lower at M6 than at M0, whereas no difference was observed for FD and GI. Between-group comparison is presented in Table 3.3

Table 3.3 Between-group comparison (t-values) of CT, FD, and GI

		Controls-M0			Controls-M6			M6-M0		
		CT	FD	GI	CT	FD	GI	CT	FD	GI
Ipsilesional hemisphere	Left	5.137**	6.454**	-1.019	7.218**	6.857**	-0.6	-2.166*	-0.197	-0.166
	Right	5.309**	6.920**	-0.980	7.371**	7.339**	-1.108	-2.166*	-0.197	0.264
Contralesional hemisphere	Left	3.333*	0.822	-0.279	3.519*	-0.076	-0.423	0.037	1.194	-0.166
	Right	3.524*	1.318	-0.158	3.326*	-0.61	-0.030	0.037	1.194	0.264
Whole brain	-	4.582**	4.512**	-0.643	6.007**	4.697**	-0.543	-1.269	0.491	0.030

CT indicates Cortical thickness, FD: Fractal dimension, GI: Gyrification index. ** indicates t-test with $p < 0.001$, * for $p < 0.05$

When analyzed at ROI-level, decreased CT was observed mainly in the damaged regions such as the insula, superior temporal sulcus, frontal and parietal operculum, auditory areas,

and inferior parietal lobule. However, additional areas also showed a significant CT decrease, despite being relatively spared by the stroke lesion (damaged in less than 10% of all patients). These regions involved the visual areas (V1, V3, V4, V8, and visual ventral area), cingulate cortex (BA 23, 24, 31, 32), and frontal cortex (BA8, 9, and 11). Interestingly, CT in the homologous contralesional regions was also decreased. To exclude the possible effects of the stroke lesion on cortical measures, we performed an analysis in patients with only a subcortical stroke, and similar results were found. Detailed t-test results at ROI level for CT are presented in Table 3.4. ROI-level comparison regarding FD showed less significant difference especially in the contralesional hemisphere. Almost no difference was found for GI. Results for FD and GI are provided in Table B.2 and Table B.3

SBM predictive values for hand motor outcome

The baseline models for the prediction of handgrip strength at M6 were built using logistic regression by introducing initial severity (NIHSS at M0) or lesion volume as predictors. The accuracy of the grip model was 0.78 with initial severity and 0.71 with lesion volume.

Then, we used several statistical and machine learning methods to predict hand motor outcomes at M6 using each of the SBM metrics separately and in combination. Predictive values represented by the AUC are provided in table 3.5. Of note, the highest predictive values were obtained when using a random forest approach, with AUC values that was higher than the baseline models. When used separately, CT was the best predictor, followed by FD and then GI. Interestingly, the predictive values were slightly higher when CT, FD, and GI were used in combination.

3.4.4 Discussion

The two main objectives of this study were to explore SBM metrics changes following a stroke over time and to determine their predictive value on hand motor outcome. To this aim, data from 107 healthy controls and 106 patients with stroke were collected regarding the T1 anatomical MRI images, and hand behavioral scores were assessed using a handgrip dynamometer. Following a stroke, decreased CT was found in both hemispheres, decreased FD only in the ipsilesional hemisphere, and no change was found for GI. CT in the ipsilesional hemisphere was reduced over time, while no change was found in the contralesional hemisphere for FD and GI. The ROI-level analysis showed that CT was decreased not only in the damaged areas but also in some undamaged areas, such as the visual areas, cingulate and frontal cortex, in both the ipsilesional and contralesional hemispheres. CT with a random

3.4 Study IV (Surface-based morphometry)

Table 3.4 Cortical thickness (CT) comparison between patients (at M0) and controls at ROI-level

ROI	%	Ipsi	Contra	ROI	%	Ipsi	Contra	ROI	%	Ipsi	Contra
Insula-G	57.01	-6.62*	-5.35*	PFm	19.63	-2.98	-2.38	ProStriate	4.67	0.20	1.69
Insula2-post	56.07	-8.13*	-4.32*	47m	18.69	-2.16	-2.04	V3	3.74	-0.76	-2.03
Insula-post	54.21	-6.25*	-2.89	Frontal-eye-fields	17.76	-3.38	-3.31	V7	3.74	1.27	1.22
OP2-3-VS	53.27	-4.54*	-6.42*	IP2	17.76	-0.73	-0.64	IPS1	3.74	-0.01	1.38
FO3	52.34	-6.93*	-3.84	Superior-Temporal-medial	16.82	-0.89	-0.19	PreCuneus-visual	3.74	-3.02	-2.97
FO2	52.34	-4.88*	-5.41*	55b	16.82	-3.54	-3.74	23d	3.74	-4.26*	-2.8
Insula-mid	50.47	-8.82*	-4.21*	1	16.82	0.75	0.56	5L	3.74	-0.49	0.52
FO1	48.60	-5.36*	-1.47	TPOJ3	16.82	-1.23	-1.91	8BL	3.74	-4.89*	-3.81
Belt-medial	47.66	-4.99*	-1.05	47r-post	16.82	0.09	-5.48*	9p	3.74	-7.39*	-5.13*
43	46.73	-3.80	-1.89	TE1-mid	15.89	-2.65	-1.6	10p-ant	3.74	-4.98*	-3.2
52	46.73	-4.39*	-1.84	6-ant	14.95	-1.80	-1.87	Entorhinal	3.74	-5.33*	-4.41*
A1	44.86	-3.47	-2.03	TG-d	14.95	-6.57*	-5.78*	Perirhinal-ectorhinal	3.74	-3.63	-6.89*
Piriform	44.86	-7.69*	-4.17*	Temporal-mid	13.08	-0.84	-0.76	PH	3.74	-1.39	-2.34
OP4-PV	43.93	-6.5*	-2.55	7PC	13.08	0.36	-0.39	Visual-dorsal-transitional	3.74	1.02	-0.51
6-rostral	42.99	-2.71	-0.61	IP-Lat-dorsal	13.08	-0.19	1.58	ParaHippocampal2	3.74	-1.94	-0.82
OP1-SII	42.99	-4.66*	-6.85*	FST	13.08	-0.70	0.88	V4t	3.74	-1.51	0.64
FO4	42.99	-4.76*	-3.45	8Av	12.15	-1.91	-1.03	25	3.74	2.55	-2.3
Belt-lateral	42.99	-4.82*	-4.55*	46	12.15	-2.00	-0.36	V6	2.80	1.97	0.54
Insula-Ag-ant	42.06	-8.77*	-3.73	9-46v-ant	12.15	-6.88*	-6.9*	V8	2.80	-2.33	-1.79
RetroInsula	41.12	-3.47	0.9	IP-Lat-ventral	11.21	-0.13	0.44	LOC2	2.80	-3.32	0.39
Para-Belt	41.12	-3.14	-5.86*	6d	11.21	-1.58	-1.79	33	2.80	-3.17	-0.8
Para-Insular	38.32	-6.33*	-3.23	47-ant	11.21	-7.65*	-3.46	32d	2.80	-4.98*	-5.08*
TA2	36.45	-6.22*	-4.46*	13l	11.21	-4.22*	-6.54*	8BM	2.80	-4.35*	-5.12*
FO	36.45	-3.29	-0.95	TE1-post	10.28	-4.17*	-2.86	10r	2.80	-6.37*	-1.36
3a	35.51	1.49	0.49	LOC3	10.28	-1.94	-1.49	10d	2.80	-0.05	3.4
IFJp	35.51	-4.24*	-3.45	IP-medial	9.35	1.03	0.36	9a	2.80	-2.04	-1.55
PFcm	35.51	-3.94*	-3.85	9-46d	9.35	-5.88*	-6.25*	10v	2.80	-3.40	-2.65
Insula-ventral-ant	35.51	-5.36*	-3.16	6-8-inf-transitional	9.35	-2.20	-2.15	ParaHippocampal1	2.80	-1.53	-1.59
44	34.58	-2.81	-1.49	PGp	9.35	1.86	-0.53	V1-VM	2.80	-0.69	0.06
Auditory-4	34.58	-4.71*	-4.06*	IP1	9.35	-1.02	-0.88	V3-VM	2.80	-0.72	-3.07
IFJa	33.64	-5.88*	-3.93*	5Mv	8.41	-1.68	1.4	V2-VM	2.80	-0.69	-2.79
PFop	32.71	-4.83*	-2.11	24d-ventral	8.41	-4.82*	-3.66	31a	2.80	-3.25	-2.44
PeriSylvian-language	28.97	-4.29*	-2.01	PGs	8.41	-3.08	-2.45	s32	2.80	-2.37	-2.3
45	28.97	-3.65	-3.38	6ma	7.48	-4.71*	-4.08*	10p-post	2.80	-2.69	-1.91
PFt	28.97	-0.50	-1.17	6mp	7.48	-4.53*	-5.44*	TG-v	2.80	-5.56*	-4.47*
IFSp	28.04	-6.28*	-5.24*	8Ad	7.48	-6.14*	-8.56*	24-post	2.80	-6.57*	-3.77
TPOJ1	28.04	-1.03	-1.28	Hippocampus	7.48	-6.71*	-2.35	SPOC2	1.87	-0.84	-0.47
Premotor-eye-fields	27.10	-2.05	0.58	TE2-ant	7.48	-3.93*	-4.0*	Superior-Frontal-language	1.87	-1.35	-2.16
8C	27.10	-1.87	-0.1	23c	6.54	-1.47	1.98	a24	1.87	-2.36	-4.41*
Auditory-5	27.10	-4.32*	-2.13	IP-ventral	6.54	-0.51	-1.12	p32	1.87	-3.36	-4.37*
PFC	27.10	-2.33	-4.34*	24prime-post	6.54	-5.89*	-6.8*	9mid	1.87	-6.45*	-2.5
Superior-Temporal-visual	26.17	-5.28*	-1.22	32	6.54	-6.03*	-3.65	ParaHippocampal3	1.87	-2.48	-1.58
47s	26.17	-6.97*	-3.57	OFC-post	6.54	1.72	-0.17	TF	1.87	-3.09	-2.98
STSd-post	26.17	-1.86	-2.15	IP0	6.54	1.42	0.68	TE2-post	1.87	-5.1*	-3.45
2	25.23	0.39	0.15	V3CD	6.54	-2.04	-0.56	31p-d	1.87	-2.05	-1.27
6v	25.23	-5.34*	-1.59	V4	5.61	-4.23*	-3.66	Visual-ventral	1.87	-1.08	-1.39
STSd-ant	25.23	-6.89*	-3.92*	LOC1	5.61	-2.30	1.27	Orbital-frontal	1.87	-4.93*	-2.8
STSV-post	25.23	-3.32	-4.96*	24d-dorsal	5.61	-6.2*	-3.52	V3A	0.93	1.27	-0.58
9-46v-post	24.30	-2.46	-0.1	24prime-ant	5.61	-7.05*	-5.48*	Fusiform-face	0.93	-3.44	-0.81
47-lat	23.36	-2.63	-1.41	11l	5.61	-6.42*	-7.41*	InferoTemporal-post	0.93	-3.20	-1.16
IFSa	23.36	-0.37	-2.71	32-ant	5.61	-5.38*	-5.19*	7P-med	0.93	-2.31	-2.54
IP-ant	23.36	-0.30	0.21	V1	4.67	0.52	0.83	7M	0.93	-2.22	-4.39*
STGa	23.36	-7.81*	-5.67*	V2	4.67	0.90	0.55	SPOC1	0.93	-4.56*	-0.9
PGi	22.43	-1.90	0.53	V3B	4.67	-1.35	0.75	23ab-ventral	0.93	-4.9*	-2.79
4	21.50	-0.45	0.08	5M	4.67	-0.58	-0.28	31p-v	0.93	-4.0*	-2.11
PHT	21.50	-4.92*	-0.44	7A	4.67	-1.19	-1.92	10p-polar	0.93	-5.28*	-1.27
TPOJ2	21.50	-2.34	0.7	Supp-Cingulate-eye	4.67	-3.45	-3.59	PreSubiculum	0.93	0.33	-0.4
STSV-ant	21.50	-3.54	-6.71*	7A-med	4.67	-0.07	-1.54	V6A	0.93	2.70	0.55
SI	19.63	2.30	1.73	7P	4.67	0.32	0.85	RetroSplenial	0.00	-5.38*	-3.61
TE1-ant	19.63	-4.13*	-4.68*	6-8-sup-transitional	4.67	-5.1*	-4.94*	23ab-dorsal	0.00	-3.96*	-3.35

Values in the table indicate t-value comparison between patients and control (negative value means decreased CT compared to controls, and vice versa), Ipsi/Contra: comparison in the ipsilesional/contralesional hemisphere, * indicates significant difference using Bonferroni correction for multiple comparison, % indicates percentage of patients having lesions in the ROI.

Table 3.5 Performance of the model represented by the area under the curve (AUC) of hand grip models using different algorithms

Predictors	LR-11	LR-12	RF	SVM
CT	0.790	0.718	0.805	0.677
FD	0.728	0.718	0.744	0.697
GI	0.595	0.631	0.733	0.390
CT-FD	0.785	0.815	0.815	0.815
CT-GI	0.790	0.795	0.815	0.764
FD-GI	0.687	0.708	0.810	0.713
CT-FD-GI	0.779	0.805	0.836	0.805

CT: Cortical thickness, FD: Fractal dimension, GI: Gyrfication index, LR: Logistic regression, 11: 11 regularization (LASSO), 12: 12 regularization (Ridge), RF: Random Forest, SVM: Support Vector Machine

forest model provided the best predictor of the motor outcome at a six-month follow-up, with an accuracy of 80%, which is similar to the baseline model based on initial severity. Models combining CT and FD or the three metrics slightly improved the accuracy of the model.

Our results regarding CT decrease in the ipsilesional hemisphere are in agreement with the growing body of stroke literature, regardless of whether the patients were scanned in the acute, (Chen et al., 2021; Duering et al., 2015; Liu et al., 2015a) subacute, (Cheng et al., 2015) or chronic (Buetefisch et al., 2018; Jones et al., 2016; Ueda et al., 2019; Zhang et al., 2014) phase of stroke. Indeed, we found that cortical thinning was not limited to the lesion but extended to undamaged regions, suggesting that neuroplastic changes may occur beyond the lesion site, especially in the regions that are structurally connected to the lesioned area. (Cheng et al., 2015; Duering et al., 2015) For example, the insular cortex was damaged in most of our stroke population (more than 50%), and is known to have a wide range of structural connectivity with the frontal, temporal, parietal, and occipital regions. (Ghaziri et al., 2017)

Furthermore, cortical thinning was also observed in the contralesional hemisphere, although to a lesser extent than in the ipsilesional hemisphere. This is in line with some previous studies (Chen et al., 2021; Cheng et al., 2020), but in contradiction with others that reported no changes (Cheng et al., 2015; Zhang et al., 2014), or even increased CT (Brodthmann et al., 2012; Liu et al., 2015a). Interestingly, we also found reduced cortical complexity (decreased FD) in the ipsilesional but not in the contralesional hemisphere and no

3.4 Study IV (Surface-based morphometry)

change for GI. As CT is a measure of a physical distance, it is expected to be more sensitive to changes in both neural and non-neural elements, as opposed to FD, which compacts detailed information into one single measure of structural complexity, or GI, which measures the brain morphology (gyri and sulci) in a more macroscopic scale. Several explanatory mechanisms, including neuroinflammatory response and degeneration through transcallosal fibers, were proposed to account for cortical thinning on the contralesional side. In contrast, compensatory processes such as increased neuronal sprouting, dendritic arborization, synaptogenesis, and angiogenesis were attributed to the interpretation of increased cortical thickness. Many methodological considerations, such as the heterogeneous clinical characteristics of the patients, delay from stroke, differences in methods and study design, may be responsible for these varying results. In particular, the brain areas where the stroke lesion is involved would be of importance, as several studies observed cortical thickness changes only in specific ROIs but not in others. For example, Zhang et al. (2014) reported decreased CT in the ipsilesional M1, and no change in contralesional hemisphere M1. Brodtmann et al. (2012) reported an increase in contralesional CT in paracentral, superior frontal gyrus, and insula, but their analysis of CT was only performed in undamaged brain regions, those that are not directly affected by the lesion or edema and that may undergo plastic changes. In our data, globally CT was significantly decreased in the contralesional hemisphere. Interestingly, at the ROI level, there was no significant CT changes in the contralesional M1 (despite being lesioned in 21% of our population) and a slight increase of CT in a part of the contralesional insula (Insula-Ag anterior), even though it was not significant. Another factor that is not taken into account in most studies is the degree of which the patients use or rely on their ipsilateral hand during recovery, as changes in CT could represent this compensatory process. Overall, with these heterogeneous results from studies with relatively small sample sizes, it can be inferred that there is still no agreement on how stroke lesions affect the CT in the contralesional side.

In addition, we found that CT predicted hand motor outcomes. The random forest algorithm reaching 80.5% and 83.6% for the three metrics did better than the baseline model based on initial severity (78%) and much better than the model using lesion volume (71%). This result indicates that morphological information coming from anatomical images could be useful in determining hand motor prognosis of stroke, even when no other clinical information is gathered. It was also observed that adding information from FD or GI improved the predictive value of the model. However, hand motor-related changes following stroke was better captured by the CT than the other metrics.

This study has several limitations in which results must be interpreted cautiously. First, it has to be noted that the effect of brain edema, if present, on the measurements of SBM

metrics have not been taken into account. Except careful qualitative inspection and exclusion of patients with edema, this remains a problem in SBM analysis that is yet to be resolved. Second, the stroke population used in this study was relatively young, with a mean age of 56 years. As younger age is known to be associated with higher cortical thickness, and higher capacity for recovery and other compensatory process, our result might be different from the general stroke population. Third, despite of higher sample size used compared to previous studies, it was not enough to build machine learning models with adequate parameter tuning and cross-validation steps, and therefore the prediction accuracy reported could be overestimated.

This study presented evidence of brain morphological changes following a stroke in the ipsilesional and contralesional hemispheres, and that cortical thickness may provide prognostic value for hand motor outcome at a six-months follow-up period. These findings may expand our understanding of structural changes occurring in the brain following stroke, and may be helpful for designing rehabilitative strategies at the individual level. However, discrepancy between studies regarding changes in the contralesional hemisphere should be further investigated with more detailed methodology while controlling several associated factors in a larger population.

3.5 Study V (VLSM)

3.5.1 Introduction

For more than a century, lesion–symptom mapping studies have yielded valuable insights into the relationships between brain and motor functions (Feys et al., 2000; Godefroy et al., 1998; Shelton and Reding, 2001). During the last decades, newer techniques have been developed, such as Voxel-based Lesion-Symptom Mapping (VLSM) analysis, which determines the voxels in which the lesion is associated with the impaired explored function (Baldo and Dronkers, 2007; Rorden et al., 2009). Several studies have used VLSM to explore the spatial location associated with upper limb motor deficits (Frenkel-Toledo et al., 2019, 2022, 2020; Lo et al., 2010; Moon et al., 2016; Plantin et al., 2019; Schoch et al., 2006) or by other voxel-based analyses such as multivoxel pattern analysis (Park et al., 2016). These studies have shown upper-limb motor deficits to be associated with lesions mainly located in the corticospinal tract (CST) et more specifically in the corona radiata (either superior [SCR] or posterior [PCR] part), and/or the posterior limb of internal capsule. Motor-related brain regions have also been reported including the insula, basal ganglia, cerebellum, as well as other white matter tracts, such as the anterior limb of the internal capsule (ALIC), superior longitudinal fasciculus (SLF), external capsule (EC), and superior fronto-occipital fasciculus (SFO). With regards to lesions associated with hand motor outcomes, lesions in the corona radiata (Frenkel-Toledo et al., 2019, 2020; Lo et al., 2010; Plantin et al., 2019) and or posterior limb of the internal capsule (Frenkel-Toledo et al., 2019; Park et al., 2016; Schiemanck et al., 2008) are the most cited for correlating with worse outcomes.

Moreover, dissociations have been reported for the neural correlates of the upper-limb and hand, *i.e.*, the proximal and distal motor components of upper limb function. Distal movement is known to depend almost exclusively on the crossed CST that form the lateral CST, while proximal movement is also supported by the uncrossed CST that form the anterior CST, with a more bilateral innervation at the spinal level (Kuypers, 2011) (Figure 1.7). However, such a dissociation is not very clear at the subcortical level. At the level of the internal capsule, in which the axons descending from the cortical areas are densely packed, a gradient in terms of somatotopy (face, UL, LL) is recognized along an anterior-posterior axis, but not in terms of functional (proximal vs. distal) that is reported to be highly overlapped (Park et al., 2001). More recently, proximal vs. distal motor deficit lesion association has been explored by Frenkel-Toledo et al. (2019, 2020) using an approach based on the hemispheric lesion side. In patients with a right hemisphere lesion, damage to the superior temporal cortex and the retro-lenticular internal capsule was associated with proximal but not distal upper limb

functions in the subacute but not in the chronic phase. Of note, in the left-lesioned stroke group, *i.e.*, no significant voxel was significantly associated with a motor deficit of the right upper limb. However, the interpretation of these dissociations is hampered by the small sample size of the splitted subgroups (acute-chronic, and left-right stroke lesions) resulting in low statistical power. In their second study (Frenkel-Toledo et al., 2020), the authors found that damage in specific voxels within the SLF, putamen, EC, SCR, and insula affected shoulder abduction and finger extension independently, but no spatially separated cluster of voxels was identified.

The studies cited above used continuous motor scores in the VLSM analysis. An advantage of these measures is that the degree of impairment is taken into account in the analysis. However, care must be taken in interpreting the results, especially when clinical implementations are expected. As each voxel from the resulting VLSM analysis is commonly represented by a z-score, an intuitive pathophysiological interpretation is that: voxels with higher z-score are associated with a worse behavioral score. In clinical settings, this arbitrary level of severity is relatively difficult to be implemented to the patients, as compared to binary state (good or bad recovery). For this reason, motor scores in this study were binarized into no motor function (score=0) or some residual motor function (score=1). This way, a lesion in a significant voxel (with a certain cluster size threshold) would be associated with a motor deficit. Association with subsequent behavioral scores (for example lesion associated motor performance assessed at the chronic phase) would be highly useful in clinical settings when informing patients and caregivers about the level of motor recovery that can be expected. In this case, lesion location predicts complete hand deficit at the chronic phase, *i.e.*, no hand recovery.

The aim of study V was to determine the lesion locations associated with distal upper limb performance and proximal motor deficits at one month post-stroke (M0) and at six-month follow-up (M6) in a relatively large sample of patients with a subacute ischemic unilateral hemispheric stroke documented by a MRI. To this aim, anatomical MRI images from 102 patients with stroke from two centers (Grenoble and Paris) were collected, and a VLSM approach was used to associate the lesion spatial location at voxel level with binarized hand (handgrip strength) and global motor scores (mNIHSS), representing distal and proximal motor performance respectively.

3.5.2 Methods

We collected anatomical MRI images from three different studies (ISIS-HERMES, IRMAS, RESSTORE) performed in two centers (Grenoble and Paris). Handgrip score was used to assess hand performance, and mNIHSS was used for the global motor outcome. mNIHSS was derived from a summation of motor arm and leg motor scores of the NIHSS (National Institute of Health Stroke Scale). Of note, as the NIHSS motor scale assesses the degree of which movement of the arm and the leg (whether or not participants can lift their arm or leg, see NIHSS scale in Appendix A.2.1), the score reflects more the proximal than distal motor ability. Voxel-based Lesion-Symptom Mapping (VLSM) analysis was performed to identify the voxels in which the lesion was associated with (1) no hand motor function (grip = 0) and then (2) some degree of motor deficit (mNIHSS score > 1), with both scores assessed at one-month post-stroke (M0) and six-months follow-up (M6). The effect of age, sex, center, lesion side, and lesion volume were introduced as covariates. The effect of stem-cell treatment was regressed when predicting any scores at M6. Permutation-based thresholding was used to control for family-wise error (FWE) at 5% ($p < 0.05$, 5000 Freedman–Lane permutations).

3.5.3 Results

Participants

A total of 102 patients from three cohorts were recruited. Detailed information on the patient characteristics, with the clinical and behavioral scores, is shown in table 3.6. The stroke lesion overlay (Figure 3.4) showed a wide distribution of lesions across the middle cerebral artery territory. Areas including the insula, corona radiata, internal and external capsule, thalamus and basal ganglia, and frontal and parietal operculum were the most frequently involved. Of note, images from patients with the right lesion were flipped along the x-axis, and thus all patients were assumed to have lesions on the left side in order to increase the statistical power.

VLSM

General findings

The statistical maps of the VLSM analysis for grip and mNIHSS at both M0 and M6 are provided in figure 3.3, with the detailed number of voxels in the involved ROI presented in table 3.7. In general, the patterns were similar between grip and mNIHSS, with lesions

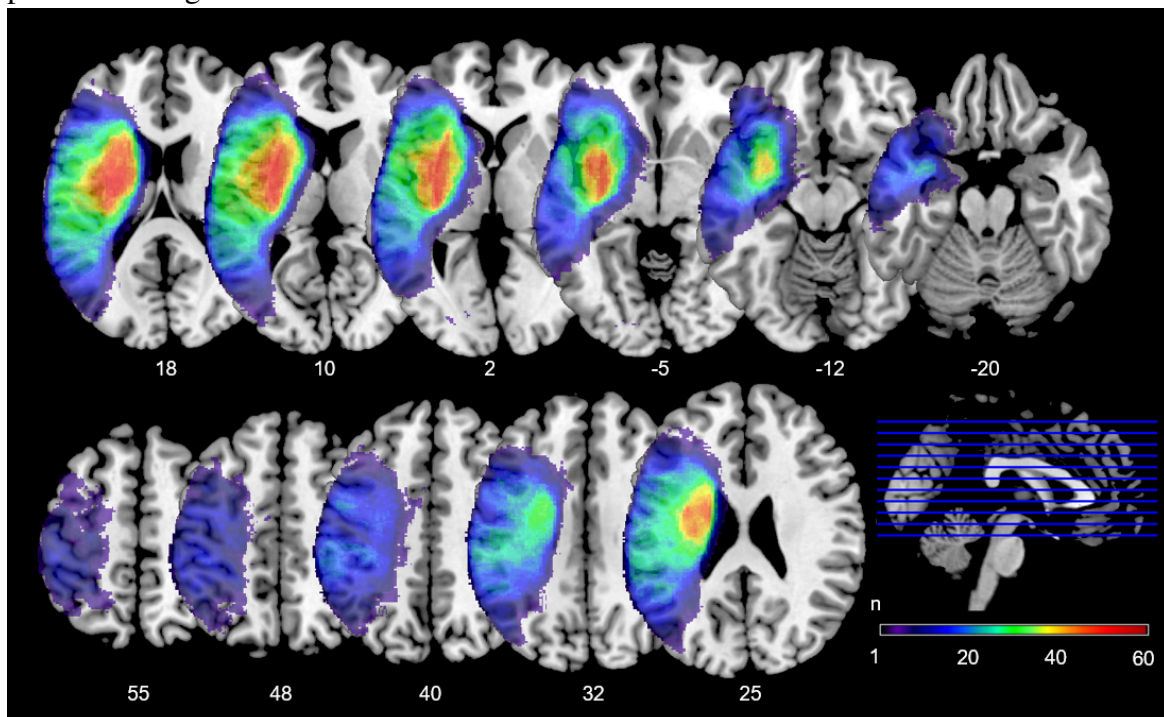
Table 3.6 Patient characteristics with clinical and behavioral scores

Categorical Variables	N	n	%
Sex (Male/Female)	102	66/36	64.71/35.29
Center (Grenoble/Paris)	102	45/57	44.12/55.88
Stem-cell Treatment (Yes/No)	102	30/72	29.41/70.59
Topology (Subcortical/Cortical/Both)	102	32/23/47	31.37/22.55/46.08
Lesion side(Right/Left)	102	51/51	50/50
Binary Grip M0 (Score>0/Score=0)	98	54/44	55/45
Binary Grip M6 (Score>0/Score=0)	91	59/32	65/35
Binary mNIHSS M0 (Score \leq 1/Score>1)	102	63/39	62/38
Binary mNIHSS M6 (Score \leq 1/Score>1)	88	41/47	47/53
Numerical Variables	N	Mean(SD)	Median(IQR)
Age (years)	102	55.98(14.06)	57(28)
Lesion volume (cc)	102	62.59(63.57)	43.75(91.83)
Grip at M0 (kg)	98	8.81(11.47)	1(14.99)
Grip at M6 (kg)	91	14.31(14.35)	12.95(24.28)
mNIHSS at M0	102	2.98(3.03)	2(5)
mNIHSS at M6	88	1.72(2.26)	0(4)
NIHSS at M0	98	7.71(6.6)	8(11)
NIHSS at M6	85	4.46(4.85)	3(8)

SD: Standard Deviation, IQR: Interquartile range, NIHSS: National Institute of Health Stroke Scale, mNIHSS: motor NIHSS

located in the superior and posterior corona radiata, and the posterior limb of the internal capsule (PLIC) were associated with worse motor performance at both time points.

Fig. 3.2 Lesion overlay of all included participants (n=102). The scale indicates number of patients having lesions in certain voxel.



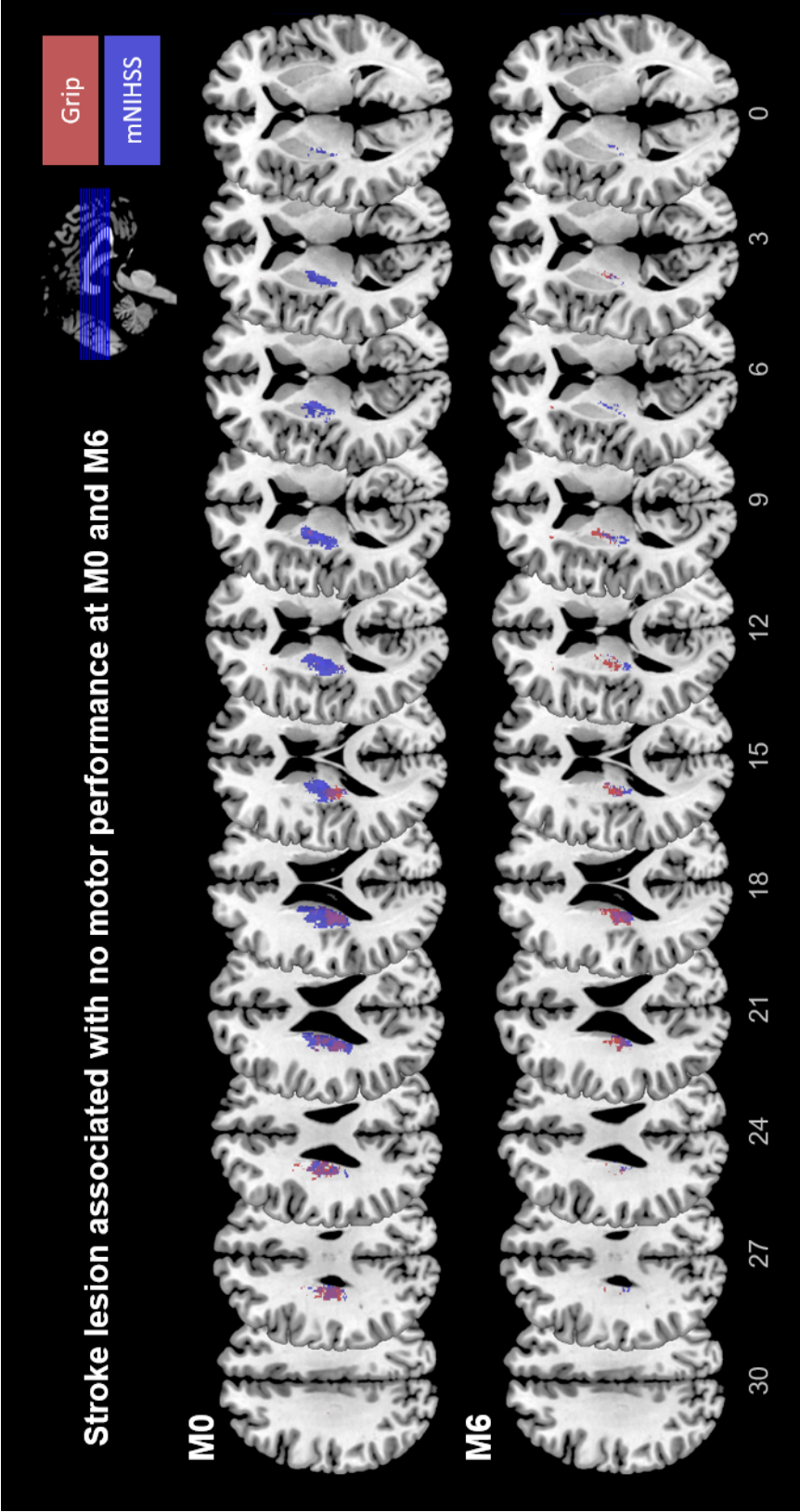


Fig. 3.3 Voxels associated with no motor performance at M0 and M6

Lesions associated with proximal and distal motor scores

At M0, the statistical maps between grip and mNIHSS overlapped. mNIHSS map (indicated with blue color in figure 3.3) covering the grip map (indicated with red color) and also areas outside of it at each level of corona radiata and internal capsule. At M6, despite some overlap between the two, a dissociation pattern was observed: the grip map covered more anteriorly, including the one-third anterior part of the PLIC and the anterior corona radiata, while the mNIHSS map covered more posterior part until the retrolenticular part of the PLIC.

Lesions associated with scores at M0 and M6

At M0, the number of significant voxels was higher than at M6. PLIC regions accounted for a higher percentage of significant voxels at M6 (30% and 41.5% for grip and mNIHSS, respectively) than at M0 (11.9% and 22.26%), while for putamen (only for mNIHSS), caudate, and pallidum, higher percentages of significant voxels were observed at M0 than at M6.

3.5.4 Discussion

This study aimed to explore the association between stroke lesion location and motor performance in a population of 102 patients with a subacute stroke using VLSM. We found that the patterns of lesion associated with complete hand paresis (grip=0) and with a more proximal motor deficit (mNIHSS > 1) were similar, including voxels located in the corona radiata (both superior [SCR] and posterior [PCR] part), posterior limb of the internal capsule (PLIC), and, with smaller clusters in the caudate, at both one-month post-stroke (M0) and six-months follow-up (M6). This result is in line with a large body of the literature (Feys et al., 2000; Frenkel-Toledo et al., 2019, 2022, 2020; Lo et al., 2010; Park et al., 2016; Schiemanck et al., 2008) and is somewhat expected considering that the dense corticospinal fibers are dedicated to voluntary motor movements and the participation of basal ganglia to motor control and learning. Regarding the period of stroke, there were more significant voxels at M0 than at M6, indicating that a wider range of spatially located lesion would relate to a subacute motor deficit, but only patients with a more specific lesion location would remain with a chronic motor deficit. Indeed, the PLIC accounts for a higher percentage of significant voxels at M6 than M0, <https://www.overleaf.com/project/62dff76ce1c9c30774781f3> confirming the importance of PLIC in motor recovery. Conversely, the reverse is observed for basal ganglia (higher percentage at M0 than M6), suggesting that patients with a lesion in the basal ganglia may show a motor deficit at the subacute phase of stroke but have a high probability of motor

Table 3.7 Number of significant voxels included in each ROI for each scores

Area	Grip M0			mNIHSS M0			Grip M6			mNIHSS M6		
	n	% vls	% area	n	% vls	% area	n	% vls	% area	n	% vls	% area
SCR	1241	65.35	16.55	1818	28.38	24.24	645	39.38	8.60	319	25.38	4.25
PLIC	226	11.90	6.02	1426	22.26	37.99	492	30.04	13.11	522	41.53	13.91
PCR	240	12.64	6.44	384	6.00	10.30	171	10.44	4.59	221	17.58	5.93
Caudate	77	4.05	1.00	331	5.17	4.31	57	3.48	0.74	38	3.02	0.49
SFO	31	1.63	6.11	261	4.07	51.48	50	3.05	9.86			
Putamen				1052	16.42	13.25	50	3.05	0.63	35	2.78	0.44
ALIC				345	5.39	10.99	43	2.63	1.37	12	0.95	0.38
ACR	27	1.42	0.39				40	2.44	0.58			
Pallidum				162	2.53	7.09	25	1.53	1.09	12	0.95	0.53
EC	23	1.21	0.41	360	5.62	6.42	20	1.22	0.36			
Insula	13	0.68	0.09	128	2.00	0.85	15	0.92	0.10			
Thalamus							13	0.79	0.15	15	1.19	0.17
RLIC				108	1.69	4.29				77	6.13	3.06
UF				21	0.33	5.53						

ROI: Region of interest, mNIHSS: motor subscale of National Institute of Health Stroke Scale

recovery at the chronic period. This is in agreement with the literature about the role of basal ganglia in motor control and of the CST in motor execution.

Somatotopic organization in the PLIC

The statistical maps of grip and mNIHSS at M0 showed a large overlap, with the mNIHSS map covering the grip map and some surrounding areas at each level of corona radiata and internal capsule. At M6, despite some overlap between the two, a dissociation was observed along an anterior-posterior axis with the grip map covering the one-third anterior part of the PLIC and the anterior corona radiata, and the mNIHSS map covering the posterior part of the PLIC until its retrolenticular part. Interestingly, although mNIHSS is composed of both upper- and lower- limb motor components the mNIHSS VLSM map covered the most posterior part of the PLIC. The somatotopic organization of the internal capsule has not been clearly defined according to the scientific findings to date. According to a classical view of the anatomical and electrophysiological literature, the motor fibers descending in the PLIC are organized along an anteromedial-posterolateral axis, meaning that hand fibers are located anteromedial to foot fibers (BERTRAND et al., 1965; Dawnay and Glees, 1986; Wells, 1983). A more recent anatomical study exploring the descending motor fibers from the different motor cortical areas in the macaque using anterograde tracers revealed an anterior-posterior organization to the cortical origin of the descending fibers, with the fibers originated from the anterior cingulate area are located in the most anterior part of the PLIC while the M1 fibers are grouped in its posterior part (Morecraft et al., 2002). In parallel electrophysiological studies in humans reported the existence of overlaps between all body part representations (BERTRAND et al., 1965). For example, Duerden et al. (2011) investigated the somatotopic organization and probabilistic mapping of motor responses in the PLIC using electrophysiological stimulation of the motor fibers in 52 patients with ventrolateral thalamotomy or deep brain stimulation surgery. They showed a somatotopic organization in the PLIC along an anteromedial to posterolateral axis for the face, arm, and leg fibers, consistently with the classical literature. However, they also found a large percentage of spatial overlap of the maps for the representation of the body parts, reaching (68.5%) for the arm and leg representations. In fact, the results regarding the overlap between the arm and leg representations are more in agreement with our findings, as they both represent proximal parts of the limbs.

Lesion dissociation between upper limb and hand (proximal vs. distal) has been explored by Frenkel-Toledo et al. (2019, 2020). In the first study, (Frenkel-Toledo et al., 2019) the authors found that in the right-lesioned stroke group, lesions in the insula, EC, SLF, ALIC,

caudate, and SFO were associated with a proximal motor deficit, while lesions in the putamen and SCR were associated with a proximal and distal motor deficit. In contrast, in the left-lesioned stroke group, they found no significant voxels but a trend for lesions in the SCR, PLIC, EC, SLF, and putamen to be associated with both proximal and distal motor deficits. In the second study, (Frenkel-Toledo et al., 2020) they found that damage in specific voxel within the SLF, putamen, EC, SCR, and insula affected shoulder abduction and finger extension independently, but no spatially separated cluster of voxels could be identified.

Taken together, all these results suggest that the spatial organization in the PLIC may follow several concomitant patterns in terms of anatomical (Cingulate, premotor, MI cortices), somatotopic (face, arm, leg), and functional (distal, proximal) organization of the motor system, explaining both the dissociation and the overlaps that are reported in most studies. This study confirms previous literature that stroke lesions in the corona radiata and PLIC are associated with motor deficits. In addition, lesions located specifically in the hand part of the PLIC and the anterior corona radiata predicted bad hand motor outcome at six months. This information could be useful in clinical settings when informing patients and caregivers about the course of the recovery.

3.6 Study VI (Multimodal MRI)

3.6.1 Introduction

In study I to study V, each MRI modality was used separately to predict hand motor outcome following stroke. Each of the modalities explored in these studies is to some extent suitable for hand-motor outcome prediction, depending on the type of hand motor outcome measure that is assessed. VLSM, SBM, and DTI define structural MRI, while task-fMRI and rs-fMRI relate to functional MRI for exploring the motor network. When used in combination, different modalities might bring either complementary or redundant information. Some studies have included multiple modalities to predict the motor outcomes of stroke patients. In most of these studies, a common practice is to combine one structural and one functional modality. Diffusion-weighted imaging, which has a high predictive value for motor outcome, is widely used in multimodal approaches, either together with resting-state fMRI (Carter et al., 2012; Chen and Schlaug, 2013; Lam et al., 2018; Lee and van Donkelaar, 2006; Lin et al., 2018; Lindow et al., 2016; Liu et al., 2015b, 2022; Rosso et al., 2013; Xia et al., 2021) or with task-fMRI. (Qiu et al., 2011; Song et al., 2014; Wang et al., 2012) Interestingly, fractional anisotropy (FA), a metric derived from DWI measuring white matter integrity, is reported in all of these studies to be associated with upper-limb motor performance. Functional features, on the other hand, were found to be also associated with motor performance but with a lower coefficient or to improve prediction accuracy but with a lower contribution to the explained variance. No study, as far as this thesis is concerned, has explored the use of SBM metrics together with DWI or fMRI modality to predict motor outcomes.

In Study VI, we explored the four MRI modalities presented in the previous studies (study I-IV, all except VLSM [Study V]), either separately or in combination. More specifically, several questions will be explored: Which MRI modality predicts hand motor outcome the best? Does a combination of two or more modalities provide better prediction than one, or do they bring redundant information to the model? Is it worth performing all of the MRI sequences to obtain better prognostic models? In this study (Study VI), the different modalities were compared and then used in combination to determine the models with the best prediction accuracy. Handgrip strength will be used as the main outcome measure of hand motor performance. Other outcome scores, including the mNIHSS and NIHSS, will also be used in order to have a better view of the contribution of each modality to more global components of stroke deficit.

3.6.2 Methods

To answer these questions, data from each modality, including surface-based morphometry, diffusion-weighted, task fMRI, and resting-state fMRI, were used in a total of 175 healthy controls and 108 patients. In patients, MRI was acquired at one-month post-stroke (M0). Pre-processing steps for each modality are detailed in chapter 2. MRI values from each modality were converted into z-scores against data from healthy controls of each cohort. Three outcome measures at six-month follow-up (M6) were binarized and tested in the models: Handgrip scores, either no (score=0) or some degree (score>0) of hand motor function; mNIHSS, and NIHSS, either no-mild (score 0 or 1) or moderate-severe (score>1) motor/neurological deficit. Prediction models were built using several statistical and machine learning algorithms, including logistic regression (LR) with l1 (LASSO) or l2 (Ridge) regularization, random forest, and support vector machine (SVM). The data were randomly split into a training and a testing dataset with a proportion of 70:30. Therefore, each model was built using the training dataset and then evaluated using the testing dataset. Model performance was evaluated using the Area under the curve (AUC).

For all MRI modalities, an ROI-based analysis was performed using the ROIs from the HCP atlas (Glasser et al., 2016), as described above, in the method chapter. For morphological imaging, an SBM analysis was performed using CAT12 to obtain three metrics: cortical thickness (CT), fractal dimension (FD), and gyrification index (GI). For RS-fMRI, we used graph theory analysis to compute 7 graph metrics: global efficiency (GE), local efficiency (LE), Betweenness Centrality (BE), average path length (APL), clustering coefficient (CC), cost (C), and degree (D). Graph theory analysis was used instead of the classical ROI-based approach to limit the number of variables, as there is only one value per graph metric and ROI. Therefore, 2260 (7 metrics x 380) ROIs were used while 144400 (380 x 380) ROI-to-ROI connectivity z-score values would have been used with the ROI-based approach. For task-fMRI, we used the Cohen's d effect sizes derived for each ROI from the t maps obtained using spm12. Finally, for diffusion MRI, we used a constrained spherical deconvolution (CSD) approach in MRtrix software to estimate the Fractional Anisotropy (FA) in 72 white matter ROIs (Wasserthal et al., 2018). Within each MRI modality, model performances were compared, and the best metric was used to be compared with the other modalities. Then, each modality was compared either independently or in a combination of two to predict each outcome measure. Of note, only the highest accuracy among different algorithms is presented for models with a combination of two modalities.

3.6.3 Results

Participants

Data from a total of 172 healthy controls (mean age 43.48 years, 78 males) and 105 patients (mean age 55.89 years, 68 males, 53 right strokes) from the three cohorts were used. A complete description of the characteristics and clinical and behavioral scores of the participants is summarized in table 3.8.

Predictive value of each modality when used independently

The model performance of each metric is provided in table B.4 for each modality. In most models, the best prediction was found using random forest analysis. For SBM, cortical thickness showed higher AUC than fractal dimension and gyrification index models, regardless of the algorithm that was used. Among RS-fMRI graph theory metrics, GE was the best predictor. Consequently, in the multimodal analysis, CT and GE were used to represent SBM and RS-fMRI modality, respectively.

Model performance using each modality independently for grip, mNIHSS, and NIHSS is reported in table 3.9. Each modality showed different predictive values for each outcome measure. The grip was best predicted by task-fMRI, mNIHSS by DWI, and NIHSS equally by SBM, DWI, and RS-fMRI. Relatively, a low prediction was found for the mNIHSS by SBM and for NIHSS by task-fMRI.

Predictive value of each modality when used in a combination of two

Model performances for the combination of 2 modalities are provided in table 3.10. Table 3.10 shows that grip is best predicted by the combination of task-fMRI and DWI, mNIHSS by DWI alone or the combination of SBM and task-fMRI, and the NIHSS by any combination of two modalities (AUC>0.9). In addition, the AUC for combined DWI and SBM modalities reached 1. Of note, as the prediction of two combined modalities is approaching 1 for all outcome measures, no additional improvement of the model seemed necessary, and therefore combinations of three and four modalities were not tested.

3.6.4 Discussion

After exploring each modality separately, this last study aimed to compare the contribution to motor outcome prediction provided by these modalities either independently or in combination. We found that hand motor outcome was best predicted by task-fMRI alone, with an

improved prediction if used together with DWI. Additionally, upper- and lower-limb motor outcome assessed with the mNIHSS was best predicted by DWI, and global neurological severity assessed with the NIHSS was equally well predicted by DWI, RS-fMRI, and SBM independently.

The best prediction of hand motor outcome assessed with the handgrip was provided by task-fMRI using a wrist flexion-extension task. This could be expected considering the fact that task-fMRI is designed to explore motor-related systems related to wrist and hand movements. Interestingly, adding another functional modality did not improve the model, but adding structural information (DWI) did. This finding confirmed the complementary relationship between structural and functional neuroimaging approaches in explaining brain changes following stroke, in line with previous studies using DWI and resting-state fMRI (Lam et al., 2018; Lin et al., 2018; Rosso et al., 2013). Studies using task-fMRI and DWI (Song et al., 2014; Wang et al., 2012), however, only reported correlations between the two instead of their independent and joint contribution to predicting hand motor outcomes.

The specificity of task-fMRI, however, brought lesser value as the outcome measures reflect a more global deficit (mNIHSS and NIHSS). We found that motor deficit that is known to be well reflected by the CST structural damage was best predicted by DWI and that adding another modality did not improve the prediction accuracy. Indeed, in other studies using global motor measures, the predictive value is usually lower for fMRI than for DWI, with FA explaining most of the motor outcome variance, while fMRI added only slight improvements to the model fits (Carter et al., 2010; Lam et al., 2018; Lee et al., 2019; Lin et al., 2018; Lindow et al., 2016; Qiu et al., 2011; Rosso et al., 2013; Xia et al., 2021). The second best model was the combination of task-fMRI and DWI for the hand and NIHSS outcomes or task-fMRI and SBM for the mNIHSS outcome, indicating that the unexplained variance of task-fMRI can be complemented by structural information. In contrast, all modalities but the task-fMRI predicted the NIHSS with high accuracy. As the NIHSS comprises additional measures than motor deficit, such as visual loss, language deficit, inattention, and level of consciousness, it could be expected that MRI modalities that bring global structural and functional information would be more relevant compared to a specific motor-task-related brain activity.

This study has several limitations. A first limitation is the heterogeneity of our data in terms of stroke populations (baseline stroke severity and delays, stem-cell treatment), MRI data acquisition (eyes open and eyes closed in RS-fMRI, an active and passive task in task-fMRI), representing potential biases for the interpretation of our findings. However, we introduced these variables as covariates in the models to account for their effects. This

3.6 Study VI (Multimodal MRI)

may also be considered as a strength since such heterogeneity reflects better the diversity of stroke populations in routine. A second limitation is the small sample size, leading to the use of the testing dataset in the hyperparameter tuning, resulting in an increased risk of overfitting in our predictive models. Indeed, this is reflected by the very high accuracy reaching up to 1, (*i.e.*, perfect prediction) in some models. Nevertheless, the main aim of this study was more to compare predictive values of different MRI modalities at the exploratory level for motor outcomes. Therefore, further studies are needed to validate our predictive models with the aim to use them in clinical settings.

MRI modalities with best prediction accuracy

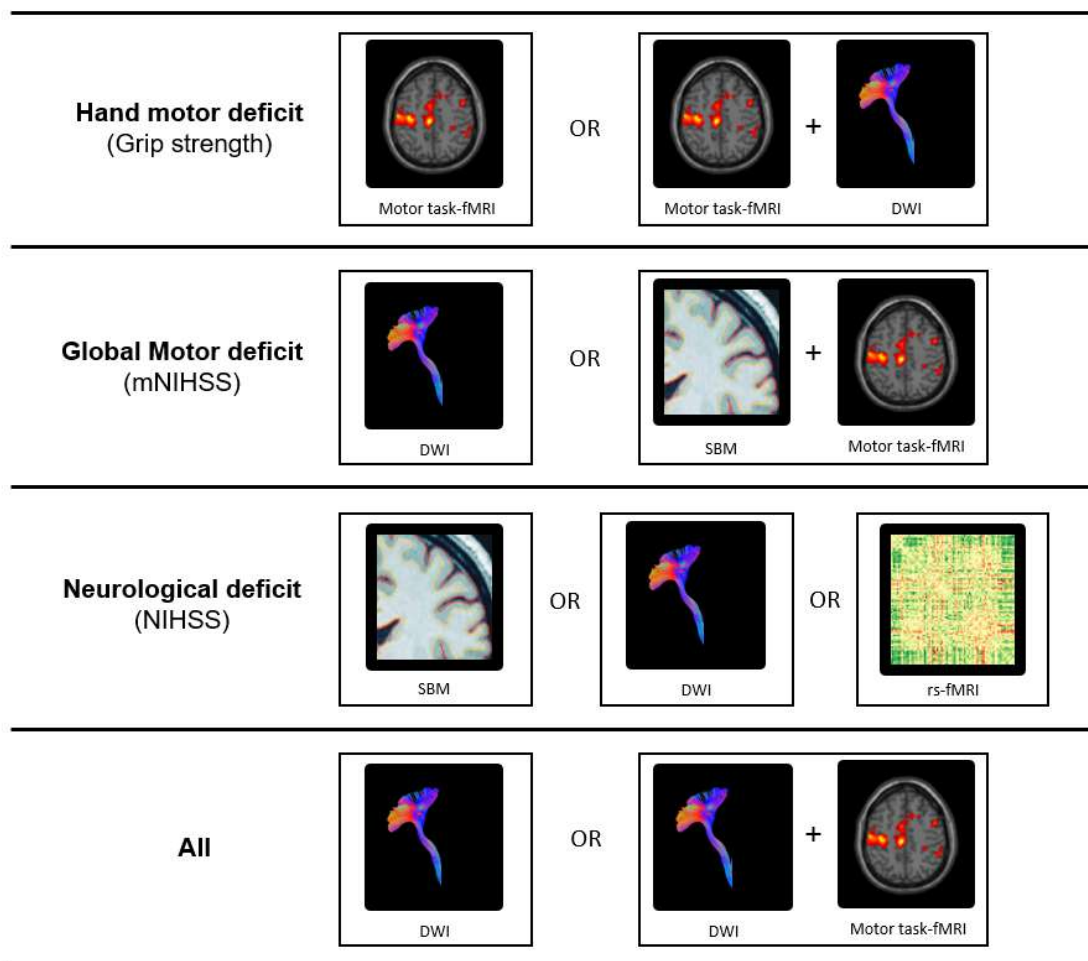


Fig. 3.4 Best MRI modality biomarkers according to outcome measures

Table 3.8 Characteristics, clinical and behavioral scores in patients and controls

Variables	Patients			Controls		
	N	n	%	N	n	%
Sex (Male/Female)	105	68/37	64.76/35.24	172	78/94	45.35/54.65
Cohort (HERMES/IRMAS/RESSTORE)	108	29/63/16	26.85/58.33/14.81	175	81/62/32	46.29/35.43/18.29
Stem-cell Treatment (Yes/No)	108	78/30	72.22/27.78	-	-	-
Topology (Subcortical/Cortical/Subcortical)	107	35/24/48	32.71/22.43/44.86	-	-	-
Lesion side(Right/Left)	108	53/55	49.07/50.93	-	-	-
Binary Grip at M0 (Score>0/Score=0)	101	56/45	55/45	-	-	-
Binary Grip at M6 (Score>0/Score=0)	93	60/33	65/35	-	-	-
Binary mNIHSS at M0 (Score \leq 1/Score>1)	105	64/41	61/39	-	-	-
Binary mNIHSS at M6 (Score \leq 1/Score>1)	90	42/48	47/53	-	-	-
Binary NIHSS at M0 (Score \leq 1/Score>1)	101	80/21	79/21	-	-	-
Binary NIHSS at M6 (Score \leq 1/Score>1)	88	55/33	63/37	-	-	-
	N	Mean(SD)	Median(IQR)	N	Mean(SD)	Median(IQR)
Age (years)	105	55.89(14.28)	57(29)	172	43.48(19.15)	37(29)
Lesion volume (cc)	108	62.59(67.7)	38.32(92.76)	-	-	-
Grip at M0	101	9.08(11.62)	1(15.96)	-	-	-
Grip at M6	93	14.43(14.52)	12.95(24.35)	-	-	-
mNIHSS at M0	105	2.98(3.07)	2(5)	-	-	-
mNIHSS at M6	90	1.7(2.25)	0(4)	-	-	-
NIHSS at M0	101	7.63(6.63)	8(11)	-	-	-
NIHSS at M6	88	4.4(4.83)	3(8)	-	-	-

3.6 Study VI (Multimodal MRI)

Table 3.9 Predictive value of each modality using different algorithms

Dependent variable	MRI Modality	LR-I1	LR-I2	RF	SVM
Grip M6	SBM	0.790	0.718	0.805	0.677
	DWI	0.849	0.855	0.836	0.803
	RS-fMRI	0.754	0.749	0.872	0.713
	task-fMRI	0.922	0.878	0.944	0.867
mNIHSS M6	SBM	0.406	0.553	0.694	0.571
	DWI	0.982	0.982	0.939	0.861
	RS-fMRI	0.726	0.673	0.827	0.577
	task-fMRI	0.917	0.906	0.865	0.844
NIHSS M6	SBM	0.988	0.952	0.958	0.927
	DWI	0.948	0.954	0.961	0.935
	RS-fMRI	0.967	0.953	0.973	0.927
	task-fMRI	0.769	0.744	0.679	0.756

Table 3.10 Predictive value of MRI modalities when used in combination of two

Dependent variable	MRI modality	DWI	RS-fMRI	SBM	task-fMRI
Grip M6	DWI	0.855	0.882	0.855	0.969
	RS-fMRI		0.872	0.872	0.944
	SBM			0.805	0.844
	task-fMRI				0.944
mNIHSS M6	DWI	0.982	0.885	0.894	0.910
	RS-fMRI		0.827	0.780	0.833
	SBM			0.694	0.979
	task-fMRI				0.917
NIHSS M6	DWI	0.961	0.979	1.000	0.987
	RS-fMRI		0.973	0.980	0.911
	SBM			0.988	0.923
	task-fMRI				0.769

Chapter 4

Discussion and Conclusion

Chapter contents

4.1	Summary of the main findings	154
4.2	Hand motor impairment after stroke	156
4.3	Predictive models and neural correlates of hand motor recovery	157
4.3.1	Clinical assessments	157
4.3.2	Lesion characteristics	158
4.3.3	Structural Imaging	159
4.3.4	Functional MRI	160
4.4	Methodological Considerations	162
4.4.1	Generalizability of the results	162
4.4.2	Sample size	162
4.4.3	Heterogeneity in study designs and confounding factors	163
4.4.4	Brain asymmetry: to flip or not to flip?	165
4.5	Clinical Implications	165
4.6	Perspectives	167
4.7	Conclusion	168

The present thesis benefited from the three cohorts (ISIS-HERMES, IRMAS, and RESTORE) performed in two centers (CHUGA and Pitié Salpêtrière Paris) in healthy participants and stroke patients assessed with clinical and multimodal MRI imaging examinations. Focusing on hand motor recovery, the current work investigates the predictive value of 5 different MRI modalities, including the task-fMRI, DTI, rs-fMRI, SBM, and VLSM, first separately (study I to study V) and then in combination. We assessed and compared the contribution of each MRI modality relative to the others when used either independently or in combination (study VI). The present chapter presents a summary of the main findings in each study and is followed by a general discussion about hand motor impairment, predictive models and neural correlates, methodological considerations reviewing the strengths and limitations of the thesis, perspectives for future studies, and a conclusion.

4.1 Summary of the main findings

Study I. Task fMRI

- Purdue pegboard test (PPT) and handgrip scores were lower in patients with stroke than healthy participants. No significant effect of age was found for both tasks but an effect of sex was observed: Men had higher scores than women in handgrip while not in PPT.
- Both PPT and handgrip in patients improved significantly over time. There was an effect of the lesion side (patients with a left-sided hemispheric stroke had better PPT scores than those with a right-sided hemispheric stroke) for the PPT. No effect of age, gender, and lesion volume on recovery was observed.
- Task-related fMRI brain activity was associated with hand behavioral scores, with a specific spatiotemporal pattern: while almost no significant correlations were found at baseline, hand motor performances positively correlated with bilateral activity in the sensorimotor network at six-month follow-up and with activity in the ipsilesional sensorimotor and parietal regions at two-year follow-up.
- There was a dissociation between the simple grasp task (handgrip) and manual dexterity task (PPT). PPT recovery was predicted by fMRI activity within MI-4p and both the dorsolateral and dorsomedial network, while handgrip was predicted by activity in the MI-4a and only the dorsolateral network.

Study II. DTI

- Impairment of the ipsilateral hand was frequent in patients with stroke, both in the whole group or in a subgroup of patients without cognitive deficit.
- Impairment of the ipsilateral hand correlated with neurological clinical scores (NIHSS, FMS, Barthel index) but not with cognitive scores.
- Decreased Fractional anisotropy (FA) in several white matter tracts, including the corticospinal tract (CST), anterior corona radiata (ACR), corpus callosum (CC), superior longitudinal fasciculus (SLF), and corticoreticulospinal pathway (CRP) was associated with the impairment of the ipsilateral hand.
- A set of white matter tract FA predicted hand motor recovery assessed using the three motor scores: PPT was predicted by ipsilesional CST at the level of PLIC and SLF, handgrip was predicted by ipsilesional CST at the level of cerebral peduncle, and contralesional ACR and movement time was predicted by CC-genu, ipsilesional SLF and CRT at the level of PLIC, and contralesional CST at the level of the pons.

Study III. Resting-state fMRI

- Handgrip scores measured at baseline and six-month follow-up were associated with functional connectivity within the sensorimotor network, connectivity between bilateral motor and occipital areas, connectivity between ipsilesional superior parietal lobule and occipital areas, and connectivity between the interhemispheric occipital areas
- Handgrip is predicted by visuomotor connectivity at both time points: at baseline by BA4a-OC1 and SPL7M-OC.lateral and at six-month by MI4a-OC.dorsal and within-sensorimotor connectivity (BA3b-BA6ma).

Study IV. SBM

- Cortical thickness (CT) is lower in patients with stroke than in healthy controls at both time points in the ipsilesional hemisphere and, to a lesser extent, the contralesional hemisphere. Fractal dimension (FD) is reduced only in the ipsilesional hemisphere, while no change was found for the gyrification index (GI).
- CT in the ipsilesional hemisphere was reduced over time (from baseline to six-months follow-up), while no change was found for FD and GI.

Discussion and Conclusion

- Using a random forest approach, CT may predict hand motor outcome with an accuracy that is similar to that of initial severity, while lower accuracy was found using FD and GI. When the three metrics were used in combination, predictive values were slightly higher.

Study V. VLSM

- Lesions located in the superior and posterior corona radiata (SCR and PCR), posterior limb of the internal capsule (PLIC), and caudate were associated with poor proximal and distal motor performance at both baseline and six-month follow-up.
- At baseline, The statistical maps of grip and mNIHSS showed a large overlap, with the mNIHSS map covering the grip map and some surrounding areas at each level of corona radiata and internal capsule. At M6, a dissociation was observed along an anterior-posterior axis with the grip map covering the one-third anterior part of the PLIC and the anterior corona radiata, and the mNIHSS map covering the posterior part of the PLIC until its retrolenticular part.

Study VI. Multimodal MRI

- Hand motor outcome was best predicted by task-fMRI, with improved prediction if used together with DWI.
- Global motor outcome was best predicted by DWI alone, and adding other modalities did not improve prediction accuracy
- Global neurological severity was equally well predicted by DWI, RS-fMRI, and SBM independently

4.2 Hand motor impairment after stroke

The fact that this thesis was focused on hand motor impairment following stroke is due to its high frequency and crucial role in patients' quality of life. In our dataset, hand motor performance was impaired in both the contralateral hand (Study I) and in the ipsilateral hand (Study II), with variable degrees of impairment depending on the measurement used. Then, we observed significant improvement in hand motor performances over time between baseline and six-month follow-up, with some degree of recovery until two-year follow-up.

4.3 Predictive models and neural correlates of hand motor recovery

This is in line with the literature on stroke recovery, that globally significant recovery occurs in the first 6 months after stroke, and that that neurologic and functional recovery should not be expected after the first 5 months.(Jørgensen et al., 1995) It needs to be noted, though, that Study I and II were based on participants of the ISIS-HERMES study with 31 patients with moderate to severe stroke (NIHSS > 6). This fact implies that even though this study benefited from a wide range of clinical, cognitive, and behavioral measurements, the nature of its inclusion criteria would surely overestimate the severity and frequency of hand impairment in the general population. For this specific reason, we have explored clinical and behavioral data from routinely assessed patients in the local stroke unit, including 209 patients with unilateral stroke, and found similar results, even though to a lesser degree. (Razak et al., 2022)

Studies reporting the frequency of ipsilateral hand impairment are still scarce. Meanwhile, impairment of the ipsilateral hand also needs to be assessed, given the fact that patients with severe sensorimotor deficits of the contralateral hand mostly rely on their ipsilateral hand and that most daily life activities require bimanual coordination of both hands. In study II and in the related published work,(Razak et al., 2022) we shed a light on the importance of assessing the ipsilateral hand: We found that the ipsilateral hand is frequent following stroke (up to 35%, depending on the type of motor task assessed), that it predicts long-term outcome assessed by modified Rankin Scale (mRS), and that it is associated with white matter disruption to a combination of white matter tracts. We recommend to integrate the ipsilateral hand assessment into rehabilitation programs, as it may bring additional information to assess and improve recovery.

4.3 Predictive models and neural correlates of hand motor recovery

4.3.1 Clinical assessments

One of the known best predictors of hand motor outcome is the hand motor performance measured at initial time points, as reported by several previous studies. (Beebe and Lang, 2009; Plantin et al., 2021; Smania et al., 2007) The limitation of prediction using initial assessment is that it is valuable only in moderately impaired patients due to the floor effect on the severely impaired patients and ceiling effect as early as 3 months after stroke. (Lindow et al., 2016) In this context, our study (Razak et al., 2022) showed that assessment of the ipsilateral hand might bring useful predictive information, particularly in severe stroke, as

Discussion and Conclusion

the subtle impairment to the ipsilateral hand may provide a more continuous scale. Indeed, ipsilateral hand impairment is reported to be more prominent in severe stroke. (Bustrén et al., 2017) It is important to note, though, that these reported predictive values are highly dependent on the type of the measurements used (strength, tapping speed, manual dexterity, etc.) for both the predictors and the outcome measures, as not all aspects of hand motor components would be captured by a single hand assessment type.

4.3.2 Lesion characteristics

Lesion volume has been suggested to be associated with stroke recovery, but varying evidence supports this notion. Recent studies reported weak to no correlation between lesion volume alone and upper-limb motor outcome (Page et al., 2013). In this thesis work, Study I evidenced no effect of lesion volume on hand motor recovery of the paretic hand. In Study II, a moderate correlation between lesion volume and movement time ($r=0.44$, $p=0.025$), a trend with manual dexterity assessed using PPT ($r=-0.38$, $p=0.058$) and handgrip ($r=-0.34$, $p=0.093$) of the ipsilateral hand were observed. In Study III, although the direct correlation between lesion volume and hand motor outcome was not reported, the effect of lesion volume was not kept by the linear regression model when predicting handgrip scores using resting-state fMRI connectivity measures. In Study IV, the logistic regression model showed that lesion volume could predict 71% of the binarized handgrip scores, either no hand function (grip=0) or some degree of hand motor function (grip>0).

Taken together, these findings indicate that lesion volume explains a good part of the hand motor outcome variance, while other factors such as stroke location may account for the residual variance. The complementary contribution of lesion volume and lesion location should not come as a surprise. Severe hand motor impairment with a low probability of recovery could result from large brain lesions affecting multiple brain areas within the motor network -or even other systems, as well as small brain lesions located in areas with dense corticospinal tract. (Parsons et al., 2010; Seitz et al., 1998) Indeed, the location of stroke has also been consistently reported to be associated with hand motor deficits. Based on results in Study V and supported by other previous studies, (Feys et al., 2000; Frenkel-Toledo et al., 2019, 2022, 2020; Lo et al., 2010; Park et al., 2016; Schiemanck et al., 2008) stroke lesion involving the superior corona radiata and, more importantly, the posterior limb of the internal capsule is associated with a lower probability of hand motor recovery.

4.3.3 Structural Imaging

One of the most important contributions of neuroimaging approach to the prediction of hand-motor outcomes is the precise quantification of the damaged structural neural resources, also known as structural reserve (Stinear, 2010). Although VLSM methods may lay out voxels in which lesions would be associated with certain behavioral deficits, it does not provide the degree of damage in the corresponding structure. In this regard, diffusion-weighted imaging strategies have been developed to accurately examine the contribution of white matter damage to the behavioral deficit and have gained huge attention in the neuroimaging field. Fractional anisotropy (FA), together with other DWI-derived metrics such as axial and radial diffusivity (AD/RD), is commonly used as a measure of "intactness" or "integrity" of the white matter.

An obvious target in the context of hand motor deficit is the corticospinal tract (CST), although other white matter tracts such as the superior longitudinal fasciculus (SLF), corpus callosum CC), and other corticocortical fibers have gained more attention in more recent studies. Within the CST, FA estimated from DWI at the subacute phase has been consistently reported to be a predictor of motor outcome, both for the upper limb (Buch et al., 2016; Byblow et al., 2015; Puig et al., 2013, 2010; Radlinska et al., 2010; Yu et al., 2009; Zhang et al., 2014) and for the hand (Imura et al., 2015; Koyama et al., 2014; Schaechter et al., 2009; Song et al., 2012). In addition to the CST, these predictive values were also reported for other white matter tracts, including corticocortical intrahemispheric tracts such as SLF (Koyama and Domen, 2017; Rodríguez-Herreros et al., 2015), interhemispheric tracts (CC) (Li et al., 2015; Sisti et al., 2012; Stewart et al., 2017), and alternate corticofugal pathway (Jang et al., 2013). For a comprehensive review, see (Koch et al., 2016). Although not explicitly reported, we found similar results in our dataset. However, the abundance of evidence for white matter integrity as a predictor of contralateral hand motor outcome is the main reason why this thesis focused on studying the ipsilateral hand instead (Study II), which has been given less attention in the literature. In this study, we found that ipsilateral hand impairment was associated with white matter disruption to a combination of different tracts (CST, SLF, ACR, and CC) depending on the motor task that is measured. Recently, similar result has been reported regarding the somatosensory outcome: contralateral touch function was correlated with the structural connectivity along the somatosensory fibers, while ipsilateral touch function correlated with connectivity in the SLF and CC. (Koh et al., 2021)

Several key points can be learned from this thesis, together with other structural brain imaging studies on hand motor outcomes following stroke. First, very strong evidence for CST integrity as a main and crucial factor explaining hand motor impairment and

Discussion and Conclusion

recovery is available. Second, other structural connectivities, those involving corticocortical intrahemispheric, interhemispheric, or corticofugal tracts, may explain the residual variance not accounted for by the CST alone. Along these lines, our results suggest that damage in a more dispersed brain network is involved in accounting for impairments of the hand ipsilateral to the lesion, in the sense that these additional tracts may serve as "collateral" pathways when the main pathway is injured. This typical biological system with one main actor followed by contributions from others with some degree of redundancy is advantageous in a case of injury. Unless the damage involved the whole related structure, some room for recovery would be available provided by the remaining structure to maintain function, at the least for functional purposes. With regard to the hand motor systems, some residual degree of hand movement, both for the contralateral and ipsilateral side, is important in performing daily life activities and in determining individual independence. This view, supported by findings in our work and others, is in favor of the old "redundancy and degeneracy" theory in biological networks. (Edelman and Gally, 2001; Tononi et al., 1999)

4.3.4 Functional MRI

The effects of stroke are known to not only damage neural structures locally within the lesion site but also to have remote effects, reflected by brain functional changes. Functional MRI (fMRI) has been used to investigate these changes both when performing a specific task (task-fMRI) and during rest (resting-state fMRI). Using passive wrist flexion and extension task, task-fMRI in healthy volunteers showed brain activity in the canonical motor areas, including the primary sensorimotor areas, dorsal premotor cortex, supplementary motor areas, parietal operculum, putamen, thalamus, and cerebellum. (Hannanu et al., 2017) Motor activity patterns provided by task-fMRI are relevant in the context of predicting hand motor recovery following stroke, as good motor recovery is usually associated with the recruitment of the original functional network. (Carey et al., 2013; Rosso et al., 2013) More specifically, motor-related brain activity follows a specific temporal pattern during stroke recovery: bilateral activity is usually observed within the sensorimotor network during the early period, followed by the restoration of physiological hemisphere activity balance at the chronic stage associated with good functional recovery. Of note, our findings in study I are in agreement with this spatiotemporal pattern. Similarly, changes in resting-state functional connectivity between brain areas following stroke, with decreased interhemispheric FC from the ipsilesional sensorimotor cortex, have been reported early after stroke, with a return to more normal connectivity in the sensorimotor networks during the recovery process.

4.3 Predictive models and neural correlates of hand motor recovery

Overall, the motor outcome of the upper limb has been associated with increased or decreased functional connectivity between the ipsilesional and contralesional motor areas (SM1, SMA, and dPMC). However, the influence of non-motor regions on hand recovery has been sparsely explored.

In this thesis, Study I and III (using task- and resting-state fMRI, respectively) were performed with a specific hypothesis based on the dual visuomotor stream theory: brain functional activity or connectivity is associated with motor recovery, with areas belonging to the visuomotor neural pathway (dorsolateral or dorsomedial) engaged depending on the type of the motor task assessed. In Study I, this hypothesis was confirmed, as distinct spatiotemporal patterns were observed for the two motor tasks. The reach and grasp task (PPT) was associated with activity within both dorsolateral and dorsomedial networks, while the simple grasp task (handgrip) was associated with activity within the dorsolateral network only. Our findings also pointed out that different subregions of M1 (M1a and M1p) are involved in simple versus highly skilled tasks requiring independent finger movements. With regards to the accuracy of the predictive models, a main advantage of task-fMRI is that brain activity is specific to the task of interest (as opposed to the resting-state fMRI where no task is performed), resulting in better predictive models. As reported in our studies, PPT and handgrip models explained 93% and 96% of the variance, respectively (Study I), while the handgrip model in rs-fMRI only explained 82% in the handgrip model (Study III). Similarly, in Study VI, using the random forest method, the task-fMRI model reached an accuracy of 94%, while the RSFC model using global efficiency reached 87.2%. Conversely, being non-task-specific, rs-fMRI offers the advantage of exploring functional connectivity in the whole brain outside the task-related regions. A limitation is that brain areas that are non-targeted by the tasks, such as the visual areas, cannot be explored with fMRI using a motor task. Resting-state fMRI, on the other hand, allowing the exploration of connectivity in the whole brain, including the visuomotor connectivity, *i.e.*, connectivity between occipital and motor areas, was our first choice to test the dual visual system hypothesis.

In Study III, we found that in addition to connectivity within the sensorimotor network, visuomotor connectivity is associated with and predicted hand motor outcome. This finding suggests that handgrip, a pure grasp motor task that does not require visual online control to be performed, also engaged visuomotor connectivity. It is possible that the visual systems influence the preparation and execution phases of motor actions during cognitive processes such as "motor imagery", in which imagined movements are the internal simulation of real movements.(Jeannerod and Decety, 1995) Indeed, it has become increasingly recognized in recent studies that the occipital areas, more specifically the primary visual cortex (V1),

Discussion and Conclusion

are involved in motor-related functions, including planning and executing object-oriented actions.(Gallivan et al., 2019; Monaco et al., 2020) Study III used data from two cohorts, ISIS-HERMES and IRMAS, to perform a validation step. However, the dissociation between the tasks could not be investigated as there were no additional behavioral scores in the IRMAS dataset. When using only the HERMES dataset, the association between PPT (reach and grasp task) with visuomotor connectivity was observed, with a stronger correlation than that of handgrip (results not reported).

Overall, studies using fMRI in this thesis may contribute to a better understanding of visuomotor actions in stroke patients. Hand motor recovery was associated with a set of sensorimotor areas depending on the task modality, and visuomotor connectivity was engaged regardless of whether or not motor action requires visual feedback. Nonetheless, further investigation is needed to confirm this view across different populations.

4.4 Methodological Considerations

4.4.1 Generalizability of the results

Stroke patients included in the three cohorts were relatively younger than the general stroke population (mean age of 56 years) due to the inclusion and exclusion criteria, as older patients tend to have either very severe outcomes or not be eligible for any behavioral or MRI assessments or presented with severe comorbid factors in other systems. Additionally, our stroke population is limited to those with first-ever lesions in the MCA territory presented with no severe leukoaraiosis or atrophy. These facts indicate that our population does not fully represent the typical patient admitted to a stroke unit, and therefore results should be cautiously generalized to the broader stroke population.

4.4.2 Sample size

A small sample size leading to a lack of statistical power is a major problem in neuroimaging field not exclusive to studies in this work. In fact, neuroimaging literature cited in this thesis used an average of 37 stroke patients, with 4 studies using less than 10 participants. This size, considering the number of statistical tests that need to be performed for any imaging analysis, is considered small with a high risk of type-1 error (false positive), overestimation of effect size, and low reproducibility. For this reason, analyses included in this thesis reported statistical analysis with correction for multiple comparisons or internal validation methods whenever necessary to minimize this risk. Additionally, data from another study

(RESSTORE) or even a center (IRMAS) with a similar study design were added at the later stage of this work (Study III-VI) to increase the statistical power while taking into consideration any heterogeneity between the studies.

In Study IV and Study VI, a machine learning approach was used in order to deal with a large number of variables available in a relatively small number of cases, often termed the "p>n" problem. Regression with regularization (either l1 [LASSO] or l2 [Ridge]) method, random forest, and support vector machine are algorithms that are known to best deal with this problem. In addition, only variables of interest, those that are known in the literature to be relevant to hand motor recovery, are included, removing a large number of unrelated variables.

The recommended practice in the machine learning method is to split the dataset into three: training, validation, and test dataset, where training and validation datasets are used iteratively to build the model, and the test dataset should be used just once to evaluate the model. However, due to the small sample size, the dataset in our studies is split into training and test datasets, in which hyperparameter tuning and cross-validation steps were performed using both training and test datasets, and therefore accuracy reported in these studies might be slightly overestimated. With this notion, we would regard the results of the two studies more as preliminary for exploratory purposes, which would require more validation in future research.

4.4.3 Heterogeneity in study designs and confounding factors

Along with the increased statistical power, the use of three different cohorts from different centers also brings some degree of heterogeneity in this work in terms of clinical (stroke population) and methodological (MRI data acquisition) point of view that is further discussed below together with other confounding factors.

Stem-cell treatment

ISIS-HERMES study is a randomized controlled trial (RCT) in which patients were randomized to receive either an IV injection of mesenchymal stem cells (MSCs) or rehabilitation alone. On the other hand, none of the participants in the IRMAS or RESSTORE studies received stem-cell treatment. The stem cell injection was administered one day after the one-month assessment (M0), and therefore the effect of stem cell was always introduced as a covariate when performing correlations or regression to scores at M6 (but not to scores

Discussion and Conclusion

at M0), regardless of whether it has a significant effect or not. Interestingly, the stem-cell treatment has no effect on all statistical tests performed.

MRI data acquisition

Task-fMRI

The task paradigm for the task-fMRI analysis is different according to the center: Grenoble center (ISIS-HERMES and RESSTORE) used a passive wrist flexion-extension task, while Paris center (IRMAS) used an active wrist flexion-extension task. Task-related brain activity during the active and passive motor tasks was reported to show no difference in terms of topography, (Guzzetta et al., 2007; Jaeger et al., 2014; Loubinoux et al., 2001; Zhavoronkova et al., 2017) although some reported higher activity and extent during active than in passive tasks (Jaeger et al., 2014; Zhavoronkova et al., 2017). With this regard, analysis using these data (Study VI) is controlled for the effect of the center.

RS-fMRI

During resting-state fMRI acquisition, patients in Grenoble center were instructed to remain still and relaxed with eyes open while looking at a white "X" sign in the middle of the black background screen, while patients in Paris center were instructed to keep their eyes closed and to avoid falling asleep. Differences in RS-fMRI functional connectivity related to the two eyes state (eyes closed vs. eyes open) have been previously reported (Laumann et al., 2015; McAvoy et al., 2008; Xu et al., 2014), in which eye state has localized effects in visual, somatomotor, and adjacent regions. In study III, correlation matrices and predictive models were built first on the IRMAS dataset and then validated using the ISIS-HERMES dataset. We found that in both datasets, RS functional connectivity within the sensorimotor network and visuomotor connectivity were associated with handgrip scores at M0 and M6. This result suggests that these connectivities are involved in grasp motor action, regardless of whether rs-fMRI was performed during eyes closed or eyes open.

Age and sex

The effect of age and sex was significant on handgrip strength and the Purdue pegboard test, in which male tends to have higher handgrip score, the female tends to have higher PPT score, and the trends may differ by age group (Beller et al., 2019; Strauss et al., 2006). These effects were therefore included in the analysis either as covariates (in partial correlation or regression analysis) or by using z-score values computed from healthy controls or normative data (Strauss et al., 2006) controlled for age and sex.

4.4.4 Brain asymmetry: to flip or not to flip?

One common practice in stroke neuroimaging studies when dealing with small sample size, or when performing whole group analysis, is to flip the images along the x-axis (left-right direction) so that all images can be assumed to have lesions on the same side and that group analysis can be performed without having to split the dataset based on lesion side. In this work, we performed the flipping step in study III and study V. The problem with this practice is that it underestimates the fact that the brain is not perfectly symmetrical, and thus flipping might cause some degree of inaccuracy: a voxel on one side of the brain might not correspond to the same area on the other side after the flip process.

In Study I, during the reviewing process for publication, we processed the data both with (the first submission) and without (the published version) the flipping step. Using this data, we observed that detailed results from both methods were slightly different, but the main results, in this case, brain areas activated by passive task-fMRI and their prediction to hand motor outcome, remained the same. This could be due to the fact that brain asymmetry is not prominent within the sensorimotor areas, those that are relevant in our task-fMRI study. On the other hand, brain asymmetry has been reported for the occipital lobes in terms of cortical thickness, surface area, and local gyrification. As this might affect our result for Study III, which focused on visuomotor connectivity, 10 anatomical occipital regions extracted from the Julich atlas (brain.eu) were grouped into 3 larger ROIs based on visual area subdivision. In Study V, the flip step was necessary in order to reach adequate statistical power for VLSM studies ($n > 90$). (Lorca-Puls et al., 2018) A previous study dividing stroke groups into subgroups based on lesion side with $n = 65$ for each subgroup reported non-significant results on left hemispheric stroke. (Frenkel-Toledo et al., 2019) In this context, we argue that the effect of the lesion side is potentially smaller when compared to the effect of the stroke itself, and therefore unless an adequate number of participants were available for each group, all participants should be analyzed jointly with the flipping step. Of note, no flipping step was performed for studies II, IV, and VI.

4.5 Clinical Implications

Among all studies presented in this thesis, the results from the VLSM study (Study V) would be the closest for clinical use. First, no additional MRI sequence and preprocessing step is needed to implement the results to incoming stroke patients, as routinely used anatomical MRI or even CT scan images would be enough to locate stroke lesions. Second, the use

Discussion and Conclusion

of binarized outcome measure to predict patients' hand motor function at a chronic period have made it easier to interpret and implement the results. Third, the proposed model is in good agreement with a large number of arguments from both basic neuroanatomy and recent neuroimaging literature, supporting its validity. Fourth, as predictions using initial severity, age, and lesion volume currently used in clinical settings are still prone to high error rates, any increase in accuracy would be advantageous. The associations proposed in this study, specifically between lesions at the level of PLIC and hand motor outcomes, are likely to be useful for medical practitioners in informing patients and caregivers about the prognosis of stroke in terms of hand motor recovery.

As this thesis focused on hand motor recovery post-stroke, the main clinical implication of this thesis would be regarding the rehabilitation point of view. In Study III, we found that there was an indication that visuomotor connectivity might be associated with better hand motor outcomes. This fact implies that motor rehabilitation therapy with visual input, such as movements while viewing mirrored movements of the contralateral hand, or viewing intended normal hand movement from a screen/virtual reality system, may be useful in rehabilitation programs to enhance hand motor recovery for patients with a motor deficit. Similarly, our results in Study II and related work (Razak et al., 2022) evidenced the importance of the assessment of the ipsilateral hand both to evaluate hand motor deficit and as an additional predictive factor to consider, especially in severe stroke or when the contralateral hand is completely plegic. In the same line, hand motor rehabilitation integrating the ipsilateral hand would be recommended. It is important to note, though, that this does not mean that focus should be shifted completely toward the ipsilateral hand while ignoring the contralateral hand. The role of brain activity in the contralesional hemisphere (activated during movements of the ipsilateral hand) in hand recovery is still under debate, with beneficial effects according to some studies but deleterious to others. Our results instead argue against the inhibition of the ipsilateral hand during rehabilitation, and in favor of the rehabilitative training for both contralesional and ipsilesional hands, separately and simultaneously with bimanual movements.

Another implication is the use of neuroimaging tools in clinical settings. Results from Study I, II, III, IV, and VI pointed out the values brought by each MRI modality, in which certain MRI sequence or processing steps can be considered to be integrated into the clinical routine as a biomarker for evaluation and prognostic purposes, depending on the specific goal of the assessment. Analyzing SBM metrics such as cortical thickness in both hemispheres from anatomical T1 would provide a better prognostic value than lesion volume and comparable to the initial deficit score. It would be of low cost, as only additional processing

resources would be needed. Passive task-fMRI would bring the most useful information for stroke patients with hand deficits in which the clinical concern is more specific toward hand motor recovery. DWI or rs-fMRI is more suitable for patients in which multiple brain systems (motor, emotion, cognitive) are concerned, providing information about the degree of white matter damage and changes in the brain functional network. An important factor to consider when integrating more MRI sequences into clinical settings is the additional resources required, especially in terms of acquisition time. DWI, in particular, may be of high interest to be implemented routinely considering its short acquisition time, with relatively high and more global predictive values. At the hyperacute phase, reducing acquisition time is crucial, and thus anatomical imaging, allowing several analyses such as stroke location, volume, and SBM, should be sufficient. Later, when wider time windows are available, additional assessments could be performed. However, our work suggests that not all of the sequences or analyses presented in this thesis should be performed on other than an exploratory basis, as information brought by more than two would be very likely to be redundant for clinical purposes. Finally, even though predictive models in these studies showed very high performance/accuracy, some factors explained in the previous section have limited their generalizability to a broader population, and therefore at this level, they are most useful in providing theoretical insights from a neurophysiological point of view, but further external validation studies in larger populations are necessary before they can be reliably used at the individual level in clinical settings.

4.6 Perspectives

First of all, models proposed in this thesis should be further tested in larger and different stroke populations, preferably using a multicentric design and accounting for more factors such as lesion side, handedness, cognitive scores, or other potential features. Another important factor that was not taken into account in this work is that patients from the two centers had varying rehabilitation programs in terms of type, frequency, and duration. Indeed, in the literature, the effects of rehabilitation are rarely documented, reported, or accounted for in the observed recovery.

The later part of this thesis, particularly Study VI, deserves deeper investigation considering its richness in multimodal MRI data availability, which is not performed due to the time constraints of this Ph.D. Consequently, the results and interpretations of Study VI are pragmatic, providing the predictive accuracy of each MRI modality when used separately or in combination. Instead, analysis of the importance of each variable (at the ROI level)

Discussion and Conclusion

in the predictive models across different algorithms, and their correlation to each other, is missing while it can provide insights about the contribution of each specific variable and their interaction in predicting hand motor recovery.

Future research investigating stroke recovery or new therapy such as noninvasive brain stimulation or stem cells could benefit from this thesis in terms of integrating suitable neuroimaging assessments.

4.7 Conclusion

This thesis explored hand motor recovery after stroke using longitudinal and multimodal MRI in an endeavor to determine hand motor outcome prediction models based on clinical and neuroimaging parameters and neural correlates of hand impairment and recovery following stroke. Based on six studies performed with different MRI modalities either separately or simultaneously, it can be concluded that each of the explored modalities brings valuable information to some extent about motor impairment and recovery depending on the specific type of the desired outcome measured, and that combination of two -preferably combining structural and functional features- would be beneficial, but more than that would be unnecessary. This thesis also highlighted associative white and grey matter regions and functional connectivity involved in hand motor impairment and recovery that would be useful both in clinical settings as potential targets to enhance recovery and in research settings when assessing and predicting outcomes during investigation of possible new therapies following stroke.

References

- Amunts, K., Mohlberg, H., Bludau, S., and Zilles, K. (2020). Julich-brain: A 3d probabilistic atlas of the human brain's cytoarchitecture. *Science*, 369(6506):988–992.
- Baier, B., zu Eulenburg, P., Geber, C., Rohde, F., Rolke, R., Maihöfner, C., Birklein, F., and Dieterich, M. (2014). Insula and sensory insular cortex and somatosensory control in patients with insular stroke. *Eur J Pain*, 18(10):1385–1393.
- Baldo, J. V. and Dronkers, N. F. (2007). Neural correlates of arithmetic and language comprehension: a common substrate? *Neuropsychologia*, 45(2):229–235.
- Bannister, L. C., Crewther, S. G., Gavrilescu, M., and Carey, L. M. (2015). Improvement in Touch Sensation after Stroke is Associated with Resting Functional Connectivity Changes. *Front Neurol*, 6:165.
- Basser, P. J., Mattiello, J., and LeBihan, D. (1994). MR diffusion tensor spectroscopy and imaging. *Biophys J*, 66(1):259–267.
- Bates, E., Wilson, S. M., Saygin, A. P., Dick, F., Sereno, M. I., Knight, R. T., and Dronkers, N. F. (2003). Voxel-based lesion-symptom mapping. *Nat Neurosci*, 6(5):448–450.
- Beckmann, C. F., DeLuca, M., Devlin, J. T., and Smith, S. M. (2005). Investigations into resting-state connectivity using independent component analysis. *Philos Trans R Soc Lond B Biol Sci*, 360(1457):1001–1013.
- Beebe, J. A. and Lang, C. E. (2009). Active range of motion predicts upper extremity function 3 months after stroke. *Stroke*, 40(5):1772–1779. [PubMed Central:PMC2718540] [DOI:10.1161/STROKEAHA.108.536763] [PubMed:2300994].
- Behrens, T. E., Berg, H. J., Jbabdi, S., Rushworth, M. F., and Woolrich, M. W. (2007). Probabilistic diffusion tractography with multiple fibre orientations: What can we gain? *Neuroimage*, 34(1):144–155.
- Beller, J., Miething, A., Regidor, E., Lostao, L., Epping, J., and Geyer, S. (2019). Trends in grip strength: Age, period, and cohort effects on grip strength in older adults from Germany, Sweden, and Spain. *SSM Popul Health*, 9:100456. [PubMed Central:PMC6700453] [DOI:10.1016/j.ssmph.2019.100456] [PubMed:9421240].
- Benjamin, E. J., Virani, S. S., Callaway, C. W., Chamberlain, A. M., Chang, A. R., Cheng, S., Chiuve, S. E., Cushman, M., Dellinger, F. N., Deo, R., de Ferranti, S. D., Ferguson, J. F., Fornage, M., Gillespie, C., Isasi, C. R., Jiménez, M. C., Jordan, L. C., Judd, S. E., Lackland, D., Lichtman, J. H., Lisabeth, L., Liu, S., Longenecker, C. T., Lutsey, P. L.,

References

- Mackey, J. S., Matchar, D. B., Matsushita, K., Mussolino, M. E., Nasir, K., O'Flaherty, M., Palaniappan, L. P., Pandey, A., Pandey, D. K., Reeves, M. J., Ritchey, M. D., Rodriguez, C. J., Roth, G. A., Rosamond, W. D., Sampson, U. K. A., Satou, G. M., Shah, S. H., Spartano, N. L., Tirschwell, D. L., Tsao, C. W., Voeks, J. H., Willey, J. Z., Wilkins, J. T., Wu, J. H., Alger, H. M., Wong, S. S., and Muntner, P. (2018). Heart Disease and Stroke Statistics-2018 Update: A Report From the American Heart Association. *Circulation*, 137(12):e67–e492. [DOI:10.1161/CIR.0000000000000558] [PubMed:29386200].
- Bernhardt, J., Hayward, K. S., Kwakkel, G., Ward, N. S., Wolf, S. L., Borschmann, K., Krakauer, J. W., Boyd, L. A., Carmichael, S. T., Corbett, D., and Cramer, S. C. (2017). Agreed definitions and a shared vision for new standards in stroke recovery research: The Stroke Recovery and Rehabilitation Roundtable taskforce. *Int J Stroke*, 12(5):444–450.
- BERTRAND, G., BLUNDELL, J., and MUSELLA, R. (1965). ELECTRICAL EXPLORATION OF THE INTERNAL CAPSULE AND NEIGHBOURING STRUCTURES DURING STEREOTAXIC PROCEDURES. *J Neurosurg*, 22:333–343. [DOI:10.3171/jns.1965.22.4.0333] [PubMed:14318109].
- Bhagat, Y. A., Emery, D. J., Shuaib, A., Sher, F., Rizvi, N. H., Akhtar, N., Clare, T. L., Leatherdale, T., and Beaulieu, C. (2006). The relationship between diffusion anisotropy and time of onset after stroke. *J Cereb Blood Flow Metab*, 26(11):1442–1450.
- Binkofski, F., Fink, G. R., Geyer, S., Buccino, G., Gruber, O., Shah, N. J., Taylor, J. G., Seitz, R. J., Zilles, K., and Freund, H. J. (2002). Neural activity in human primary motor cortex areas 4a and 4p is modulated differentially by attention to action. *J Neurophysiol*, 88(1):514–519.
- Biswal, B., Yetkin, F. Z., Haughton, V. M., and Hyde, J. S. (1995). Functional connectivity in the motor cortex of resting human brain using echo-planar MRI. *Magn Reson Med*, 34(4):537–541.
- Blatow, M., Reinhardt, J., Riffel, K., Nennig, E., Wengenroth, M., and Stippich, C. (2011). Clinical functional MRI of sensorimotor cortex using passive motor and sensory stimulation at 3 Tesla. *J Magn Reson Imaging*, 34(2):429–437.
- Borovsky, A., Saygin, A. P., Bates, E., and Dronkers, N. (2007). Lesion correlates of conversational speech production deficits. *Neuropsychologia*, 45(11):2525–2533.
- Borra, E., Gerbella, M., Rozzi, S., and Luppino, G. (2017). The macaque lateral grasping network: A neural substrate for generating purposeful hand actions. *Neurosci Biobehav Rev*, 75:65–90.
- Boscolo Galazzo, I., Storti, S. F., Formaggio, E., Pizzini, F. B., Fiaschi, A., Beltramello, A., Bertoldo, A., and Manganotti, P. (2014). Investigation of brain hemodynamic changes induced by active and passive movements: a combined arterial spin labeling-BOLD fMRI study. *J Magn Reson Imaging*, 40(4):937–948.
- Brihmat, N., Tarri, M., Gasq, D., Marque, P., Castel-Lacanal, E., and Loubinoux, I. (2020). Cross-Modal Functional Connectivity of the Premotor Cortex Reflects Residual Motor Output After Stroke. *Brain Connect*, 10(5):236–249. [DOI:10.1089/brain.2020.0750] [PubMed:32414294].

- Brodal, A. (1973). Self-observations and neuro-anatomical considerations after a stroke. *Brain*, 96(4):675–694.
- Brodtmann, A., Pardoe, H., Li, Q., Lichter, R., Ostergaard, L., and Cumming, T. (2012). Changes in regional brain volume three months after stroke. *J Neurol Sci*, 322(1-2):122–128. [DOI:10.1016/j.jns.2012.07.019] [PubMed:22858417].
- Brott, T., Adams, H. P., Olinger, C. P., Marler, J. R., Barsan, W. G., Biller, J., Spilker, J., Holleran, R., Eberle, R., and Hertzberg, V. (1989). Measurements of acute cerebral infarction: a clinical examination scale. *Stroke*, 20(7):864–870. [DOI:10.1161/01.str.20.7.864] [PubMed:2749846].
- Buch, E. R., Rizk, S., Nicolo, P., Cohen, L. G., Schnider, A., and Guggisberg, A. G. (2016). Predicting motor improvement after stroke with clinical assessment and diffusion tensor imaging. *Neurology*, 86(20):1924–1925.
- Bueteifisch, C. M., Reville, K. P., Haut, M. W., Kowalski, G. M., Wischnewski, M., Pifer, M., Belagaje, S. R., Nahab, F., Cobia, D. J., Hu, X., Drake, D., and Hobbs, G. (2018). Abnormally reduced primary motor cortex output is related to impaired hand function in chronic stroke. *J Neurophysiol*, 120(4):1680–1694. [PubMed Central:PMC6230804] [DOI:10.1152/jn.00715.2017] [PubMed:9166922].
- Buma, F. E., Lindeman, E., Ramsey, N. F., and Kwakkel, G. (2010). Functional neuroimaging studies of early upper limb recovery after stroke: a systematic review of the literature. *Neurorehabil Neural Repair*, 24(7):589–608.
- Bustrén, E. L., Sunnerhagen, K. S., and Alt Murphy, M. (2017). Movement Kinematics of the Ipsilesional Upper Extremity in Persons With Moderate or Mild Stroke. *Neurorehabil Neural Repair*, 31(4):376–386.
- Byblow, W. D., Stinear, C. M., Barber, P. A., Petoe, M. A., and Ackerley, S. J. (2015). Proportional recovery after stroke depends on corticomotor integrity. *Ann Neurol*, 78(6):848–859. [DOI:10.1002/ana.24472] [PubMed:26150318].
- Canedo, A. (1997). Primary motor cortex influences on the descending and ascending systems. *Progress in Neurobiology*, 51(3):287–335.
- Carel, C., Loubinoux, I., Boulanouar, K., Manelfe, C., Rascol, O., Celsis, P., and Chollet, F. (2000). Neural substrate for the effects of passive training on sensorimotor cortical representation: a study with functional magnetic resonance imaging in healthy subjects. *J Cereb Blood Flow Metab*, 20(3):478–484.
- Carey, L. M., Abbott, D. F., Egan, G. F., Bernhardt, J., and Donnan, G. A. (2005). Motor impairment and recovery in the upper limb after stroke: behavioral and neuroanatomical correlates. *Stroke*, 36(3):625–629. [DOI:10.1161/01.STR.0000155720.47711.83] [PubMed:15677574].
- Carey, L. M., Abbott, D. F., Egan, G. F., O’Keefe, G. J., Jackson, G. D., Bernhardt, J., and Donnan, G. A. (2006). Evolution of brain activation with good and poor motor recovery after stroke. *Neurorehabil Neural Repair*, 20(1):24–41.

References

- Carey, L. M., Seitz, R. J., Parsons, M., Levi, C., Farquharson, S., Tournier, J.-D., Palmer, S., and Connelly, A. (2013). Beyond the lesion: neuroimaging foundations for post-stroke recovery. *Future Neurology*, 8(5):507–527.
- Carrera, E. and Tononi, G. (2014). Diaschisis: past, present, future. *Brain*, 137(Pt 9):2408–2422.
- Carter, A. R., Astafiev, S. V., Lang, C. E., Connor, L. T., Rengachary, J., Strube, M. J., Pope, D. L., Shulman, G. L., and Corbetta, M. (2010). Resting interhemispheric functional magnetic resonance imaging connectivity predicts performance after stroke. *Ann Neurol*, 67(3):365–375.
- Carter, A. R., Patel, K. R., Astafiev, S. V., Snyder, A. Z., Rengachary, J., Strube, M. J., Pope, A., Shimony, J. S., Lang, C. E., Shulman, G. L., and Corbetta, M. (2012). Upstream dysfunction of somatomotor functional connectivity after corticospinal damage in stroke. *Neurorehabil Neural Repair*, 26(1):7–19. [PubMed Central:PMC3822763] [DOI:10.1177/1545968311411054] [PubMed:16400157].
- Cavina-Pratesi, C., Connolly, J. D., Monaco, S., Figley, T. D., Milner, A. D., Schenk, T., and Culham, J. C. (2018). Human neuroimaging reveals the subcomponents of grasping, reaching and pointing actions. *Cortex*, 98:128–148.
- Cavina-Pratesi, C., Monaco, S., Fattori, P., Galletti, C., McAdam, T. D., Quinlan, D. J., Goodale, M. A., and Culham, J. C. (2010). Functional magnetic resonance imaging reveals the neural substrates of arm transport and grip formation in reach-to-grasp actions in humans. *J Neurosci*, 30(31):10306–10323.
- Chen, H., Shi, M., Geng, W., Jiang, L., Yin, X., and Chen, Y. C. (2021). A preliminary study of cortical morphology changes in acute brainstem ischemic stroke patients. *Medicine (Baltimore)*, 100(1):e24262. [PubMed Central:PMC7793415] [DOI:10.1097/MD.00000000000024262] [PubMed:33429834].
- Chen, J. L. and Schlaug, G. (2013). Resting state interhemispheric motor connectivity and white matter integrity correlate with motor impairment in chronic stroke. *Front Neurol*, 4:178. [PubMed Central:PMC3819700] [DOI:10.3389/fneur.2013.00178] [PubMed:16888796].
- Cheng, B., Dietzmann, P., Schulz, R., Boenstrup, M., Krawinkel, L., Fiehler, J., Gerloff, C., and Thomalla, G. (2020). Cortical atrophy and transcallosal diaschisis following isolated subcortical stroke. *J Cereb Blood Flow Metab*, 40(3):611–621.
- Cheng, B., Forkert, N. D., Zavaglia, M., Hilgetag, C. C., Golsari, A., Siemonsen, S., Fiehler, J., Pedraza, S., Puig, J., Cho, T. H., Alawneh, J., Baron, J. C., Ostergaard, L., Gerloff, C., and Thomalla, G. (2014). Influence of stroke infarct location on functional outcome measured by the modified rankin scale. *Stroke*, 45(6):1695–1702.
- Cheng, B., Schulz, R., Bönstrup, M., Hummel, F. C., Sedlacik, J., Fiehler, J., Gerloff, C., and Thomalla, G. (2015). Structural plasticity of remote cortical brain regions is determined by connectivity to the primary lesion in subcortical stroke. *J Cereb Blood Flow Metab*, 35(9):1507–1514. [PubMed Central:PMC4640340] [DOI:10.1038/jcbfm.2015.74] [PubMed:22858417].

- Chestnut, C. and Haaland, K. Y. (2008). Functional significance of ipsilesional motor deficits after unilateral stroke. *Arch Phys Med Rehabil*, 89(1):62–68.
- Chi, N. F., Ku, H. L., Chen, D. Y., Tseng, Y. C., Chen, C. J., Lin, Y. C., Hsieh, Y. C., Chan, L., Chiou, H. Y., Hsu, C. Y., and Hu, C. J. (2018). Cerebral Motor Functional Connectivity at the Acute Stage: An Outcome Predictor of Ischemic Stroke. *Sci Rep*, 8(1):16803. [PubMed Central:PMC6235876] [DOI:10.1038/s41598-018-35192-y] [PubMed:22019881].
- Colebatch, J. G. and Gandevia, S. C. (1989). The distribution of muscular weakness in upper motor neuron lesions affecting the arm. *Brain*, 112 (Pt 3):749–763.
- Collins, K. C., Kennedy, N. C., Clark, A., and Pomeroy, V. M. (2018). Getting a kinematic handle on reach-to-grasp: a meta-analysis. *Physiotherapy*, 104(2):153–166.
- Cordes, D., Haughton, V. M., Arfanakis, K., Wendt, G. J., Turski, P. A., Moritz, C. H., Quigley, M. A., and Meyerand, M. E. (2000). Mapping functionally related regions of brain with functional connectivity MR imaging. *AJNR Am J Neuroradiol*, 21(9):1636–1644.
- Cramer, S. C., Shah, R., Juranek, J., Crafton, K. R., and Le, V. (2006). Activity in the peri-infarct rim in relation to recovery from stroke. *Stroke*, 37(1):111–115.
- Culham, J. C., Cavina-Pratesi, C., and Singhal, A. (2006). The role of parietal cortex in visuomotor control: what have we learned from neuroimaging? *Neuropsychologia*, 44(13):2668–2684.
- Cunha, B. P., de Freitas, S. M. S. F., and de Freitas, P. B. (2017). Assessment of the Ipsilesional Hand Function in Stroke Survivors: The Effect of Lesion Side. *J Stroke Cerebrovasc Dis*, 26(7):1615–1621.
- Damoiseaux, J. S., Rombouts, S. A., Barkhof, F., Scheltens, P., Stam, C. J., Smith, S. M., and Beckmann, C. F. (2006). Consistent resting-state networks across healthy subjects. *Proc Natl Acad Sci U S A*, 103(37):13848–13853.
- Davare, M., Andres, M., Cosnard, G., Thonnard, J. L., and Olivier, E. (2006). Dissociating the role of ventral and dorsal premotor cortex in precision grasping. *J Neurosci*, 26(8):2260–2268.
- Dawnay, N. A. and Glees, P. (1986). Somatotopic analysis of fibre and terminal distribution in the primate corticospinal pathway. *Brain Res*, 391(1):115–123. [DOI:10.1016/0165-3806(86)90013-1] [PubMed:3955378].
- de C Hamilton, A. F. (2015). The neurocognitive mechanisms of imitation. *Current Opinion in Behavioral Sciences*, 3:63–67. Social behavior.
- de Groot-Driessen, D., van de Sande, P., and van Heugten, C. (2006). Speed of finger tapping as a predictor of functional outcome after unilateral stroke. *Arch Phys Med Rehabil*, 87(1):40–44.
- Debaere, F., Van Assche, D., Kiekens, C., Verschueren, S. M., and Swinnen, S. P. (2001). Coordination of upper and lower limb segments: deficits on the ipsilesional side after unilateral stroke. *Exp Brain Res*, 141(4):519–529.

References

- Dell'Acqua, F., Simmons, A., Williams, S. C., and Catani, M. (2013). Can spherical deconvolution provide more information than fiber orientations? Hindrance modulated orientational anisotropy, a true-tract specific index to characterize white matter diffusion. *Hum Brain Mapp*, 34(10):2464–2483.
- Dell'Acqua, F. and Tournier, J. D. (2019). Modelling white matter with spherical deconvolution: How and why? *NMR Biomed*, 32(4):e3945.
- Descoteaux, M., Deriche, R., Knösche, T. R., and Anwander, A. (2009). Deterministic and probabilistic tractography based on complex fibre orientation distributions. *IEEE Trans Med Imaging*, 28(2):269–286.
- Desrosiers, J., Bourbonnais, D., Bravo, G., Roy, P. M., and Guay, M. (1996). Performance of the 'unaffected' upper extremity of elderly stroke patients. *Stroke*, 27(9):1564–1570.
- Detante, O., Jaillard, A., Moisan, A., Barbieux, M., Favre, I. M., Garambois, K., Hommel, M., and Remy, C. (2014). Biotherapies in stroke. *Rev Neurol (Paris)*, 170(12):779–798. [DOI:10.1016/j.neurol.2014.10.005] [PubMed:25459115].
- Di Pino, G., Pellegrino, G., Assenza, G., Capone, F., Ferreri, F., Formica, D., Ranieri, F., Tombini, M., Ziemann, U., Rothwell, J. C., and Di Lazzaro, V. (2014). Modulation of brain plasticity in stroke: a novel model for neurorehabilitation. *Nat Rev Neurol*, 10(10):597–608.
- Dotson, V. M., Szymkowicz, S. M., Sozda, C. N., Kirton, J. W., Green, M. L., O'Shea, A., McLaren, M. E., Anton, S. D., Manini, T. M., and Woods, A. J. (2015). Age Differences in Prefrontal Surface Area and Thickness in Middle Aged to Older Adults. *Front Aging Neurosci*, 7:250.
- Doughty, C., Wang, J., Feng, W., Hackney, D., Pani, E., and Schlaug, G. (2016). Detection and Predictive Value of Fractional Anisotropy Changes of the Corticospinal Tract in the Acute Phase of a Stroke. *Stroke*, 47(6):1520–1526.
- Doyon, J., Penhune, V., and Ungerleider, L. G. (2003). Distinct contribution of the cortico-striatal and cortico-cerebellar systems to motor skill learning. *Neuropsychologia*, 41(3):252–262.
- Duerden, E. G., Finnis, K. W., Peters, T. M., and Sadikot, A. F. (2011). Three-dimensional somatotopic organization and probabilistic mapping of motor responses from the human internal capsule. *J Neurosurg*, 114(6):1706–1714. [DOI:10.3171/2011.1.JNS10136] [PubMed:21375376].
- Duering, M., Righart, R., Wollenweber, F. A., Zietemann, V., Gesierich, B., and Dichgans, M. (2015). Acute infarcts cause focal thinning in remote cortex via degeneration of connecting fiber tracts. *Neurology*, 84(16):1685–1692. [PubMed Central:PMC4409580] [DOI:10.1212/WNL.0000000000001502] [PubMed:22858417].
- Dum, R. P. and Strick, P. L. (1991). The origin of corticospinal projections from the premotor areas in the frontal lobe. *J Neurosci*, 11(3):667–689. [PubMed Central:PMC6575356] [PubMed:1705965].

- Dum, R. P. and Strick, P. L. (2002). Motor areas in the frontal lobe of the primate. *Physiol Behav*, 77(4-5):677–682. [DOI:10.1016/s0031-9384(02)00929-0] [PubMed:12527018].
- Edelman, G. M. and Gally, J. A. (2001). Degeneracy and complexity in biological systems. *Proc Natl Acad Sci U S A*, 98(24):13763–13768. [PubMed Central:PMC61115] [DOI:10.1073/pnas.231499798] [PubMed:7768323].
- Eickhoff, S. B., Paus, T., Caspers, S., Grosbras, M. H., Evans, A. C., Zilles, K., and Amunts, K. (2007). Assignment of functional activations to probabilistic cytoarchitectonic areas revisited. *Neuroimage*, 36(3):511–521. [DOI:10.1016/j.neuroimage.2007.03.060] [PubMed:17499520].
- Favre, I., Zeffiro, T. A., Detante, O., Krainik, A., Hommel, M., and Jaillard, A. (2014). Upper limb recovery after stroke is associated with ipsilesional primary motor cortical activity: a meta-analysis. *Stroke*, 45(4):1077–1083.
- Feigin, V. L., Lawes, C. M., Bennett, D. A., and Anderson, C. S. (2003). Stroke epidemiology: a review of population-based studies of incidence, prevalence, and case-fatality in the late 20th century. *Lancet Neurol*, 2(1):43–53.
- Feigin, V. L., Stark, B. A., Johnson, C. O., Roth, G. A., Bisignano, C., Abady, G. G., Abbasifard, M., Abbasi-Kangevari, M., Abd-Allah, F., Abedi, V., Abualhasan, A., Abu-Rmeileh, N. M., Abushouk, A. I., Adebayo, O. M., Agarwal, G., Agasthi, P., Ahinkorah, B. O., Ahmad, S., Ahmadi, S., Ahmed Salih, Y., Aji, B., Akbarpour, S., Akinyemi, R. O., Al Hamad, H., Alahdab, F., Alif, S. M., Alipour, V., Aljunid, S. M., Almoustanyir, S., Al-Raddadi, R. M., Al-Shahi Salman, R., Alvis-Guzman, N., Ancuceanu, R., Anderlini, D., Anderson, J. A., Ansar, A., Antonazzo, I. C., Arabloo, J., Ärnlov, J., Artanti, K. D., Aryan, Z., Asgari, S., Ashraf, T., Athar, M., Atreya, A., Ausloos, M., Baig, A. A., Baltatu, O. C., Banach, M., Barboza, M. A., Barker-Collo, S. L., Bärnighausen, T. W., Barone, M. T. U., Basu, S., Bazmandegan, G., Beghi, E., Beheshti, M., Béjot, Y., Bell, A. W., Bennett, D. A., Bensenor, I. M., Bezabhe, W. M., Bezabih, Y. M., Bhagavathula, A. S., Bhardwaj, P., Bhattacharyya, K., Bijani, A., Bikbov, B., Birhanu, M. M., Bloor, A., Bonny, A., Brauer, M., Brenner, H., Bryazka, D., Butt, Z. A., Caetano Dos Santos, F. L., Campos-Nonato, I. R., Cantu-Brito, C., Carrero, J. J., Castañeda-Orjuela, C. A., Catapano, A. L., Chakraborty, P. A., Charan, J., Choudhari, S. G., Chowdhury, E. K., Chu, D. T., Chung, S. C., Colozza, D., Costa, V. M., Costanzo, S., Criqui, M. H., Dadras, O., Dagnew, B., Dai, X., Dalal, K., Damasceno, A. A. M., D'Amico, E., Dandona, L., Dandona, R., Darega Gela, J., Davletov, K., De la Cruz-Góngora, V., Desai, R., Dhamnetiya, D., Dharmaratne, S. D., Dhimal, M. L., Dhimal, M., Diaz, D., Dichgans, M., Dokova, K., Doshi, R., Douiri, A., Duncan, B. B., Eftekharzadeh, S., Ekholuenetale, M., El Nahas, N., Elgendy, I. Y., Elhadi, M., El-Jaafary, S. I., Endres, M., Endries, A. Y., Erku, D. A., Faraon, E. J. A., Farooque, U., Farzadfar, F., Feroze, A. H., Filip, I., Fischer, F., Flood, D., Gad, M. M., Gaidhane, S., Ghanei Gheshlagh, R., Ghashghaee, A., Ghith, N., Ghazali, G., Ghazy, S., Gialluisi, A., Giampaoli, S., Gilani, S. A., Gill, P. S., Gnedovskaya, E. V., Golechha, M., Goulart, A. C., Guo, Y., Gupta, R., Gupta, V. B., Gupta, V. K., Gyanwali, P., Hafezi-Nejad, N., Hamidi, S., Hanif, A., Hankey, G. J., Hargono, A., Hashi, A., Hassan, T. S., Hassen, H. Y., Havmoeller, R. J., Hay, S. I., Hayat, K., Hegazy, M. I., Herteliu, C., Holla, R., Hostiuc, S., Househ, M., Huang, J., Humayun, A., Hwang, B. F., Iacoviello, L., Iavicoli, I., Ibitoye, S. E., Ilesanmi, O. S., Ilic, I. M., Ilic, M. D., Iqbal, U., Irvani, S. S. N., Islam, S. M. S., Ismail, N. E., Iso, H., Isola, G., Iwagami, M., Jacob, L., Jain, V., Jang, S. I., Jayapal, S. K., Jayaram, S.,

References

- Jayawardena, R., Jeemon, P., Jha, R. P., Johnson, W. D., Jonas, J. B., Joseph, N., Jozwiak, J. J., Jürisson, M., Kalani, R., Kalhor, R., Kalkonde, Y., Kamath, A., Kamiab, Z., Kanchan, T., Kandel, H., Karch, A., Katoto, P. D., Kayode, G. A., Keshavarz, P., Khader, Y. S., Khan, E. A., Khan, I. A., Khan, M., Khan, M. A., Khatib, M. N., Khubchandani, J., Kim, G. R., Kim, M. S., Kim, Y. J., Kisa, A., Kisa, S., Kivimäki, M., Kolte, D., Koolivand, A., Koulmane Laxminarayana, S. L., Koyanagi, A., Krishan, K., Krishnamoorthy, V., Krishnamurthi, R. V., Kumar, G. A., Kusuma, D., La Vecchia, C., Lacey, B., Lak, H. M., Lallukka, T., Lasrado, S., Lavados, P. M., Leonardi, M., Li, B., Li, S., Lin, H., Lin, R. T., Liu, X., Lo, W. D., Lorkowski, S., Lucchetti, G., Lutzky Saute, R., Magdy Abd El Razek, H., Magnani, F. G., Mahajan, P. B., Majeed, A., Makki, A., Malekzadeh, R., Malik, A. A., Manafi, N., Mansournia, M. A., Mantovani, L. G., Martini, S., Mazzaglia, G., Mehndiratta, M. M., Menezes, R. G., Meretoja, A., Mersha, A. G., Miao Jonasson, J., Miazgowski, B., Miazgowski, T., Michalek, I. M., Mirrakhimov, E. M., Mohammad, Y., Mohammadian-Hafshejani, A., Mohammed, S., Mokdad, A. H., Mokhayeri, Y., Molokhia, M., Moni, M. A., Montasir, A. A., Moradzadeh, R., Morawska, L., Morze, J., Muruet, W., Musa, K. I., Nagarajan, A. J., Naghavi, M., Narasimha Swamy, S., Nascimento, B. R., Negoi, R. I., Neupane Kandel, S., Nguyen, T. H., Norrving, B., Noubiap, J. J., Nwatah, V. E., Oancea, B., Odukoya, O. O., Olagunju, A. T., Orru, H., Owolabi, M. O., Padubidri, J. R., Pana, A., Parekh, T., Park, E. C., Pashazadeh Kan, F., Pathak, M., Peres, M. F. P., Perianayagam, A., Pham, T. M., Piradov, M. A., Podder, V., Polinder, S., Postma, M. J., Pourshams, A., Radfar, A., Rafiei, A., Raggi, A., Rahim, F., Rahimi-Movaghar, V., Rahman, M., Rahman, M. A., Rahmani, A. M., Rajai, N., Ranasinghe, P., Rao, C. R., Rao, S. J., Rath, P., Rawaf, D. L., Rawaf, S., Reitsma, M. B., Renjith, V., Renzaho, A. M. N., Rezapour, A., Rodriguez, J. A. B., Roeber, L., Romoli, M., Rynkiewicz, A., Sacco, S., Sadeghi, M., Saeedi Moghaddam, S., Sahebkar, A., Saif-Ur-Rahman, K. M., Salah, R., Samaei, M., Samy, A. M., Santos, I. S., Santric-Milicevic, M. M., Sarrafzadegan, N., Sathian, B., Sattin, D., Schiavolin, S., Schlaich, M. P., Schmidt, M. I., Schutte, A. E., Sepanlou, S. G., Seylani, A., Sha, F., Shahabi, S., Shaikh, M. A., Shannawaz, M., Shawon, M. S. R., Sheikh, A., Sheikhbahaei, S., Shibuya, K., Siabani, S., Silva, D. A. S., Singh, J. A., Singh, J. K., Skryabin, V. Y., Skryabina, A. A., Sobaih, B. H., Stortecky, S., Stranges, S., Tadesse, E. G., Tarigan, I. U., Temsah, M. H., Teuschl, Y., Thrift, A. G., Tonelli, M., Tovani-Palone, M. R., Tran, B. X., Tripathi, M., Tsegaye, G. W., Ullah, A., Unim, B., Unnikrishnan, B., Vakilian, A., Valadan Tahbaz, S., Vasankari, T. J., Venketasubramanian, N., Vervoort, D., Vo, B., Volovici, V., Vosoughi, K., Vu, G. T., Vu, L. G., Wafa, H. A., Waheed, Y., Wang, Y., Wijeratne, T., Winkler, A. S., Wolfe, C. D. A., Woodward, M., Wu, J. H., Wulf Hanson, S., Xu, X., Yadav, L., Yadollahpour, A., Yahyazadeh Jabbari, S. H., Yamagishi, K., Yatsuya, H., Yonemoto, N., Yu, C., Yunusa, I., Zaman, M. S., Zaman, S. B., Zamanian, M., Zand, R., Zandifar, A., Zastrozhin, M. S., Zastrozhina, A., Zhang, Y., Zhang, Z. J., Zhong, C., Zuniga, Y. M. H., and Murray, C. J. L. (2021). Global, regional, and national burden of stroke and its risk factors, 1990-2019: a systematic analysis for the Global Burden of Disease Study 2019. *Lancet Neurol*, 20(10):795–820.
- Feng, W., Wang, J., Chhatbar, P. Y., Doughty, C., Landsittel, D., Lioutas, V. A., Kautz, S. A., and Schlaug, G. (2015). Corticospinal tract lesion load: An imaging biomarker for stroke motor outcomes. *Ann Neurol*, 78(6):860–870.
- Ferri, S., Peeters, R., Nelissen, K., Vanduffel, W., Rizzolatti, G., and Orban, G. A. (2015). A human homologue of monkey F5c. *Neuroimage*, 111:251–266.

- Feys, H., Hetejbrij, J., Wilms, G., Dom, R., and De Weerd, W. (2000). Predicting arm recovery following stroke: value of site of lesion. *Acta Neurol Scand*, 102(6):371–377. [DOI:10.1034/j.1600-0404.2000.102006371.x] [PubMed:11125752].
- Fischl, B. and Dale, A. M. (2000). Measuring the thickness of the human cerebral cortex from magnetic resonance images. *Proc Natl Acad Sci U S A*, 97(20):11050–11055. [PubMed Central:PMC27146] [DOI:10.1073/pnas.200033797] [PubMed:7583616].
- Fjell, A. M., Westlye, L. T., Amlien, I., Espeseth, T., Reinvang, I., Raz, N., Agartz, I., Salat, D. H., Greve, D. N., Fischl, B., Dale, A. M., and Walhovd, K. B. (2009). High consistency of regional cortical thinning in aging across multiple samples. *Cereb Cortex*, 19(9):2001–2012.
- Fornito, A. and Bullmore, E. T. (2015). Connectomics: a new paradigm for understanding brain disease. *Eur Neuropsychopharmacol*, 25(5):733–748.
- Fox, M. D., Snyder, A. Z., Vincent, J. L., Corbetta, M., Van Essen, D. C., and Raichle, M. E. (2005). The human brain is intrinsically organized into dynamic, anticorrelated functional networks. *Proc Natl Acad Sci U S A*, 102(27):9673–9678.
- Franceschini, M., La Porta, F., Agosti, M., Massucci, M., Franceschini, M., Branchini, W., Brianti, R., De Camillis, E., Ferrari, L., Galvagni, R., Lenti, G., Manca, M., Mayer, R., Molteni, F., Perdon, L., Procičchiani, D., Todeschini, E., Zaccala, M., Agosti, M., Citterio, A., Massucci, M., Spizzichino, L., Vallasciani, M., Branchini, W., Recupero, E., Finocchiaro, F., Santagati, A., Greco, S., Longo, P., Comessatti, C., Perdon, L., Taroni, B., Manca, M., Cosentino, E., Mayer, F., Biondi, T., Mugelli, C., Maria Rossi, R., Lombardi, G., Serra, A., Molteni, F., Bretoni, M., Meinecke, C., Fabbri, S., Gonfalonieri, D., Zaccala, M., Ceruti, R., Fortina, C., Galvagni, R., Zaccaria, B., Meneghetti, S., Robuschi, K., Michelotti, V., Cavaldonati, A., Sandrini, G., Arrigo, A., Lenti, G., Antenucci, R., Gandolfi, P., Gatta, G., Procičchiani, D., Boschini, L., Brianti, R., Dardani, M., Massucci, M., Braconi, A. R., De Camillis, E., Bortoluzzi, N., and Timar, J. (2010). Is health-related-quality of life of stroke patients influenced by neurological impairments at one year after stroke? *Eur J Phys Rehabil Med*, 46(3):389–399.
- Fregni, F. and Pascual-Leone, A. (2006). Hand motor recovery after stroke: tuning the orchestra to improve hand motor function. *Cogn Behav Neurol*, 19(1):21–33. [DOI:10.1097/00146965-200603000-00003] [PubMed:16633016].
- Frenkel-Toledo, S., Fridberg, G., Ofir, S., Bartur, G., Lowenthal-Raz, J., Granot, O., Handzelts, S., and Soroker, N. (2019). Lesion location impact on functional recovery of the hemiparetic upper limb. *PLoS One*, 14(7):e0219738. [PubMed Central:PMC6641167] [DOI:10.1371/journal.pone.0219738] [PubMed:29042216].
- Frenkel-Toledo, S., Levin, M. F., Berman, S., Liebermann, D. G., Baniña, M. C., Solomon, J. M., Ofir-Geva, S., and Soroker, N. (2022). Shared and distinct voxel-based lesion-symptom mappings for spasticity and impaired movement in the hemiparetic upper limb. *Sci Rep*, 12(1):10169. [PubMed Central:PMC9206020] [DOI:10.1038/s41598-022-14359-8] [PubMed:23090951].

References

- Frenkel-Toledo, S., Ofir-Geva, S., and Soroker, N. (2020). Lesion Topography Impact on Shoulder Abduction and Finger Extension Following Left and Right Hemispheric Stroke. *Front Hum Neurosci*, 14:282. [PubMed Central:PMC7379861] [DOI:10.3389/fnhum.2020.00282] [PubMed:15064880].
- Fries, W., Danek, A., Scheidtmann, K., and Hamburger, C. (1993). Motor recovery following capsular stroke. Role of descending pathways from multiple motor areas. *Brain*, 116 (Pt 2):369–382.
- Gallivan, J. P., Chapman, C. S., Gale, D. J., Flanagan, J. R., and Culham, J. C. (2019). Selective Modulation of Early Visual Cortical Activity by Movement Intention. *Cereb Cortex*, 29(11):4662–4678. [PubMed Central:PMC6917518] [DOI:10.1093/cercor/bhy345] [PubMed:23558106].
- Gaser, C., Dahnke, R., Thompson, P. M., Kurth, F., Luders, E., and (2022). Cat – a computational anatomy toolbox for the analysis of structural mri data. *bioRxiv*.
- Gemba, H. and Sasaki, K. (1984). Distribution of potentials preceding visually initiated and self-paced hand movements in various cortical areas of the monkey. *Brain Res*, 306(1-2):207–214.
- Geva, S., Baron, J. C., Jones, P. S., Price, C. J., and Warburton, E. A. (2012). A comparison of VLSM and VBM in a cohort of patients with post-stroke aphasia. *Neuroimage Clin*, 1(1):37–47.
- Geyer, S., Ledberg, A., Schleicher, A., Kinomura, S., Schormann, T., Bürgel, U., Klingberg, T., Larsson, J., Zilles, K., and Roland, P. E. (1996). Two different areas within the primary motor cortex of man. *Nature*, 382(6594):805–807.
- Ghaziri, J., Tucholka, A., Girard, G., Houde, J. C., Boucher, O., Gilbert, G., Descoteaux, M., Lippé, S., Rainville, P., and Nguyen, D. K. (2017). The Corticocortical Structural Connectivity of the Human Insula. *Cereb Cortex*, 27(2):1216–1228. [DOI:10.1093/cercor/bhv308] [PubMed:26683170].
- Glasser, M. F., Coalson, T. S., Robinson, E. C., Hacker, C. D., Harwell, J., Yacoub, E., Ugurbil, K., Andersson, J., Beckmann, C. F., Jenkinson, M., Smith, S. M., and Van Essen, D. C. (2016). A multi-modal parcellation of human cerebral cortex. *Nature*, 536(7615):171–178. [PubMed Central:PMC4990127] [DOI:10.1038/nature18933] [PubMed:18641121].
- Godefroy, O., Duhamel, A., Leclerc, X., Saint Michel, T., Hénon, H., and Leys, D. (1998). Brain-behaviour relationships. Some models and related statistical procedures for the study of brain-damaged patients. *Brain*, 121 (Pt 8):1545–1556. [DOI:10.1093/brain/121.8.1545] [PubMed:9712015].
- Goldberg, G. (1985). Supplementary motor area structure and function: Review and hypotheses. *Behavioral and Brain Sciences*, 8(4):567–588.
- Goodale, M. A. and Milner, A. D. (1992). Separate visual pathways for perception and action. *Trends Neurosci*, 15(1):20–25.
- Gowers WR, C. A. (1887). A manual of diseases of the nervous system. *Journal of Mental Science*, 32(140):594–596.

- Grafton, S. T. (2010). The cognitive neuroscience of prehension: recent developments. *Exp Brain Res*, 204(4):475–491. [PubMed Central:PMC2903689] [DOI:10.1007/s00221-010-2315-2] [PubMed:19747280].
- Grefkes, C., Nowak, D. A., Eickhoff, S. B., Dafotakis, M., Küst, J., Karbe, H., and Fink, G. R. (2008). Cortical connectivity after subcortical stroke assessed with functional magnetic resonance imaging. *Ann Neurol*, 63(2):236–246. [DOI:10.1002/ana.21228] [PubMed:17896791].
- Griffa, A., Baumann, P. S., Thiran, J. P., and Hagmann, P. (2013). Structural connectomics in brain diseases. *Neuroimage*, 80:515–526.
- Groisser, B. N., Copen, W. A., Singhal, A. B., Hirai, K. K., and Schaechter, J. D. (2014). Corticospinal tract diffusion abnormalities early after stroke predict motor outcome. *Neurorehabil Neural Repair*, 28(8):751–760.
- Guzzetta, A., Staudt, M., Petacchi, E., Ehlers, J., Erb, M., Wilke, M., Krägeloh-Mann, I., and Cioni, G. (2007). Brain representation of active and passive hand movements in children. *Pediatr Res*, 61(4):485–490. [DOI:10.1203/pdr.0b013e3180332c2e] [PubMed:17515876].
- Hampson, M., Peterson, B. S., Skudlarski, P., Gatenby, J. C., and Gore, J. C. (2002). Detection of functional connectivity using temporal correlations in MR images. *Hum Brain Mapp*, 15(4):247–262.
- Han, X., Jovicich, J., Salat, D., van der Kouwe, A., Quinn, B., Czanner, S., Busa, E., Pacheco, J., Albert, M., Killiany, R., Maguire, P., Rosas, D., Makris, N., Dale, A., Dickerson, B., and Fischl, B. (2006). Reliability of MRI-derived measurements of human cerebral cortical thickness: the effects of field strength, scanner upgrade and manufacturer. *Neuroimage*, 32(1):180–194.
- Hannanu, F. F., Zeffiro, T. A., Lamalle, L., Heck, O., Renard, F., Thuriot, A., Krainik, A., Hommel, M., Detante, O., Jaillard, A., Garambois, K., Barbieux-Guillot, M., Favre-Wiki, I., Grand, S., Le Bas, J. F., Moisan, A., Richard, M. J., De Fraipont, F., Gere, J., Marcel, S., Vadot, W., Rodier, G., Perennou, D., Chrispin, A., Davoine, P., Naegle, B., Antoine, P., Tropres, I., and Renard, F. (2017). Parietal operculum and motor cortex activities predict motor recovery in moderate to severe stroke. *Neuroimage Clin*, 14:518–529.
- Hansen, J., Koeppen, B., Netter, F., Craig, J., and Perkins, J. (2002). *Atlas of Neuroanatomy and Neurophysiology: Selections from the Netter Collection of Medical Illustrations*. Icon Custom Communication.
- Harris, A. D., Pereira, R. S., Mitchell, J. R., Hill, M. D., Sevvick, R. J., and Frayne, R. (2004). A comparison of images generated from diffusion-weighted and diffusion-tensor imaging data in hyper-acute stroke. *J Magn Reson Imaging*, 20(2):193–200.
- He, B. J., Snyder, A. Z., Vincent, J. L., Epstein, A., Shulman, G. L., and Corbetta, M. (2007). Breakdown of functional connectivity in frontoparietal networks underlies behavioral deficits in spatial neglect. *Neuron*, 53(6):905–918.
- He, S. Q., Dum, R. P., and Strick, P. L. (1993). Topographic organization of corticospinal projections from the frontal lobe: motor areas on the lateral surface of the hemisphere. *J Neurosci*, 13(3):952–980.

References

- Heiss, W. and Kidwell, C. (2014). Imaging for prediction of functional outcome and assessment of recovery in ischemic stroke. *Stroke*, 45(4):1195–1201.
- Hermisdörfer, J., Ulrich, S., Marquardt, C., Goldenberg, G., and Mai, N. (1999). Prehension with the ipsilesional hand after unilateral brain damage. *Cortex*, 35(2):139–161.
- Hilbig, H., Bidmon, H. J., Blohm, U., and Zilles, K. (2001). Wisteria floribunda agglutinin labeling patterns in the human cortex: a tool for revealing areal borders and subdivisions in parallel with immunocytochemistry. *Anat Embryol (Berl)*, 203(1):45–52. [DOI:10.1007/s004290000135] [PubMed:11195088].
- Hong, W., Lin, Q., Cui, Z., Liu, F., Xu, R., and Tang, C. (2019). Diverse functional connectivity patterns of resting-state brain networks associated with good and poor hand outcomes following stroke. *Neuroimage Clin*, 24:102065. [PubMed Central:PMC6889370] [DOI:10.1016/j.nicl.2019.102065] [PubMed:15070770].
- Horn, U., Grothe, M., and Lotze, M. (2016). MRI Biomarkers for Hand-Motor Outcome Prediction and Therapy Monitoring following Stroke. *Neural Plast*, 2016:9265621.
- Howells, H., Thiebaut de Schotten, M., Dell’Acqua, F., Beyh, A., Zappalà, G., Leslie, A., Simmons, A., Murphy, D. G., and Catani, M. (2018). Frontoparietal Tracts Linked to Lateralized Hand Preference and Manual Specialization. *Cereb Cortex*, 28(7):2482–2494. [PubMed Central:PMC6005057] [DOI:10.1093/cercor/bhy040] [PubMed:13174710].
- Huettel, S. A. (2012). Event-related fMRI in cognition. *Neuroimage*, 62(2):1152–1156.
- Hurtz, S., Woo, E., Kebets, V., Green, A. E., Zoumalan, C., Wang, B., Ringman, J. M., Thompson, P. M., and Apostolova, L. G. (2014). Age effects on cortical thickness in cognitively normal elderly individuals. *Dement Geriatr Cogn Dis Extra*, 4(2):221–227.
- Imura, T., Nagasawa, Y., Inagawa, T., Imada, N., Izumi, H., Emoto, K., Tani, I., Yamasaki, H., Ota, Y., Oki, S., Maeda, T., and Araki, O. (2015). Prediction of motor outcomes and activities of daily living function using diffusion tensor tractography in acute hemiparetic stroke patients. *J Phys Ther Sci*, 27(5):1383–1386.
- Jaeger, L., Marchal-Crespo, L., Wolf, P., Riener, R., Michels, L., and Kollias, S. (2014). Brain activation associated with active and passive lower limb stepping. *Front Hum Neurosci*, 8:828. [PubMed Central:PMC4211402] [DOI:10.3389/fnhum.2014.00828] [PubMed:23616742].
- Jaillard, A., Martin, C. D., Garambois, K., Lebas, J. F., and Hommel, M. (2005). Vicarious function within the human primary motor cortex? A longitudinal fMRI stroke study. *Brain*, 128(Pt 5):1122–1138.
- Jang, S. H., Chang, C. H., Lee, J., Kim, C. S., Seo, J. P., and Yeo, S. S. (2013). Functional role of the corticoreticular pathway in chronic stroke patients. *Stroke*, 44(4):1099–1104. [DOI:10.1161/STROKEAHA.111.000269] [PubMed:23444306].
- Jansons, K. M. and Alexander, D. C. (2003). Persistent Angular Structure: new insights from diffusion MRI data. Dummy version. *Inf Process Med Imaging*, 18:672–683.

- Jeannerod, M. and Decety, J. (1995). Mental motor imagery: a window into the representational stages of action. *Curr Opin Neurobiol*, 5(6):727–732. [DOI:10.1016/0959-4388(95)80099-9] [PubMed:8805419].
- Jeurissen, B., Leemans, A., Tournier, J. D., Jones, D. K., and Sijbers, J. (2013). Investigating the prevalence of complex fiber configurations in white matter tissue with diffusion magnetic resonance imaging. *Hum Brain Mapp*, 34(11):2747–2766.
- Johansen-Berg, H. and Behrens, T. E. (2009). Diffusion mri. In *Diffusion MRI*, page iv. Academic Press, San Diego.
- Jones, P. W., Borich, M. R., Vavsour, I., Mackay, A., and Boyd, L. A. (2016). Cortical thickness and metabolite concentration in chronic stroke and the relationship with motor function. *Restor Neurol Neurosci*, 34(5):733–746.
- Jones, R. D., Donaldson, I. M., and Parkin, P. J. (1989). Impairment and recovery of ipsilateral sensory-motor function following unilateral cerebral infarction. *Brain*, 112 (Pt 1):113–132.
- Jung, H. Y., Yoon, J. S., and Park, B. S. (2002). Recovery of proximal and distal arm weakness in the ipsilateral upper limb after stroke. *NeuroRehabilitation*, 17(2):153–159.
- Jørgensen, H. S., Nakayama, H., Raaschou, H. O., Vive-Larsen, J., Støier, M., and Olsen, T. S. (1995). Outcome and time course of recovery in stroke. Part II: Time course of recovery. The Copenhagen Stroke Study. *Arch Phys Med Rehabil*, 76(5):406–412. [DOI:10.1016/s0003-9993(95)80568-0] [PubMed:7741609].
- Katrak, P., Bowring, G., Conroy, P., Chilvers, M., Poulos, R., and McNeil, D. (1998). Predicting upper limb recovery after stroke: The place of early shoulder and hand movement. *Archives of Physical Medicine and Rehabilitation*, 79(7):758–761.
- Kelly, R. M. and Strick, P. L. (2003). Cerebellar loops with motor cortex and prefrontal cortex of a nonhuman primate. *Journal of Neuroscience*, 23(23):8432–8444.
- Ketcham, C. J., Rodriguez, T. M., and Zihlman, K. A. (2007). Targeted aiming movements are compromised in nonaffected limb of persons with stroke. *Neurorehabil Neural Repair*, 21(5):388–397.
- Kim, S. H., Pohl, P. S., Luchies, C. W., Stylianou, A. P., and Won, Y. (2003). Ipsilateral deficits of targeted movements after stroke. *Arch Phys Med Rehabil*, 84(5):719–724.
- King, M., Rauch, H. G., Stein, D. J., and Brooks, S. J. (2014). The handyman’s brain: a neuroimaging meta-analysis describing the similarities and differences between grip type and pattern in humans. *Neuroimage*, 102 Pt 2:923–937.
- Kitsos, G. H., Hubbard, I. J., Kitsos, A. R., and Parsons, M. W. (2013). The ipsilesional upper limb can be affected following stroke. *ScientificWorldJournal*, 2013:684860.
- Koch, P., Schulz, R., and Hummel, F. C. (2016). Structural connectivity analyses in motor recovery research after stroke. *Ann Clin Transl Neurol*, 3(3):233–244. [PubMed Central:PMC4774263] [DOI:10.1002/acn3.278] [PubMed:16888796].

References

- Koh, C. L., Yeh, C. H., Liang, X., Vidyasagar, R., Seitz, R. J., Nilsson, M., Connelly, A., and Carey, L. M. (2021). Structural Connectivity Remote From Lesions Correlates With Somatosensory Outcome Poststroke. *Stroke*, 52(9):2910–2920. [DOI:10.1161/STROKEAHA.120.031520] [PubMed:34134504].
- Kortier, H. G., Sluiter, V. I., Roetenberg, D., and Veltink, P. H. (2014). Assessment of hand kinematics using inertial and magnetic sensors. *J Neuroeng Rehabil*, 11:70. [PubMed Central:PMC4019393] [DOI:10.1186/1743-0003-11-70] [PubMed:15077642].
- Koski, L., Wohlschläger, A., Bekkering, H., Woods, R. P., Dubeau, M. C., Mazziotta, J. C., and Iacoboni, M. (2002). Modulation of motor and premotor activity during imitation of target-directed actions. *Cereb Cortex*, 12(8):847–855.
- Koyama, T. and Domen, K. (2017). Diffusion Tensor Fractional Anisotropy in the Superior Longitudinal Fasciculus Correlates with Functional Independence Measure Cognition Scores in Patients with Cerebral Infarction. *J Stroke Cerebrovasc Dis*, 26(8):1704–1711. [DOI:10.1016/j.jstrokecerebrovasdis.2017.03.034] [PubMed:28478977].
- Koyama, T., Marumoto, K., Miyake, H., and Domen, K. (2014). Relationship between diffusion tensor fractional anisotropy and long-term motor outcome in patients with hemiparesis after middle cerebral artery infarction. *J Stroke Cerebrovasc Dis*, 23(9):2397–2404.
- Kumar, P., Kathuria, P., Nair, P., and Prasad, K. (2016). Prediction of Upper Limb Motor Recovery after Subacute Ischemic Stroke Using Diffusion Tensor Imaging: A Systematic Review and Meta-Analysis. *J Stroke*, 18(1):50–59. [PubMed Central:PMC4747076] [DOI:10.5853/jos.2015.01186] [PubMed:3503832].
- Kuperberg, G. R., Broome, M. R., McGuire, P. K., David, A. S., Eddy, M., Ozawa, F., Goff, D., West, W. C., Williams, S. C., van der Kouwe, A. J., Salat, D. H., Dale, A. M., and Fischl, B. (2003). Regionally localized thinning of the cerebral cortex in schizophrenia. *Arch Gen Psychiatry*, 60(9):878–888.
- Kuypers, H. (2011). *Anatomy of the Descending Pathways*, volume II.
- Kuypers, N. J., James, K. T., Enzmann, G. U., Magnuson, D. S., and Whittemore, S. R. (2013). Functional consequences of ethidium bromide demyelination of the mouse ventral spinal cord. *Exp Neurol*, 247:615–622.
- Lam, T. K., Binns, M. A., Honjo, K., Dawson, D. R., Ross, B., Stuss, D. T., Black, S. E., Chen, J. J., Fujioka, T., and Chen, J. L. (2018). Variability in stroke motor outcome is explained by structural and functional integrity of the motor system. *Sci Rep*, 8(1):9480. [PubMed Central:PMC6013462] [DOI:10.1038/s41598-018-27541-8] [PubMed:8524021].
- Lang, N., Siebner, H. R., Ward, N. S., Lee, L., Nitsche, M. A., Paulus, W., Rothwell, J. C., Lemon, R. N., and Frackowiak, R. S. (2005). How does transcranial DC stimulation of the primary motor cortex alter regional neuronal activity in the human brain? *Eur J Neurosci*, 22(2):495–504.

- Laumann, T. O., Gordon, E. M., Adeyemo, B., Snyder, A. Z., Joo, S. J., Chen, M. Y., Gilmore, A. W., McDermott, K. B., Nelson, S. M., Dosenbach, N. U., Schlaggar, B. L., Mumford, J. A., Poldrack, R. A., and Petersen, S. E. (2015). Functional System and Areal Organization of a Highly Sampled Individual Human Brain. *Neuron*, 87(3):657–670. [PubMed Central:PMC4642864] [DOI:10.1016/j.neuron.2015.06.037] [PubMed:8524021].
- Le Bihan, D., Breton, E., Lallemand, D., Grenier, P., Cabanis, E., and Laval-Jeantet, M. (1986). MR imaging of intravoxel incoherent motions: application to diffusion and perfusion in neurologic disorders. *Radiology*, 161(2):401–407.
- Lee, J. H., Kyeong, S., Kang, H., and Kim, D. H. (2019). Structural and functional connectivity correlates with motor impairment in chronic supratentorial stroke: a multimodal magnetic resonance imaging study. *Neuroreport*, 30(7):526–531. [DOI:10.1097/WNR.0000000000001247] [PubMed:30932970].
- Lee, J. H. and van Donkelaar, P. (2006). The human dorsal premotor cortex generates on-line error corrections during sensorimotor adaptation. *J Neurosci*, 26(12):3330–3334.
- Lemaitre, H., Goldman, A. L., Sambataro, F., Verchinski, B. A., Meyer-Lindenberg, A., Weinberger, D. R., and Mattay, V. S. (2012). Normal age-related brain morphometric changes: nonuniformity across cortical thickness, surface area and gray matter volume? *Neurobiol Aging*, 33(3):1–9.
- Lemon, R. N. (1997). Review : Mechanisms of cortical control of hand function. *The Neuroscientist*, 3(6):389–398.
- Lemon, R. N. (2008). Descending pathways in motor control. *Annu Rev Neurosci*, 31:195–218.
- Li, P., Li, S., Dong, Z., Luo, J., Han, H., Xiong, H., Guo, Z., and Li, Z. (2012). Altered resting state functional connectivity patterns of the anterior prefrontal cortex in obsessive-compulsive disorder. *Neuroreport*, 23(11):681–686.
- Li, Q., Zhao, Y., Chen, Z., Long, J., Dai, J., Huang, X., Lui, S., Radua, J., Vieta, E., Kemp, G. J., Sweeney, J. A., Li, F., and Gong, Q. (2020). Meta-analysis of cortical thickness abnormalities in medication-free patients with major depressive disorder. *Neuropsychopharmacology*, 45(4):703–712.
- Li, R., Wu, X., Chen, K., Fleisher, A. S., Reiman, E. M., and Yao, L. (2013). Alterations of directional connectivity among resting-state networks in Alzheimer disease. *AJNR Am J Neuroradiol*, 34(2):340–345.
- Li, Y., Wu, P., Liang, F., and Huang, W. (2015). The microstructural status of the corpus callosum is associated with the degree of motor function and neurological deficit in stroke patients. *PLoS One*, 10(4):e0122615. [PubMed Central:PMC4398463] [DOI:10.1371/journal.pone.0122615] [PubMed:16888796].
- Lin, L. Y., Ramsey, L., Metcalf, N. V., Rengachary, J., Shulman, G. L., Shimony, J. S., and Corbetta, M. (2018). Stronger prediction of motor recovery and outcome post-stroke by cortico-spinal tract integrity than functional connectivity. *PLoS One*, 13(8):e0202504. [PubMed Central:PMC6107181] [DOI:10.1371/journal.pone.0202504] [PubMed:18468545].

References

- Lindow, J., Domin, M., Grothe, M., Horn, U., Eickhoff, S. B., and Lotze, M. (2016). Connectivity-Based Predictions of Hand Motor Outcome for Patients at the Subacute Stage After Stroke. *Front Hum Neurosci*, 10:101. [PubMed Central:PMC4783389] [DOI:10.3389/fnhum.2016.00101] [PubMed:24553104].
- Liu, G., Dang, C., Peng, K., Xie, C., Chen, H., Xing, S., Chen, X., and Zeng, J. (2015a). Increased spontaneous neuronal activity in structurally damaged cortex is correlated with early motor recovery in patients with subcortical infarction. *Eur J Neurol*, 22(12):1540–1547. [DOI:10.1111/ene.12780] [PubMed:26453239].
- Liu, H., Peng, X., Dahmani, L., Wang, H., Zhang, M., Shan, Y., Rong, D., Guo, Y., Li, J., Li, N., Wang, L., Lin, Y., Pan, R., Lu, J., and Wang, D. (2020). Patterns of motor recovery and structural neuroplasticity after basal ganglia infarcts. *Neurology*, 95(9):e1174–e1187. [PubMed Central:PMC7538227] [DOI:10.1212/WNL.0000000000010149] [PubMed:9931269].
- Liu, J., Qin, W., Zhang, J., Zhang, X., and Yu, C. (2015b). Enhanced interhemispheric functional connectivity compensates for anatomical connection damages in subcortical stroke. *Stroke*, 46(4):1045–1051. [DOI:10.1161/STROKEAHA.114.007044] [PubMed:25721013].
- Liu, J., Wang, C., Cheng, J., Miao, P., and Li, Z. (2022). Dynamic Relationship Between Interhemispheric Functional Connectivity and Corticospinal Tract Changing Pattern After Subcortical Stroke. *Front Aging Neurosci*, 14:870718. [PubMed Central:PMC9120434] [DOI:10.3389/fnagi.2022.870718] [PubMed:27706924].
- Lo, R., Gitelman, D., Levy, R., Hulvershorn, J., and Parrish, T. (2010). Identification of critical areas for motor function recovery in chronic stroke subjects using voxel-based lesion symptom mapping. *Neuroimage*, 49(1):9–18.
- Lorca-Puls, D. L., Gajardo-Vidal, A., White, J., Seghier, M. L., Leff, A. P., Green, D. W., Crinion, J. T., Ludersdorfer, P., Hope, T. M. H., Bowman, H., and Price, C. J. (2018). The impact of sample size on the reproducibility of voxel-based lesion-deficit mappings. *Neuropsychologia*, 115:101–111. [PubMed Central:PMC6018568] [DOI:10.1016/j.neuropsychologia.2018.03.014] [PubMed:18633328].
- Lotze, M., Beutling, W., Loibl, M., Domin, M., Platz, T., Schminke, U., and Byblow, W. D. (2012). Contralesional motor cortex activation depends on ipsilesional corticospinal tract integrity in well-recovered subcortical stroke patients. *Neurorehabil Neural Repair*, 26(6):594–603.
- Loubinoux, I., Carel, C., Alary, F., Boulanouar, K., Viallard, G., Manelfe, C., Rascol, O., Celsis, P., and Chollet, F. (2001). Within-session and between-session reproducibility of cerebral sensorimotor activation: a test–retest effect evidenced with functional magnetic resonance imaging. *J Cereb Blood Flow Metab*, 21(5):592–607. [DOI:10.1097/00004647-200105000-00014] [PubMed:11333370].
- Loubinoux, I., Carel, C., Pariente, J., Dechaumont, S., Albucher, J. F., Marque, P., Manelfe, C., and Chollet, F. (2003). Correlation between cerebral reorganization and motor recovery after subcortical infarcts. *Neuroimage*, 20(4):2166–2180.

- Loubinoux, I., Dechaumont-Palacin, S., Castel-Lacanal, E., De Boissezon, X., Marque, P., Pariente, J., Albucher, J. F., Berry, I., and Chollet, F. (2007). Prognostic value of FMRI in recovery of hand function in subcortical stroke patients. *Cereb Cortex*, 17(12):2980–2987.
- Lowe, M. J., Mock, B. J., and Sorenson, J. A. (1998). Functional connectivity in single and multislice echoplanar imaging using resting-state fluctuations. *Neuroimage*, 7(2):119–132.
- Lövblad, K. O., Baird, A. E., Schlaug, G., Benfield, A., Siewert, B., Voetsch, B., Connor, A., Burzynski, C., Edelman, R. R., and Warach, S. (1997). Ischemic lesion volumes in acute stroke by diffusion-weighted magnetic resonance imaging correlate with clinical outcome. *Ann Neurol*, 42(2):164–170.
- Manto, M., Bower, J. M., Conforto, A. B., Delgado-García, J. M., da Guarda, S. N., Gerwig, M., Habas, C., Hagura, N., Ivry, R. B., Mariën, P., Molinari, M., Naito, E., Nowak, D. A., Oulad Ben Taib, N., Pelisson, D., Tesche, C. D., Tilikete, C., and Timmann, D. (2012). Consensus paper: roles of the cerebellum in motor control—the diversity of ideas on cerebellar involvement in movement. *Cerebellum*, 11(2):457–487.
- Markham, C. H. (1987). Vestibular control of muscular tone and posture. *Can J Neurol Sci*, 14(3 Suppl):493–496.
- Marshall, R. S., Perera, G. M., Lazar, R. M., Krakauer, J. W., Constantine, R. C., and DeLaPaz, R. L. (2000). Evolution of cortical activation during recovery from corticospinal tract infarction. *Stroke*, 31(3):656–661.
- Matsuzaka, Y., Aizawa, H., and Tanji, J. (1992). A motor area rostral to the supplementary motor area (presupplementary motor area) in the monkey: neuronal activity during a learned motor task. *J Neurophysiol*, 68(3):653–662. [DOI:10.1152/jn.1992.68.3.653] [PubMed:1432040].
- Mattiello, J., Bassar, P. J., and Le Bihan, D. (1997). The b matrix in diffusion tensor echo-planar imaging. *Magn Reson Med*, 37(2):292–300.
- Mawase, F., Cherry-Allen, K., Xu, J., Anaya, M., Uehara, S., and Celnik, P. (2020). Pushing the Rehabilitation Boundaries: Hand Motor Impairment Can Be Reduced in Chronic Stroke. *Neurorehabil Neural Repair*, 34(8):733–745.
- McAvoy, M., Larson-Prior, L., Nolan, T. S., Vaishnavi, S. N., Raichle, M. E., and d’Avossa, G. (2008). Resting states affect spontaneous BOLD oscillations in sensory and paralimbic cortex. *J Neurophysiol*, 100(2):922–931. [PubMed Central:PMC2525732] [DOI:10.1152/jn.90426.2008] [PubMed:9345548].
- McCrea, P. H., Eng, J. J., and Hodgson, A. J. (2003). Time and magnitude of torque generation is impaired in both arms following stroke. *Muscle Nerve*, 28(1):46–53.
- Metrot, J., Froger, J., Hauret, I., Mottet, D., van Dokkum, L., and Laffont, I. (2013). Motor recovery of the ipsilesional upper limb in subacute stroke. *Arch Phys Med Rehabil*, 94(11):2283–2290.

References

- Meyer, M. J., Pereira, S., McClure, A., Teasell, R., Thind, A., Koval, J., Richardson, M., and Speechley, M. (2015). A systematic review of studies reporting multivariable models to predict functional outcomes after post-stroke inpatient rehabilitation. *Disabil Rehabil*, 37(15):1316–1323.
- Mishkin, M. and Ungerleider, L. G. (1982). Contribution of striate inputs to the visuospatial functions of parieto-preoccipital cortex in monkeys. *Behav Brain Res*, 6(1):57–77.
- Molenberghs, P., Gillebert, C. R., Peeters, R., and Vandenberghe, R. (2008). Convergence between lesion-symptom mapping and functional magnetic resonance imaging of spatially selective attention in the intact brain. *J Neurosci*, 28(13):3359–3373.
- Monaco, S., Malfatti, G., Culham, J. C., Cattaneo, L., and Turella, L. (2020). Decoding motor imagery and action planning in the early visual cortex: Overlapping but distinct neural mechanisms. *Neuroimage*, 218:116981. [DOI:10.1016/j.neuroimage.2020.116981] [PubMed:32454207].
- Moon, H. I., Pyun, S.-B., Tae, W.-S., and Kwon, H. (2016). Neural substrates of lower extremity motor, balance, and gait function after supratentorial stroke using voxel-based lesion symptom mapping. *Neuroradiology*, 58.
- Moore, M. J., Gillebert, C. R., and Demeyere, N. (2021). Right and left neglect are not anatomically homologous: A voxel-lesion symptom mapping study. *Neuropsychologia*, 162:108024.
- Morecraft, R. J., Herrick, J. L., Stilwell-Morecraft, K. S., Louie, J. L., Schroeder, C. M., Ottenbacher, J. G., and Schoolfield, M. W. (2002). Localization of arm representation in the corona radiata and internal capsule in the non-human primate. *Brain*, 125(Pt 1):176–198.
- Moseley, M. E., Cohen, Y., Kucharczyk, J., Mintorovitch, J., Asgari, H. S., Wendland, M. F., Tsuruda, J., and Norman, D. (1990). Diffusion-weighted MR imaging of anisotropic water diffusion in cat central nervous system. *Radiology*, 176(2):439–445.
- Moulton, E., Valabregue, R., Lehericy, S., Samson, Y., and Rosso, C. (2019). Multivariate prediction of functional outcome using lesion topography characterized by acute diffusion tensor imaging. *Neuroimage Clin*, 23:101821.
- Muakkassa, K. F. and Strick, P. L. (1979). Frontal lobe inputs to primate motor cortex: evidence for four somatotopically organized 'premotor' areas. *Brain Res*, 177(1):176–182. [DOI:10.1016/0006-8993(79)90928-4] [PubMed:115545].
- Ng, Y. S., Stein, J., Ning, M., and Black-Schaffer, R. M. (2007). Comparison of clinical characteristics and functional outcomes of ischemic stroke in different vascular territories. *Stroke*, 38(8):2309–2314. [DOI:10.1161/STROKEAHA.106.475483] [PubMed:17615368].
- Nichols-Larsen, D. S., Clark, P. C., Zeringue, A., Greenspan, A., and Blanton, S. (2005). Factors influencing stroke survivors' quality of life during subacute recovery. *Stroke*, 36(7):1480–1484.

- Nijland, R. H., van Wegen, E. E., Harmeling-van der Wel, B. C., Kwakkel, G., Kwakkel, G., Harmeling-van der Wel, B. C., Veerbeek, J. M., Nijland, R. H., van Wegen, E. E., van der Beek, M. A., Cornelissen, W. A., Goos, A. A., Steeg, C. S., Timmermans, J. M., and Tichelaar, R. (2010). Presence of finger extension and shoulder abduction within 72 hours after stroke predicts functional recovery: early prediction of functional outcome after stroke: the EPOS cohort study. *Stroke*, 41(4):745–750.
- Noskin, O., Krakauer, J. W., Lazar, R. M., Festa, J. R., Handy, C., O'Brien, K. A., and Marshall, R. S. (2008). Ipsilateral motor dysfunction from unilateral stroke: implications for the functional neuroanatomy of hemiparesis. *J Neurol Neurosurg Psychiatry*, 79(4):401–406.
- Nowak, D. A., Grefkes, C., Dafotakis, M., Küst, J., Karbe, H., and Fink, G. R. (2007). Dexterity is impaired at both hands following unilateral subcortical middle cerebral artery stroke. *Eur J Neurosci*, 25(10):3173–3184.
- Ogawa, S. and Lee, T. M. (1990). Magnetic resonance imaging of blood vessels at high fields: in vivo and in vitro measurements and image simulation. *Magn Reson Med*, 16(1):9–18.
- Ogawa, S., Lee, T. M., Kay, A. R., and Tank, D. W. (1990a). Brain magnetic resonance imaging with contrast dependent on blood oxygenation. *Proc Natl Acad Sci U S A*, 87(24):9868–9872.
- Ogawa, S., Lee, T. M., Nayak, A. S., and Glynn, P. (1990b). Oxygenation-sensitive contrast in magnetic resonance image of rodent brain at high magnetic fields. *Magn Reson Med*, 14(1):68–78.
- Okuda, B., Tanaka, H., Tomino, Y., Kawabata, K., Tachibana, H., and Sugita, M. (1995). The role of the left somatosensory cortex in human hand movement. *Exp Brain Res*, 106(3):493–498.
- Otti, A., Guendel, H., Wohlschläger, A., Zimmer, C., and Noll-Hussong, M. (2013). Frequency shifts in the anterior default mode network and the salience network in chronic pain disorder. *BMC Psychiatry*, 13:84.
- Page, S., Gauthier, L., and White, S. (2013). Size doesn't matter: Cortical stroke lesion volume is not associated with upper extremity motor impairment and function in mild, chronic hemiparesis. *Archives of physical medicine and rehabilitation*, 94.
- Park, C. H., Chang, W. H., Ohn, S. H., Kim, S. T., Bang, O. Y., Pascual-Leone, A., and Kim, Y. H. (2011). Longitudinal changes of resting-state functional connectivity during motor recovery after stroke. *Stroke*, 42(5):1357–1362.
- Park, C. H., Kou, N., and Ward, N. S. (2016). The contribution of lesion location to upper limb deficit after stroke. *J Neurol Neurosurg Psychiatry*, 87(12):1283–1286. [PubMed Central:PMC5136717] [DOI:10.1136/jnnp-2015-312738] [PubMed:10860804].
- Park, M. C., Belhaj-Saïf, A., Gordon, M., and Cheney, P. D. (2001). Consistent features in the forelimb representation of primary motor cortex in rhesus macaques. *J Neurosci*, 21(8):2784–2792. [PubMed Central:PMC6762507] [PubMed:5711137].

References

- Parsons, M. W., Christensen, S., McElduff, P., Levi, C. R., Butcher, K. S., De Silva, D. A., Ebinger, M., Barber, P. A., Bladin, C., Donnan, G. A., and Davis, S. M. (2010). Pretreatment diffusion- and perfusion-MR lesion volumes have a crucial influence on clinical response to stroke thrombolysis. *J Cereb Blood Flow Metab*, 30(6):1214–1225. [PubMed Central:PMC2949206] [DOI:10.1038/jcbfm.2010.3] [PubMed:19509116].
- Pereira, F., Mitchell, T., and Botvinick, M. (2009). Machine learning classifiers and fMRI: a tutorial overview. *Neuroimage*, 45(1 Suppl):199–209.
- Picard, N. and Strick, P. L. (1996). Motor areas of the medial wall: a review of their location and functional activation. *Cereb Cortex*, 6(3):342–353. [DOI:10.1093/cercor/6.3.342] [PubMed:8670662].
- Pinto, A., Mckinley, R., Alves, V., Wiest, R., Silva, C. A., and Reyes, M. (2018). Stroke Lesion Outcome Prediction Based on MRI Imaging Combined With Clinical Information. *Front Neurol*, 9:1060.
- Plantin, J., Pennati, G. V., Roca, P., Baron, J. C., Laurencikas, E., Weber, K., Godbolt, A. K., Borg, J., and Lindberg, P. G. (2019). Quantitative Assessment of Hand Spasticity After Stroke: Imaging Correlates and Impact on Motor Recovery. *Front Neurol*, 10:836.
- Plantin, J., Verneau, M., Godbolt, A. K., Pennati, G. V., Laurencikas, E., Johansson, B., Krumlinde-Sundholm, L., Baron, J. C., Borg, J., and Lindberg, P. G. (2021). Recovery and Prediction of Bimanual Hand Use After Stroke. *Neurology*, 97(7):e706–e719. [PubMed Central:PMC8377875] [DOI:10.1212/WNL.0000000000012366] [PubMed:30420830].
- Ploner, C. J., Gaymard, B. M., Rivaud-Péchoix, S., and Pierrot-Deseilligny, C. (2005). The prefrontal substrate of reflexive saccade inhibition in humans. *Biol Psychiatry*, 57(10):1159–1165.
- Power, J. D., Cohen, A. L., Nelson, S. M., Wig, G. S., Barnes, K. A., Church, J. A., Vogel, A. C., Laumann, T. O., Miezin, F. M., Schlaggar, B. L., and Petersen, S. E. (2011). Functional network organization of the human brain. *Neuron*, 72(4):665–678.
- Prados-Román, E., Cabrera-Martos, I., López-López, L., Rodríguez-Torres, J., Torres-Sánchez, I., Ortiz-Rubio, A., and Valenza, M. C. (2021). Deficits underlying handgrip performance in mildly affected chronic stroke persons. *Topics in Stroke Rehabilitation*, 28(3):190–197. PMID: 32758034.
- Preul, C., Hund-Georgiadis, M., Forstmann, B. U., and Lohmann, G. (2006). Characterization of cortical thickness and ventricular width in normal aging: a morphometric study at 3 Tesla. *J Magn Reson Imaging*, 24(3):513–519.
- Preusser, S., Thiel, S. D., Rook, C., Roggenhofer, E., Kosatschek, A., Draganski, B., Blankenburg, F., Driver, J., Villringer, A., and Pleger, B. (2015). The perception of touch and the ventral somatosensory pathway. *Brain*, 138(Pt 3):540–548.
- Prigatano, G. P. and Wong, J. L. (1997). Speed of finger tapping and goal attainment after unilateral cerebral vascular accident. *Arch Phys Med Rehabil*, 78(8):847–852.

- Puig, J., Blasco, G., Daunis-I-Estadella, J., Thomalla, G., Castellanos, M., Soria, G., Prats-Galino, A., Sánchez-González, J., Boada, I., Serena, J., and Pedraza, S. (2013). Increased corticospinal tract fractional anisotropy can discriminate stroke onset within the first 4.5 hours. *Stroke*, 44(4):1162–1165.
- Puig, J., Pedraza, S., Blasco, G., Daunis-I-Estadella, J., Prats, A., Prados, F., Boada, I., Castellanos, M., Sánchez-González, J., Remollo, S., Laguillo, G., Quiles, A. M., Gómez, E., and Serena, J. (2010). Wallerian degeneration in the corticospinal tract evaluated by diffusion tensor imaging correlates with motor deficit 30 days after middle cerebral artery ischemic stroke. *AJNR Am J Neuroradiol*, 31(7):1324–1330.
- Qiu, M., Darling, W. G., Morecraft, R. J., Ni, C. C., Rajendra, J., and Butler, A. J. (2011). White matter integrity is a stronger predictor of motor function than BOLD response in patients with stroke. *Neurorehabil Neural Repair*, 25(3):275–284. [PubMed Central:PMC3579586] [DOI:10.1177/1545968310389183] [PubMed:11834603].
- Radlinska, B., Ghinani, S., Leppert, I. R., Minuk, J., Pike, G. B., and Thiel, A. (2010). Diffusion tensor imaging, permanent pyramidal tract damage, and outcome in subcortical stroke. *Neurology*, 75(12):1048–1054.
- Raghavan, P. (2007). The nature of hand motor impairment after stroke and its treatment. *Curr Treat Options Cardiovasc Med*, 9(3):221–228.
- Raichle, M. E., MacLeod, A. M., Snyder, A. Z., Powers, W. J., Gusnard, D. A., and Shulman, G. L. (2001). A default mode of brain function. *Proc Natl Acad Sci U S A*, 98(2):676–682.
- Rajashekar, D., Wilms, M., Hecker, K. G., Hill, M. D., Dukelow, S., Fiehler, J., and Forkert, N. D. (2020). The Impact of Covariates in Voxel-Wise Lesion-Symptom Mapping. *Front Neurol*, 11:854.
- Rapin, I., Tourk, L. M., and Costa, L. D. (1966). Evaluation of the Purdue Pegboard as a screening test for brain damage. *Dev Med Child Neurol*, 8(1):45–54. [DOI:10.1111/j.1469-8749.1966.tb08272.x] [PubMed:5922056].
- Rathelot, J. A. and Strick, P. L. (2009). Subdivisions of primary motor cortex based on cortico-motoneuronal cells. *Proc Natl Acad Sci U S A*, 106(3):918–923.
- Rathore, S. S., Hinn, A. R., Cooper, L. S., Tyroler, H. A., and Rosamond, W. D. (2002). Characterization of incident stroke signs and symptoms: findings from the atherosclerosis risk in communities study. *Stroke*, 33(11):2718–2721.
- Razak, R. A., Hannanu, F. F., Naegele, B., Hommel, M. J. G., Detante, O., and Jaillard, A. (2022). Ipsilateral hand impairment predicts long-term outcome in patients with subacute stroke. *Eur J Neurol*, 29(7):1983–1993. [DOI:10.1111/ene.15323] [PubMed:35276028].
- Rehme, A. K., Eickhoff, S. B., Rottschy, C., Fink, G. R., and Grefkes, C. (2012). Activation likelihood estimation meta-analysis of motor-related neural activity after stroke. *Neuroimage*, 59(3):2771–2782.
- Rehme, A. K., Volz, L. J., Feis, D. L., Eickhoff, S. B., Fink, G. R., and Grefkes, C. (2015). Individual prediction of chronic motor outcome in the acute post-stroke stage: Behavioral parameters versus functional imaging. *Hum Brain Mapp*, 36(11):4553–4565.

References

- Reynolds, A. M., Peters, D. M., Vendemia, J. M., Smith, L. P., Sweet, R. C., Baylis, G. C., Krotish, D., and Fritz, S. L. (2014). Neuronal injury in the motor cortex after chronic stroke and lower limb motor impairment: a voxel-based lesion symptom mapping study. *Neural Regen Res*, 9(7):766–772.
- Richards, L. G., Stewart, K. C., Woodbury, M. L., Senesac, C., and Cauraugh, J. H. (2008). Movement-dependent stroke recovery: a systematic review and meta-analysis of TMS and fMRI evidence. *Neuropsychologia*, 46(1):3–11.
- Riddle, C. N., Edgley, S. A., and Baker, S. N. (2009). Direct and indirect connections with upper limb motoneurons from the primate reticulospinal tract. *J Neurosci*, 29(15):4993–4999.
- Rizzolatti, G. and Matelli, M. (2003). Two different streams form the dorsal visual system: anatomy and functions. *Exp Brain Res*, 153(2):146–157.
- Rodríguez-Herreros, B., Amengual, J. L., Gurtubay-Antolín, A., Richter, L., Jauer, P., Erdmann, C., Schweikard, A., López-Moliner, J., Rodríguez-Fornells, A., and Münte, T. F. (2015). Microstructure of the superior longitudinal fasciculus predicts stimulation-induced interference with on-line motor control. *Neuroimage*, 120:254–265. [DOI:10.1016/j.neuroimage.2015.06.070] [PubMed:26143205].
- Rojas Albert, A., Backhaus, W., Graterol Pérez, J. A., Braa, H., Schön, G., Choe, C. U., Feldheim, J., Bönstrup, M., Cheng, B., Thomalla, G., Gerloff, C., and Schulz, R. (2022). Cortical thickness of contralesional cortices positively relates to future outcome after severe stroke. *Cereb Cortex*. [DOI:10.1093/cercor/bhac040] [PubMed:35169830].
- Ropper, A. H., Samuels, M. A., and Klein, J. P. (2014). *Chapter 34. Cerebrovascular Diseases*. The McGraw-Hill Companies, New York, NY.
- Rorden, C., Fridriksson, J., and Karnath, H. O. (2009). An evaluation of traditional and novel tools for lesion behavior mapping. *Neuroimage*, 44(4):1355–1362. [PubMed Central:PMC2667945] [DOI:10.1016/j.neuroimage.2008.09.031] [PubMed:17702605].
- Rosas, H. D., Liu, A. K., Hersch, S., Glessner, M., Ferrante, R. J., Salat, D. H., van der Kouwe, A., Jenkins, B. G., Dale, A. M., and Fischl, B. (2002). Regional and progressive thinning of the cortical ribbon in Huntington’s disease. *Neurology*, 58(5):695–701.
- Rosso, C., Valabregue, R., Attal, Y., Vargas, P., Gaudron, M., Baronnet, F., Bertasi, E., Humbert, F., Peskine, A., Perlberg, V., Benali, H., Lehericy, S., and Samson, Y. (2013). Contribution of corticospinal tract and functional connectivity in hand motor impairment after stroke. *PLoS One*, 8(9):e73164. [PubMed Central:PMC3785485] [DOI:10.1371/journal.pone.0073164] [PubMed:24488093].
- Rost, N. S., Bottle, A., Lee, J. M., Randall, M., Middleton, S., Shaw, L., Thijs, V., Rinkel, G. J., Hemmen, T. M., Thijs, V., Eleopra, R., van Oostenbrugge, R. J., Rinkel, G., Fenwick, C., Pelly, M., Shaw, L., Vaux, E., van Wyk, A., Randall, M., Spencer, M., Lee, J. M., Matzkiw, G. H., Newman, J., Rost, N., and Hemmen, T. (2016). Stroke Severity Is a Crucial Predictor of Outcome: An International Prospective Validation Study. *J Am Heart Assoc*, 5(1).

- Roy, C. S. and Sherrington, C. S. (1890). On the Regulation of the Blood-supply of the Brain. *J Physiol*, 11(1-2):85–158.
- Sailer, M., Fischl, B., Salat, D., Tempelmann, C., Schönfeld, M. A., Busa, E., Bodammer, N., Heinze, H. J., and Dale, A. (2003). Focal thinning of the cerebral cortex in multiple sclerosis. *Brain*, 126(Pt 8):1734–1744.
- Salat, D. H., Buckner, R. L., Snyder, A. Z., Greve, D. N., Desikan, R. S., Busa, E., Morris, J. C., Dale, A. M., and Fischl, B. (2004). Thinning of the cerebral cortex in aging. *Cereb Cortex*, 14(7):721–730.
- Sasaki, K. and Gemba, H. (1984). Compensatory motor function of the somatosensory cortex for dysfunction of the motor cortex following cerebellar hemispherectomy in the monkey. *Exp Brain Res*, 56(3):532–538.
- Sato, S., Toyoda, K., Uehara, T., Toratani, N., Yokota, C., Moriwaki, H., Naritomi, H., and Minematsu, K. (2008). Baseline nih stroke scale score predicting outcome in anterior and posterior circulation strokes. *Neurology*, 70(24 Part 2):2371–2377.
- Saygin, A. P., Wilson, S. M., Dronkers, N. F., and Bates, E. (2004). Action comprehension in aphasia: linguistic and non-linguistic deficits and their lesion correlates. *Neuropsychologia*, 42(13):1788–1804.
- Schaechter, J. D., Fricker, Z. P., Perdue, K. L., Helmer, K. G., Vangel, M. G., Greve, D. N., and Makris, N. (2009). Microstructural status of ipsilesional and contralesional corticospinal tract correlates with motor skill in chronic stroke patients. *Hum Brain Mapp*, 30(11):3461–3474.
- Schaechter, J. D., Moore, C. I., Connell, B. D., Rosen, B. R., and Dijkhuizen, R. M. (2006). Structural and functional plasticity in the somatosensory cortex of chronic stroke patients. *Brain*, 129(Pt 10):2722–2733. [DOI:10.1093/brain/awl214] [PubMed:16921177].
- Schaechter, J. D. and Perdue, K. L. (2008). Enhanced cortical activation in the contralesional hemisphere of chronic stroke patients in response to motor skill challenge. *Cereb Cortex*, 18(3):638–647.
- Schaefer, P. W., Ozsunar, Y., He, J., Hamberg, L. M., Hunter, G. J., Sorensen, A. G., Koroshetz, W. J., and Gonzalez, R. G. (2003). Assessing tissue viability with MR diffusion and perfusion imaging. *AJNR Am J Neuroradiol*, 24(3):436–443.
- Schiemanck, S. K., Kwakkel, G., Post, M. W., Kappelle, L. J., and Prevo, A. J. (2008). Impact of internal capsule lesions on outcome of motor hand function at one year post-stroke. *J Rehabil Med*, 40(2):96–101. [DOI:10.2340/16501977-0130] [PubMed:18509572].
- Schmahmann, J. and Pandya, D. (2006). *Fiber Pathways of the Brain*, volume xviii.
- Schoch, B., Dimitrova, A., Gizewski, E. R., and Timmann, D. (2006). Functional localization in the human cerebellum based on voxelwise statistical analysis: a study of 90 patients. *Neuroimage*, 30(1):36–51.

References

- Scrutinio, D., Ricciardi, C., Donisi, L., Losavio, E., Battista, P., Guida, P., Cesarelli, M., Pagano, G., and D'Addio, G. (2020). Machine learning to predict mortality after rehabilitation among patients with severe stroke. *Sci Rep*, 10(1):20127. [PubMed Central:PMC7674405] [DOI:10.1038/s41598-020-77243-3] [PubMed:28835194].
- Seitz, R. J., Höflich, P., Binkofski, F., Tellmann, L., Herzog, H., and Freund, H. J. (1998). Role of the premotor cortex in recovery from middle cerebral artery infarction. *Arch Neurol*, 55(8):1081–1088.
- Sharma, N., Jones, P. S., Carpenter, T. A., and Baron, J. C. (2008). Mapping the involvement of BA 4a and 4p during Motor Imagery. *Neuroimage*, 41(1):92–99.
- Shaw, M. E., Abhayaratna, W. P., Sachdev, P. S., Anstey, K. J., and Cherbuin, N. (2016). Cortical Thinning at Midlife: The PATH Through Life Study. *Brain Topogr*, 29(6):875–884.
- Shelton, F. N. and Reding, M. J. (2001). Effect of lesion location on upper limb motor recovery after stroke. *Stroke*, 32(1):107–112.
- Sisti, H. M., Geurts, M., Gooijers, J., Heitger, M. H., Caeyenberghs, K., Beets, I. A., Serbruyns, L., Leemans, A., and Swinnen, S. P. (2012). Microstructural organization of corpus callosum projections to prefrontal cortex predicts bimanual motor learning. *Learn Mem*, 19(8):351–357. [DOI:10.1101/lm.026534.112] [PubMed:22837217].
- Smania, N., Paolucci, S., Tinazzi, M., Borghero, A., Manganotti, P., Fiaschi, A., Moretto, G., Bovi, P., and Gambarin, M. (2007). Active finger extension: a simple movement predicting recovery of arm function in patients with acute stroke. *Stroke*, 38(3):1088–1090. [DOI:10.1161/01.STR.0000258077.88064.a3] [PubMed:17255546].
- Son, S., Nam, S., Kang, K., and Kim, D. (2018). Relationship between ipsilateral motor deficits on the less-affected side and motor function stage on the affected side. *The Journal of Korean Physical Therapy*, 30:234–238.
- Song, F., Zhang, F., Yin, D. Z., Hu, Y. S., Fan, M. X., Ni, H. H., Nan, X. L., Cui, X., Zhou, C. X., Huang, C. S., Zhao, Q., Ma, L. H., Xu, Y. M., and Xia, Q. J. (2012). Diffusion tensor imaging for predicting hand motor outcome in chronic stroke patients. *J Int Med Res*, 40(1):126–133.
- Song, J., Young, B. M., Nigogosyan, Z., Walton, L. M., Nair, V. A., Grogan, S. W., Tyler, M. E., Farrar-Edwards, D., Caldera, K. E., Sattin, J. A., Williams, J. C., and Prabhakaran, V. (2014). Characterizing relationships of DTI, fMRI, and motor recovery in stroke rehabilitation utilizing brain-computer interface technology. *Front Neuroeng*, 7:31. [PubMed Central:PMC4114288] [DOI:10.3389/fneng.2014.00031] [PubMed:14293031].
- Stejskal, E. O. and Tanner, J. E. (1965). Spin diffusion measurements: Spin echoes in the presence of a time-dependent field gradient. *The Journal of Chemical Physics*, 42(1):288–292.
- Stewart, J. C., Dewanjee, P., Tran, G., Quinlan, E. B., Dodakian, L., McKenzie, A., See, J., and Cramer, S. C. (2017). Role of corpus callosum integrity in arm function differs based on motor severity after stroke. *Neuroimage Clin*, 14:641–647. [PubMed Central:PMC5357692] [DOI:10.1016/j.nicl.2017.02.023] [PubMed:20876483].

- Stinear, C. (2010). Prediction of recovery of motor function after stroke. *The Lancet Neurology*, 9(12):1228–1232.
- Strauss, E., Sherman, E., and Spreen, O. (2006). *A Compendium of Neuropsychological Tests: Administration, Norms, and Commentary*. Oxford University Press.
- Sunderland, A., Bowers, M. P., Sluman, S. M., Wilcock, D. J., and Ardron, M. E. (1999). Impaired dexterity of the ipsilateral hand after stroke and the relationship to cognitive deficit. *Stroke*, 30(5):949–955.
- Sunderland, A., Tinson, D., Bradley, L., and Hewer, R. L. (1989). Arm function after stroke. An evaluation of grip strength as a measure of recovery and a prognostic indicator. *J Neurol Neurosurg Psychiatry*, 52(11):1267–1272. [PubMed Central:PMC1031635] [DOI:10.1136/jnnp.52.11.1267] [PubMed:6875585].
- Tang, C., Zhao, Z., Chen, C., Zheng, X., Sun, F., Zhang, X., Tian, J., Fan, M., Wu, Y., and Jia, J. (2016). Decreased Functional Connectivity of Homotopic Brain Regions in Chronic Stroke Patients: A Resting State fMRI Study. *PLoS One*, 11(4):e0152875. [PubMed Central:PMC4830618] [DOI:10.1371/journal.pone.0152875] [PubMed:17389628].
- Tanji, J. and Shima, K. (1994). Role for supplementary motor area cells in planning several movements ahead. *Nature*, 371(6496):413–416. [DOI:10.1038/371413a0] [PubMed:8090219].
- Tatu, L., Moulin, T., Bogousslavsky, J., and Duvernoy, H. (1998). Arterial territories of the human brain. *Neurology*, 50(6):1699–1708.
- Tessitore, A., Amboni, M., Esposito, F., Russo, A., Picillo, M., Marcuccio, L., Pellecchia, M. T., Vitale, C., Cirillo, M., Tedeschi, G., and Barone, P. (2012). Resting-state brain connectivity in patients with Parkinson’s disease and freezing of gait. *Parkinsonism Relat Disord*, 18(6):781–787.
- Thickbroom, G. W., Byrnes, M. L., Archer, S. A., and Mastaglia, F. L. (2002). Motor outcome after subcortical stroke: Meps correlate with hand strength but not dexterity. *Clinical Neurophysiology*, 113(12):2025–2029.
- Tononi, G., Sporns, O., and Edelman, G. M. (1999). Measures of degeneracy and redundancy in biological networks. *Proc Natl Acad Sci U S A*, 96(6):3257–3262. [PubMed Central:PMC15929] [DOI:10.1073/pnas.96.6.3257] [PubMed:8197179].
- Tournier, J. D., Calamante, F., and Connelly, A. (2007). Robust determination of the fibre orientation distribution in diffusion MRI: non-negativity constrained super-resolved spherical deconvolution. *Neuroimage*, 35(4):1459–1472.
- Tournier, J. D., Calamante, F., and Connelly, A. (2009). Improved probabilistic streamlines tractography by 2nd order integration over fibre orientation distributions.
- Tuch, D. S. (2004). Q-ball imaging. *Magn Reson Med*, 52(6):1358–1372.
- Tuch, D. S., Reese, T. G., Wiegell, M. R., Makris, N., Belliveau, J. W., and Wedeen, V. J. (2002). High angular resolution diffusion imaging reveals intravoxel white matter fiber heterogeneity. *Magn Reson Med*, 48(4):577–582.

References

- Tzourio-Mazoyer, N., Landeau, B., Papathanassiou, D., Crivello, F., Etard, O., Delcroix, N., Mazoyer, B., and Joliot, M. (2002). Automated anatomical labeling of activations in SPM using a macroscopic anatomical parcellation of the MNI MRI single-subject brain. *Neuroimage*, 15(1):273–289. [DOI:10.1006/nimg.2001.0978] [PubMed:11771995].
- Uddin, L. Q., Kelly, A. M., Biswal, B. B., Margulies, D. S., Shehzad, Z., Shaw, D., Ghaffari, M., Rotrosen, J., Adler, L. A., Castellanos, F. X., and Milham, M. P. (2008). Network homogeneity reveals decreased integrity of default-mode network in ADHD. *J Neurosci Methods*, 169(1):249–254.
- Ueda, R., Yamada, N., Abo, M., and Senoo, A. (2019). Correlation analysis of motor function improvement and brain structure for upper limb paralysis. *Neuroreport*, 30(2):77–81. [DOI:10.1097/WNR.0000000000001160] [PubMed:30399028].
- van den Heuvel, M. P., Stam, C. J., Boersma, M., and Hulshoff Pol, H. E. (2008). Small-world and scale-free organization of voxel-based resting-state functional connectivity in the human brain. *Neuroimage*, 43(3):528–539.
- van Niftrik, C. H. B., Sebök, M., Muscas, G., Wegener, S., Luft, A. R., Stippich, C., Regli, L., and Fierstra, J. (2021). Investigating the Association of Wallerian Degeneration and Diaschisis After Ischemic Stroke With BOLD Cerebrovascular Reactivity. *Front Physiol*, 12:645157. [PubMed Central:PMC8264262] [DOI:10.3389/fphys.2021.645157] [PubMed:22492515].
- van Swieten, J. C., Koudstaal, P. J., Visser, M. C., Schouten, H. J., and van Gijn, J. (1988). Interobserver agreement for the assessment of handicap in stroke patients. *Stroke*, 19(5):604–607. [DOI:10.1161/01.str.19.5.604] [PubMed:3363593].
- Varghese, R. and Winstein, C. J. (2019). Relationship Between Motor Capacity of the Contralesional and Ipsilesional Hand Depends on the Side of Stroke in Chronic Stroke Survivors With Mild-to-Moderate Impairment. *Front Neurol*, 10:1340.
- Venkataraman, A., Whitford, T. J., Westin, C. F., Golland, P., and Kubicki, M. (2012). Whole brain resting state functional connectivity abnormalities in schizophrenia. *Schizophr Res*, 139(1-3):7–12.
- Viganò, L., Fornia, L., Rossi, M., Howells, H., Leonetti, A., Puglisi, G., Conti Nibali, M., Bellacicca, A., Grimaldi, M., Bello, L., and Cerri, G. (2019). Anatomico-functional characterisation of the human "hand-knob": A direct electrophysiological study. *Cortex*, 113:239–254.
- von Monakow, C. (1914). Die lokalisation im grosshirn und der abbau der funktion durch kortikale herde.
- Waller, A. (1850). Experiments on the Section of the Glossopharyngeal and Hypoglossal Nerves of the Frog, and Observations of the Alterations Produced Thereby in the Structure of Their Primitive Fibres. *Philosophical Transactions of the Royal Society of London Series I*, 140:423–429.
- Wang, L., Yu, C., Chen, H., Qin, W., He, Y., Fan, F., Zhang, Y., Wang, M., Li, K., Zang, Y., Woodward, T. S., and Zhu, C. (2010). Dynamic functional reorganization of the motor execution network after stroke. *Brain*, 133(Pt 4):1224–1238.

- Wang, L. E., Tittgemeyer, M., Imperati, D., Diekhoff, S., Ameli, M., Fink, G. R., and Grefkes, C. (2012). Degeneration of corpus callosum and recovery of motor function after stroke: a multimodal magnetic resonance imaging study. *Hum Brain Mapp*, 33(12):2941–2956. [PubMed Central:PMC6870435] [DOI:10.1002/hbm.21417] [PubMed:19253405].
- Ward, N. S., Brown, M. M., Thompson, A. J., and Frackowiak, R. S. (2003). Neural correlates of motor recovery after stroke: a longitudinal fMRI study. *Brain*, 126(Pt 11):2476–2496. [PubMed Central:PMC3717457] [DOI:10.1093/brain/awg245] [PubMed:9549504].
- Warren, J. E., Crinion, J. T., Lambon Ralph, M. A., and Wise, R. J. (2009). Anterior temporal lobe connectivity correlates with functional outcome after aphasic stroke. *Brain*, 132(Pt 12):3428–3442.
- Wasserthal, J., Neher, P., and Maier-Hein, K. H. (2018). TractSeg - Fast and accurate white matter tract segmentation. *Neuroimage*, 183:239–253. [DOI:10.1016/j.neuroimage.2018.07.070] [PubMed:30086412].
- Wells, J. (1983). Human neuroanatomy, 8th edition. edited by w. b. carpenter, j. sutin, 872 pp, williams & wilkins, baltimore, md, 1983. \$44.00. *Muscle & Nerve*, 6:462–462.
- Wetter, S., Poole, J. L., and Haaland, K. Y. (2005). Functional implications of ipsilesional motor deficits after unilateral stroke. *Arch Phys Med Rehabil*, 86(4):776–781.
- Wolfe, C. D. (2000). The impact of stroke. *Br Med Bull*, 56(2):275–286.
- Wolpert, D. M. and Flanagan, J. R. (2001). Motor prediction. *Curr Biol*, 11(18):R729–732.
- World Health Organization (2019). Global health estimates: Life expectancy and leading causes of death and disability. Technical report, Genf, Schweiz.
- Wouters, A., Nysten, C., Thijs, V., and Lemmens, R. (2018). Prediction of Outcome in Patients With Acute Ischemic Stroke Based on Initial Severity and Improvement in the First 24 h. *Front Neurol*, 9:308.
- Xia, Y., Huang, G., Quan, X., Qin, Q., Li, H., Xu, C., and Liang, Z. (2021). Dynamic Structural and Functional Reorganizations Following Motor Stroke. *Med Sci Monit*, 27:e929092. [PubMed Central:PMC7962416] [DOI:10.12659/MSM.929092] [PubMed:25721013].
- Xu, P., Huang, R., Wang, J., Van Dam, N. T., Xie, T., Dong, Z., Chen, C., Gu, R., Zang, Y. F., He, Y., Fan, J., and Luo, Y. J. (2014). Different topological organization of human brain functional networks with eyes open versus eyes closed. *Neuroimage*, 90:246–255. [DOI:10.1016/j.neuroimage.2013.12.060] [PubMed:24434242].
- Yarosh, C. A., Hoffman, D. S., and Strick, P. L. (2004). Deficits in movements of the wrist ipsilateral to a stroke in hemiparetic subjects. *J Neurophysiol*, 92(6):3276–3285.
- Yelnik, A., Bonan, I., Debray, M., Lo, E., Gelbert, F., and Bussel, B. (1996). Changes in the execution of a complex manual task after ipsilateral ischemic cerebral hemispheric stroke. *Arch Phys Med Rehabil*, 77(8):806–810.
- Yeterian, E. H., Pandya, D. N., Tomaiuolo, F., and Petrides, M. (2012). The cortical connectivity of the prefrontal cortex in the monkey brain. *Cortex*, 48(1):58–81.

References

- Yu, C., Zhu, C., Zhang, Y., Chen, H., Qin, W., Wang, M., and Li, K. (2009). A longitudinal diffusion tensor imaging study on Wallerian degeneration of corticospinal tract after motor pathway stroke. *Neuroimage*, 47(2):451–458. [DOI:10.1016/j.neuroimage.2009.04.066] [PubMed:19409500].
- Zaaimi, B., Edgley, S. A., Soteropoulos, D. S., and Baker, S. N. (2012). Changes in descending motor pathway connectivity after corticospinal tract lesion in macaque monkey. *Brain*, 135(Pt 7):2277–2289.
- Zarei, M., Ibarretxe-Bilbao, N., Compta, Y., Hough, M., Junque, C., Bargallo, N., Tolosa, E., and Martí, M. J. (2013). Cortical thinning is associated with disease stages and dementia in Parkinson's disease. *J Neurol Neurosurg Psychiatry*, 84(8):875–881.
- Zhang, J., Meng, L., Qin, W., Liu, N., Shi, F. D., and Yu, C. (2014). Structural damage and functional reorganization in ipsilesional m1 in well-recovered patients with subcortical stroke. *Stroke*, 45(3):788–793. [DOI:10.1161/STROKEAHA.113.003425] [PubMed:24496396].
- Zhang, L., Butler, A. J., Sun, C. K., Sahgal, V., Wittenberg, G. F., and Yue, G. H. (2008). Fractal dimension assessment of brain white matter structural complexity post stroke in relation to upper-extremity motor function. *Brain Res*, 1228:229–240. [PubMed Central:PMC2655112] [DOI:10.1016/j.brainres.2008.06.008] [PubMed:10968303].
- Zhang, M., Lin, Q., Lu, J., Rong, D., Zhao, Z., Ma, Q., Liu, H., Shu, N., He, Y., and Li, K. (2015). Pontine infarction: diffusion-tensor imaging of motor pathways-a longitudinal study. *Radiology*, 274(3):841–850.
- Zhang, Y., Li, K. S., Ning, Y. Z., Fu, C. H., Liu, H. W., Han, X., Cui, F. Y., Ren, Y., and Zou, Y. H. (2016a). Altered structural and functional connectivity between the bilateral primary motor cortex in unilateral subcortical stroke: A multimodal magnetic resonance imaging study. *Medicine (Baltimore)*, 95(31):e4534. [PubMed Central:PMC4979863] [DOI:10.1097/MD.0000000000004534] [PubMed:23090951].
- Zhang, Y., Liu, H., Wang, L., Yang, J., Yan, R., Zhang, J., Sang, L., Li, P., Wang, J., and Qiu, M. (2016b). Relationship between functional connectivity and motor function assessment in stroke patients with hemiplegia: a resting-state functional MRI study. *Neuroradiology*, 58(5):503–511. [DOI:10.1007/s00234-016-1646-5] [PubMed:8524021].
- Zhavoronkova, L., Boldyreva, G., Kuptsova, S., Sharova, E., Smirnov, A., and Pronin, I. (2017). fmri responses of the brain during active and passive movements in left-handed subjects. *Human Physiology*, 43:191–198.
- Ziemann, U., Ishii, K., Borgheresi, A., Yaseen, Z., Battaglia, F., Hallett, M., Cincotta, M., and Wassermann, E. M. (1999). Dissociation of the pathways mediating ipsilateral and contralateral motor-evoked potentials in human hand and arm muscles. *J Physiol*, 518 (Pt 3):895–906.

Appendix A

Supplementary materials and methods

A.1 Inclusion and exclusion criteria of cohorts

A.1.1 ISIS-HERMES study

Inclusion Criteria

- Right or left carotid ischemic stroke in the 14 previous days, confirmed by MRI
- Persistent neurological deficit (NIHSS ≥ 7)
- Optimal medical treatment (antithrombotics, antihypertensive, statins)
- General state compatible with a program of functional rehabilitation

Exclusion Criteria

- Severe extensive stroke implying vital prognosis.
- Severe persistent neurological deficit (NIHSS > 24)
- Medical history of neurological pathology with a deficit as consequence (Rankin < 3 before stroke)
- Serious psychiatric disease
- Myocardial infarction less than 3 months old
- Recurring thromboembolic disease or less than 6 months old
- Patient with organ transplantation
- Medical history of infection (HIV, HTLV, HBV, HCV)
- Current immunosuppressive/immunomodulating treatment
- Medical history of cancer
- Medical history of chemotherapy
- Known chronic kidney failure (clearance of creatinin < 90 ml/min/1.73m²)

Supplementary materials and methods

- Known hepatic failure(diminution of prothrombin level (TP) not corrigible with vitamin K)
- Obesity hindering the bone-marrow sampling in the iliac crest
- Pathology implying vital prognosis in the 3 month following stroke
- Refusal to participate
- Patient unable to give personally his/her consent
- Pregnant, parturient and feeding women
- Woman in age to procreate who could not receive an effective method of contraception during the study
- Participation to another therapeutic clinical trial or in period of exclusion of a therapeutic clinical study
- Privation of liberty with a decision of justice or administration, legal protection
- Non affiliation to social security

A.1.2 RESSTORE study

Inclusion Criteria

- Male or female > 18 year-old
- Subtentorial ischemic stroke (> 1.5 cm on 2 slices), admitted in stroke unit in the first 24h after stroke onset
- Inclusion from 1 to 4 days post-stroke
- NIHSS 7
- No decompressive craniectomy
- Patient able to follow a rehabilitation program
- Rankin scale = 0 before stroke onset
- Obtaining signed informed consent from patient or the proxy

Exclusion Criteria

- Contraindication for MRI.
- Coma (score of 2 or more on item 1a of the NIHSS related to awareness)
- Evidence on neuroimaging (CT or MRI) of a brain tumor, cerebral edema with midline shift and a clinically significant compression of ventricles, cerebellar or brainstem infarction, or subarachnoid hemorrhage, or intracerebral parenchymal hematoma
- Severe leucoariosis and/or severe cortical atrophy on cerebral imaging
- Previous territorial ischemic stroke
- Active infectious disease (HIV, hepatitis B, hepatitis C)

- History of cancer
- Pre-existing dementia
- A health status, any clinical condition (eg, short life expectancy, and coexisting disease) or other characteristic that precludes appropriate diagnosis, treatment, or follow-up in the trial
- Pregnancy / Breast feeding
- Patients who are participating in another therapeutic trial
- Inability or unwillingness of the individual or their legal guardian/representative to provide written informed consent

A.1.3 IRMAS study

Inclusion Criteria

- First-ever ischemic stroke in the carotid territory
- Initial MRI with DWI performed within 12 hours of stroke onset
- Neurological deficit score of ≥ 1 on the National Institutes of Health Stroke Scale (NIHSS)

Exclusion Criteria

- Younger than 18 years old or under the care of a legal guardian
- Functionally dependent before the stroke (modified Rankin score >2)
- Severe white matter lesions (Fazekas score 3),
- addicted to alcohol or drugs or diagnosed with a life-threatening pathology that would potentially limit the 3-month follow-up visit

A.2 Clinical score measurement

A.2.1 National Institutes of Health Stroke Scale

N I H STROKE SCALE

Patient Identification. ____-____-____

Pt. Date of Birth ____/____/____

Hospital _____ (____-____)

Date of Exam ____/____/____

Interval: ☐ Baseline ☐ 2 hours post treatment ☐ 24 hours post onset of symptoms ± 20 minutes ☐ 7-10 days
☐ 3 months ☐ Other _____ (____)

Time: ____:____ ☐ am ☐ pm

Person Administering Scale _____

Administer stroke scale items in the order listed. Record performance in each category after each subscale exam. Do not go back and change scores. Follow directions provided for each exam technique. Scores should reflect what the patient does, not what the clinician thinks the patient can do. The clinician should record answers while administering the exam and work quickly. Except where indicated, the patient should not be coached (i.e., repeated requests to patient to make a special effort).

Instructions	Scale Definition	Score
1a. Level of Consciousness: The investigator must choose a response if a full evaluation is prevented by such obstacles as an endotracheal tube, language barrier, orotracheal trauma/bandages. A 3 is scored only if the patient makes no movement (other than reflexive posturing) in response to noxious stimulation.	0 = Alert; keenly responsive. 1 = Not alert; but arousable by minor stimulation to obey, answer, or respond. 2 = Not alert; requires repeated stimulation to attend, or is obtunded and requires strong or painful stimulation to make movements (not stereotyped). 3 = Responds only with reflex motor or autonomic effects or totally unresponsive, flaccid, and areflexic.	_____
1b. LOC Questions: The patient is asked the month and his/her age. The answer must be correct - there is no partial credit for being close. Aphasic and stuporous patients who do not comprehend the questions will score 2. Patients unable to speak because of endotracheal intubation, orotracheal trauma, severe dysarthria from any cause, language barrier, or any other problem not secondary to aphasia are given a 1. It is important that only the initial answer be graded and that the examiner not "help" the patient with verbal or non-verbal cues.	0 = Answers both questions correctly. 1 = Answers one question correctly. 2 = Answers neither question correctly.	_____
1c. LOC Commands: The patient is asked to open and close the eyes and then to grip and release the non-paretic hand. Substitute another one step command if the hands cannot be used. Credit is given if an unequivocal attempt is made but not completed due to weakness. If the patient does not respond to command, the task should be demonstrated to him or her (pantomime), and the result scored (i.e., follows none, one or two commands). Patients with trauma, amputation, or other physical impediments should be given suitable one-step commands. Only the first attempt is scored.	0 = Performs both tasks correctly. 1 = Performs one task correctly. 2 = Performs neither task correctly.	_____
2. Best Gaze: Only horizontal eye movements will be tested. Voluntary or reflexive (oculocephalic) eye movements will be scored, but caloric testing is not done. If the patient has a conjugate deviation of the eyes that can be overcome by voluntary or reflexive activity, the score will be 1. If a patient has an isolated peripheral nerve paresis (CN III, IV or VI), score a 1. Gaze is testable in all aphasic patients. Patients with ocular trauma, bandages, pre-existing blindness, or other disorder of visual acuity or fields should be tested with reflexive movements, and a choice made by the investigator. Establishing eye contact and then moving about the patient from side to side will occasionally clarify the presence of a partial gaze palsy.	0 = Normal. 1 = Partial gaze palsy; gaze is abnormal in one or both eyes, but forced deviation or total gaze paresis is not present. 2 = Forced deviation, or total gaze paresis not overcome by the oculocephalic maneuver.	_____

N I H STROKE SCALE

Patient Identification. _____

Pt. Date of Birth ____/____/____

Hospital _____ (____-____)

Date of Exam ____/____/____

Interval: ☐ Baseline ☐ 2 hours post treatment ☐ 24 hours post onset of symptoms \pm 20 minutes ☐ 7-10 days
☐ 3 months ☐ Other _____ (____)

<p>3. Visual: Visual fields (upper and lower quadrants) are tested by confrontation, using finger counting or visual threat, as appropriate. Patients may be encouraged, but if they look at the side of the moving fingers appropriately, this can be scored as normal. If there is unilateral blindness or enucleation, visual fields in the remaining eye are scored. Score 1 only if a clear-cut asymmetry, including quadrantanopia, is found. If patient is blind from any cause, score 3. Double simultaneous stimulation is performed at this point. If there is extinction, patient receives a 1, and the results are used to respond to item 11.</p>	<p>0 = No visual loss.</p> <p>1 = Partial hemianopia.</p> <p>2 = Complete hemianopia.</p> <p>3 = Bilateral hemianopia (blind including cortical blindness).</p>	<p>_____</p>
<p>4. Facial Palsy: Ask – or use pantomime to encourage – the patient to show teeth or raise eyebrows and close eyes. Score symmetry of grimace in response to noxious stimuli in the poorly responsive or non-comprehending patient. If facial trauma/bandages, orotracheal tube, tape or other physical barriers obscure the face, these should be removed to the extent possible.</p>	<p>0 = Normal symmetrical movements.</p> <p>1 = Minor paralysis (flattened nasolabial fold, asymmetry on smiling).</p> <p>2 = Partial paralysis (total or near-total paralysis of lower face).</p> <p>3 = Complete paralysis of one or both sides (absence of facial movement in the upper and lower face).</p>	<p>_____</p>
<p>5. Motor Arm: The limb is placed in the appropriate position: extend the arms (palms down) 90 degrees (if sitting) or 45 degrees (if supine). Drift is scored if the arm falls before 10 seconds. The aphasic patient is encouraged using urgency in the voice and pantomime, but not noxious stimulation. Each limb is tested in turn, beginning with the non-paretic arm. Only in the case of amputation or joint fusion at the shoulder, the examiner should record the score as untestable (UN), and clearly write the explanation for this choice.</p>	<p>0 = No drift; limb holds 90 (or 45) degrees for full 10 seconds.</p> <p>1 = Drift; limb holds 90 (or 45) degrees, but drifts down before full 10 seconds; does not hit bed or other support.</p> <p>2 = Some effort against gravity; limb cannot get to or maintain (if cued) 90 (or 45) degrees, drifts down to bed, but has some effort against gravity.</p> <p>3 = No effort against gravity; limb falls.</p> <p>4 = No movement.</p> <p>UN = Amputation or joint fusion, explain: _____</p> <p>5a. Left Arm</p> <p>_____</p> <p>5b. Right Arm</p> <p>_____</p>	<p>_____</p> <p>_____</p>
<p>6. Motor Leg: The limb is placed in the appropriate position: hold the leg at 30 degrees (always tested supine). Drift is scored if the leg falls before 5 seconds. The aphasic patient is encouraged using urgency in the voice and pantomime, but not noxious stimulation. Each limb is tested in turn, beginning with the non-paretic leg. Only in the case of amputation or joint fusion at the hip, the examiner should record the score as untestable (UN), and clearly write the explanation for this choice.</p>	<p>0 = No drift; leg holds 30-degree position for full 5 seconds.</p> <p>1 = Drift; leg falls by the end of the 5-second period but does not hit bed.</p> <p>2 = Some effort against gravity; leg falls to bed by 5 seconds, but has some effort against gravity.</p> <p>3 = No effort against gravity; leg falls to bed immediately.</p> <p>4 = No movement.</p> <p>UN = Amputation or joint fusion, explain: _____</p> <p>6a. Left Leg</p> <p>_____</p> <p>6b. Right Leg</p> <p>_____</p>	<p>_____</p>

N I H STROKE SCALE

Patient Identification. ____-____-____

Pt. Date of Birth ____/____/____

Hospital _____ (____-____)

Date of Exam ____/____/____

Interval: ☐ Baseline ☐ 2 hours post treatment ☐ 24 hours post onset of symptoms ± 20 minutes ☐ 7-10 days
☐ 3 months ☐ Other _____ (____)

<p>7. Limb Ataxia: This item is aimed at finding evidence of a unilateral cerebellar lesion. Test with eyes open. In case of visual defect, ensure testing is done in intact visual field. The finger-nose-finger and heel-shin tests are performed on both sides, and ataxia is scored only if present out of proportion to weakness. Ataxia is absent in the patient who cannot understand or is paralyzed. Only in the case of amputation or joint fusion, the examiner should record the score as untestable (UN), and clearly write the explanation for this choice. In case of blindness, test by having the patient touch nose from extended arm position.</p>	<p>0 = Absent.</p> <p>1 = Present in one limb.</p> <p>2 = Present in two limbs.</p> <p>UN = Amputation or joint fusion, explain: _____</p>	<p>_____</p>
<p>8. Sensory: Sensation or grimace to pinprick when tested, or withdrawal from noxious stimulus in the obtunded or aphasic patient. Only sensory loss attributed to stroke is scored as abnormal and the examiner should test as many body areas (arms [not hands], legs, trunk, face) as needed to accurately check for hemisensory loss. A score of 2, "severe or total sensory loss," should only be given when a severe or total loss of sensation can be clearly demonstrated. Stuporous and aphasic patients will, therefore, probably score 1 or 0. The patient with brainstem stroke who has bilateral loss of sensation is scored 2. If the patient does not respond and is quadriplegic, score 2. Patients in a coma (item 1a=3) are automatically given a 2 on this item.</p>	<p>0 = Normal; no sensory loss.</p> <p>1 = Mild-to-moderate sensory loss; patient feels pinprick is less sharp or is dull on the affected side; or there is a loss of superficial pain with pinprick, but patient is aware of being touched.</p> <p>2 = Severe to total sensory loss; patient is not aware of being touched in the face, arm, and leg.</p>	<p>_____</p>
<p>9. Best Language: A great deal of information about comprehension will be obtained during the preceding sections of the examination. For this scale item, the patient is asked to describe what is happening in the attached picture, to name the items on the attached naming sheet and to read from the attached list of sentences. Comprehension is judged from responses here, as well as to all of the commands in the preceding general neurological exam. If visual loss interferes with the tests, ask the patient to identify objects placed in the hand, repeat, and produce speech. The intubated patient should be asked to write. The patient in a coma (item 1a=3) will automatically score 3 on this item. The examiner must choose a score for the patient with stupor or limited cooperation, but a score of 3 should be used only if the patient is mute and follows no one-step commands.</p>	<p>0 = No aphasia; normal.</p> <p>1 = Mild-to-moderate aphasia; some obvious loss of fluency or facility of comprehension, without significant limitation on ideas expressed or form of expression. Reduction of speech and/or comprehension, however, makes conversation about provided materials difficult or impossible. For example, in conversation about provided materials, examiner can identify picture or naming card content from patient's response.</p> <p>2 = Severe aphasia; all communication is through fragmentary expression; great need for inference, questioning, and guessing by the listener. Range of information that can be exchanged is limited; listener carries burden of communication. Examiner cannot identify materials provided from patient response.</p> <p>3 = Mute, global aphasia; no usable speech or auditory comprehension.</p>	<p>_____</p>
<p>10. Dysarthria: If patient is thought to be normal, an adequate sample of speech must be obtained by asking patient to read or repeat words from the attached list. If the patient has severe aphasia, the clarity of articulation of spontaneous speech can be rated. Only if the patient is intubated or has other physical barriers to producing speech, the examiner should record the score as untestable (UN), and clearly write an explanation for this choice. Do not tell the patient why he or she is being tested.</p>	<p>0 = Normal.</p> <p>1 = Mild-to-moderate dysarthria; patient slurs at least some words and, at worst, can be understood with some difficulty.</p> <p>2 = Severe dysarthria; patient's speech is so slurred as to be unintelligible in the absence of or out of proportion to any dysphasia, or is mute/anarthric.</p> <p>UN = Intubated or other physical barrier, explain: _____</p>	<p>_____</p>

NIH STROKE SCALE

Patient Identification. ____-____-____

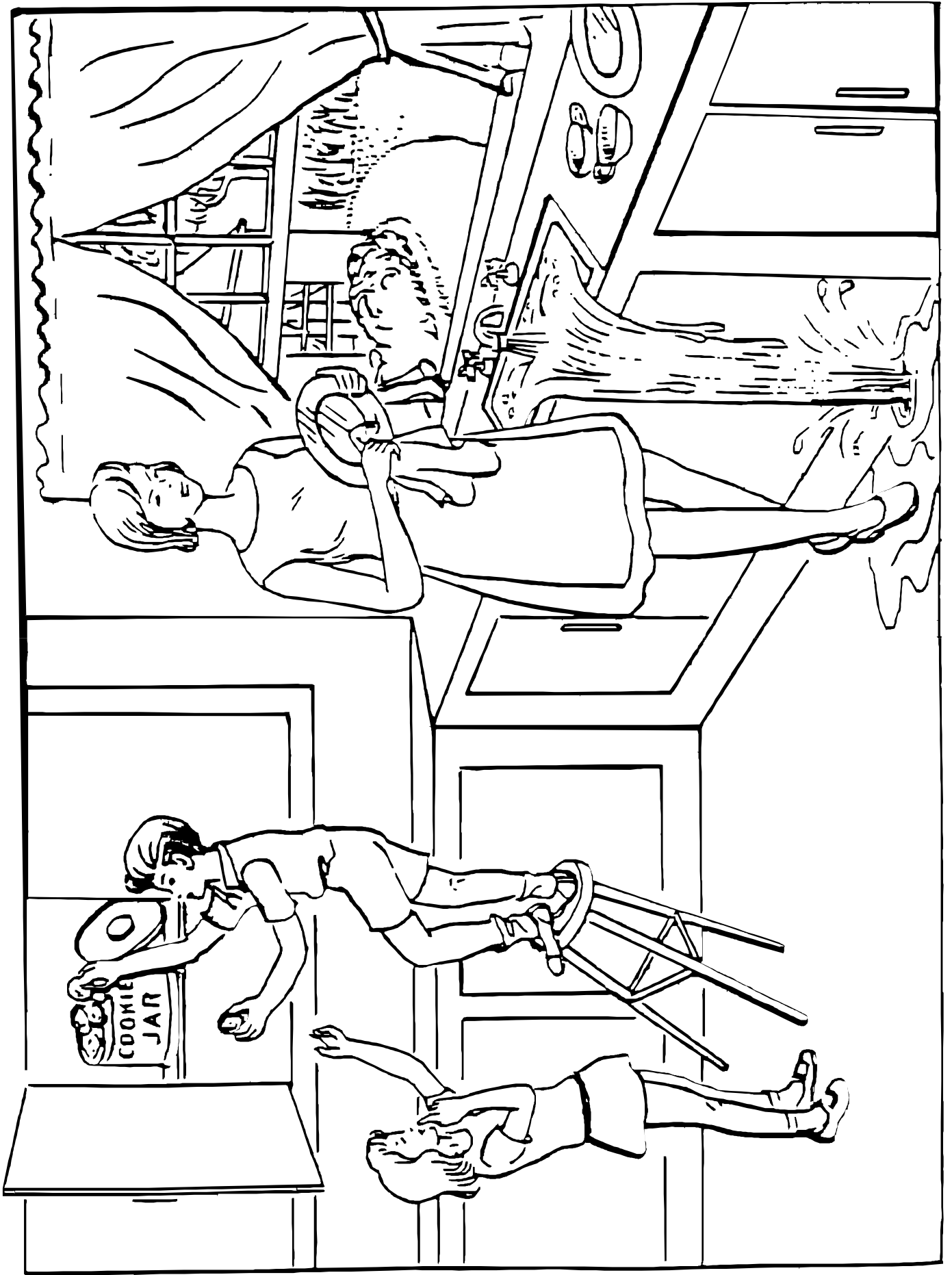
Pt. Date of Birth ____/____/____

Hospital _____ (____-____)

Date of Exam ____/____/____

Interval: ☐ Baseline ☐ 2 hours post treatment ☐ 24 hours post onset of symptoms \pm 20 minutes ☐ 7-10 days
☐ 3 months ☐ Other _____ (____)

<p>11. Extinction and Inattention (formerly Neglect): Sufficient information to identify neglect may be obtained during the prior testing. If the patient has a severe visual loss preventing visual double simultaneous stimulation, and the cutaneous stimuli are normal, the score is normal. If the patient has aphasia but does appear to attend to both sides, the score is normal. The presence of visual spatial neglect or anosagnosia may also be taken as evidence of abnormality. Since the abnormality is scored only if present, the item is never untestable.</p>	<p>0 = No abnormality.</p> <p>1 = Visual, tactile, auditory, spatial, or personal inattention or extinction to bilateral simultaneous stimulation in one of the sensory modalities.</p> <p>2 = Profound hemi-inattention or extinction to more than one modality; does not recognize own hand or orients to only one side of space.</p>	<p>_____</p>
---	--	--------------



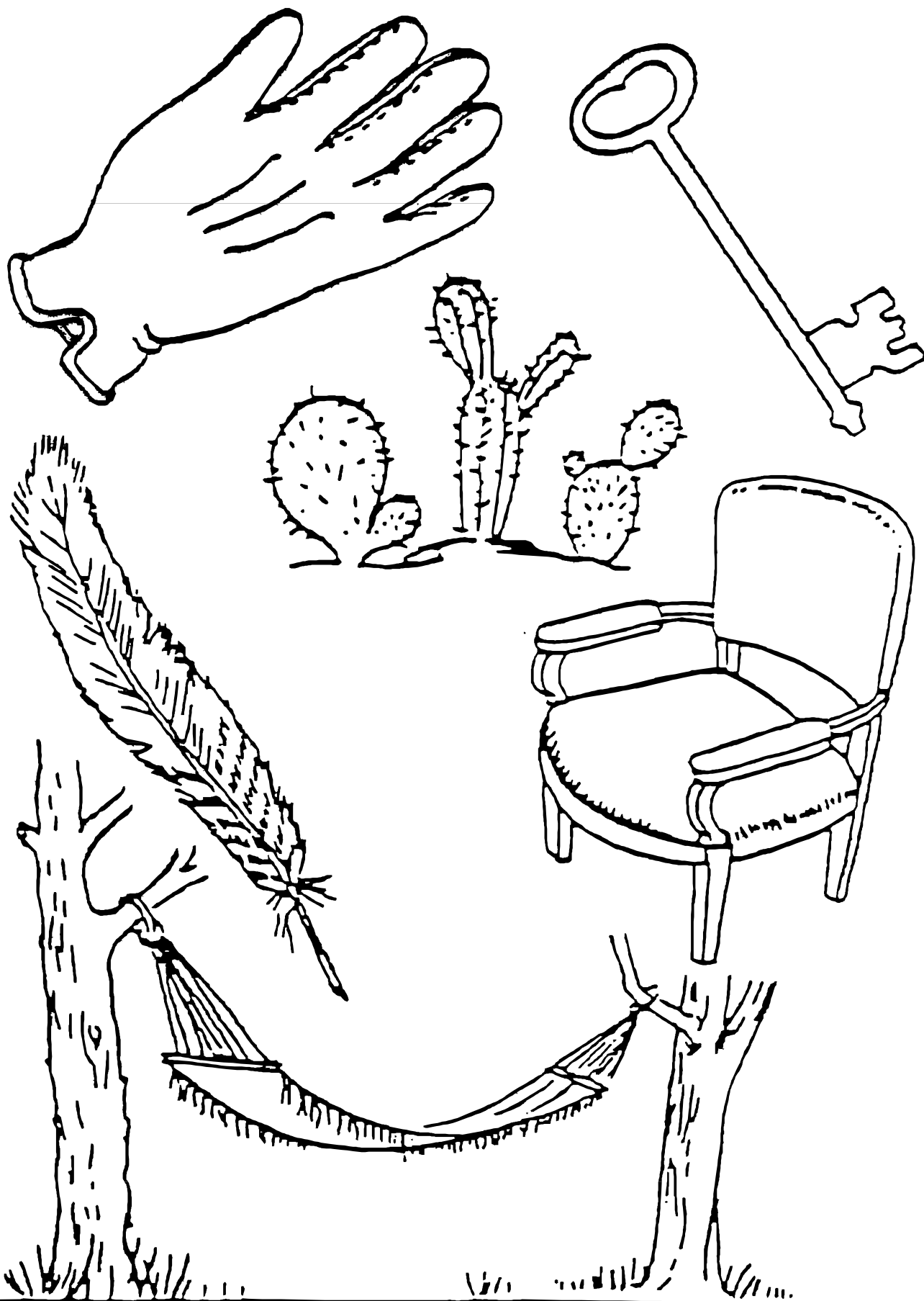
You know how.

Down to earth.

I got home from work.

**Near the table in the dining
room.**

**They heard him speak on the
radio last night.**



MAMA

TIP – TOP

FIFTY – FIFTY

THANKS

HUCKLEBERRY

BASEBALL PLAYER

A.2.2 modified Rankin Scale

**University of North Carolina Hospitals
Chapel Hill, NC 27514
Department of Neurology**

**MODIFIED RANKIN SCALE (MRS)
MIM # 721**

Rater Name: _____

Date: _____

Score Description

- | | |
|---|---|
| 0 | No symptoms at all |
| 1 | No significant disability despite symptoms; able to carry out all usual duties and activities |
| 2 | Slight disability; unable to carry out all previous activities, but able to look after own affairs without assistance |
| 3 | Moderate disability; requiring some help, but able to walk without assistance |
| 4 | Moderately severe disability; unable to walk without assistance and unable to attend to own bodily needs without assistance |
| 5 | Severe disability; bedridden, incontinent and requiring constant nursing care and attention |
| 6 | Dead |

TOTAL (0–6): _____

Rater Sign / pager: _____

Provider Sign / MD# / pager: _____

HDF 536 / 4/03

References

Rankin J. "Cerebral vascular accidents in patients over the age of 60." *Scott Med J* 1957;2:200-15
Bonita R, Beaglehole R. "Modification of Rankin Scale: Recovery of motor function after stroke." *Stroke* 1988 Dec;19(12):1497-1500
Van Swieten JC, Koudstaal PJ, Visser MC, Schouten HJ, van Gijn J. "Interobserver agreement for the assessment of handicap in stroke patients." *Stroke* 1988;19(5):604-7

Appendix B

Supplementary Results

B.1 Study IV. Surface-based Morphometry

Table B.1 Mean and SD of the SBM metrics for controls, patients at M0 and patients at M6

Metrics	Hemisphere	Controls		Patients-M0		Patients-M6	
		Mean	SD	Mean	SD	Mean	SD
Cortical Thickness	Left ipsilesional	2.551	0.117	2.345	0.187	2.280	0.184
	Right/contralesional	2.551	0.116	2.413	0.154	2.405	0.152
	Whole brain	2.551	0.116	2.379	0.162	2.342	0.153
Fractal Dimension	Left ipsilesional	2.588	0.031	2.535	0.045	2.528	0.053
	Right/contralesional	2.575	0.033	2.559	0.033	2.562	0.039
	Whole brain	2.581	0.029	2.547	0.034	2.545	0.040
Gyrification Index	Left ipsilesional	28.364	0.495	28.467	0.665	28.358	0.776
	Right/contralesional	28.456	0.486	28.411	0.513	28.451	0.571
	Whole brain	28.410	0.473	28.439	0.552	28.404	0.628

Supplementary Results

Table B.2 Fractal dimension (FD) comparison between patients (at M0) and controls at ROI-level

ROI	%	Ipsi	Contra	ROI	%	Ipsi	Contra	ROI	%	Ipsi	Contra
Insula-G	57.01	-4.79*	-2.59	PFm	19.63	-3.07	-3.87	ProStriate	4.67	-4.86*	-1.52
Insula2-post	56.07	0.44	1.54	47m	18.69	-3.20	-2.28	V3	3.74	-4.77*	-5.7*
Insula-post	54.21	0.26	2.75	Frontal-eye-fiels	17.76	-4.63*	-4.69*	V7	3.74	-1.05	-1.53
OP2-3-VS	53.27	-3.40	-5.78*	IP2	17.76	-2.54	-3.39	IPS1	3.74	-2.56	-1.81
FO3	52.34	-0.02	0.2	Superior-Temporal-medial	16.82	-3.28	-4.05*	PreCuneus-visual	3.74	-2.73	-0.16
FO2	52.34	0.24	0.03	55b	16.82	-3.55	-5.56*	23d	3.74	-2.03	-2.62
Insula-mid	50.47	-0.10	2.12	1	16.82	-4.37*	-3.51	5L	3.74	-3.45	-1.68
FO1	48.60	-4.2*	-0.61	TPOJ3	16.82	-2.95	-3.49	8BL	3.74	-0.62	-0.77
Belt-medial	47.66	-8.61*	-3.56	47r-post	16.82	-1.88	-3.85	9p	3.74	-2.00	-1.11
43	46.73	-1.67	-0.25	TE1-mid	15.89	-5.0*	-3.04	10p-ant	3.74	-3.54	-2.19
52	46.73	-2.80	-0.99	6-ant	14.95	-6.44*	-4.56*	Entorhinal	3.74	1.09	3.15
A1	44.86	-6.54*	-4.2*	TG-d	14.95	0.44	0.51	Perirhinal-ectorhinal	3.74	3.61	0.73
Piriform	44.86	0.57	2	Temporal-mid	13.08	-3.79	-5.06*	PH	3.74	-2.28	-3.57
OP4-PV	43.93	0.49	2.02	7PC	13.08	-3.13	-2.57	Visual-dorsal-transitional	3.74	-3.58	-4.11*
6-rostral	42.99	-7.81*	-4.59*	IP-Lat-dorsal	13.08	-2.06	-0.96	ParaHippocampal2	3.74	-4.11*	-1.93
OP1-SII	42.99	-0.05	-2.17	FST	13.08	-3.51	-2.15	V4t	3.74	-4.5*	-2.62
FO4	42.99	-3.18	-2.71	8Av	12.15	-5.24*	-3.77	25	3.74	-2.82	-6.43*
Belt-lateral	42.99	-6.9*	-4.87*	46	12.15	-7.93*	-3.38	V6	2.80	-2.81	-2.83
Insula-Ag-ant	42.06	0.04	2.64	9-46v-ant	12.15	-3.22	-3.72	V8	2.80	-2.91	-0.32
RetroInsula	41.12	-7.46*	-3.76	IP-Lat-ventral	11.21	-2.66	-2.37	LOC2	2.80	-3.81	0.06
Para-Belt	41.12	-3.92*	-4.98*	6d	11.21	-4.82*	-4.48*	33	2.80	-3.82	-1.78
Para-Insular	38.32	-1.65	2.69	47-ant	11.21	-5.66*	-2	32d	2.80	-0.12	-0.89
TA2	36.45	-8.31*	-4.22*	13l	11.21	-0.98	1.4	8BM	2.80	-0.62	-2.16
FO	36.45	-4.74*	-5.12*	TE1-post	10.28	-5.57*	-2.06	10r	2.80	-3.79	-1.22
3a	35.51	-4.32*	-4.33*	LOC3	10.28	-2.52	-4.55*	10d	2.80	-3.73	-1.92
IFJp	35.51	-4.6*	-1.56	IP-medial	9.35	-2.28	-3.1	9a	2.80	-1.81	-4.27*
PFcm	35.51	-3.68	-3.96*	9-46d	9.35	-6.88*	-3.66	10v	2.80	-3.30	-3.96*
Insula-ventral-ant	35.51	-0.91	1.19	6-8-inf-transitional	9.35	-4.25*	-4.46*	ParaHippocampal1	2.80	-2.75	-4.18*
44	34.58	-6.45*	-4.37*	PGp	9.35	-0.61	-2.76	V1-VM	2.80	-2.02	-1.92
Auditory-4	34.58	-5.4*	-3.48	IP1	9.35	-1.93	-2.39	V3-VM	2.80	-5.14*	-5.16*
IFJa	33.64	-3.96*	-3.4	5Mv	8.41	-6.43*	-1.64	V2-VM	2.80	-2.67	-3.65
PFop	32.71	-4.46*	1.13	24d-ventral	8.41	-4.22*	-1.55	31a	2.80	-1.83	-0.16
PeriSylvian-language	28.97	-5.44*	-2.84	PGs	8.41	-2.36	-1.14	s32	2.80	-1.37	-1.08
45	28.97	-7.02*	-5.13*	6ma	7.48	0.85	-0.23	10p-post	2.80	-5.71*	-2.92
PFt	28.97	-5.28*	-3.78	6mp	7.48	-1.70	-1.45	TG-v	2.80	1.65	1.55
IFSp	28.04	-3.40	-2.59	8Ad	7.48	-2.99	-2	24-post	2.80	-2.58	-0.05
TPOJ1	28.04	-4.75*	-2.75	Hippocampus	7.48	-0.44	-0.11	SPOC2	1.87	-5.01*	-2.79
Premotor-eye-fields	27.10	-6.55*	-2.29	TE2-ant	7.48	-1.96	-0.52	Superior-Frontal-language	1.87	-1.09	-2.77
8C	27.10	-6.33*	-4.47*	23c	6.54	-5.03*	-2.74	a24	1.87	2.56	0.73
Auditory-5	27.10	-7.82*	-3.09	IP-ventral	6.54	-2.65	-1.3	p32	1.87	1.46	-0.12
PFC	27.10	-2.59	-4.53*	24prime-post	6.54	-1.71	-3.58	9mid	1.87	-4.49*	-2.59
Superior-Temporal-visual	26.17	-6.52*	0.15	32	6.54	-2.91	0.57	ParaHippocampal3	1.87	-4.91*	-2.78
47s	26.17	-4.11*	-0.99	OFC-post	6.54	-6.27*	-3.52	TF	1.87	-0.47	-0.6
STSd-post	26.17	-4.85*	-5.21*	IP0	6.54	-1.71	-3.32	TE2-post	1.87	1.02	-0.99
2	25.23	-4.9*	-3.85	V3CD	6.54	-3.49	-1.83	31p-d	1.87	-6.01*	-2.49
6v	25.23	-4.88*	-5.11*	V4	5.61	-6.49*	-3.38	Visual-ventral	1.87	-5.34*	-4.35*
STSd-ant	25.23	-8.68*	-3.46	LOC1	5.61	-3.51	-2.63	Orbital-frontal	1.87	-0.25	2.55
STSV-post	25.23	-3.71	-3.38	24d-dorsal	5.61	-6.84*	-1.15	V3A	0.93	-1.47	-2.72
9-46v-post	24.30	-5.97*	-4.18*	24prime-ant	5.61	-2.71	-0.33	Fusiform-face	0.93	-1.87	-0.03
47-lat	23.36	-5.78*	-3.13	11l	5.61	1.08	0.74	InferoTemporal-post	0.93	-2.79	0
IFSa	23.36	-4.35*	-3.97*	32-ant	5.61	-1.42	-0.34	7P-med	0.93	-3.54	-2.47
IP-ant	23.36	-4.35*	-3.93*	V1	4.67	-3.71	-3.77	7M	0.93	-4.89*	-2.33
STGa	23.36	-4.4*	0.08	V2	4.67	-3.63	-3.97*	SPOC1	0.93	-3.50	0.13
PGi	22.43	-4.7*	-3.94*	V3B	4.67	-4.99*	-2.13	23ab-ventral	0.93	0.41	0.3
4	21.50	-5.91*	-4.96*	5M	4.67	-3.12	-2.31	31p-v	0.93	-2.12	-1.55
PHT	21.50	-3.52	1.16	7A	4.67	-2.78	-2.11	10p-polar	0.93	-4.83*	-1.91
TPOJ2	21.50	-4.78*	-1.85	Supp-Cingulate-eye	4.67	-1.18	-1.15	PreSubiculum	0.93	-4.74*	-4.11*
STSV-ant	21.50	-0.09	-2.72	7A-med	4.67	-2.18	-0.38	V6A	0.93	-1.05	-2.14
SI	19.63	-4.15*	-3.57	7P	4.67	-2.80	-1.28	RetroSplenial	0.00	-0.28	0.88
TE1-ant	19.63	2.03	0.55	6-8-sup-transitional	4.67	-1.46	-1.77	23ab-dorsal	0.00	-0.97	-0.03

Values in the table indicate t-value comparison between patients and control (negative value means decreased CT compared to controls, and vice versa), Ipsi/Contra: comparison in the ipsilesional/contralesional hemisphere, * indicates significant difference using Bonferroni correction for multiple comparison, % indicates percentage of patients having lesions in the ROI.

B.1 Study IV. Surface-based Morphometry

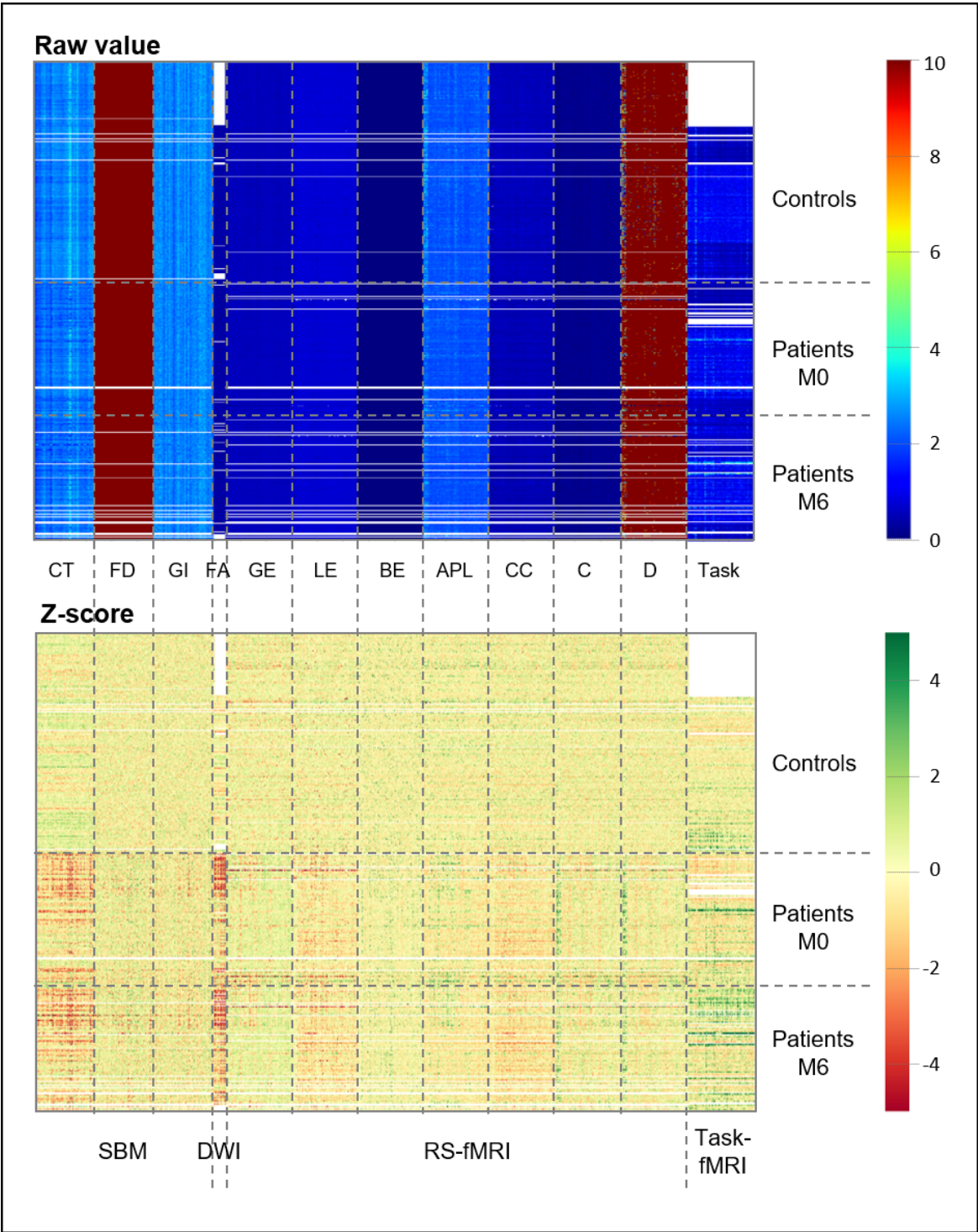
Table B.3 Gyrification Index (GI) comparison between patients (at M0) and controls at ROI-level

ROI	%	Ipsi	Contra	ROI	%	Ipsi	Contra	ROI	%	Ipsi	Contra
Insula-G	57.01	-1.83	-2.26	PFm	19.63	-2.07	0.09	ProStriate	4.67	-6.05*	0.43
Insula2-post	56.07	5.51*	0.1	47m	18.69	-1.17	-0.49	V3	3.74	-0.50	0.68
Insula-post	54.21	3.61	-5.31*	Frontal-eye-fields	17.76	2.37	-0.95	V7	3.74	1.45	-0.86
OP2-3-VS	53.27	-0.76	-2.33	IP2	17.76	-0.09	-0.67	IPS1	3.74	4.56*	-2.1
FO3	52.34	3.09	-3.22	Superior-Temporal-medial	16.82	-0.78	-0.6	PreCuneus-visual	3.74	-0.92	0.52
FO2	52.34	0.49	-2.83	55b	16.82	-1.88	0.99	23d	3.74	0.03	-1.68
Insula-mid	50.47	1.97	-1.6	1	16.82	-1.56	-1.64	5L	3.74	2.25	0.28
FO1	48.60	2.35	0.25	TPOJ3	16.82	-0.42	-0.98	8BL	3.74	1.63	2.06
Belt-medial	47.66	1.43	-2.22	47r-post	16.82	-1.09	-0.79	9p	3.74	-0.01	-2.37
43	46.73	-1.36	-1.71	TE1-mid	15.89	2.97	-0.8	10p-ant	3.74	0.30	-0.49
52	46.73	-0.51	-3.6	6-ant	14.95	3.00	2.14	Entorhinal	3.74	2.81	-2.97
A1	44.86	0.41	-2.56	TG-d	14.95	3.51	0.55	Perirhinal-ectorhinal	3.74	-1.68	1.22
Piriform	44.86	3.28	-2.17	Temporal-mid	13.08	2.43	0.26	PH	3.74	2.10	0.94
OP4-PV	43.93	-2.05	-1.4	7PC	13.08	0.52	-0.15	Visual-dorsal-transitional	3.74	1.47	3.77
6-rostral	42.99	-0.01	-0.64	IP-Lat-dorsal	13.08	0.29	-0.13	ParaHippocampal2	3.74	-1.23	0.78
OP1-SII	42.99	-1.30	-1.97	FST	13.08	0.43	0.74	V4t	3.74	-1.05	-0.73
FO4	42.99	-0.70	-1.43	8Av	12.15	3.24	-1.76	25	3.74	-1.17	1.43
Belt-lateral	42.99	-1.41	0.87	46	12.15	-0.05	1.2	V6	2.80	-0.68	-0.53
Insula-Ag-ant	42.06	4.73*	-0.61	9-46v-ant	12.15	1.23	-0.23	V8	2.80	1.07	-0.07
RetroInsula	41.12	-2.31	-0.35	IP-Lat-ventral	11.21	2.27	0.51	LOC2	2.80	-0.38	-1.9
Para-Belt	41.12	1.28	1.18	6d	11.21	1.66	3.38	33	2.80	2.32	-3.53
Para-Insular	38.32	-3.55	-3.3	47-ant	11.21	0.53	-0.74	32d	2.80	-4.0*	0.59
TA2	36.45	2.73	-0.15	13l	11.21	-0.28	1.48	8BM	2.80	0.62	1.14
FO	36.45	-1.60	-2.13	TE1-post	10.28	2.95	2.62	10r	2.80	2.21	-2.08
3a	35.51	-3.90	-0.09	LOC3	10.28	0.38	2.19	10d	2.80	-1.32	-4.58*
IFJp	35.51	0.04	-1.13	IP-medial	9.35	-2.19	1.93	9a	2.80	0.57	-4.02*
PFcm	35.51	-0.60	0.62	9-46d	9.35	-4.27*	-0.65	10v	2.80	0.79	0.84
Insula-ventral-ant	35.51	-1.75	-0.93	6-8-inf-transitional	9.35	0.70	0.29	ParaHippocampal1	2.80	0.88	-3.89*
44	34.58	-1.68	-2.15	PGp	9.35	-2.52	-1.17	V1-VM	2.80	-0.64	0.88
Auditory-4	34.58	3.32	-0.09	IP1	9.35	0.97	0.25	V3-VM	2.80	1.11	4.62*
IFJa	33.64	-1.75	-0.47	5Mv	8.41	-2.57	1.88	V2-VM	2.80	-2.38	-0.25
PFop	32.71	-3.88	-2.18	24d-ventral	8.41	-0.26	1.95	31a	2.80	-1.77	2.13
PeriSylvian-language	28.97	0.57	-3.92*	PGs	8.41	-1.23	-1.78	s32	2.80	3.43	-0.93
45	28.97	-0.35	0.45	6ma	7.48	-0.66	1.06	10p-post	2.80	-1.41	-0.65
PFt	28.97	-2.17	0.17	6mp	7.48	1.01	-0.08	TG-v	2.80	1.05	0.78
IFSp	28.04	-1.51	-0.19	8Ad	7.48	-0.28	1.76	24-post	2.80	1.65	-0.17
TPOJ1	28.04	-0.67	-0.6	Hippocampus	7.48	-1.44	4.89*	SPOC2	1.87	0.11	1.14
Premotor-eye-fields	27.10	1.70	0.09	TE2-ant	7.48	3.36	0.4	Superior-Frontal-language	1.87	4.07*	-1.38
8C	27.10	2.69	-0.09	23c	6.54	1.54	-3.57	a24	1.87	-0.14	-0.99
Auditory-5	27.10	0.62	3.89*	IP-ventral	6.54	-1.19	-0.73	p32	1.87	-1.14	2.33
PFC	27.10	-3.42	-1.16	24prime-post	6.54	-0.79	-1.57	9mid	1.87	1.03	-2.41
Superior-Temporal-visual	26.17	-1.02	0.72	32	6.54	-0.14	0.78	ParaHippocampal3	1.87	3.57	0.58
47s	26.17	2.33	0.25	OFC-post	6.54	2.38	1.43	TF	1.87	-0.60	1.94
STSd-post	26.17	2.59	1.8	IP0	6.54	-1.21	2	TE2-post	1.87	0.32	3.48
2	25.23	-0.71	-1.82	V3CD	6.54	-0.57	-0.1	31p-d	1.87	1.83	1
6v	25.23	0.76	2.19	V4	5.61	1.46	-0.17	Visual-ventral	1.87	1.63	-1.69
STSd-ant	25.23	4.84*	-0.87	LOC1	5.61	0.44	-0.22	Orbital-frontal	1.87	-2.42	-0.31
STSV-post	25.23	-0.38	5.04*	24d-dorsal	5.61	2.82	0.37	V3A	0.93	-1.11	2.29
9-46v-post	24.30	2.42	-0.07	24prime-ant	5.61	1.34	-2.15	Fusiform-face	0.93	-1.34	1.2
47-lat	23.36	2.21	-0.59	11l	5.61	-0.75	5.01*	InferoTemporal-post	0.93	0.63	0.82
IFSa	23.36	-3.22	-1.15	32-ant	5.61	-0.47	1.01	7P-med	0.93	-0.67	-1.33
IP-ant	23.36	-1.15	0.18	V1	4.67	2.20	1.23	7M	0.93	0.64	1.32
STGa	23.36	3.44	-1.82	V2	4.67	-1.09	-0.16	SPOC1	0.93	-0.91	0.05
PGi	22.43	-0.93	-2.2	V3B	4.67	-0.68	-1.11	23ab-ventral	0.93	-0.39	1.15
4	21.50	1.74	-0.85	5M	4.67	-0.97	-0.67	31p-v	0.93	-0.67	-0.99
PHT	21.50	0.39	1.97	7A	4.67	-0.43	0.08	10p-polar	0.93	1.53	-2.9
TPOJ2	21.50	0.68	-1.3	Supp-Cingulate-eye	4.67	-1.19	-0.01	PreSubiculum	0.93	-1.25	-3.57
STSV-ant	21.50	-3.18	6.26*	7A-med	4.67	-1.09	-0.01	V6A	0.93	0.54	-0.81
SI	19.63	0.56	1.09	7P	4.67	0.72	1.49	RetroSplenial	0.00	1.46	-0.58
TE1-ant	19.63	2.74	2.36	6-8-sup-transitional	4.67	2.94	2.8	23ab-dorsal	0.00	1.12	-1.5

Values in the table indicate t-value comparison between patients and control (negative value means decreased CT compared to controls, and vice versa), Ipsi/Contra: comparison in the ipsilesional/contralesional hemisphere, * indicates significant difference using Bonferroni correction for multiple comparison, % indicates percentage of patients having lesions in the ROI.

B.2 Study VI. Multimodal MRI

Fig. B.1 Heatplot of raw value and z-scores



B.2 Study VI. Multimodal MRI

Table B.4 Predictive value of metrics in each modality using different methods

Dependent variable	MRI modality	Metrics	LR-I1	LR-I2	RF	SVM
Grip M6	SBM	CT	0.790	0.718	0.805	0.677
		FD	0.728	0.718	0.744	0.697
		GI	0.595	0.631	0.733	0.390
	DWI	FA	0.849	0.855	0.836	0.803
		GE	0.754	0.749	0.872	0.713
	RS-fMRI	LE	0.615	0.582	0.813	0.593
		BE	0.805	0.821	0.800	0.795
		APL	0.816	0.632	0.724	0.553
		CC	0.615	0.516	0.692	0.484
		C	0.779	0.759	0.790	0.692
		D	0.779	0.759	0.795	0.692
	Task-fMRI		0.922	0.878	0.944	0.867
mNIHSS M6	SBM	CT	0.406	0.553	0.694	0.571
		FD	0.694	0.682	0.729	0.665
		GI	0.659	0.753	0.718	0.729
	DWI	FA	0.982	0.982	0.939	0.861
		GE	0.726	0.673	0.827	0.577
	RS-fMRI	LE	0.643	0.488	0.679	0.488
		BE	0.750	0.649	0.631	0.631
		APL	0.880	0.861	0.843	0.824
		CC	0.619	0.464	0.583	0.488
		C	0.821	0.714	0.685	0.619
		D	0.821	0.714	0.685	0.619
	Task-fMRI		0.917	0.906	0.865	0.844
NIHSS M6	SBM	CT	0.988	0.952	0.958	0.927
		FD	0.976	0.903	0.867	0.915
		GI	0.861	0.830	0.794	0.830
	DWI	FA	0.948	0.954	0.961	0.935
		GE	0.967	0.953	0.973	0.927
	RS-fMRI	LE	0.701	0.623	0.714	0.623
		BE	0.900	0.907	0.913	0.867
		APL	0.780	0.760	0.830	0.700
		CC	0.662	0.636	0.688	0.623
		C	0.980	0.967	0.933	0.947
		D	0.980	0.967	0.933	0.940
	Task-fMRI		0.769	0.744	0.679	0.756

SBM: Surface-based morphometry, CT: Cortical thickness, FD: Fractal dimension, GI: Gyrfication index, DWI: Diffusion weighted imaging, FA: Fractional anisotropy, RS-fMRI: Resting-state functional MRI, GE: Global efficiency, LE: Local efficiency, APL: Average path length, CC: Clustering coefficient, C: cost, D: Degree

